# Experimental Investigations and Numerical Modelling of Lateral Variations of Hydraulics and Sediment Transport in Braided Rivers

Submitted by **Michael Mehari Moges**
to the University of Exeter
as a thesis for the degree of Doctor of Philosophy
in Geography in the College of Life and Environmental Sciences
November 2012



I certify that all material in this thesis which is not my own work has been identified and that no material has previously been submitted and approved for the award of a degree by this or any other University.

……..
Michael Mehari Moges

# ABSTRACT

Measurement and prediction of cross section averaged bedload transport rates in braided rivers have been long standing problem. Moreover, because bedload transport is non-linear, width averaged calculations of sediment transport will underestimate the true bedload flux where there is marked spatial and temporal variability in hydraulic parameters. However, at present very little is known about this effect or the actual lateral distribution of bedload. This thesis presents results from a series of micro-scale laboratory experiments designed to quantify the role of lateral variation of sediment transport as controls on braided river evolution. The experimental approach follows the "similarity of processes" concept and is therefore not scaled to a real world prototype. In all the five runs, the water discharge was held constant and the sediment feed rate was varied to simulate consecutive aggradation and degradation scenarios.

The qualitative observations of the experiments were supplemented with sediment transport data at the flume outlet and quantitative analysis of high resolution laser profiler attached to the experimental apparatus which measured bed elevations of the experimental channels as they evolved. This allowed the construction of a time series of data on the sediment storage and channel morphology and the changing lateral hydraulic variability on the channel. Aggradation was associated with channel multiplication and an increase in braiding intensity. During degradation, channel pattern was transformed to single thread. Simple averaging of sediment transport computations over the width of the channel is found to underestimate the sediment transport rate. A clear relationship appears to exist between braiding intensity and the width of shear stress distribution shape parameter. Maxima in braiding intensity and minima in shape parameter values occur around the flume outlet. In contrast, minima in braiding intensity and maxima in shape parameter values occur at the flume entrance. The experimental data generated provides a unique opportunity to observe in detail the spatial and temporal changes in the width of shear stress shape parameter that occurred on the channels as they evolved. The digital elevation models collected from the experiments were also used to run a two-dimensional hydraulic model that helped to understand the controls of shear stress on the experimental channels. A relationship was established that relates the width of

shear stress distribution shape parameter and channel morphological parameters (channel width to depth ratio and braiding intensity) and the relationship was also compared with observations of the Megech gravel bed braided river in the Northern Ethiopia.

Overall, the investigation has demonstrated the potential for micro scale physical models to investigate aggradation and degradation scenarios and provide rich data concerning the lateral variability of sediment transport in braided channels. These data demonstrate the idea that increasing braiding intensity is a morphological response to high sediment load from upstream. Channel aggradation increases sediment transport by promoting lateral flow variability. This in turn feeds back to further aggradation depending on the response of the channel. This process will continue up to a point where there is no substantial variation in channel width to depth ratio. Beyond this point, there will be a reduction in sediment transport rates as a result of reduction in mean shear stress. This will in turn feed back to promote further aggradation.

# TABLE OF CONTENTS

# LIST OF TABLES

# LIST OF FIGURES

# ACKNOWLEDGEMENT

This dissertation would not have come to fruition without the support and encouragement of different individuals and organizations. First, I would like to thank my second supervisor Dr. Andrew Nicholas for not only critically reading my dissertation but also for the interesting discussions we always had on all matters of this thesis. I am indebted to him for useful suggestions and encouragement. It would not have been possible for me to complete this PhD without his resourcefulness and help. I would like to thank my first supervisor Prof. Timothy Quine for giving me the opportunity to study this PhD under his supervision, for his invaluable advices and continuous support of all kind throughout the research period. Diane Fraser and Neville England provided a great deal of support in computing and laboratory experimentation, and Helen Pisarska provided much-needed administrative support both in the period leading up to my move to the UK, and throughout my PhD. I thank the University of Exeter for providing me the funding for this research through internal scholarship.

Fieldwork in Ethiopia would not have been possible without the assistance of Bahir Dar University, School of Civil and Water Resources Engineering for providing me the total station and Amhara Water Resources Development Bureau for providing me the current meter for velocity measurement. Thanks to my friend Bewketu Destaw, who helped me tirelessly in challenging field conditions and helping me to get additional total station set while the one at hand was not working.

I am grateful to my relatives and friends for their encouragement and wishes of successful accomplishment. Many thanks are due to my mother, brothers and sisters and all other members of my family for their prayers, unconditional love and support. My heartfelt gratitude goes to my lovely wife, Belaynesh for her constant encouragement, patience and strength in shouldering diverse responsibilities in my absence. Very special thanks to my little daughter, Afomi; you are my inspiration. I should not finish without expressing my gratitude to my Ethiopian friends in London (Halefom, his wife Saba and their children Bruk and Rubi). So much fun and good times I have shared with you. Thank you for all your supports and comforts. You made my stay in the UK lively.

# 1. INTRODUCTION

## 1.1. INTRODUCTION

The term 'braided river' has been given several definitions in literature over the past 40 years (Bristow and Best, 1993). Most focus on the physical characteristics associated with the presence of multiple flowing channels. For example:

"Braided rivers are characterized by having a number of alluvial channels with bars and islands between meeting and dividing again, and presenting from the air the intertwining effect of a braid" (Lane, 1957).

"A braided river is one which flows in two or more channels around alluvial islands" (Leopold and Wolman, 1957).

There are a lot of other definitions in the literature. The main characteristics of the braided reach is the repeated division and joining of channels and their associated flow patterns, referred to as zones of confluence and diffluence. Braided river reaches occur in diverse climatic settings and are abundant in many areas. They are mainly characterised by their multi-threaded planform and are agents of substantial sediment transport, erosion and deposition. Typically, braiding is associated with high values of valley slope, abundant sediment supply, non-cohesive bank materials, and higher values of stream power, shear stress, width to depth ratio and bedload transport rate than straight or meandering channels (Schumm and Khan, 1972;Ferguson, 1993).

The high rates of sediment transport, erosion and deposition, and the frequent shifting of river channel positions in braided rivers pose many significant problems to a whole range of disciplines (Bristow and Best, 1993). Despite this, braided rivers have been relatively understudied when compared to the wealth of material on meandering rivers (Bristow and Best, 1993). The neglect of braided river study is probably due in part to the nature of braided rivers, and the difficulty of undertaking field work and characterising complex features in this rapidly changing environment. This relative disregard of braided rivers has resulted in the development of our understanding of braided river behaviour being impeded. Although advances have been made in the

qualitative and quantitative understanding of flow and sediment processes in braided river systems, several key issues still remain to be addressed.

Measurement and prediction of cross section averaged bedload transport rates in braided rivers have been long standing problems for several reasons. One of these reasons is the complexity and instability of braided river morphology. Braided rivers change their morphology continuously, which makes measurement very difficult. The second reason is due to the lateral and temporal variation in flow and sediment transport that makes representative measurement of bedload flux almost impossible, due to the number and frequency of samples required to represent the whole channel (Bertoldi *et al.*, 2009). Conventional approaches to bedload transport computation based upon rectangular channels are understood to be of limited utility in braided rivers where there is marked spatial and temporal variability in hydraulic parameters (Nicholas, 2000;Bertoldi *et al.*, 2009;Carson and Griffiths, 1987;Ferguson, 2003). However, at present very little is known about this effect or the actual lateral distribution of bedload. Previous studies suggest that in real river cross sections the bedload transport may be several times greater than that estimated using the equivalent uniform, rectangular cross section (Nicholas, 2000;Bertoldi *et al.*, 2009;Ferguson, 2003;Paola, 1996). Flow and sediment transport in braided rivers may also be confined to narrow and active zones, which signify the fact that section averaged variables result in significant underestimation of the actual bedload transport (Carson and Griffiths, 1987). This phenomenon also introduces another complexity for the relationship between bedload transport and stream braiding. At the moment, the role played by channel pattern indices (e.g., channel width to depth ratio, braiding intensity) in bedload transport is very unclear. For example, the laboratory experiments of Ashmore (1988) and Davies and Lee (1988) show that a reduction in braid intensity and/or channel width is associated with increased bedload transport for equilibrium braided streams. However, Warburton and Davies (1994) recognize the opposite trend in their data, with bedload transport rates being directly proportional to braid intensity. This indicates that there is no consistent relationship between bedload transport rate and channel pattern indices. The feedback mechanisms between flow-sediment transport and river morphology is clearly described in Figure 1.1. “There is a tendency for channel multiplication to occur in aggrading reaches,

which may accelerate aggradation as the newly formed or occupied channels evolve toward their own equilibrium shapes and as a greater proportion of total water discharge is over bars where bedload transport rates are low. Thus changes in channel planform which are themselves responses to aggradation may induce further aggradation. Degradation of one channel leads to capture of a greater proportion of total flow by that channel. This in turn causes further degradation as the increased flow is associated with different equilibrium channel geometry" (Hoey and Sutherland, 1991).

Despite this, until recently there has been no systematic assessment of the effect of cross section averaging and this is an area that requires more research. Recent research on the effect of lateral variation in hydraulic parameters and morphology on estimates of bedload transport has focussed on the application of probability density functions of either flow depth or shear stress to sediment flux calculations (Nicholas, 2000;Paola, 1996;Hoey *et al.*, 2001). The development of this method has been hindered mainly because of the requirement of a large number of measurements of channel morphology to derive the input parameters, and the difficulty of obtaining high resolution datasets to investigate the issue for different environmental conditions (including non-equilibrium channels).

This study has emerged from the above considerations. There is a need for an investigation into how lateral flow variability affects the estimation of sediment transport in braided rivers, and how these factors influence and are influenced by changes in channel morphology. Moreover, there is a need to identify relationships that will help to incorporate lateral flow variability into bedload flux calculations without measuring the full PDF of the relevant hydraulic parameter. This project will attempt to enhance understanding in these areas. The next section will outline the structure of the thesis to be presented.

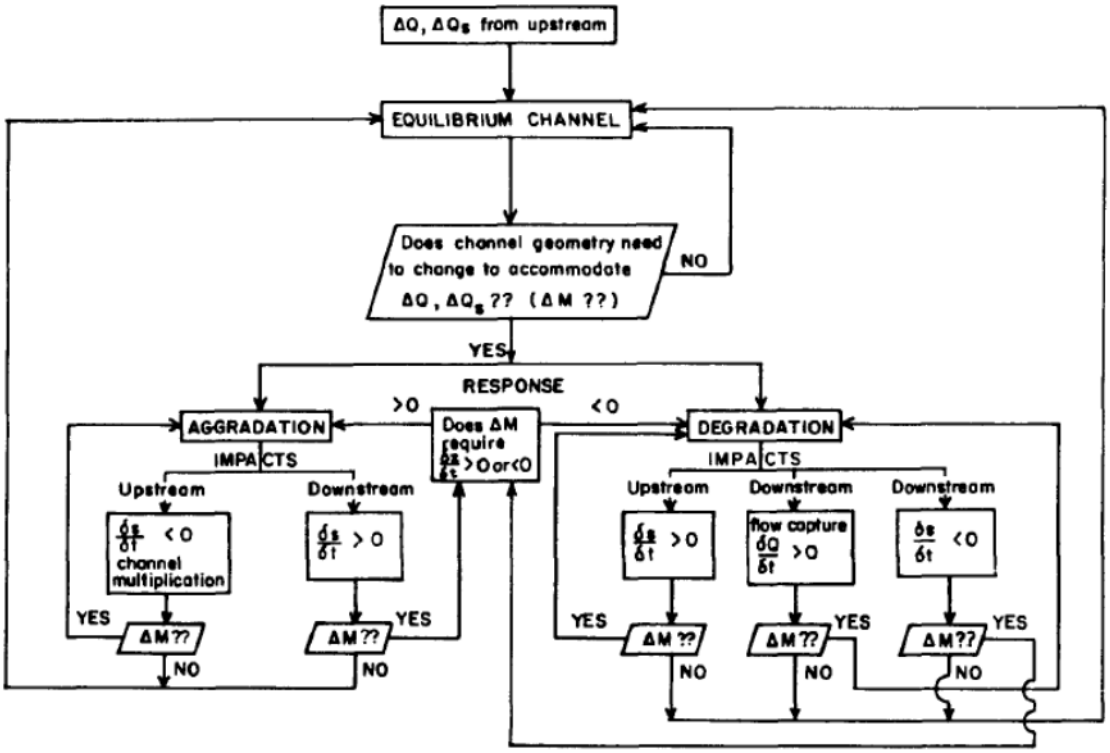


**Figure 1-1 Schematic representation of the controls over aggradation and degradation defined in terms of channel adjustment toward equilibrium. ΔQ = Water discharge input from upstream; ΔM = 'Is a change in channel morphology required to offset the effects of changes in water and sediment discharge (ΔQ and $\Delta Q_s$)?; S = Water surface slope; $\bar{z}$ = mean bed elevation; t = time.**

## 1.2. THESIS STRUCTURE

**Chapter 2** sets the research background for this investigation, examining the existing literature on braided river research to establish the socio-economic and environmental importance of braided rivers; this is followed by a comprehensive examination of braided river morphodynamics, including details on mechanics of braiding, the different approaches to estimate sediment transport in braided rivers and the primary controls on shear stress in braided rivers. The chapter then concludes with an outline of the aims and objectives of this project. **Chapter 3** reviews the three main approaches used in the study of braided rivers; field measurement, physical and numerical modelling. Each technique is expanded upon, providing examples from the literature of its use in braided river studies and exploring the associated advantages and disadvantages of each approach. This is followed by an explanation of the methods to be employed in this project.

**Chapter 4** provides a detailed overview of the physical model to be used in the experimental section of this project. This chapter gives details of the experimental design, the scaling relations used and the five experimental scenarios used in this project.

**Chapter 5** details the quantitative analysis of the effects of aggradation and degradation on the morphology and sediment storage of the experimental channels. The changes in sediment transport, channel morphology and longitudinal profile evolution over the course of the experiments are examined and the results interpreted in terms of current understanding of braided rivers. **Chapter 6** presents the hydraulic and sediment transport characteristics of the experimental channels. The effect of flow variability on sediment transport and the variation of sediment transport along the flume are examined. A relationship is established between sediment transport, channel morphological parameters and the gamma distribution shape parameter.

The next chapter compares the experimental results with output from a two dimensional hydraulic model (**Chapter 7**) to attempt to gain a better understanding of the controls on the shear stress distribution in the experimental channels and its influence on sediment transport and channel evolution. Finally, **Chapter 8** provides a synopsis of the thesis and summarises the main findings from the research in the context of the original aims and objectives of the project, as well as offering suggestions for potential future development of the work using some preliminary data collected from field located at the highlands of Ethiopia.

# 2. BRAIDED RIVER RESEARCH: STATE OF THE ART

## 2.1. INTRODUCTION

The hydraulics of rivers and open channels have long been the focus of many engineering and geomorphological studies mainly for the purpose of designing irrigation, drainage, flood control and navigation structures etc (Chow, 1964). Sediment transport also has been of much interest, primarily because of its effect on reservoirs, river infrastructure like bridges, shoaling of navigable rivers and estuaries (Chanson, 1999;Chow, 1964). Understanding of sediment transport processes is essential for integrated river management and river engineering.

The chapter begins by highlighting the importance of studying braided rivers from social, economic and environmental viewpoint. Key topics within the study of braided rivers are introduced by means of literature review. These include mechanisms of braiding, causes and significance of aggradation and degradation in braided rivers. Different methods for estimating shear stress and sediment transport in braided rivers are discussed by highlighting the foundation papers and how these have developed and expanded to provide the contemporary issues of interest. This chapter will then conclude with an outline of the research to be undertaken in this study, stating the aims and objectives of the project.

## 2.2. IMPORTANCE OF STUDYING BRAIDED RIVERS

Braided rivers represent high-energy fluvial environments often characterized by steep valley gradients, non-cohesive banks lacking vegetation and, and consequently, high rates of bank erosion and bedload transport. They change their geometry so rapidly, thereby modifying their boundaries and floodplains, that key management questions are difficult to resolve. They are sensitive to changes in their flood regime or sediment influx and, can completely modify their geometry over a few decades (Ferguson, 1993).

Braided rivers can be agents of significant erosion and sediment transport. They are distinctive because of their high stream power and subsequent high rates of erosion, deposition and channel change compared to other channel types. The potential for high rates of sediment erosion, transport and deposition within channels, frequent channel switching and bank erosion can lead to problems for engineers when designing channel or braidplain edge structures, such as bridges and roads or other hydraulic structures (Bristow and Best, 1993).

The importance of investigating braided rivers can be identified in three areas: (1) social; (2) economic; and (3) environmental. Each of these will now be expanded on.
From a social perspective, braided river floodplains, or braidplains, and the land bordering the braidplain can provide sites for industrial, urban and agricultural development due to their flat topography and, in some cases, the fertility of their soil. Moreover, the nearby flat topography of the adjacent land makes them ideal for irrigation development. Nevertheless, unlike straight or meandering single-channel rivers, braided rivers are intrinsically dynamic and unstable. Therefore, societies exploiting braided rivers and the surround environment face associated risks of flooding. The risk of flooding at high discharges common to all rivers is heightened in braided rivers by the potential for rapid within channel aggradation. Moreover, there is also a risk of channels migrating, switching positions and producing rapid bank erosion. This can lead to areas of the braidplain that were previously out of reach of the river becoming inundated. This dynamic environment poses significant management challenges and, from an engineering point of view, the high rates of sediment transport, erosion and deposition combined with frequent channel shifting and rapid bank erosion may pose considerable design and operation problems both to within channel structures, such as bridge piers and braidplain edge constructions such as roads, highways and railways(Bristow and Best, 1993). Management strategies proposed for controlling braided rivers include protecting the floodplain by engineered structures, regulating sediment from contributing tributaries etc. Although river training structures such as revetments, bed and bank protection walls are constructed in some sections of the braided rivers, this is not successful most of the time due to the feedback mechanisms

and unpredictable nature of braided rivers. A typical example here is the case of Waiho River in New Zealand. The river presently has an active braiding form constrained laterally over the greater part of its length by manmade river protection measures (e.g., stopbanks, rock rip rap facing, and rock rip rap groynes). Those protection interventions has exacerbated the problem by promoting aggradation, generate deep scour and aggressive sediment movement. Aggradation rates are increasing and are higher in the upper reaches, diminishing as we move downstream (Hall, 2012). Figure 2-1 shows an amazing picture taken in a braided gravel bed river in northern Ethiopia. The picture was taken immediately after the flood receded. However, it can be seen from the colour of the river water that an intense rainfall has fallen upstream and there is indication that the channel started to migrate towards the true right of the river, although the major reason for the failure of the bridge pier seems to be scour and degradation at the middle of the channel. The floodplains of large braided river systems have long been a focus of human settlement, providing ideal locations for development and agriculture, important sources for food and construction materials, although statistics is not available. As people continue to live in those floodplains, flooding and channel erosion have prompted river engineering solutions to minimize these impacts, and costly maintenance program to ensure effectiveness and safety (Schumm and Winkley, 1994).

Much of the social importance of studying braided rivers has an economic dimension (costs of management and consequences of instability); however, the economic importance of studying braided rivers is also a consequence of the nature of their sediments. Braided alluvial deposits form substantial hydrocarbon reservoirs (Martin, 1993), sites for the deposition and accumulation of heavy minerals (Smith and Minter, 1980;Slingerland and Smith, 1986) and important sand and gravel reservoirs.

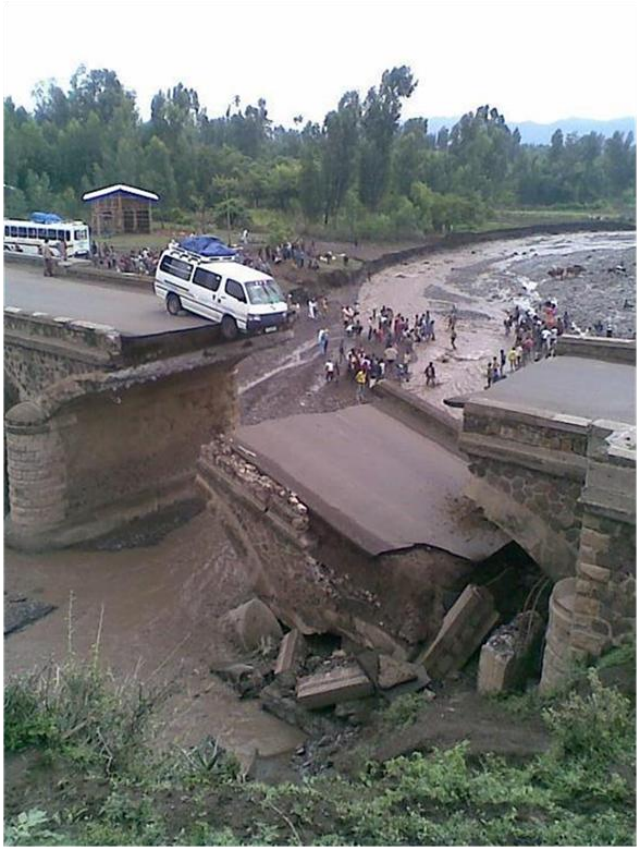

**Figure 2-1 Bridge failure due to flooding and channel switching of a gravel bed Braided river in Northern Ethiopia (image taken April 2, 2012, http://imhabesha.blogspot.com/2012/04/lucky-driver-escapes-bridge-collapse-in.html)**

An understanding of braided rivers, in terms of their depositional processes, is necessary to identify and exploit these deposits. Braided river floodplains have also been exploited for their reserves of sand and gravel aggregates (Bristow and Best, 1993). Braided rivers can also provide the source of hydroelectric power generation. For example, the Harper and Avoca Rivers, New Zealand flow into Lake Coleridge, where a hydroelectric plant is situated. In addition, braided rivers are often utilized for navigation, and can become a tourist attraction and location for riverine activities like fishing.

The environmental importance of rivers in general was summarized by Hey (1997) who stated that a river's morphology, hydraulic variability, water quality and temperature exert a control on habitat formation and its success. Braided rivers are environmentally important because they show very high overall biodiversity (Tockner and Stanford, 2002). The unique characteristics of braided rivers such as multiple channels, flow

instability, high levels of sediment supply and movement etc provide outstanding habitats for braided river birds. Moreover, they are also key areas for conservation and restoration since they provide habitat for highly endangered fauna and flora (Tockner *et al.*, 2003). Any adjustment to the river that affects flow and sediment transport conditions can alter channel characteristics which may have negative impacts upon the river's fauna and flora. Mosley and Jowett (1999) state that river management needs in New Zealand have encouraged research regarding the environmental aspects of braided rivers, including the influence of flow regime on river ecosystems. Mosley (1982) cites studies by Bovee (1978b) and Smith (1979) on "habitat suitability criteria" which indicated preference of some salmonid species for certain water depths, mean velocities, temperature and bed sediment type. Mosley (1982) observed that, for the braided Ohau River, New Zealand, as discharge increased existing channels increased in width, depth and velocity, and new channels were formed which possessed similar hydraulic characteristics to the original channels at the lower discharge. This would suggest that for fish and invertebrate species (or other in-stream uses requiring these lower depths and velocities) the surface area available in a braided river remains fairly constant over a range of discharges, compared to a single channel in which depth and velocity increase progressively with discharge. Therefore, the understanding of the braided rivers natural complexity and dynamics forms the prerequisite for developing sustainable management schemes in this regard.

## 2.3.CAUSES OF BRAIDING

The continuous change and interaction between channel geometry, water flow and sediment transport in braided rivers makes understanding the real cause of braiding a major challenge. The mechanisms of braiding, in terms of the initiation of braiding and bar development, have been investigated through the use of laboratory flume experiments (e.g., Leopold and Wolman, 1957;Ashmore, 1982)) and field studies (e.g., Ferguson and Werritty, 1983;Davoren and Mosley, 1986;Ferguson *et al.*, 1992). Many researchers gave different suggestions on why river tend to braid. Most ideas for initiation of braiding are related to either the geometry of the channel (slope, width to depth ratio) or sediment type & size (dominant bedload, non-cohesive banks etc). There has been acknowledgment of the fact that there is no single universal mode of braid

development (Ferguson, 1993) and that bars can be a product of depositional or erosional processes.

It was indicated in a more general way by Church and Gilbert (1975) that local inability of the flow to transport the imposed sediment loads as the basic cause of braiding. The most important early work in this regard include Fahnestock (1963), Leopold and Wolman (1957), Schumm and Khan (1972) which demonstrated the contribution of the above mentioned factors in river braiding; most of the time braiding occurs in steep slopes and non-cohesive bank materials with a high proportion of sediment carried as bed load. Leopold and Wolman (1957) proposed two primary controlling variables on channel pattern; discharge and slope. For a given discharge and bed material, there are threshold slopes between which channels will braid. Moreover, the critical slope decreases with increasing discharge or decreasing sediment size. Nevertheless, Tal and Paola (2007) referring to Parker (1976) commented that in laboratory experiments the tendency to braid is inevitable even if sediment and water discharge, grain size and slope are set to values that should theoretically lead to meandering. Moreover, it has been shown that braiding is basically independent of the grain size distribution as it was possible to reproduce braided pattern using uniform sediment (Métivier and Meunier, 2003), although a general conclusion may not be reached as this is a laboratory based study. That means the mechanism of river braiding is probably not controlled by the grain size distribution. However, other field based studies show that braiding occurs at lower slopes and/or discharges as grain size decreases (Ferguson and Ashworth, 1991).

Bristow and Best (1993) noted that some authors have even suggested that fluctuations in flow stage or discharge are a prerequisite for river braiding (e.g., Doeglas, 1962;Miall, 1977), although this hypothesis has been discounted in many cases by the physical modelling of braided river planforms in steady discharge flume experiments (Ashmore, 1991a;Ashmore, 1982). Ashmore (1982) reproduced the forms and processes of natural gravel braided rivers in constant discharge, constant slope flume experiments with equilibrium maintained using an adjustable sediment feed. This led him to conclude that the mechanisms of bar initiation proposed by Douglas (1962) and Miall (1977) which rely on a variable or falling discharge are not uniquely responsible for

braiding. It has also been shown that bars may disappear at high flow stage, the implication being that some braided systems act as single channels at bankfull stage and only adopt the characteristic braided pattern on the falling stage (Bluck, 1979;Carson, 1984;Smith, 1974). However, the idea that braided rivers act as single channels during high flow stages and only exhibit a braided channel form at low flow stages was not generally accepted as observations of this kind are generally rare. At high discharges (and hence high flow depths) a lot of sediment will be transported. During this time, channels within the braided system are often scoured and mid-channel bars may be entirely eroded. ‘’During lower magnitude flow events maximum sediment deposition ensues, channel beds start to aggrade and any new high-stage bed-forms may be modified. It is during these low flow stages that new bars may be formed or existing bars may be enlarged as sediment is deposited; and as the flow stage falls further, some mid-channel bars may become emergent and be dissected by low stage channels, forming another braid level within the system’’ (Bristow and Best, 1993).

The pioneering work by Ashmore (1991a) explained the mechanism of braiding in much more detail from an initial straight channel. According to him braiding basically occurs by four different processes: deposition and accumulation of a central bar, chute cut-off of point bars, conversion of single transverse unit bars to mid-channel braid bars and dissection of multiple bars, the predominant mechanism being dependent up on the availability of excess bed shear stress and bed-form regime. Chute cut-off was the most common in Ashmore’s experiments. Regardless of the exact braiding process, local short-term pulses in bedload supply are also identified as initiating and maintaining braiding. Ashmore (1991a) identified two types of central channel deposition (mid channel bars and chutes & lobes) and two erosional processes (chute cut-off and lobe dissection). Mid-channel bars are elongated, often almost symmetrical deposits without a distal avalanche face that develop in the centre of a channel expansion (Ferguson, 1993). Chute cut-offs involve the headward incision of flow across bars. This is illustrated in Figure 2-2.

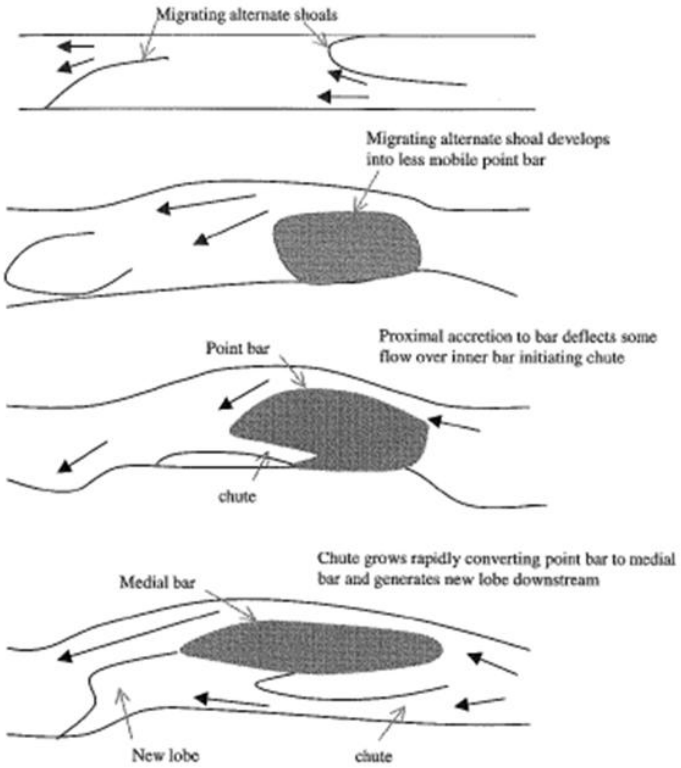


**Figure 2-2 Braid development by chute cut-off. Flow over top of bar incises into it causing partial within channel avulsion. Taken from Ferguson's (1993) summary of Ashmore's (1991) flume experiments.**

Multiple dissection of lobes is a two stage process according to Rundle (1985a). A lobe is deposited at a flow expansion during periods of high discharge. As water level falls flow is concentrated in channels on the lobe surface. These channels dissect the bar by headward erosion. This mechanism is reported to have occurred in flumes that were very wide, shallow and steep, and where multiple bars develop into fewer, larger bars that concentrate the flow into scour pools resulting in dissection (Figure 2-4). Multiple dissection of lobes has been considered to be the characteristic mechanism of braiding in New Zealand rivers (Rundle, 1985b) although, Ashmore (1991a) reports them as being uncommon in his flume experiments, possibly as a result of inadequate flume width. Carson and Griffiths (1987) suggested that bars are a consequence, and not a cause of braiding.

The above discussion associates braiding mostly with a combination of externally imposed environmental factors like discharge and sediment supply. There is a second class of hypothesis that associates braiding with the inherent instability of flow and sediment transport using theoretical stability analysis of channel scale bed forms

(primarily bars) in two dimensional flow regimes (Parker, 1976;Hayashi and Ozaki, 1980).

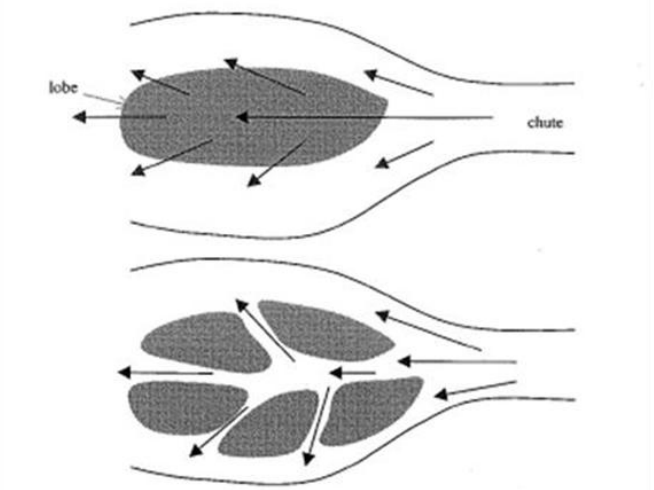


**Figure 2-3 Illustration of sedimentary mechanics for braid bar initiation (Knighton, 1998).**

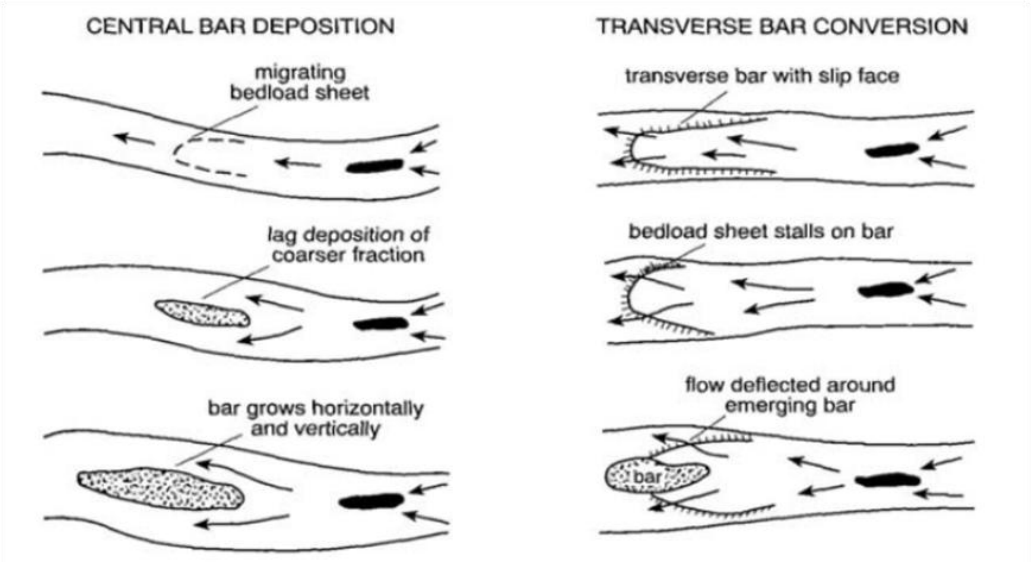


**Figure 2-4 Braid development by multiple lobe dissection. Diverging flow over lobe below chutedissects lobe margin at one or more points. Taken from Ferguson's (1993) summary of Rundle's (1985) study.**

Theoretical stability analyses use equation of motion and define thresholds for meandering and braiding. According to this, the primary factor causing instability is the phase difference between the shear stress gradient (a function of fluctuating water elevations) and bed form gradient (elevations of the channel bed) (Hayashi and Ozaki, 1980). Engelund and Skovgaard (1973), based on the method of stability analysis, found that the primary control on braiding is a width to depth ratio more than 50. This was

further reconfirmed by Fredsøe (1978) and Fukuoka (1989), although Fukuoka found that slope is also a critical parameter. Parker (1976) derived a theoretical relationship for a system's stable number of braids using stability analysis. Parker's analysis indicates that rivers have the tendency to form bars and braids even when they are in equilibrium. However, this contradicts the traditional hypothesis that braiding is caused by sediment load in excess of the transport capacity that results in bar deposition and general channel aggradation. The laboratory experiment of Ashmore (1991a) also confirms that braiding can be formed in equilibrium conditions.

The initiation of braiding has been linked to a number of factors, some of which were mentioned in the previous sections. The most important of these can be grouped into three. First is an explanation relating braiding to external and environmental factors such as discharge and sediment supply. The second associates braiding to theoretical stability analysis of channel bars in two dimensional flow regimes. The third one focuses on physical processes such as sedimentary and hydraulic conditions that begin the braiding process (Ashmore, 1991a). Braiding can also develop in more than one way. However, there is a need to identify the range of hydraulic and other conditions in which different braiding mechanisms occur (Ferguson, 1993).

## 2.4.AGGRADATION AND DEGRADATION IN BRAIDED RIVERS

The bottom of river channels may aggrade or degrade if the balance between water discharge, sediment flow and the channel shape is disturbed. It has been suggested that if a river channel is in equilibrium then the rate of sediment supply will be equal to the total sediment transport rate, and if the sediment supply to a reach is altered this will induce a change in channel form (e.g., Gilbert, 1917;Griffiths, 1979;Hoey and Sutherland, 1991;Germanoski and Schumm, 1993). Such a disturbance may be due to anthropogenic or man-made factors, such as construction of a dam, land use changes resulting in change in the sediment supply rate, lowering of the channel bottom etc. The main modifier of river flow induced by humans involves dam construction. As the effects are coupled, it is not easy to foresee the effects of river engineering projects like dams. But generally a dam holds back sediments, especially the heavy cobble and gravel. The river, deprived of its sediment load, tends to recapture it by eroding the

downstream channel and banks, undermining bridges and other river bank structures. Riverbeds are typically eroded by several meters within a decade of first closing a dam (Church, 1995;McCartney *et al.*, 2000). The damage can extend for tens or even hundreds of kilometres below the dam.

Typical responses include the reduction in channel bed slope downstream of the dam and degradation of the river channel. One result of degradation is a coarsening in the texture of the material left in the stream bed (i.e. an armoured bed). Many other studies report channel incision and bed surface coarsening immediately downstream of dams in response to sediment impoundment (Williams and Wolman, 1984;Gilbert, 1917). In many instances, a change from sand to gravel is observed and, in some, scour can proceed to bedrock (McCartney *et al.*, 2000). These tendencies can influence downstream infrastructure such as bridges, leaving diversion intakes at the wrong elevations etc. As an example, the reduction in channel bed elevation and water level on the lower River Nile due to the high Aswan Dam caused the abandonment of the barrage and associated navigation lock at a place called Esna, 167 km downstream of the dam (Gasser, 1996). On most rivers, however, these effects are constrained to the first few kilometers or tens of kilometers below the dam. Degradation of up to 7.5 m has been observed in large rivers and 1-3 m of degradation occurred within a decade or two of regulation in the Colorado River below the Hoover dam (Church, 1995). Degradation in the order of 2.5 m has been observed downstream of the High Aswan Dam (McCartney *et al.*, 2000). Further downstream, increased sedimentation (aggradation) may occur because the regulated flows may not be able to move sediments entrained from tributaries so quickly through the channel system. Channel widening and multiplication is a frequent follower of aggradation. River channel planform may eventually be changed from braided to single thread and from less towards more sinuous as a consequence of the reduction in sediment transport (Consultants, 1983). After the construction of the High Aswan Dam, the Nile has been transformed towards being a more stable, single channel (El-Belasy A.M, 1996).

Effects of variation in sediment supply have also been investigated through laboratory experiments. An increase in sediment supply resulting in aggradation has been found to

encourage braiding, whilst a decrease in sediment supply produces degradation and results in a decrease in braiding (e.g., Ashmore, 1988;Hoey and Sutherland, 1991;Germanoski and Schumm, 1993;Smith and Smith, 1984). In their flume experiments, Germanoski and Schumm (1993) enforced aggradation and degradation by increasing and decreasing sediment supply. They observed that aggradation occurred over the entire channel length, but was locally variable according to channel geometry and morphology, and aggradation amounts were greatest at the upstream end of the flume. Aggradation resulted in an increase in the braiding index, an increase in number of bars and a general overall increase in channel pattern complexity. In addition, an increase in overall channel width due to flow being directed into banks, resulting in lateral erosion, was observed as a consequence of bar development. Degradation, induced by reduction in sediment supply, resulted in incision of the channels, with the greatest incision occurring upstream. They observed that in some degrading channels, sediment discharge also increased, so they proposed that actual sediment transport rates are related to transport capacity of the channels than sediment supply. Degradation resulted in a decrease in braiding index and number of bars. Despite this progress, there is no clear information whether the process of stream braiding results in an increase in bedload transport, thus enabling the increased load to be conveyed, or it is fully a consequence of sediment supply.

Nowadays there is an increased pressure on rivers for a variety of in-stream and external uses of water that may ultimately distort their nature and form. This increased pressure on rivers requires an ability to quantitatively describe how a river's form changes with discharge and sediment supply variations. Research has shown that these changes will eventually distort the natural equilibrium of the river, and through time the river will adjust to the new conditions by changing one of its parameters: longitudinal slope, roughness, bed material grain size, cross sectional geometry of the channel or ultimately its pattern. Such knowledge is important since channel change can affect in-channel and off-channel resources (Madej *et al.*, 2009). Moreover, it is very important for river engineering purposes to manage hydraulic structures and prevent disasters from flooding, and for environmental engineering purposes, to maintain river ecosystems and landscapes (Gilvear, 1993;Marston *et al.*, 1995). From a practical point of view,

predicting the changes in the river channel using traditional hydraulic geometry relations will be problematic because these are generally based on the assumption of river equilibrium (Mosley, 1982). For example, in their flume experiments, Hoey and Sutherland (1991) observed that when using equilibrium formulae (e.g. Bagnold's (1980) bedload equation), sediment transport rates were over predicted for aggrading channels and those in equilibrium, and under predicted in degrading channels. Channel non-equilibrium has been suggested as the main cause of this variation between predicted and measured transport rates.

## 2.5.ESTIMATING SEDIMENT TRANSPORT IN BRAIDED RIVERS

There are different reasons why understanding of sediment transport processes is indispensable from an engineering perspective. Boundary conditions like water discharge, maximum and minimum water level, velocities and lowest river bed level that may occur in the river and any future changes in the morphological characteristic of the river are basic inputs for the design of any hydraulic structure. It is likely that those parameters and possible changes are affected by interaction between flow and sediment transport.

The need for an efficient means of estimating sediment transport extends to applied problems. Reservoir sedimentation is a serious problem. Often reservoir sedimentation happens due to the fact that either the upstream sediment supply was never considered or the seriousness of the process was underestimated because of insufficient data or changes in sediment yield, for instance due to changes in land use in the upstream catchment. To remedy the loss in storage capacity, changes in the operation of the reservoir are often required, sometimes with drastic and costly consequences e.g. the reduction of power production. Sediment entering through the headwork is often deposited in irrigation canals. This may be due to the fact that sediment transport in the river was not properly assessed and appears to be much larger than anticipated. Another possible reason is that there are always feedbacks between water flow, sediment transport and the structure in place which jeopardize the measures taken to exclude sediment when withdrawing water. All kinds of remedial measures like regular cleaning of canals or rehabilitation of the intake are very costly. Broader questions of watershed

management, such as the downstream effects of changes in land use or flow regime, also would benefit from an efficient sediment transport methodology, which would allow tracking of sediment flux through a channel system (Wilcock, 2001).

Modelling of rivers and open channels require information on the hydraulic geometry and flow conditions in the water course as well as roughness, discharge and sediment characteristics. One of the major problems of river modelling is the estimation of sediment load using one of the traditional transport predictors. However, it is becoming increasingly clear that sediment transport formulae based on idealized hydraulic principles fail to predict transport accurately. This is especially the case where there is huge spatial and temporal variability of river morphology like that in braided rivers making it difficult to set representative hydraulic parameters (see Figure 2-5 for typical lateral variation of hydraulic parameters in the wandering gravel bed Fraser River, Canada). Estimation of sediment transport in multi-thread channel systems has been a long standing problem for many reasons. The main reasons include: (Ashmore, 1988;Gomez and Church, 1989;Young and Davies, 1991;Hoey and Sutherland, 1991):

1) The complexity and instability in Braided River morphology

It is very difficult to describe the shape, direction, number and size of channels (Pickup and Higgins, 1979) and all hydraulic parameters change very rapidly. Individual channels can also migrate quite often with competent flow (Ferguson, 1993).

2) The hazards and difficulty involved in making a direct measurement of bedload flux

Numerous attempts have been made to measure bedload transport directly using a variety of sampling devices and traps. This approach requires an extensive field effort because the spatial and temporal variability associated with sediment movement makes observation and collection of transported sediment exceedingly difficult (Gomez, 1991). Sampling difficulties are amplified by the fact that most sediment transport in braided rivers occurs during high flow events when direct observation and measurement is difficult. Concerns over the accuracy of sampling devices themselves raise an additional problem that requires sampler calibration and adjustment for trapping inefficiencies

(Hubbell, 1987;McLean *et al.*, 1999). Overall, problems related to sediment measurement in braided rivers can be summarized by the following points:

- Particularly at high flows, high velocities and coarse sediment load makes sampling hazardous (Pickup and Higgins, 1979).
- Changes in morphology take place very quickly and often at rates which makes useful measurements impossible to obtain.
- Most importantly sampling is almost impossible because of the number and frequency of samples needed to represent the lateral and temporal variation (Bertoldi *et al.*, 2009).

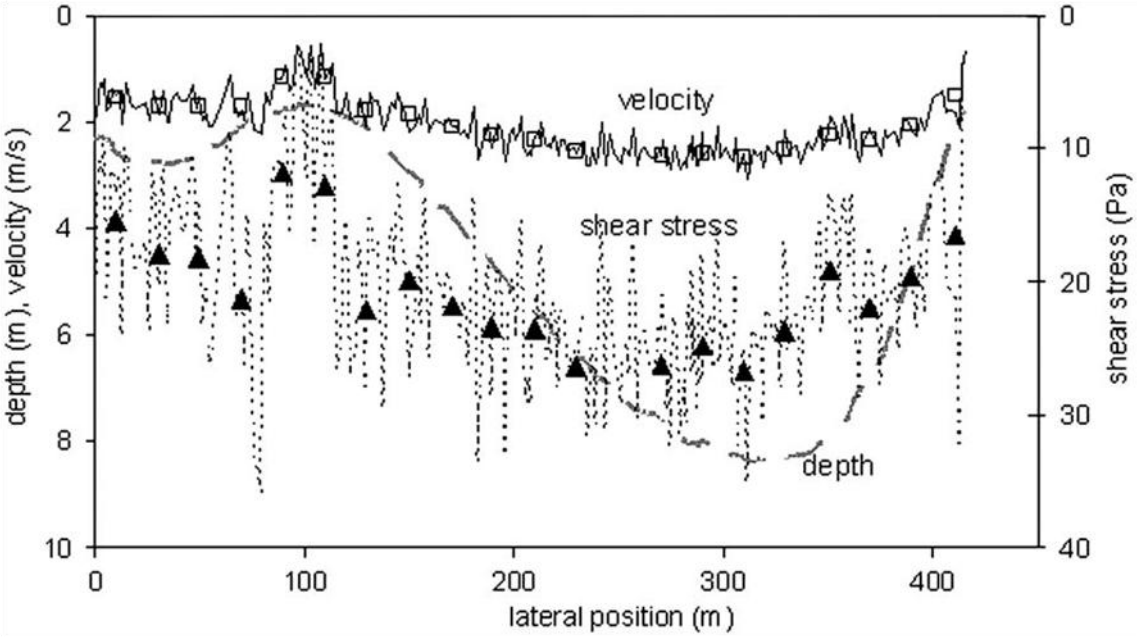


**Figure 2-5 Section across lower Fraser River, western Canada, Showing lateral variability in hydraulic properties as show by moving boat ADCP measurements at a mean spacing of about 1m. Dashed grey line shows local depth. Solid line shows local vertically average velocity with open symbols for average over successive 20m bins. Dotted lines show local shear stress estimated from local mean velocity with solid symbols (Taken from Ferguson, 2007)**

For these reasons braided rivers cannot routinely be treated in the same way as single-channel rivers when applying sediment transport predictions. Since channel form is a direct result of bed load transport, a first requirement is the ability to predict the rate of bed load transport for a given discharge so as to predict changes in channel morphology reasonably well. Several methods have been proposed and used in the past to make a reasonable prediction of bedload flux in braided rivers. The methods are explained in the following sub-sections.

### 2.5.1. Conventional Bedload Functions (equations)

Researchers have developed a wide range of different equations for bed load transport prediction. Gomez and Church (1989) after analysing four sets of river data and three sets of flume data, grouped those empirical bed load transport laws into four categories as discharge, tractive force, stochastic and stream power (Table 2-1 and Figure 2-6). Because the effectiveness of discharge in moving sediment varies with channel geometry, planform and roughness, a suitably scaled flow variable (typically bed shear stress or stream power) is required for transport calculations (Wilcock, 2001). Consequently, the majority of bed load formulae represent a functional relation between bed load discharge and shear stress. Moreover, most of the equations require information related to grain size of the river bed and the channel geometry of the reach. Most formulae predict the sediment transport capacity, which is the maximum bed material discharge under equilibrium conditions for particular hydraulic and sediment characteristics. Equilibrium corresponds to steady, uniform flow conditions, where the respective bed material discharge entering and leaving a particular reach are the same and where bed conditions remain unchanged. It should be noted that the wash load does not form part of the sediment transport capacity of a stream.

**Table 2-1 Ten contemporary sediment transport equations from Gomez and Church (1989)**

| Formula | Type |
|---|---|
| **Meyer Peter (1934)** | Discharge |
| **Schoklitsch (1934)** | Discharge |
| **Schoklitsch (1943)** | Discharge |
| **Meyer-Peter and Muller (1948)** | Tractive force |
| **Einstein (1950)** | Tractive force |
| **Du Boys-Straub (1935)** | Tractive force |
| **Parker (1982)** | Stochastic |
| **Yalin (1963)** | Tractive force |
| **Ackers and White (1973)** | Tractive force |
| **Bagnold (1980)** | Stream power |

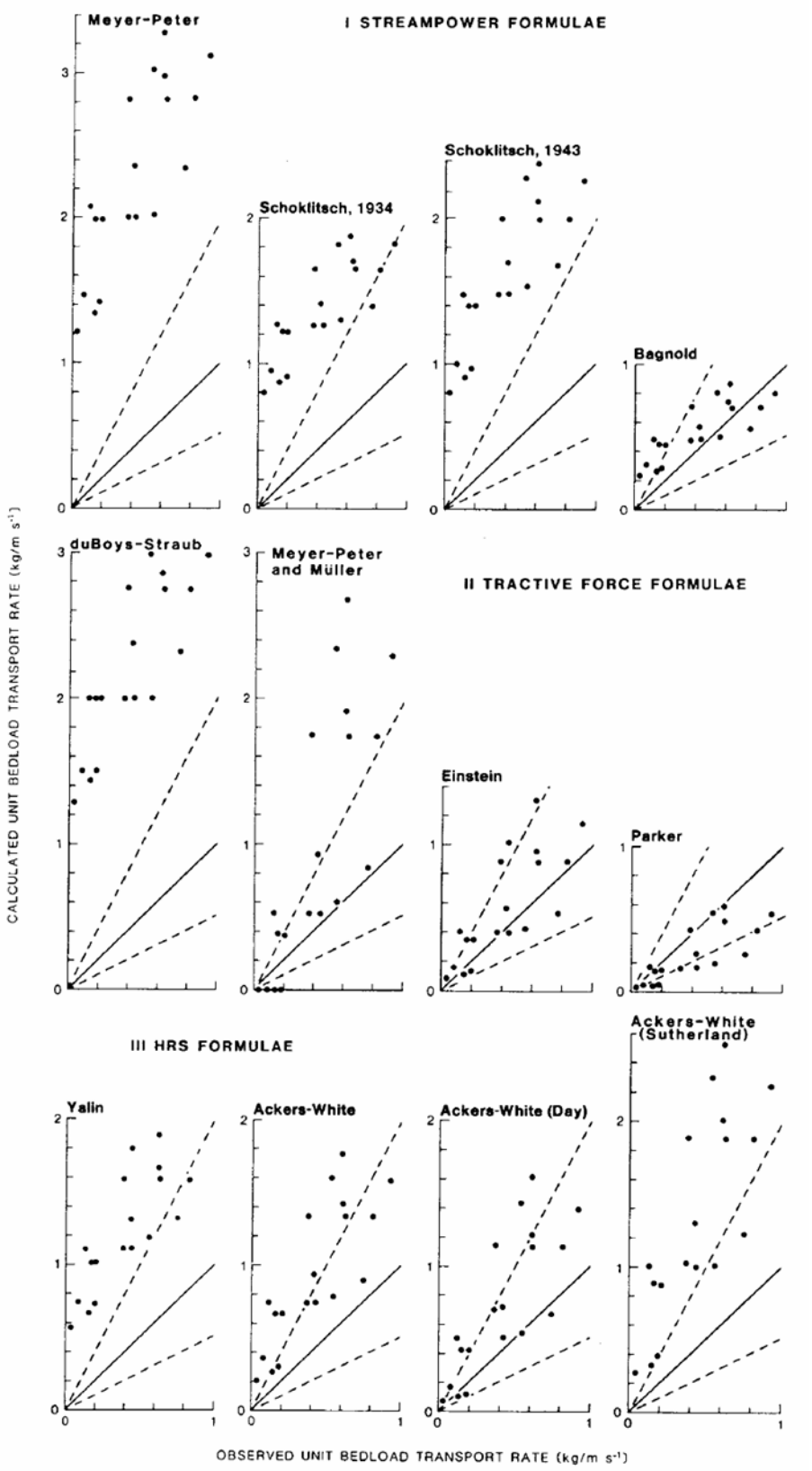


**Figure 2-6 Performance of observed versus predicted sediment discharge rates for Elbow River, From Gomez and Church (1989).**

The Du Boys-Straub formula is mainly based on data from small flume experiments. The Schoklitsch (1934) based mainly on data from experiments by Gilbert (1914), with well sorted sediments, and also on data of graded sediments with median size of 0.3 mm-5 mm. Although the Einstein formula is also based on flume data with well sorted sediments having median size in the range of 0.3 mm to 7 mm (river sediments), it has also another set of data with 28.6 mm gravel and 5.21 mm mix of gravel barite and coal for other sets of data (ASCE, 1975). The Yalin (1963) formula is based on a theoretical assumption that bedload discharge rate is a function of the range of particles in saltation rather than their number (Alonso et al, 1981). Gomez and Church (1989) described a comprehensive assessment of bedload transport formulae. They evaluated twelve formulae using seven datasets. They conclude that in general situations Bagnold's formula is best, but where detailed local hydraulic information is available, the Einstein and Parker methods might also be appropriate. A similar assessment was undertaken by Bathurst *et al.* (1987) on six sediment transport equations in the context of steep mountain rivers. They concluded that most tractive force type equations breakdown with slopes greater than 0.1 and with relative submergence ($Y/d_{50}$) less than 10. They pointed out that the Schoklitsch equation performs better, although the equation does not represent wide ranges of grain sizes.

An important advantage unique to the bedload transport equations is the ability to predict transport under conditions other than the present, making possible predictions of channel change (Wilcock, 2001). However, it is usually difficult to apply those equations directly as those formulae were either developed from a theoretical background (e.g., Einstein, 1950;Yalin, 1963) or direct field observation (e.g., Schoklitsch, 1934) and compared directly to the Author's own data only. Consequently, the formulae provide reasonable results when compared to the source dataset but limited improvement over theoretical relationships when used with other data. For example, Ashmore (1988) using bed load data from his flume studies on braided rivers, tried to reproduce the experimental result with the Meyer-Peter and Muller formula. However, to obtain an agreement between observed and calculated values, he required a modification of the original Meyer-Peter and Muller equation. This demonstrated that a direct application of bed load transport equations, without any possibility of calibration, will usually fail.

Another important source of uncertainty and error in the empirical equations arises from the propagation of error in the measured variable used to calculate transport (Wilcock, 2001). An investigation by McLean (1985) to estimate the uncertainty in transport rates calculated for the Fraser River in British Colombia, Canada shows that the uncertainty, expressed as $\Delta q_b / q_b$ varied between +/-0.4 to +/-3.6 for five different transport formulae; where $q_b$ is the transport rate and $\Delta q_b$ is the error in transport rate.
Empirical bed load functions have been developed for predicting mean bed load from river discharge or stream power (Ashmore, 1988;Young and Davies, 1991;Davies, 1987;Shvidchenko and Kopaliani, 1998). Total transport over time has a well defined relationship with total discharge. However, because there are very few field and experimental cases, it is not clear what the appropriate coefficients are, why they vary and if they are generally applicable. Unit transport rates can be predicted from standard bed load transport functions (Carson and Griffiths, 1987;Ashmore, 1988;Carson and Griffiths, 1989); but the uncertainties related to the choice of formula and entrainment threshold are amplified by the lateral variation in morphology, grain size and hydraulics and the tendency for transport to be focussed in only a few zones or channels (Carson and Griffiths, 1987).

A range of decisions is necessary when developing an estimate of sediment transport based on one of the empirical bedload equations. This starts from the choice of a range of predictive formulae. We need to decide on the range of grain-sizes in transport, which sometimes can be represented using one, two, or many size fractions. There is a question of time and space scales to be used when developing an estimate of sediment transport. Is the total sediment load needed or the transport rate of individual size fractions? Is the annual flux through a section needed or local estimates over short time periods?

Attempts to relate sediment transport and morphologic development to hydraulic variables in rivers have been largely unsuccessful due to non-uniformity and unsteadiness of flow (Ferguson and Ashworth, 1992;Gomez, 1991). Ashmore and Church (1998) point out that those functional relations are statements of equilibrium

conditions which are rare in nature. Consequently, predictions may be under-estimated when input parameters and channel dimensions are averaged over larger temporal and spatial scales. In particular, most bedload equations fail to adequately perform on systems for which they were not developed, having been calibrated for a particular grain-size distribution and set of flow parameters that may simply not translate to other systems. Furthermore, as a consequence of the difficulty and expense in measuring bedload accurately, there is a shortage of datasets although, there are many transport equations. Consequently, there is no universally accepted sediment transport equation. Nevertheless, their use remains significant in numerical modelling studies where a sediment transport function is specified, although uncertainty in the reliability of such functions may require an independent means of calibration if the models are to be used in predicting bed level changes (Della Morte, 2004).

### 2.5.2. Morphological Approach

The development of morphological approach dates back to Popov (1962a) and Popov (1962b) where he outlined sediment balance of river reaches and its use to characterize channel processes (Della Morte, 2004). Neill (1971); Neill (1987) then demonstrated the possibility to estimate sediment transfer on meandering rivers by measuring average bank transfer rates from maps and aerial photos. The method of Neill, however, requires data for the volume of sediment mobilized per unit length of channel and the average travel distance. The latter was defined as the distance that eroded bed material is transported downstream during a time interval (Lane and Richards, 1997), this he assumed to be one-half the meander wave length for regularly meandering rivers. A typical advantage of this method is that it does not require knowledge of boundary transport condition but, it would underestimate actual transport volume when the travel distance assumed was too short and will overestimate if materials move only locally (Ashmore and Church, 1998). A more general outline of the method was proposed by Church et al (1986) where estimation of sediment transport everywhere along the reach can be made by knowledge of changes in sediment storage in a reach and an estimate of local transport at one section. The method was also used in rivers of complex morphologies (Church *et al.*, 1987). This approach to some extent avoided the need for 'the travel distance concept' proposed earlier by Neill (1971). It

works with repeat topographic surveys or aerial photo analysis of the channel bed, bars and islands to quantify volumetric changes of bed and bank sediment. Previous studies used comparison of digital elevation models produced from topographic surveys to detect bed level changes associated with sediment erosion, transport and deposition. In this method a sediment budget technique will be followed to relate changes in channel morphology and sediment transport. The basic equation for this approach can be expressed as:

$$\mathbf{V_o = V_i - (1 - p)\Delta V - V_d} \qquad \textbf{2-1}$$

Where Vo is the volumetric sediment output;

$V_i$ is volumetric sediment input to the reach during some specified time period;

$V_d$ accounts for any kind of sediment removed from the system, for instance, by dredging;

p is the term that accounts for the porosity;

ΔV is the storage within the channel system measured as the net difference between scour and fill along the channel bed.

This equation will further be reduced to a mean transport rate by dividing all the terms by the time between successive survey intervals (Martin and Church, 1995),

$$\boldsymbol{Q_0 = Q_i - (1 - p)\Delta V/\Delta t} \qquad \textbf{2-2}$$

Where $Q_i$ is the volumetric transport into a reach per unit time ($\Delta t$), p is porosity of the sediment pile and $Q_o$ is the volumetric transport out of a reach per unit time and $\Delta t$ is the time between surveys. The morphological method for calculating sediment transport relies on the assumption that there is no sediment throughput. That is, all transported sediment is involved in local deposition and erosion and not simply transported through the reach without contributing to the changing channel morphology. It has been argued that this assumption often may not be met and that this method can only yield a minimum sediment transport rate. Thus, transport rates estimated in this way have to be treated with caution (Ham and Church, 2000).

The morphology based approach is very important in that it will produce outputs useful for long term monitoring as well as quantification of historical channel change and linking those changes with controls on channel morphology. McLean (1990), Ham and

Church (2000) provide examples for bank erosion, channel widening and changes in channel morphology utilizing planimetry-based studies. Other researchers have demonstrated the magnitude and dynamics of channel scour and fill along surveyed cross-sections (Ferguson and Ashworth, 1992;Goff and Ashmore, 1994;Hickin, 1995;Paige and Hickin, 2000). Three-dimensional surfaces of difference have been generated to illustrate complex patterns of sediment erosion and deposition distributed along entire channel reaches (McLean, 1990;Eaton and Lapointe, 2001;Lane *et al.*, 2003). As is the case with the other transport prediction methods, the morphological approach is not free from limitations. The first and foremost is the requirement for high quality and long-term datasets. Such high resolution topographic datasets are available for only a few rivers around the world. Other problems are related to the data itself and the method. This includes the reliability and accuracy of historic channel and floodplain topographic surveys and the accuracy with which these data can be converted to interpolated surfaces to reflect the actual topographic variability as data can be compiled from different source. There are also concerns relating to the spatial and temporal resolution of the surveys that can limit applicability, although recent advances in data acquisition techniques have begun to address these. Although there is no previous application of this method in laboratory flumes, it appears that most of the concerns regarding data collection and quality will be reduced as compared to field conditions.

While there are concerns regarding the accuracy and reliability of data sources and the developments in the morphological method remain incomplete, it appears clear that observations of morphodynamic changes may usefully provide a means to better understand form and process relations in alluvial rivers. As such, the morphological approach provides a valuable tool for estimating sediment transport and to predict channel responses to disturbances.

### 2.5.3. Stochastic Approaches to Bedload Prediction

The use of standard bedload functions to estimate bedload flux has come under increasing scrutiny especially in multi-thread channel systems due to the lateral variation in morphology, grain size and hydraulics (Carson and Griffiths, 1987;Paola, 1996;Ferguson, 2003;Nicholas, 2000) and the tendency of transport to be focussed in

only a few active zones of channels (Carson and Griffiths, 1987;Thompson, 1985). Moreover, in braided rivers different sets of channel conditions are possible at any one discharge value (Pickup and Higgins 1979). Due to this, the hydraulic parameters to be used in the standard sediment transport equations must fully represent the range of conditions which occur in the river and they must be representative of the various channel conditions. Two possible approached to obtaining representative hydraulic parameters to be used in sediment transport estimation of Braided Rivers are mentioned in literature (Pickup and Higgins, 1979); these are based on averaging and frequency distributions.

The first approach involves measurement of individual channels in the cross section; and then deriving weighted average parameters based on the proportion of the discharge carried by each channel. There are some drawbacks to this method. Firstly, taking measurements of individual channels in a braided network is very difficult and almost impossible. Channel parameters like number of channels, direction, shape and size vary over short distances as flow paths join and divide (Pickup and Higgins, 1979;Ferguson and Ashworth, 1992). Secondly, this averaging option, although it gives a better prediction of bedload transport than in the equivalent rectangular cross section with a uniform depth, it doesn't produce the same sediment transport rate as that obtained when each channel is treated separately. Moreover, lumping individual channel parameters to derive a composite value is difficult.

The second approach has focussed on the application of frequency distributions of hydraulic parameters (either flow depth or shear stress). In this approach, it will be assumed that a certain frequency distribution fits the data (flow depth or shear stress) and if it is possible to derive the distribution parameters, then it will be possible to generate sets of hydraulic conditions similar to those occurring in the river (Pickup and Higgins, 1979). Based on this approach, Pickup and Higgins (1979) used frequency distributions of number of channels and their dimension from which bedload is calculated as the sum of transport in individual channels in a cross section. They used a random number technique to generate data related to channel number, discharge, width to depth ratio, slope and resistance to flow and they used these data in association with a

sediment transport equation of the Meyer-Peter-Muller to estimate the bedload discharge. They got a satisfactory result with an absolute mean error of 16.3% for the river data they considered. Later a similar approach was used by Hoey *et al.*(2001) estimating the PDF for transport rate in an individual anabranch and applying this to a stochastic model of anabranch numbers and widths. The result was a PDF of bed load flux for the river which could be compared with the measured PDF of bed load flux (from flume experiments) in order to model temporal variability. Paola (1996) used a method in which gamma frequency distributions of shear stress or depth in a reach are estimated, irrespective of location or dimension of a particular anabranch. Although Paola's approach yields promising results when compared with both field and flume data for laterally unconstrained channels at a single discharge, it has a number of limitations when discharge varies or channel width is imposed. Paola determined the mean boundary shear stress using the theory of Parker (1978), which can be used to relate the mean boundary shear stress to the critical shear stress and is independent of discharge. However, determination of mean annual bedload yield involves integration of sediment transport rates over a range of discharges (Nicholas, 2000). Further to this Nicholas (2000) argues that the theory of Parker (1978) is applicable only to straight gravel bed rivers and not braided channels. Although Carson and Griffiths (1989) have shown that bank erosion within anabranches represents a fundamental mechanism of bedload transport in braided rivers, the theory of Parker (1978) represents a stability condition under which bank erosion will not occur. Based on this, Nicholas (2000) extended and modified Paola's (1996) work to include a range of discharges for a given river reach. Nicholas (2000) defined the boundary shear stress distribution using an alternative approach that involves a relationship between flow discharge, channel geometry and the degree of variability exhibited by flow depths at a channel cross section. He has shown that the model generates improved estimates of bedload yield, when compared with conventional approaches that underestimate bedload transport rates (Carson and Griffiths, 1987). Later Ferguson (2003) adapted this approach and developed a general analytical and theoretical insight into the effect of incorporating lateral variability in hydraulic parameters into bedload calculations. He used a uniform probability density function and analyses the effects on bedload transport capacity of spatial variations in shear stress and critical shear stress, separately and in combination.

He developed a statistical model to represent variability in shear stress, with allowances for differences between sand and gravel-bed rivers and for below bakfull flow. Results show that bedload flux increases greatly with the variance of shear stress, especially in gravel-bed rivers. However, variability in critical shear stress may increase, reduce or make little difference to bedload flux depending on the correlation between shear stress and critical shear stress. Furthermore, the study highlighted the severe underestimation of bedload flux due to simple width averaging.

Previous investigators using the stochastic approach for bedload prediction have stated that the approach has improved bedload yield predictions when compared to conventional approaches (Nicholas, 2000;Pickup and Higgins, 1979). In particular, the stochastic approach gives a better estimate for braided rivers where there is a huge lateral variability in hydraulic parameters. However, stochastic approaches to bed load prediction initially require a large number of measurements of channel morphology in order to derive the input parameters of the distribution at a range of discharges. Detailed sets of channel morphological data are either unavailable or very costly to collect. At present it is not clear whether these parameters and distributions are generally applicable, what easily-measured morphological variables they may correlate with, how and why the shape of the distributions may vary, or how these distributions may be affected by channel aggradation and degradation. So there is a need to have an understanding of the distribution parameters and rises a question of whether there is a more direct way of calculating the distribution parameters without the need to measure or estimate the full PDF of the relevant hydraulic parameter.

## 2.6.ESTIMATION OF SHEAR STRESS

Shear stress is an important parameter in hydraulics and river engineering which provides an index of fluid force per unit area on the stream bed and is related to sediment transport and deposition in many theoretical and empirical treatments of sediment transport. The rate of sediment transport in a channel depends on the shear stress $\tau$. But for typical range of flows in most rivers the shear stress $\tau$ rarely exceeds the critical value $\tau_c$ for initiation of sediment transport and for flows for which shear stress exceeds $\tau_c$ most transport models shows that the relationship between $\tau$ and transport is

strongly non-linear. This might be due to the nature of the transport models as most models predict the sediment transport capacity of the rivers, which is the maximum bed material discharge under equilibrium condition. Moreover, in most transport models the relationship between sediment transport and flow variable (e.g., shear stress) is greater than one. Due to this non-linearity, a small error in $\tau$ can lead to very large errors in estimated transport rate. Moreover, it is only the portion of the total shear stress called the grain stress which acts on the movable grains to produce transport. Estimation of this portion of the stress is possible but approximate. A further thing which makes sediment transport prediction complicated is the spatial variability in shear stress. Shear stress tends to vary across and along the channel. Although the total shear stress on a cross section can be determined, prediction of transport based on this average value is inaccurate as shear stress tends to vary laterally even in straight reaches with relatively simple cross sections (Carson and Griffiths, 1987;Paola, 1996;Nicholas, 2000;Ferguson, 2003;Wilcock, 1996). The rate of transport in areas of shear stress greater than the mean will be much larger than the rate of transport in areas where shear stress is smaller than the mean (Ferguson, 2003). Paola *et al.* (1999) estimated that this lateral variation in topography can increase transport rates through a section by as much as a factor of three. To understand this we can take a simpler case where the mean shear stress $\tau$ is less than the critical shear stress $\tau_c$. In the case of conventional sediment transport equations utilizing the mean shear stress this would mean no transport in the section. But in actual situations there are still locations where the shear stress $\tau$ is greater than the critical $\tau_c$ and hence sediment transport takes place. There are ways to estimate local shear stress to account for this spatial variation in sediment transport, but these require local measurements, or extensive and costly detailed information about the channel topography and bed material (Wilcock, 2001).Several methods are available to predict the boundary shear stress which can be broadly categorized into reach averaged relations, theoretical methods and direct measurement of turbulence.

The most familiar method to estimate reach-averaged bed shear stress is using the cross sectioned hydraulic parameters of depth and slope (regardless of whether the flow is laminar or turbulent and the primary assumption being that the flow is steady and uniform):

$$\tau_o = \rho g R S_o \qquad 2\text{-}3$$

Where R is the hydraulic radius which is essentially equal to the depth of flow for wide rivers and $S_o$ is the friction slope. This method is relatively easy and serves as an index of the total resistance by all frictional influences on the flow as grain, bed form, bar, bank, and planform resistance. However, in many studies this method is considered to be inappropriate for estimation of local bed shear stress (e.g., Biron *et al.*, 2004) and unable to provide information on spatial variation in resistance at sub-reach scale. Furthermore, it is not always clear under what conditions it applies; however, Paola (2000) states two basic conditions that must be satisfied for a reasonable application of the above equation:

$$U/gS_oT \ll 1 \qquad 2\text{-}4$$

$$H/S_oL \ll 1 \qquad 2\text{-}5$$

Where U is the average flow velocity, $S_o$ is longitudinal bed slope and H is average flow depth. In the second condition, $H/S_o$ is usually termed as an estimate of the 'backwater length' L upstream of a point to which backwater effects are felt. This means the normal flow approximation generally is valid when the reach length of interest is long compared to the backwater length $H/S_o$. Having said this, for a given shear stress if flow depth is large and longitudinal slope is small, the back water length is larger and vice versa. Consequently the depth-slope product as an estimate of bed shear stress works best for mountainous, shallow and high-slope streams (Paola, 2000).

Alternative approaches to estimate local and small scale variation in shear stress include the logarithmic relation and the quadratic stress law. The logarithmic relation is the most widely used (Lawless and Robert, 2001;Wilcock, 1996) and models local bed shear stress by relating shear velocity and average velocity with height (Schlichting and Gersten, 2000). It is based on the assumption that the velocity profile in the lower portion (15-20%) of an open channel flow has a logarithmic structure.

$$U/U_* = 1/\kappa \ln\left[Z/Z_o\right] \qquad 2\text{-}6$$

Where U is the flow velocity and $U_*$ is the shear velocity, which is computed by dividing the bed shear stress by fluid density under square root $(\tau_o/\rho)^{0.5}$, Z is the height above the bed and $Z_o$ is the characteristic roughness height (height above bed where velocity goes to zero). The logarithmic law is probably only valid for the bottom 20% of the flow; however a logarithmic relation is often assumed to approximate the velocity for the entire flow depth (Bathurst, 1997). The logarithmic approach provides local measures for shear stress and can be used to map spatial patterns of shear stress and roughness height at sub-reach scale. However, it is reported to be not valid for complex flows as the velocity profile may not be logarithmic (Biron *et al.*, 2004). Previous researchers (Wilkinson, 1984;Whiting and Dietrich, 1989;Williams, 1995) all observed uncertainties in fitting a logarithmic profile to velocity data. Moreover considerable deviation of velocity profiles from the logarithmic was observed in shallow flows, having a variation near the tops of the roughness elements (Wiberg and Smith, 1991). Errors in measurement of flow velocity and height above the bed can highly influence the results.

There are different variants on the logarithmic law. The first and most commonly used method is using multiple observations of U in a single vertical. The slope of the least square line fitted to (U, Ln (Z)) is seen to be $U_*/\kappa$. An advantage of this method is the fact that it does not need an independent estimate of $Z_o$ because the shear velocity depends only on the slope of the profile and not its intercept. Moreover, measures of uncertainty in shear velocity can be obtained from the standard error of the slope of the curve fitted between U and Ln (Z) (Wilcock, 1996). An alternative to using multiple observations of U involves using a single velocity observation in the lower 20% of the flow or using the depth averaged velocity U and the depth integrated form of equation 2.6. In both approaches, an independent estimate of $Z_o$ is required, which may be estimated as a function of grain size. The fact that a single measurement of U is required offers considerable logistic advantage and requires only small log layer, although the latter may require measurements of velocity profile to determine the mean. Based on replicate observations of the depth-averaged and near bed measurements, Wilcock (1996) revealed that using the depth-averaged velocity offers the highest precision, whereas the slope of the velocity profile offers the lowest precision and requires the

most restrictive flow condition for accuracy but offers the advantage that it may be made without the knowledge of the bed roughness.

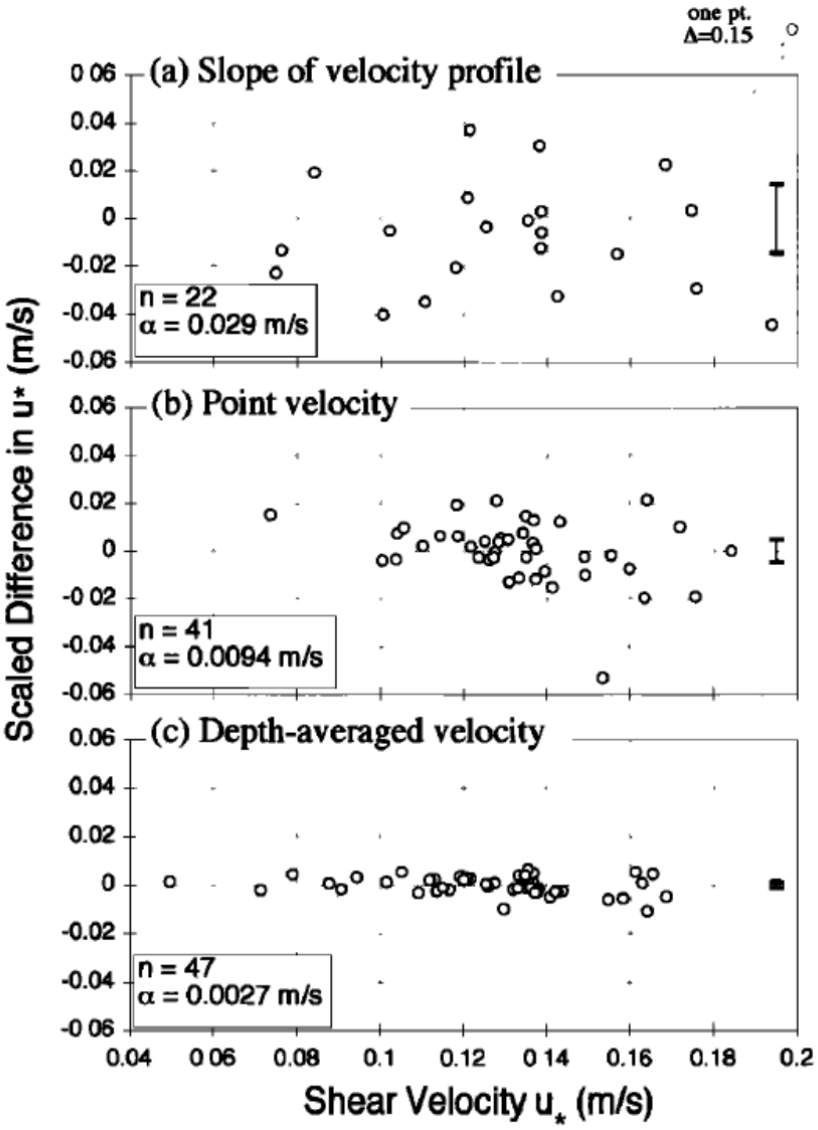


**Figure 2-7 Differences between replicate calculations of u* plotted as a function of mean u*. α refers to the standard error (adopted from Wilcock, 1996).**

The quadratic stress law works by relating the average bed shear stress to the square of the average fluid velocity (U) by a drag coefficient ($C_f$) (Schlichting and Gersten, 2000):

$$U = \sqrt{\tau_o / \rho C_f} \qquad 2\text{-}7$$

Some researchers treat the drag coefficient $C_f$ as constant (e.g., Paola, 1996) which is basically not the case as the drag coefficient depends on the ratio of depth to local bed roughness (Paola, 2000). It has been suggested that this is one of the weakest links of the method as the coefficient is difficult to estimate accurately (Whiting and Dietrich,

1989). Paola (1996) also explained the effect of constant $C_f$ as causing the estimate of the variance in the stress to be slightly high, since deeper flows, which generally produce the highest stress, would be expected to have lower relative roughness and hence lower drag coefficient. Nicholas (2000) expresses the drag coefficient in terms of a roughness relationship using the Darcy-Weisbach friction coefficient f. Use of the Chezy C, the Manning's n or the Darcy-Weisbach f is more or less the same since those coefficients can be used interchangeably; but according to Ferguson (2007), use of the Darcy-Weisbach friction coefficient yields two advantages. It is non-dimensional and physically interpretable as a drag coefficient if resistance is equated with gravitational driving force per unit bed area and assumed proportional to the square of velocity:

$$\tau_o = \rho g H S_o = \rho V^2 \, f/8 \qquad 2\text{-}8$$

Measurement of near bed turbulence or the divergences of the depth averaged velocity field are other methods for measuring local bed shear stress. However, these methods require precision or techniques that are not generally feasible under typical field conditions (e.g., Whiting and Dietrich, 1991). The reason for this partly due to the complexity and expensive nature of the devices used for measurement.

Evaluation of the precision of shear stress estimates based on the various approaches is done using replicate observations made under constant conditions. However, there are only few studies regarding this due, in part, to logistical restrictions and the typical variation of flow and sediment transport in time and space (Wilcock, 1996). However, Wilcock (1996) mentioned that estimates of $U_*$ and hence shear stress using the slope of the velocity profile is found to be the least precise from the other indirect methods to calculate shear stress. But, this method has the advantage that an independent estimate of the bed roughness $Z_o$.

The main reason for reliable estimate of local bed shear stress is to calculate the transport field and related scour, deposition and channel change. Although, several methods are available for calculation of the local bed shear stress with different underlying assumptions, they do not produce comparable results. In field studies, direct measurement of shear stress is rarely attempted and different indirect methods have been used. Investigation and comparison of the different indirect methods of shear stress

estimates in complex flow fields provide the basis for selecting the most appropriate and advantageous method for different conditions and purposes.

## 2.7.OUTLINE OF CURRENT RESEARCH PROJECT

In the braided river research there appears to be a gap in understanding regarding the effects of lateral flow variability in sediment transport. Theoretical approaches to estimating sediment transport in braided rivers have limitations since they represent braided channels using simple cross section shapes that do not fully represent the lateral variability in hydraulic parameters. The developments of alternative stochastic approaches to bedload prediction that include lateral variability are hindered by the requirement of large amounts of channel morphological data to derive the distribution parameters (Bertoldi et al, 2009). At present, there is a lack of relationships for estimating distribution parameters from mean morphological parameters, and accounting for temporal and spatial changes in distribution parameters for non-equilibrium condition. Such relationships would be useful to enable the stochastic approach to be applied when estimating long-term sediment flux for engineering, geomorphology and ecology, in addition to supporting the development of improved one-dimensional sediment routing models. One of the main intentions of this study is then to use experimental micro-scale physical modelling to obtain an improved understanding of lateral variability of sediment transport as a control on braided river evolution.

The current study also intends to use the quantitative data and digital elevation models derived from the micro-scale physical model to gain more insight into the effects of varying sediment supply in braided river evolution, and investigate the relationship between channel pattern indices (channel width to depth ratio and braiding index) and sediment transport. Detailed examination of these relationships will be used to improve understanding and quantification of sediment transport dynamics in braided rivers.

### 2.7.1. Aims and objectives

The aims of this investigation are:

- To develop a micro-scale physical model and exploit its potential for braided river evolution studies.

- To obtain an improved understanding of lateral variability of sediment transport as a control on braided river evolution.

The objectives of this study are:

1. To exploit the potential of micro-scale modelling in braided river studies and to use this modelling approach in controlled laboratory conditions to investigate and quantify the effects of varying sediment supply on channel morphology and hydraulic geometry of braided rivers.
2. To assess the effect of lateral flow variability on sediment transport and investigate the relationship between a measure of lateral flow variability, sediment transport rate and channel morphological parameters.
3. To use the quantitative data and digital elevation models gained from the micro-scale physical model in a two-dimensional hydraulic model to predict flow depth and shear stress and attempt to use the model results to gain a better understanding of the controls on the shear stress distribution in the experimental channels and its influence on sediment transport and channel evolution.

# 3. METHODS FOR UNDERSTANDING BRAIDING RIVER PROCESSES AND FORM: BENEFITS, DIFFICULTIES & LIMITATIONS

## 3.1. INTRODUCTION

This chapter will evaluate the approaches available to investigate fluvial processes and morphology, with a particular focus on braided rivers, and will conclude with a summary of the rationale for choice of methodology in this study. The broad approaches may be divided into three groups.

First, field observations, maps and aerial photographs of rivers and their valley floors provide a historical perspective for studying current fluvial processes (Petts *et al.*, 1989). Furthermore, a number of researchers have tried to understand how a braided rivers respond to external environmental forcing by analysing historical maps and aerial photographs in a GIS environment (Piégay *et al.*, 2006;Surian, 2006;Surian and Rinaldi, 2003;Winterbottom, 1995;Winterbottom and Gilvear, 1997;Winterbottom, 2000). Nevertheless, given a river influenced by many environmental factors, it can be difficult to understand the physical process involved. Moreover, separating the exact nature and cause of channel change in the presence of climatic variability and anthropogenic impacts is problematic (Winterbottom, 2000).

Second, laboratory modelling of rivers has provided new insights into braided river behaviour (Ashmore, 1991b;Ashmore *et al.*, 1985). This method is advantageous in that several processes can be studied in a single model with different boundary conditions (Warburton *et al.*, 1996). In addition, models are controllable at a laboratory scale and experience an increased rate of geomorphic evolution (Young and Warburton, 1996) unlike field conditions, which are generally episodic and slow (Warburton *et al.*, 1996). More recently, researchers have started using micro-scale physical models, which have some differences from the more-established Froude scale models, but are able to

reproduce typical braided patterns in a flume as small as 10cm wide and 1m long over shorter time scales. Research has demonstrated the applicability of hydraulic scale models in the following areas: understanding sediment transport in braided rivers (Ashmore, 1988;Ashmore *et al.*, 1985;Ashmore, 1991a;Ashworth *et al.*, 1992;Hoey and Sutherland, 1991;Young and Davies, 1991;Warburton and Davies, 1994); testing design equations for determining the characteristic of single thread-channels (Griffiths, 1989); and, simulating flooding conditions in a field prototype (Warburton *et al.*, 1996) etc. Nevertheless, (Warburton, 1996) also emphasized the difficulty of producing a flume model of sufficient size to reproduce both the mechanics of gravel transport and the overall form of a braided channel.

Third, braided river form and process can be conveniently investigated by means of mathematical models if the quantitative description or mathematical formulation of the subject is available. Representation of coupled flow-sediment transport-morphology systems provides a problem of considerable interest in modelling river processes. The most extensively used fluvial models are either 1D or 2D depth averaged, which are based on the basic hydraulic principles (e.g., The Saint-venant equations). More recently, researchers have started using cellular automata to simulate braided river processes. The most significant of these works is that of Murray and Paola (1994). They used simple water and bed load sediment routing techniques and produced a model which gives visually realistic simulation of braided river flow with constantly migrating channels and similar form and statistical characteristics. This model is also able to produce sediment pulses even when the discharge is kept constant, as has been observed in flume experiments (e.g., Hoey and Sutherland, 1991;Ashmore, 1988). Since then this approach has been developed substantially. Examples of such works include Murray and Paola (1997), Thomas and Nicholas (2002), Thomas *et al.*(2002), Nicholas *et al.*(2006), Coulthard *et al.*(2007) etc.

While these three broad approaches can be identified, it is common for two or more to be employed in the same investigation. For example, faced with a real-world 'river problem', it is not uncommon for engineers to use a physical model to study a range of scenarios and collect enough data to calibrate computational models, and then use the

calibrated computational model to analyze more scenarios before making recommendations for field application. Similarly, in geomorphological studies there is growing appreciation of the advantages to be gained by combining approaches, for example field and numerical (Nicholas and Quine, 2007); field and laboratory model (Davis and Korup, 2000); numerical and laboratory models (Clarke *et al.*, 2010). The challenge is therefore, not solely to identify the advantages and disadvantages of the individual approaches but to find the optimum combination of methods.

## 3.2.FIELD STUDIES OF BRAIDED RIVERS

### 3.2.1. Field measurements used in braided river studies

Field measurements have been used for numerous investigations to progress the understanding of the dynamics and sedimentary history of braided rivers. This section will provide a selection of referenced examples of braided river studies that have utilised field work in their investigations to illustrate the techniques that can be used and the understanding that can be gained from field-based research.

Field-based studies of braided rivers have provided the basis from which the other approaches have developed, although the majority of past studies have involved small-scale reaches or short time scales (e.g.Mosley, 1982;Ashworth and Ferguson, 1986;Davoren and Mosley, 1986;Ferguson *et al.*, 1992;Warburton *et al.*, 1993;Goff and Ashmore, 1994;McLelland *et al.*, 1996).

Some field-based research on braided rivers has focused on understanding the effects of human impacts, usually through dams and/or water abstractions. Those human impacts typically damp flood regimes and alter relative sediment supplies. Reduction of peak flows can eliminate the flow needed to scour vegetation and re-set the dynamics of braided systems. The process of channel narrowing will be accelerated if there is no periodic scouring and vegetation begins to colonize bars and other exposed surfaces. Surian and Rinaldi (2003) summarized the main types of channel adjustment in Italian alluvial rivers. They recognized incision of 3 to 4 meters and channel width reduction of up to 50% or more. In some reaches these adjustments have led to changes in channel pattern from braided to wandering. Such channel adjustments were mainly attributed to

sediment extraction, dams and channelization. However, it was not possible to extract the contribution of each factor. Sediment mining and dams have resulted in a remarkable decrease in sediment supply. This decrease was recorded in several rivers, for instance 38% in the Po River, 23% in the Adige River, and 68% in the Brenta River (Bondesan, 2001).

Contemporary and recent field-based research on braided rivers has focused on understanding the obvious association between sediment transport and morphologic change and developing an alternative approach to estimate sediment transport. Since the morphology displayed by a channel reach is a direct consequence of sediment transport (McLean and Church, 1999), observations of channel deformation can reveal details of sediment transfer in rivers (cf. Ashmore and Church, 1998). Neill(1971) was the first to recognize this association in rivers displaying a regular downstream progression of meanders and used it to estimate the rate of bed material transport on a large braided river. He demonstrated that an estimate of sediment transfer could be made on braided rivers by measuring average bank recession rates from maps and air-photos. However, Neill (1987) also mentioned that the method would underestimate actual transport volumes when the assumed transfer length was too short; or overestimate the actual short-term transport volume if material moves only locally (Ashmore and Church, 1998). Church (1987) adapted this association between morphologic measurement and sediment transport to estimate sediment transfer in rivers with complex morphologies. Advances in measurement technologies have allowed more recent studies to describe temporal changes in local bed material transport rates (McLean, 1990;Goff and Ashmore, 1994;Lane *et al.*, 1995;Ham and Church, 2000;Lane *et al.*, 2003;Ferguson and Ashworth, 1992). The technique reveals details of spatial and temporal channel change that other approaches do not. These efforts have begun to reveal details of the association between channel form and process rates on braided rivers, although developments remain incomplete. The approach is also a valuable tool for monitoring and evaluating the sensitivity of riverine systems to environmental changes, hence to predict channel response to disturbances.

Although some of the studies of braiding dynamics and mechanisms of braiding are flume-based, field based studies have also made important complementary contributions to this field. Reinfelds and Nanson (1993) described the three predominant mechanisms in the development of the Waimakariri River's floodplain in New Zealand. First, riverbed abandonment by lateral migration of the active riverbed (usually in the lee of tributary fans and bed rock spurs), followed by aggradation during high magnitude flood events and, finally, localized riverbed incision. Rundle (1985a;Rundle, 1985b) considered multiple dissection of lobes to be the characteristic braiding mechanism in New Zealand rivers and identified dissected lobes as basic morphologic units. Ashworth and Ferguson (1986) demonstrated that the spatial patterns of shear stress and of channel erosion or deposition can alter considerably with an increase in discharge through a reach, causing drastic channel change or even avulsion. Warburton et al. (1993) gathered data from an active gravel bed braided river in New Zealand and examined channel changes and determined the main mechanisms which produce the braidplain morphology. According to this study the dominant mechanism of channel change in the Ashley River, New Zealand are avulsion and bank notching. They concluded that small changes at critical points in the braided network may have a large effect on the channel pattern downstream.

Field based studies have made important contributions to the debate over whether braided rivers can be considered stable or in dynamic equilibrium. A wide braided river may not appear to be stable when its flood banks are forming, mid-channel bars are destroyed and its active channel is changing. Moreover, sediment pulses from episodic events, such as landslides, often results in a wave of sediment migrating downstream, causing aggradation and degradation of the riverbed. Korup (2005) used historical aerial photography and geomorphic and morpho-stratigraphic evidence from 250 landslides in south-western New Zealand to describe the channel-altering effects of landslides. According to this investigation 6% of landslides caused major avulsions (channel shifting) and it is likely that the characteristic instability of braided rivers is accentuated by sediment pulses (Hicks *et al.*, 2007). Goff and McFadgen (2002), Cullen et al.(2003) and Korup (2005) have all documented evidence of several periodic seismic events that have caused river aggradation and driven vegetation destruction and channel instability

throughout New Zealand. This is indicator of the fact that over longer time scales (hundreds of years) it would be less accurate to view these rivers as being in a state of equilibrium, although appearance of equilibrium state is dependent on both time scale of observation and periodicity of drivers.

The drawbacks of field-based approaches in braided river studies stem mainly from the inherent variability present in braided river processes combined with the practical difficulty involved in measuring variables such as discharge, flow depth, bedload transport rates, and flow velocity over greater spatial or temporal scales. More recently however, the development of new technologies of data collection (e.g. ADCP, photogrammetry, etc.) has allowed braided rivers to be studied in the field at larger spatial scales and in greater detail (e.g. Richardson and Thorne, 1998;McLelland *et al.*, 1999;Lane, 2000). Another common problem in field studies of braided rivers is that several controls can change simultaneously so that it is typically difficult to isolate the effects of one control (e.g., dams can reduce sediment supply and regulate flows, which can both facilitate encroachment of vegetation). In this regard, laboratory and numerical models – where all other factors can be held fixed – are useful for inspiring questions, testing hypotheses, identifying processes and key parameters, accelerating time scales, and quantifying relationships. In particular, some recent physical modelling works in laboratory has advanced our understanding of the processes and form in braided gravel-bed rivers (Ashmore, 1991a;Ashmore, 1993;Ashmore, 1982;Ashmore, 1988;Ashmore, 1991b;1985). Also, numerical modelling is now used to examine river morphological change at basin scales (Coulthard *et al.*, 2007). Nevertheless, the use of field data in parameterising these models and providing verification of the results is vital (Dikau, 1999).

### 3.3.PHYSICAL MODELLING FOR BRAIDED RIVER STUDIES

Although there is increasing use of mathematical models in river engineering, management and geomorphology a large number of problems have to be solved by scale models. The use of physical modelling has played an important part in geomorphology over the last few decades. Mosley and Zimpfer (1978, p 457) , Young and Warburton (1996) and others identified several advantages in their use:

- They allow several components and processes to be included in a single model and can accommodate various boundary and initial conditions.
- They allow control in a laboratory scale with increased rate of geomorphic evolution.
- Careful observation of these models may reveal previously unsuspected phenomena and open new lines of enquiry.
- They allow easy visualization of geomorphic phenomena and thereby aid understanding and education.

However, the above advantages are counter balanced by prototype to model scaling difficulties and comparability (Peakall *et al.*, 1996):

- Initial and boundary conditions in the model may not be similar to those in nature or may influence model behaviour to an indeterminate or undesirable extent.
- Materials and processes in the model may be dissimilar to those in nature and there may be no obvious way of relating model behaviour to that of the prototype. In particular, it is difficult to relate model behaviour under constant rate of operation of processes (constant material input) to prototype behaviour, where highly variable rates of operation of processes are usual.
- Studying only one or two processes or independent variables may mask interactions that occur in nature.
- As model size decreases, there is a trade-off between precision of measurement and observation and accuracy of representation of the prototype. Confidence in the model results may therefore decline.

### 3.3.1. Classes of Physical Models

In the literature two kinds of boundary conditions for scale models are identified: fixed bed models with non-erodible boundaries and no sediment transport and movable bed models, where the substrate is free to move in the constrained or unconstrained channel (Peakall *et al.*, 1996). The growing insight into sediment transport and morphological processes has given a sounder basis for the latter. The

interaction of water and sediment movement can, however, still lead to large errors if no check on the scales is made (Jansen *et al.*, 1979).

Based on the degree to which the model replicates a prototype and the temporal/spatial scale at which they are applicable, physical models are classified as: one-to-one replicas of the field prototype; scaled by Froude numbers only; have different horizontal and vertical scales (distorted models); or un-scaled experimental analogues that attempt to reproduce some properties of the prototype (Peakall *et al.*, 1996). The following figure (Figure 3-1) clearly demonstrates the decrease in replication of prototype characteristics when we move from 1:1 models through Froude scale models, distorted scale models to analogue models. Peakall *et al.* (1996) mentioned two points on the spacing of the boxes with respect to replication of prototype. First the significant decrease in replicability when moving from 1:1 to scaled models and from scaled to analogue models and second the smaller loss of model replicabilty in the transition from Froude scale models to distorted models. Micro scale models seem to be located in between the distorted scale models and the analogue models in Figure 3-1. The major difference between the micro scale models and the distorted scale models is the fact that micro scale models use highly exaggerated vertical scaling that in turn will have problems in replicating water surface slopes. It is important to bridge the gap between different types of physical models so that understanding can be shared. Figure 3-1 also suggests that, although different models use different scales and hence replicate prototypes differently, results from one model may inform the other specially when models are scaled.

A one-to-one scale model attempts to create an exact scaled reproduction of the prototype. However, this can only be achieved for small spatial and temporal scales, with little or no difference from the natural prototype. For a medium to large scale prototype, a scaled physical model would be required which needs to satisfy similarity conditions. For engineering purposes a model needs to satisfy three conditions of similitude- geometric, kinematic and dynamic similarity (Henderson, 1966). The systems, for which the criteria of geometric, kinematic and dynamic similarity are simultaneously satisfied, are called mechanically similar. This means the ratio of all

homologous dimensions must be equal and the ratio of all homogeneous forces must be the same. Mechanical similarity always includes dynamic and geometric similarity.

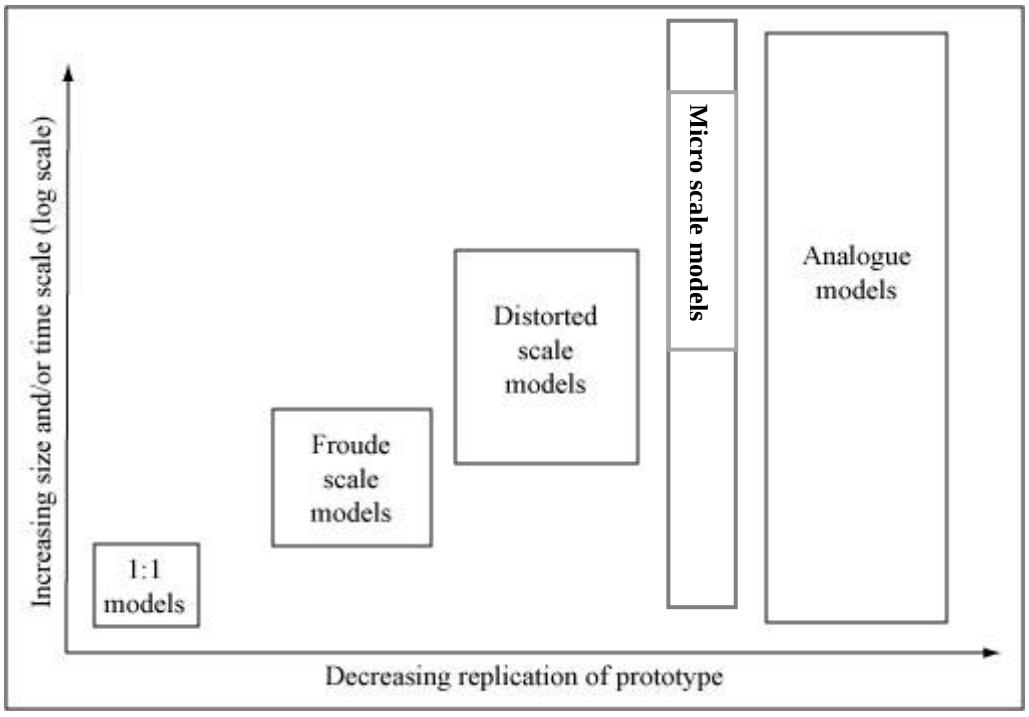


**Figure 3-1 Schematic view of the balance between model specificity and spatial/temporal scales for different modelling techniques, (Source: Peakall et al, 1996, p 223)**

But some practical considerations can either impede or simply prevent the realization of a dynamically similar small scale hydraulic model. Some of the practical considerations include, but are not limited to, the use of water as a fluid in both model and prototype in conventional hydraulic models and the significant contribution of more than one force in a system. To reduce some of those complexities, investigators have used distortion of geometric scales particularly in movable bed models where precise modelling of sediment movement is attempted (Peakall *et al.*, 1996). Model distortion implies that the vertical scale and the lateral scales are not identical. If this vertical model scale is different from the downstream horizontal scale, the model is said to be tilted. Distortion allows the use of different scale factors for flow depth and sediment grain-size. Distortion allows using higher flow depth values in models. This will probably have an effect of increasing lateral sediment transport in models. In movable bed modelling it is also usual to adjust other scales like valley slope, grain size, sediment density, flow velocity, and discharge (Peakall *et al.*, 1996) for the best representation of the prototype.

However, model distortion is acceptable only when vertical and lateral accelerations of the water can be neglected with respect to the gravitational acceleration.

There is a wide variety of river problems in nature. Some of the problems require perfect similarity to discover how a certain reach of a particular river is likely to behave under given circumstances. Others are more general problems that require investigation of interactions between variables. The difficulty in achieving reasonable accuracy of modelling with reasonable economics and time added with those varieties of problems in nature has resulted in a more general principle of similitude to be employed. Such a model is referred to as 'generic model' (Ashmore, 1991a;Ashmore, 1991b;Ashworth *et al.*, 1994) and this model is expected to be hydraulically similar to some general prototype since it is not scaled from a specific prototype. Those models will allow conclusions about the operation of processes, controlling variables and the resultant landforms to be reached (Peakall *et al.*, 1996) and give order of magnitude indications of the rates of operation of processes in general prototypes.

The final types of physical model are those that are unscaled or 'analogue' models. Experimental analogue models are based on the assumption that aspects of a natural system can be reproduced in a laboratory setting and that the processes which formed the prototype will form similar features in a model environment. Such a natural system can be considered scale independent, and was termed a "similarity of process and performance" model by Hooke (1968). The basic requirements for analogue models are that: the gross scaling relationships be met; the model reproduce some morphologic characteristic of the prototype; and the process which produced this characteristic in the experiment can logically be assumed to have the same effect on the prototype (Hooke and Rohrer, 1979). The main advantage of analogue models is the speed and simplicity in setting up experiments and the reduced space and budget costs which constrain other modelling approaches (Peakall *et al.*, 1996). Also using this approach, the generally recognized disadvantages of scale models – scaling ratios, initial conditions and boundary conditions – are avoided, and (as shown in Figure 3-1) analogue models are applicable over a wide range of space and time scales. However, when comparing these models to field examples it has to be remembered that they are not scale models and

therefore care must be taken when interpreting the results in a field environment. Koss *et al* (1994) noted that the most serious problem with analogue models is relating experimental time to real time, because there is no way to scale time absolutely it must be viewed as relative. Numerous investigations have successfully used analogue models in geomorphology and they have proved extremely useful, especially for prediction and gaining an understanding of initial and boundary conditions that were unknown from field observations prior to the onset of the experiment. Examples from previous users of analogue models includes: analogue models of drainage basins to try to determine autocyclic oscillations in erosion rate and terrace formation (e.g. Hasbergen and Paola, 2000), observation of overland flow and erosion patterns (e.g. Hancock and Willgoose, 2001;Hancock and Willgoose, 2003;Hancock *et al.*, 2006), and determination of the geomorphic response to tectonic uplift (e.g. Lague *et al.*, 2003). There has also been work into alluvial architecture looking into mesoscale fluvial dynamics (Sheets *et al.*, 2002;Hickson *et al.*, 2005) , exploring the potential bias of the recorded allogenic forcings preserved in the stratigraphic record (Van Heijst and Postma, 2001) and investigation of autogenic behaviour during alluvial fan evolution (Clarke *et al.*, 2010).

### 3.3.2. Froude Scale Modelling

The most important parameter which characterizes free surface open channel flows is the Froude number. For this to be the same in model and prototype, the ratios of inertial and gravity forces in the model and prototype has to be the same. Hence: -

$$\rho L^3 (V^2/L) \Big/ (gL^3) = V^2/gL = F_r^2 \qquad 3\text{-}1$$

Where ρ is density of the fluid, L is length of the reach under consideration, V is average flow velocity, g is the acceleration due to gravity and $F_r$ is the Froude number. The Froude model law represents the condition of dynamic similarity for flow in model and prototype governed by gravity. The focus on the Froude number implies that other forces such as frictional, capillarity, resistance of viscous fluid etc either do not affect the flow or the effect may be neglected.

However, if only the parameters in equation 2.1 are considered, true similarity will rarely be achieved. But the presence of more than one condition of similarity at the same time forces to deviate to a certain extent from the original conditions, introducing scale effects. Scale effects are said to be present if the scale factor is not only a function of other scales but also varies in the model (Jansen *et al.*, 1979). They generally arise due to imperfect modelling of geometric and kinematic conditions rather than a mistake in the basic theory of dynamic similarity(Sabersky *et al.*, 1971).

The primary source of scale effects is the wish to satisfy multiple scaling conditions at the same time. For example if we consider a case of free surface flow for which viscosity is also present; both Froude condition and Reynolds condition have to be fulfilled at the same time. The latter describes the ratio of inertia to viscous force and is referred to by the Reynolds number. If the same fluid is used both in model and prototype which is generally the case, the following relation should hold:

$$\mathbf{n_{R_e} = 1 \Rightarrow n_V = {n_L}^{-1}}$$

$$\mathbf{n_{F_r} = 1 \Longrightarrow n_V = {n_L}^{1/2}} \qquad \textbf{3-2}$$

Where $n_{Re}$, $n_{Fr}$, $n_V$, $n_L$ represents the scales of the Reynolds number, the Froude number the velocity and the length respectively. The two conditions can never be fulfilled at the same time unless $n_V = n_L = 1$ is selected, which is a full scale (1-to-1) model. For this reason, in Froude modelling, it is considered acceptable to deviate from the Reynolds criterion ($n_{Re} \neq 1$) as long as the flow is turbulent in the model, the transition occurring at around Re=500 to Re =600. This remark indicates the key role played by scale effects in the procedure of scaling.

If a model is designed exclusively according to the Froude modelling condition, the following conditions should be met for an approximate dynamic similarity between model and prototype (Young and Warburton, 1996): sediment density should be equal in model and prototype; the model fluid should be water; grain size should be scaled by length scale; rough turbulent flow should prevail in the model; and, bed slope should be equal in the model and prototype. For a dynamic similarity between model and prototype, the scale factor for length will be (Yalin, 1971):

$$n_L = \left[ R^*_{em} \Big/ R^*_{ep} \right]^{2/3} \qquad 3\text{-}3$$

Where $R_{em}$ and $R_{ep}$ represents Reynolds number in the model and prototype. Substitution of an appropriate range of values in equation 2-3 for gravel-bed rivers will limit the possibility of model to prototype scaling ratio to an average value of 1:50. This is based on the requirement of rough turbulent flow in Froude scaled models. Under these conditions and with the aim to limit model sediment sizes less than 0.1 mm (which is usually the case), it will be problematic to design model grain size ranges in some gravel bed rivers as it excludes sediment sizes finer than 5 mm (Young and Warburton, 1996). Moreover, with modelling scales of the order of 1:50, it was noted that parts of the braided river channel, especially areas of shallow depth and low velocity, do not always appear to satisfy the criteria for hydraulic similarity (Warburton and Davies, 1994;e.g. Ashworth *et al.*, 1994;Sapozhnikov and Foufoula-Georgiou, 1997). Large river systems, such as the Waimakariri and Rakaia in New Zealand, Brahmaputra-Jamuna river system in Bangladesh are thousands of metres wide, making them impractical or costly to simulate at the usual 1:50 to 1:75 scale (Warburton, 1996). Although some degree of similarity can be achieved in Froude scale models with respect to planform geometry and flow conditions of the prototype, it is extremely difficult or impossible to reproduce the full environmental system that includes differing grain shapes, vegetation and other environmental factors which are usually neglected.

The Froude modelling procedure in engineering and geomorphology in which the theorems of similarity mechanics observed in studies performed as a rule with water, offers certain advantages. A great number of river problems have been solved using this approach during recent decades. The major advantage of this type of model is that the results can, to some extent, be scaled to compare to the field prototype to validate the findings. However, this does restrict the applicability of the model, as it is limited to one field prototype and the results cannot easily be scaled to other areas. Nevertheless, an increasing number of problems have been encountered for which the solution obtained by this method is either insufficiently accurate, too time consuming, or too expensive. A

typical example is modelling of braided rivers. Models usually need to be verified using prototype data. One of the problems with this is the need to model the total braided river flood plain width. In this case laboratory models are often limited by flume walls, and are unable to describe the complex geometry of braided rivers fully because the lateral development of braids will be limited by the flume width, although part of the problem may be attributed to difference in bank strength and difference in flow history (time of model rum)(Young and Warburton, 1996) . This may not by itself pose a big problem for some braided rivers as flow rarely fills the full width of the braid plain and the active width. Much of the geomorphic change occurs in an area that is much smaller than the full braid plain width (Warburton *et al.*, 1993). However, in extreme discharges, which are very important because of their high transporting capacity, the braided river usually occupies the full bed width (Young and Warburton, 1996). In most of these cases even if the planform geometry is to some extent statistically similar to the prototype, it is hardly possible to exactly reproduce the geometry of a given braided river reach(Young and Warburton, 1996).

Using morphological modelling to assess changes in downstream river morphology as a result of flow obstruction or any hydrological disturbance and long profile evolution is very difficult. Practically, there are limitations in flume size, sediment management and cost because of the requirement of rough turbulent flow in Froude scaled models. Comparison of sediment transport processes is also another challenge in Froude scaled models. The considerable variability of bed load transport in braided rivers made it less meaningful to compare instantaneous bed load transport in model and prototype (Young and Warburton, 1996). Direct measurement of bed load transport in the field is an almost impossible task due to the inherent temporal variability and errors associated with the sampling devices although it is easier in laboratory flumes. These limitations constrain the applicability of Froude scaled models to the investigation of larger system dynamics that is attracting increasing interest from fluvial geomorphologists and some engineers. This change in scale of investigation away from the single reach or individual reach elements, has been one of the basic motivations to develop methods of investigation in a smaller scale (micro-scale) without the same attention being given to most of the dimensionless scaling parameters.

### 3.3.3. Micro-Scale Modelling

Micro-scale modelling is an extension of formal physical hydraulic modelling, using extremely small-scale representations that deliberately ignore some aspects of dynamic similarity for convenience of scale (Davies *et al.*, 2003). It has been suggested that this approach was developed in 1994 by the St. Louis District of the US Army of Corps of Engineers (Maynord, 2006) to give quick answers to river engineering problems. They have primarily used it for the design of navigable channels (Gaines and Maynord, 2001). However, geomorphologists started using micro-scale rivers in 1968 for investigation of alluvial fan dynamics (Hooke, 1968).

Graf (1984) grouped movable bed physical models into two as rational and empirical. This classification is based on similarity of dimensionless parameters in model and prototype. Rational models are the most rigorous type basically used for modelling sediment transport. They are semi-quantitative with low vertical scale distortion and low Froude number exaggeration. In those models, the Shields parameter is similar in both models and prototype. The empirical models are less rigorous than the rational. They use normal vertical scale distortion and Froude number exaggeration. In those models as the objective is just to generate a movable bed, the Shield's parameter is usually less than in the prototype. Due to this, their use is limited to study of bathymetric response (Maynord, 2006). Micro-scale models resemble these empirical models. A comparison made by (Maynord, 2006) put their significant difference from the empirical models as their smaller size, large vertical scale distortion, and large Froude number/slope distortion.

There are important differences from formal Froude scale models: For example, In Froude scale models the dimensionless variables like flow and grain Reynolds number, Froude number, relative density and relative depth, in the model should correctly represent the prototype. Of course, depending on the importance of the different forces, force combinations and type of flow, the Reynolds number may be relaxed as long as it is in the turbulent range. Turbulent range Reynolds number is achieved by imposing relatively large magnitude flow, which basically requires large experimental flumes.

Due to this, Froude scale models often operate on long time scales (Malverti *et al.*, 2008). In micro-scale modelling there is no attempt to achieve the same range of Reynolds number in the model as in the prototype, hence the flow is often laminar in the model (Davies *et al.*, 2003;Malverti *et al.*, 2008;Métivier and Meunier, 2003) and operates with very small flow depths. To induce sediment transport, bed slope is usually much steeper than the prototype (Davies *et al.*, 2003;Maynord, 2006). This has its own drawback in reproducing flow patterns similar to a prototype as it may lead to greater Froude numbers (Maynord, 2006). However, the Froude number is sometimes of secondary importance since it has limited significance for low values typical of alluvial rivers (Maynord, 2006) and hence it might be acceptable to deviate ($n_{Fr}<1$, where $n_{Fr}$ is the scale of the Froude number) provided that this does not lead to excessively large Froude numbers in the model (Struiksma, 1986). Having said this, there is no strict limit as to what is meant by 'excessively large' Froude numbers in models, and different researchers have put different exaggeration limits on the Froude number. Gujar (1981) put 1.67 as acceptable Froude number exaggeration limits ($Fr_m/Fr_p$) and Latteux (1986) suggested 2.2.

In micro-scale modelling, values such as the water and sediment flow rate, sediment grain size, and bed slope are usually selected arbitrarily unlike in the Froude scale models, which have interrelationships based on established scaling principles. Davis *et al.* (2003) obtained appreciable similarity between a micro-scale model and the Waiho River, but suggested that this correspondence was simply coincidental. Despite these similarities, no effort was put to derive time scales and relate the amount of aggradation in the model to that of the prototype as the model is not 'dynamically' similar to the prototype. The latter would require a formal Froude scale hydraulic model. More recently a general procedure is developed to set boundary conditions and scales in micro scale models (Malverti *et al.*, 2008). This is done by relating the longitudinal profile development of a micro scale laminar river and a natural turbulent river. Details are provided in chapter 4 (section 4.3.1).

Traditional Froude scale models are usually calibrated and verified to see how much they have been able to reproduce the actual prototype (Young and Warburton, 1996;Maynord, 2006). Validation involves running the model for a known & different

set of boundary condition to see if there is a satisfactory level of similarity with the prototype. For screening different project alternatives this step is replaced by a base test in the case of micro-scale modelling (Maynord, 2006). The calibrated model will be run for a certain water and sediment discharge combination, and the output will be taken as a reference or base test and hence deviation of all successive runs from the base test is assumed to occur in the prototype (Maynord, 2006). Two problems can be identified with this approach. First, since there is no scaled relationship between the model and prototype, extrapolation of the results will be questionable. Second, if different water-sediment discharge combinations are to be considered, then it may be necessary to run the model several times. It can be very difficult to achieve a similar level of accuracy for successive runs in a micro-scale model and it is time consuming, although possible.

More generally, important differences between micro models and empirical models include their smaller size, larger vertical scale distortion, larger Froude number/slope distortion and lack of correspondence of stages; the operation of which results in larger departure from similarity criteria. Micro-scale modelling, even if intended to be used for the purpose of demonstration, education or communication only (Maynord, 2006) is still used by many researchers and geomorphologists as an alternative technique to traditional Froude scale physical modelling. The method has also attracted attention due to its capacity to explore larger scale systems. A typical example is investigation of the continuous aggradation of the Waiho River, South Westland, New Zealand at the head of its alluvial fan which repeatedly damaged river control works and reduced the effectiveness of flood hazard mitigation in the vicinity. An area of the Wahio River fanhead approximately 6 km by 6 km was represented at a linear scale of 1:3333 using a 2 m wide modelling tray, which otherwise would require a space of 50 m by 50 m using a formal Froude scale physical model (Davies and McSaveney, 2001). Moreover, recently researchers have shown that micro rivers and natural rivers obey similar sediment transport relations (Malverti *et al.*, 2008).

#### 3.3.3.1.Reliability of Micro-Scale Modelling

To studying morphological problems using scale models, it is a precondition that both water movement and sediment movement have to be reproduced to a certain extent

to simulate bed level and bed level changes correctly (DeVries *et al.*, 1989). Micro-scale modelling avoids consideration of the usual dynamic similitude criteria (e.g. Shields parameter for sediment movement) (Gaines and Maynord, 2001). So, it bases similarity considerations on an overall assessment of how well the model reproduces the gross features of the prototype bathymetry.

The issue of surface tension has become a point of discussion in micro-scale modelling. Such forces will become significant when flow depths and flow velocities are small. Peakall and Warburton (1996) mentioned that in small hydraulic river models, the potential influence of surface tension should be assessed. However, Malverti *et al.* (2008) demonstrated that surface tension is important only if the micro scale river width is in the order of or smaller than the capillary length. They used a dimensionless parameter called channel Bond number ($B_{oc}$) to describe the magnitude of surface tension effects where $B_{oc}$ is equal to:

$$B_{oc} = {\rho g W_c^2}/{\sigma} = {W_c^2}/{l_c^2} \qquad 3\text{-}4$$

Where ρ = fluid density; $W_c$ = channel width; $l_c = \sqrt{\sigma/\rho g}$ = capillary length; σ = surface tension and g = acceleration due to gravity.
If the bond number is more than 1, the effect of surface tension can be neglected (Malverti *et al.*, 2008). Since capillary length for water within air is in the order of 2.6 mm (Malverti *et al.*, 2008), it seems that the effect of surface tension can be neglected as long as the width of the laminar river is more than 2.6 mm which is generally the case.

Another important issue in micro-scale modelling is the selection of bed material, since the mobility of sediment particles is crucial for morphological development. So far in micro-scale modelling different kinds of sediments have been used like crushed walnut shell, sand, acrylic, urea type II plastic (Gaines and Maynord, 2001;Davies *et al.*, 2003), and glass (Métivier and Meunier, 2003;Meunier and Métivier, 2006). Most of the earlier micro model experiments in USACE used urea type II plastic, mainly because it is light enough to be transported by smaller discharges and retains the bed configuration after

the test, hence collection of bathymetric data will be facilitated (Gaines and Maynord, 2001). However, as the transport of sediments is facilitated by the relatively steeper slope of the micro-model in which 4% is stated to be the minimum at which bed materials would move without turbulence (Le and Davies, 1979), alternative sediment types should be considered to fulfil other modelling criteria. For example using fine sand in the model will help to keep reasonable similarity of depth/sediment grain size ratio in the model and prototype (Davies *et al.*, 2003) in addition to similarity in relative density if the model fluid is water. Recent researchers have even used a model slope much flatter than 4%; Malverti *et al*.(2008) with 2%; Meunier and Métivier (2006) with a slope as low as 2.6%. Although, sediment movement is initiated by using steeper slope in micro scale models, this will have its own implications in magnifying the Froude number and water surface slopes. As the shear stress is the function of the water surface slope and sediment transport is a function of shear stress, it is imperative that the sediment transport will be increased as the result of the steeper slope in micro models.

More comments and evaluation on the applicability and reliability of micro-scale modelling have been given by users in the engineering profession (Gaines and Maynord, 2001;Maynord, 2006). It seems that modelling from an engineering perspective has concentrated on specific cases and comparatively short term predictions aimed at identifying how various flow obstructions and structural alternatives affect flow and thereby the bathymetry. In those cases, good prototype-model relationships are sought and distortions should be minimal. In contrast, in geomorphological problems, qualitative questions are often considered that do not look into a specific prototype, hence ‘generic’ models are often used. Such models are often required to have typical prototype characteristics, but no strict similarities are required so long as some dimensionless parameters are within the limits of natural rivers.

#### 3.3.3.2.Previous Physical Model Studies of Braided Rivers

Peter Ashmore was reportedly known to be the first to highlight the potential use of physical models based on the Froude scaling principle for understanding and

quantifying complex and dynamic braided fluvial environments. In particular there has been an abundance of research using Froude-scale modelling to examine the form and evolution of braided rivers. Following on from his earlier work (Ashmore, 1982), he continued to apply Froude-scale models to different aspects of braided river research, using a scaled model of the Sunwapta River in Canada to investigate bed load pulses on sedimentation patterns (Ashmore, 1991;Ashmore, 1993). Other important studies using a physical modelling approach have included investigation of braiding (Southard *et al.*, 1984), bedload transport rates and channel morphology of braided rivers (Hoey and Sutherland, 1991;Warburton, 1996;Warburton and Davies, 1994;Stojic *et al.*, 1998), examination of bar formation (Fujita, 1989), braided alluvial architecture (Moreton *et al.*, 2002), description of sedimentary architecture(Ashworth *et al.*, 1994) and avulsion frequency on braided rivers (Ashworth *et al.*, 2004;Ashworth *et al.*, 2006).

Ashmore (1982, 1988, 1991a) used Froude scale model to classify the main mechanisms of braiding, explain the processes of bar formation and down bar fining and relate the internal generation of bed load pulses and bed load variability to channel change and bar creation. It was shown that the main mechanism of braiding identified were through deposition of central bars, conversion of a single transverse unit bar to a mid-channel bar and dissection of multiple bars. In Ashmore's experiments the chute cut-off mechanism was the most common process of braiding. Ashmore continued to apply Froude-scale models to different aspects of braided river research, using a scaled model of the Sunwapta River in Canada to investigate bed load pulses on sedimentation patterns (Ashmore, 1991a;Ashmore, 1993;Ashmore, 1991b).

Warburton (1996) investigated the influence of bed width on bed load transport and channel morphology. He showed that bed load transport capacity is greater in narrower braided systems. However, Carson and Griffiths (1987) indicated that an optimum channel width exists at which the bed load transport is maximized but recognized the limitation of representing braided channels using simple cross sectional shapes.

Bed load transport time series show considerable variability in braided river models, indicating minor and major fluctuations in the bed load transport rate. Physical model experiments Hoey and Sutherland (1991), Ashmore (1991a), Bertoldi et al.(2009),

Warburton and Davies (1994) all have identified a series of fluctuations with large amplitude and different time scales. Bed load flux data sets from the above mentioned experiments show an initial phase of gradually decreasing average transport rate during the development of a braided network. Moreover, they have demonstrated that those fluctuations are related to morphological changes. However, those model studies of braided rivers still lack a consistent measurement of the complexity of the braided pattern.

Cycles of increasing and then decreasing sediment supply are often accompanied by a transition from single thread river to a braided network during stream bed aggradation and higher sediment feed from upstream followed by reversion to a seemingly single thread channel as sediment supply declines and degradation progressed (Church, 1983;Knighton, 1989). The physical modelling experiments of Ashmore *et al.* (1985) and Germanoski and Schumm (1993) conducted in a tilting flume at the Engineering Research Centre at Colorado State University to a large extent mimicked those results from field studies. They found that aggradation took place over the entire channel length and resulted in the development of more braid bars and caused an increase in the braiding intensity for both sand and gravel bed channels. When sediment feed reduced rapid degradation was observed in the sand bed, the greatest incision being in the upstream region, that converted the upstream part of the channel to a single thread flanked by terraces where as the downstream part remained braided owing to the delivery of large quantities of incision-derived sediment from upstream. They also found that degradation resulted in a decrease in braiding index and number of bars whereas the size of bars increased as a result of abandonment of smaller channels thus forming more composite bars. Sediment discharge was found to increase in some degrading channels and as a result they proposed that the actual sediment transport rates are related to the transport capacity of the channel rather than sediment supply. The flume studies of Germanoski and Schumm (1993) showed that ‘’changes in sediment load had no tangible influence on the fundamental kinematics of braided river behaviour.’’

Physical modelling has been used for understanding the long-term occurrence, behaviour and triggers of avulsions on braided rivers. Ashworth *et al*. (2004;2006) used Froude-scale modelling to observe avulsions in braided rivers, and found that avulsion frequency increases with sediment supply and also increases at a rate slower than the increase in the sediment feed rate. This is in contrast with the findings of Bryant *et al.*(1995) who used Froude scale modelling and measured avulsion frequency as a function of sediment feed rate in fluvial fans, and found that as sediment flux increased the avulsion rate first increased and then stabilized as mass flows began to influence deposition. It was also discovered that less total sediment volume is needed to trigger an avulsion as the sediment supply rate increased. Ashworth *et al.* (2004, p 24) suggested four possible reasons for the differences in behaviour observed in their study from that seen by Bryant *et al.*(1995):

(1) Their varying definition of what constituted an avulsion. Bryant *et al.*(1995) defined avulsion as a newly created channel that carried at least fifty per cent of the discharge from the old channel. Ashworth *et al.*(2004) used maps of change in position of channels, bars, and abandoned braid-plain over time and defined avulsion as where a channel moved laterally by at least 300mm in a 15 min period and sustained that position for a further 15 min. This spatial-temporal definition of an avulsion therefore specifically excluded any channel relocation caused by progressive lateral migration. However, although this variation may have altered the absolute number of avulsions counted it is unlikely to have had an impact on the rate of change in avulsion frequency with sediment supply

(2) The role of bed slope. The bed slopes of Bryant *et al* (1995) (0.076 to 0.113) were an order of magnitude steeper than those of Ashworth *et al* (2004) (0.008 to 0.014). These steep multi-channel systems may be inherently less stable and the probability of avulsion is likely to be greater with a smaller change in sediment supply

(3) Sediment discharge: the much higher sediment discharge values in the alluvial fan experiments may contribute to the observed rapid rise in avulsion frequency with only a small increase in sediment supply

(4) The distinction between braided rivers and alluvial fans.

Ashworth *et al* (2004) concluded that the most probable cause of the differing findings was the relation between avulsion frequency and sediment supply being dependent on bed slope. The avulsion dynamics of unconfined braided channels may, therefore, be very different from those of steep alluvial fans.

Micro-scale rivers have been used for numerous investigations in river engineering and fluvial geomorphology to investigate alluvial fan dynamics (Hooke, 1968;Schumm *et al.*, 1987;Whipple *et al.*, 1998), river braiding and sediment transport (Malverti *et al.*, 2008;Métivier and Meunier, 2003;Meunier and Métivier, 2006;Le and Davies, 1979;Meunier and Métivier, 2000;Le, 1978), anthropogenic aggradation (Davies *et al.*, 2003), model drainage basin evolution (Hasbargen and Paola, 2000), predict the bathymetry and flow pattern trends for proposed river training structures (Davinroy, 1996a;Davinroy, 1996b;Davinroy, 1997;Ettema and Maynord, 2004), base level change studies (Koss *et al.*, 1994;Muto and Swenson, 2005) and the response the drainage network to tectonic uplift (Lague *et al.*, 2003).

The use of Micro-scale rivers dates back to the 1960s with the work of Roger Hooke (Hooke, 1968) to investigate fan morphology with a very small working area as small as 1.5m by 1.5m. Le(1978) and Le and Davies (1979) used a micro-scale river to investigate the hypothesis that the geometric properties of braided streams are constant over a range of stream sizes and demonstrated that some degree of geometric similarity existed between the model channel pattern and the Rakaia River, New Zealand. However, no channel was observed to divide with the classical braiding mechanism observed in Ashmore's laboratory experiments. They used time-lapse films and showed the main mechanism of braiding as meander migration, cut-off formation and channel abandonment. Such an experimental approach was also used by Métivier and Meunier (2003) to investigate the correlation between input and output sediment fluxes and to show that sediment transport can reach steady-state even though braiding remains unstable. The correlation between input and output mass fluxes enabled them to define a dimensionless stream-power that quantified the balance between eroding power and transport capacity which in turn permitted the definition of braided river stability with regard to bed load transport. The study of Métivier and Meunier (2003) was extended

further by Meunier and Métivier (2006) using a micro-scale modelling approach. They conducted 159 experiments with varying slope, water discharge, input sediment discharge, grain size and flood plain length. Bed load transport at the outlet is correlated with both stream power index and input flux for all the grain sizes. The correlation of input/output solid fluxes showed to be enforced with coarse material. The high input sediment load tends to decrease the bed load transport rate and forced the river to braid. The idea that increasing braiding intensity is a morphological response to a high sediment load and coarse grain size confirms previous works by Hoey and Sutherland (1991) and Warburton and Davies (1994). They further explored the influence of different characteristic length scales (flow depth, flood plain length) on the transport dynamics. They showed that bed load is probably related to the ratio of water depth to grain size as suggested by Bagnold (1973).

The response of an alluvial river to a vertical offset of its bed has also been investigated using the micro-scale modelling technique. Malverti *et al.*(2007) used a laminar micro-scale river to investigate the response of an alluvial river to a vertical offset of its bed generated by faulting. They developed a model to predict the evolution of bed elevation by solving sediment mass conservation together with transport law and shallow water equations. Predictions of the model were found to be in good agreement with the experimental observation. Moreover, the equations governing the evolution of a natural or an experimental micro-scale river are found to be identical. The difference in time and length scales at work in experimental and natural rivers are found to be encoded in the expression of two parameters, namely the critical slope that defines the threshold slope below which no sediment is transported and a diffusion coefficient. This justifies the use of a micro-scale river and provides the key to extrapolate the experimental results to the field scale.

Anthropogenic aggradation of the Waiho River, South Westland, New Zealand has been investigated using micro-scale modelling (Davies and McSaveney, 2001). A 1:3333 scale micro model was constructed and allowed to develop to equilibrium with steady inputs of water and sediment. After the boundaries of the model were altered to represent the presence of control banks and hence restriction of the ability of the river to move over the whole of its natural fan head, the model fan head was found to aggrade in

a spatial pattern similar to that recorded in the Waiho River. They concluded that the aggradation in the Waiho is a result of the lateral restriction of the river by stop banks.
With the popularity of micro-scale modelling to investigate natural processes such as alluvial fan dynamics, knick point migration and channel morphologies as braiding and meandering, a question has been raised on how to extrapolate the results from a micro-scale to natural rivers. When comparing these models to field examples it has to be remembered that they are not exact scale models and therefore care must be taken when interpreting the results in a field environment. This was addressed by Malverti *et al.*(2008) by measuring average flow velocity and sediment transport in an experimental micro-scale river. The sediment transport in the micro-scale river is found to be consistent with the law of Meyer-Peter and Muller (1948) commonly used to describe sediment transport in natural rivers, although with a different coefficient. The average flow velocity was also correctly predicted from the Navier-Stokes equation solved for a steady-uniform laminar flow. On this basis, a set of equations were derived to rescale bed elevation, downstream distance, time and uplift rate from an experimental micro-scale river to the field scale. They also showed how the set of equations can be used to rescale these same parameters in the case of a temporally varying discharge. Numerous investigations have successfully used micro-scale models in geomorphology and they have proved extremely useful, especially for prediction and gaining an understanding of initial and boundary conditions that were unknown from field observations prior to the onset of the experiment.

### 3.4.NUMERICAL MODELLING

A numerical model uses numerical methods to solve equations that represent the processes governing a particular phenomenon of interest. Kirkby (1996) defined numerical models as ”simulating the effects of an actual or hypothetical set of processes, and forecasting one or more possible outcomes”. Evolution of geomorphic features over long periods of time cannot be directly observed or measured easily and so, according to Kirkby (1996), a model can be used to extrapolate measurements from short-term processes to the long-term. Initial and boundary conditions are rarely known with accuracy and hence models are needed to interpret the observations in terms of

process understanding; allowing the exploration of ideas, formulation of initial hypotheses and, ultimately, behaviour prediction (Bras *et al.*, 2003).

### 3.4.1. Description of Fluvial Models

There are different types of numerical models, which serve different purposes and help to answer different types of questions. They can be categorized in various ways, the most common being according to the number of dimensions in which they represent the spatial domain and processes, one-, two-, or three-dimensional models can be identified.

The most general approach to model free surface flow, although not the most often used, is to compute the fully three dimensional flow with a specific treatment of the free surface boundary. But, it is not very efficient to use this approach mainly because of its computational cost and data requirement. They are most complicated and resource consuming. Though the approximation error decreases as model resolution is increased, this has been highly limited by computer speed and memory resources, although this constraint is declining (Wu, 2007). Examples of three dimensional models includes Lane *et al.* (1999), Nicholas and Sambrook Smith (1999). But there are a lot of commercially available three dimensional models.

In order to address the limited applicability of full 3D flow simulation, those equations used in modelling three dimensional free surface flow are commonly further simplified to derive the depth averaged shallow water equations, commonly called St. Venant equations or two dimensional shallow water equations. They are obtained after vertical integration of the three dimensional shallow water equations. The resulting equations are widely used to model free surface water flows, overland flows or flows in open channels. According to Wu (2007) if the vertical variation of flow and sediment quantities in a water body are sufficiently small or can be determined analytically, their variation in a horizontal plane can be approximately described by a depth-averaged two dimensional model. The main hypothesis which has been done to drive the two dimensional shallow water equations is the assumption of a hydrostatic pressure distribution. This assumption implies that in shallow water open channel flows the

vertical scale is much smaller than the horizontal scale; an assumption which depends on flow conditions and hydraulic geometry. The derivation of the two dimensional shallow water equations consists basically of integrating the X- and Y- component of the three dimensional momentum equations over the vertical direction, applying Leibnitz's rule and using the kinematic free surface and bed surface conditions. For flow over a mobile bed boundary, these shallow water equations are coupled to equations of conservation of sediment mass and evolution of bed topography. Many two dimensional models are user-friendly and popular because of the easy data input and visualization of results. They provide spatially varied information about water depth and bed elevation within rivers, lakes and estuaries. Three of the most commonly used 2D hydrodynamic models are *MIKE21* (Water, 2002) , *CCHE2D* (Wu, 2001), and *HSCTM2D* (Hayter *et al.*, 1999) . MIKE21 is a comprehensive modelling system for simulation of flow, wave, sediment and ecology in rivers, lakes, estuaries, coastal areas and seas in two dimensions. It can be applied to any two dimensional free surface flows where stratification can be neglected. CCHE2D is a two dimensional depth averaged unsteady flow and sediment transport model. It can be used to simulate non-uniform sediment (both cohesive and non cohesive) using non-equilibrium sediment transport approaches. *HSCTM2D* is composed of two parts; a hydrodynamic model called *HYDRO2D* and contaminant and sediment transport model called *CS2D*. However, there are many other commercially available two dimensional hydraulic and hydrodynamic models. Simulation of secondary flow and its influence on transport processes is mentioned to be the weakest part in most two-dimensional models (Duc *et al.*, 2004).

One-dimensional models utilise the most simplified assumptions of the three and two-dimensional models. They assume that the primary component of interest is only one dimensional (generally longitudinal). These models are quick to run and it is relatively easy to alter the boundary conditions, whilst also providing informative simulations. Early one-dimensional models were used to derive slope simulations and explore basic concepts in hill-slope profile development (e.g. Ahnert, 1970;Kirkby, 1971). Since then they have been used to investigate a variety of fields within geomorphology. Despite the simplifying assumptions in one-dimensional models they have been found to adequately

describe in-channel flow, providing a prediction of water surface elevation and velocity as well as large scale sediment transport processes. However, there are clear limitations to one-dimensional modelling approaches as they treat flow and sediment transport processes on a width-averaged basis. As a result, they underestimate the bedload flux in channels with substantial lateral variability in hydraulic conditions (Ferguson, 2003).

The most extensively used fluvial models are either one-dimensional or two-dimensional depth averaged. Most of the numerical models developed so far are based on the following five equations: continuity and momentum equations for water flow; the sediment continuity equation, commonly called as the Exner's equation; hydraulic resistance estimator; and, sediment transport equation. Those equations can be adapted either for one-dimensional, two-dimensional or three-dimensional cases depending on the problem under consideration.

Another major challenge for modelling shallow water flows and sediment transport is representation of resistance. Previous researchers used different roughness estimators for similar studies and they often calibrate roughness coefficients to reconcile modelling outputs with measurements (Cao and Carling, 2002). Associated with sediment transport are bed features such as ripples and dunes. These features can change their size and form as the sediment transport varies. Alluvial channels are subjected to considerable difference in sediment transport rate that will give rise to significant differences in roughness and hence the roughness cannot be assumed to be fixed. The roughness does at least vary between the main channel and floodplains.

The sediment transport capacity equation can be described as a function of flow parameters using a standard sediment transport equation (e.g. Cui and Parker, 2005;Cui *et al.*, 1996;Wong and Parker, 2006;Miglio *et al.*, 2009) or may be estimated by an empirical power function (Bhallamudi, 1991;Jaramillo, 1984) depending on the data. Many investigators have developed both analytical and numerical frameworks to solve the shallow water equations.

### 3.4.2. Numerical Modelling in Braided River studies

Numerical models developed to investigate braided river processes include two-dimensional flow models (Lane *et al.*, 1995;Nicholas, 2003;Lane and Richards, 1998), three-dimensional flow models (Lane *et al.*, 1999;Bradbrook *et al.*, 2000;Nicholas and Sambrook Smith, 1999) and flow models that incorporate sediment transport functions (McArdell and Faeh, 2001et al, 2001;Olesen and Tjerry, 2002;Kurabayashi *et al.*, 2001). One-dimensional models of braiding are unable to represent two-dimensional process-form dynamics. However, there are a few examples of such models (Paola, 1996;Nicholas, 2000).

Lane *et al.*(1995) and Lane and Richards (2000) applied a model called STREMR which solves the Reynolds averaged and depth-averaged momentum (Navier-Stokes) equation. Using input parameters that included bed topography, discharge, bed roughness and water surface, it was possible to derive spatially distributed patterns of velocity and eddy viscosity. Lane *et al.*(1995) showed that two-dimensional models were able to provide reasonable estimates of the depth averaged velocity field. Lane *et al.* (1995) also suggested that flow patterns are a result of the interaction between inertial and topographic effects and list grid resolution and boundary conditions as factors that need particular investigation in order to improve model prediction. However, there remained considerable uncertainty over the extent to which the model was representing adequately the effects of three-dimensional processes upon the two-dimensional velocity field (Lane *et al.*, 1999). Of more interest to this project are the numerical models that are used to simulate the reach-scale hydraulic characteristics of braided rivers and their dependence on discharge (Nicholas, 2003). Nicholas (2003) applied a two-dimensional hydraulic model to the braided reach of the Avoca River, New Zealand. Parameterization of bed friction was optimized using measured water surface elevation, flow depth and velocity at low flow. He showed that the systematic trends in the measured flow variables are reproduced by the model, although there are differences in the scale of processes measured in the field and represented by the model. Modelled shear stress distributions of runs conducted at higher discharges fit gamma distributions and showed a clear systematic trend of the gamma shape parameter with

increasing discharge. He notes that the approach is a powerful tool for generating hydraulic data that would be difficult to obtain in the field at the same spatial resolution, however, evaluating the accuracy of process representation is confounded by the lack of field data. Moreover, such approaches have important limitations. They are computationally expensive, which precludes their application to braided river evolution at large temporal and spatial scales. This has led to the development of cellular automata models for addressing larger scale problems.

The two-dimensional cellular models have recently been applied in braided river studies. Those models use relatively simple relationships but offer the potential to provide a semi-quantitative understanding of the interaction between flow, sediment transport and channel morphology. Considerable interest in the application of cellular modelling for braided river studies has been inspired by the landmark paper of Murray and Paola (1994). The Murray and Paola (1994;Murray and Paola, 1997) model showed that even a relatively simple geomorphological model can replicate many of the characteristics of braiding. It simulated the development of braided rivers by routing water discharge through a grid of cells representing the channel and braid plain according to local variations in bed slope. The model provides the insights into fundamental controls on the maintenance of braided channel pattern and a number of the general morphological and dynamic features of braided rivers in a simplified form (Murray and Paola, 1994;Murray and Paola, 1997). Murray and Paola (2003) integrated a simple vegetation growth model to examine how stabilizing the braid plain with vegetation would alter the channel pattern. The vegetation enhances bank resistance to erosion causing the development of a single channel instead of a rapidly changing, multiple channel (braided) pattern. Recently, the representation of braided channel morphodynamics in the Murray and Paola model was also tested against the known characteristics (mainly from a sequence of high resolution digital elevation models) of a physical model of braided stream (Doeschl-Wilson and Ashmore, 2005). The modelled evolution shows little resemblance to the real evolution of the small-scale laboratory river and does not reproduce the real bar-scale topography and dynamics even when the grid scale and amplitude of topography are adapted to be equivalent to the original Murray and Paola results (Doeschl-Wilson and Ashmore, 2005). Strong dependence of

the modelled processes on local bed slope rather than energy slope was suggested to be one of the causes of the differences between numerical model results and physical model morphology and dynamics. Although, the Murray and Paola (1994, 1997) model offers the potential to provide a semi-quantitative understanding of flow and sediment transport processes, the model suffers from a number of limitation particularly the inability to generate realistic predictions of distributed flow and inundation patterns, resulting from the simplified process representations that their water routing schemes typically incorporate (Thomas, 2003). Thomas and Nicholas (2002) and Thomas *et al.*(2002) presented a new cellular model of flow, sediment transport and morphological change with an improved physical basis that addressed the limitations of past cellular automata approaches. This model provides an example of a high-resolution reduced-complexity approach that seeks to represent flow-sediment transport interactions at sub-width scales. This improved cellular model of Thomas and Nicholas (2002) was tested in the braided reach of the Avoca River, New Zealand and is capable of replicating the flow patterns observed in the field at low discharge and the predictions of a more sophisticated two-dimensional hydraulic model, *hydro2de* at high flows. The coupled flow-sediment transport model has also been tested in real braided channels and by considering the morphological characteristics of channels generated in numerical experiments. Evaluation of modelled braided channels indicates that the simulated channels are statistically similar to natural streams. In addition, modelled morphological change in response to changes in upstream sediment supply was seen to reproduce channel characteristics that were similar to those reported in the literature (Nicholas *et al.*, 2006). Overall, it has been suggested that cellular automata models "succeed in capturing the complex balance of positive and negative feedbacks that control the emergence and maintenance of channel form, despite parameterising water and sediment routing merely as functions of local bed slope'' (Hardy, 2008 ,p219).

Most two-dimensional numerical models simulate flow only and relatively few studies have coupled flow models based on the Navier-Stokes equation with sediment transport equations to predict braided river morphology and channel changes. A two-dimensional finite element hydrodynamic model *(2dmbe)* that solves the depth-averaged shallow water equations coupled with sediment transport (suspended load and/or bedload) and

mobile bed component was developed by McArdell and Faeh (2001). Their model produces braiding including the emergence of mid channel bars to form flow dividing islands, although at a small spatial scale. Moreover, it could be used to address the distribution of flow across known topography. However, limitations that were identified include inability to address the possible effects of secondary flows probably due to the depth averaged flow treatment and lack of dry areas possibly due to underdevelopment of the bed topography or use of inappropriate values of constant discharge.

Three-dimensional computational fluid dynamics models have also been used to simulate flow hydraulics around mid-channel bars and in channel confluences (e.g. Lane *et al.*, 1999;Nicholas and Sambrook Smith, 1999;Bradbrook *et al.*, 2000;Nicholas and McLelland, 2004). These studies have shown that simulation results are generally qualitatively consistent with flow structures observed in the field and offer an improvement from similar two-dimensional models. Quantitative comparison between field and model velocities indicated positive correlation between the two, but highlight the sensitivity of model results to the parameterization of roughness and turbulence. DELFT3D, which solves the Navier-Stokes equations in three-dimensions, is a widely used commercial model that has state-of-the-art sediment transport routines and includes the effects of wind and waves on flow and sediment transport (Hydraulics, 1999). Hibma *et al.* (2004) have used DELFT3D and modelled a braiding like pattern of sub-aqueous shoals and channels in a large tidal estuary. However, they concluded that the complexity of the model makes it very difficult to understand why it produced the estuarine bathymetric patterns that it did. There has been a recent trend towards three-dimensional modelling; however Lane *et al.* (1999) mentioned that the move towards increasingly sophisticated models must be weighed against a considerable increase in computational time and resources and the need to understand the fundamental assumptions that lie behind model development.

### 3.5.APPROACH TO BE USED IN THIS PROJECT

The literature reviewed demonstrates that achievement of the aims outlines in section 2.6.1is dependant on generation of dataset that can demonstrate the effects of variable

sediment supply scenarios on braided rivers. Therefore, to fulfil the objectives of this project a three-fold integrated methodology will be embarked upon:

(1) Physical model experimentation to allow observation of the effects of aggradation and degradation on channel morphology and sediment transport of a braided river as it develops in scaled time and space. A micro-scale physical model, following a 'generic' approach will be built to enable observation and recording of braided river evolution over varying sediment supply scenarios (Chapter 4). The output from this will provide a wealth of qualitative and quantitative data (Chapter 5 and 6).

(2) The resultant experimental data and digital elevation models from the micro-scale physical model will be used in a two-dimensional hydraulic model to generate flow depth and shear stress predictions. This will assist in the understanding of the controls on shear stress distribution and its effect on sediment transport and channel evolution. The numerical model used is described in Chapter 7.

(3) Comparison of the trends observed on the experimental channels with those identified in field observations from the Megech gravel bed river in the highlands of the upper Blue Nile basin, Ethiopia (Future work section of Chapter 8).

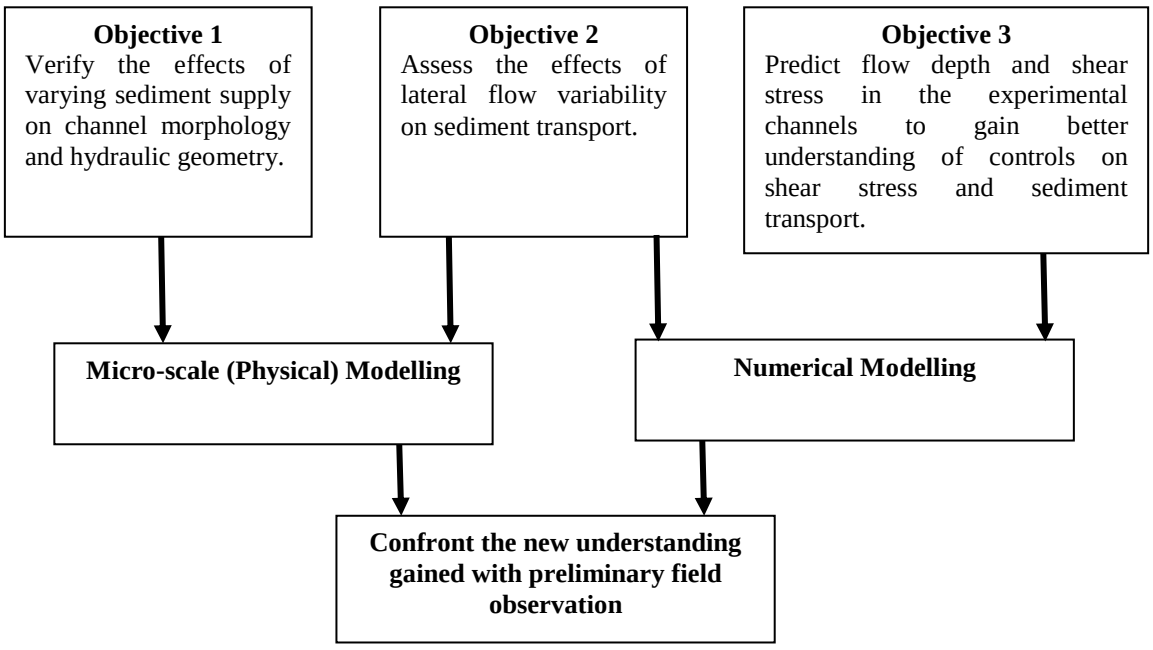


**Figure 3-2 Flow chart showing the integrated methodology used to address the research objectives**

## 3.6.SUMMARY

This chapter reviewed the three main methodological approaches used in braided river research: field measurement, physical modelling and numerical modelling. Field measurements have been used for numerous investigations into braided rivers, but this can often be problematic when investigating the impact of aggradation and degradation on sediment transport and channel morphology of braided rivers as it is difficult to monitor the influence of these in isolation and it will take very long time to perceive their effects. Advances in physical and numerical modelling approaches have enabled braided river researchers to recreate braided rivers in controlled conditions and observe the main braiding mechanisms and changes in sediment transport and channel morphology over long time periods to determine the influences of varying sediment input to the system. The chapter concludes with an explanation of the methods that will be used in this project; experimental micro-scale physical modelling to provide an improved understanding of braided river responses to sediment supply variations, and using two dimensional hydraulic model and field measurements to assist in the understanding of the controls on shear stress distribution and its effect on sediment transport and channel evolution.

# 4. PHYSICAL MODEL EXPERIMENTAL DESIGN AND DATA COLLECTION

## 4.1. OVERVIEW

In the preceding chapter, the broad methodological approaches to braided river investigation were summarised and the rationale for the approach used in this study was provided. The approach will include, physical modelling, numerical modelling and field observations. The aim of this chapter is to explain the experimental design used in the physical modelling element of this research. After a brief description of the main features of the experimental apparatus, previous studies employing physical hydraulic modelling at micro-scales are used to develop an approximate scaling procedure; this is used to determine model parameters. This is followed by a short description of the experimental scenarios employed and of the series of initial experiments that were undertaken to evaluate the potential of micro-scale experiments. On the basis of these experiments it was possible to establish that the approach was effective and that appropriate boundary conditions could be defined. Finally, the basis for selecting five experimental scenarios for further analysis is outlined.

## 4.2. EXPERIMENTAL APPARATUS

For this study a physical model will be used to investigate changes in channel morphology and sediment transport of braided rivers as a result of aggradation and degradation. To achieve this, a micro-scale model approach has been adopted. The model is not scaled to any specific prototype, but an utmost effort is made to make realistic representations of boundary conditions where possible (see Section 3.3.2 for more detail on micro-scale modelling). The boundary conditions include that of the water and sediment input to the experimental channel. The requirement for this is described in section 4.3.1 in greater detail. The model is intended only to represent gravel-bed braided rivers due to the fact that in the case of sand bed rivers model grain sizes will be reduced to unacceptable limit.

The work for this project was carried out in the University of Exeter Experimental Landscapes Facility in a multi-purpose contemporary terrain modeller (sedimentation tank). The purpose-built sedimentation tank, designed by Dr James Brighton (JBL Design & Cranfield University) has internal dimensions of 5m length, 2.7m clear width and 1m depth. Rails running longitudinally on either side provide location and measurement datum to within +/-3mm under any loading condition (JLB Design Ltd, 2007). A false floor was constructed up to 0.75 m depth to reduce the depth of sand required to 0.25 m.

The tank is pivoted at its lower edge and can be angled to a maximum of $15^0$ from the horizontal. The tank is equipped with four 150mm wide cuts to simulate lateral flows if required and if not there are plates to cover the cuts. To facilitate base level change studies, the elevation of both the upstream run-on plane/inlet channel and the vertical downstream weir can be adjusted remotely using the hard-wired computer controller (see Figure 4-1). Bed topography can be measured by a laser micro-topographic scanner which can traverse the whole 5m length of the tank along a carriage mounted on a high accuracy rail system. The scanner measures output bed topography to a resolution of 1mm in cross stream (y) and downstream (x) directions and 0.1mm in elevation (z). The carriage and laser were both automatically controlled by software (run from the control station labelled in Figure 4-1). Water is pumped to the upstream inlet from a 100 litre water tank. The tank is supplied with mains water via a float controlled inlet valve so that a constant pumping head can be maintained. Sediment is supplied at a controlled rate to the upstream inlet using a variable speed gravity-fed sediment hopper. The sediment drops into the inlet groove made of steel where it mixes with the water, being fed at a specified discharge, before reaching the basin. At the point where the mixed water and sediment drop vertically onto the flume surface, smaller gravel is placed on the surface to dissipate the energy of the incoming water and thereby to prevent bed disturbance. Potassium permanganate solution was added regularly to the flow to facilitate flow visualization and identification in imagery.

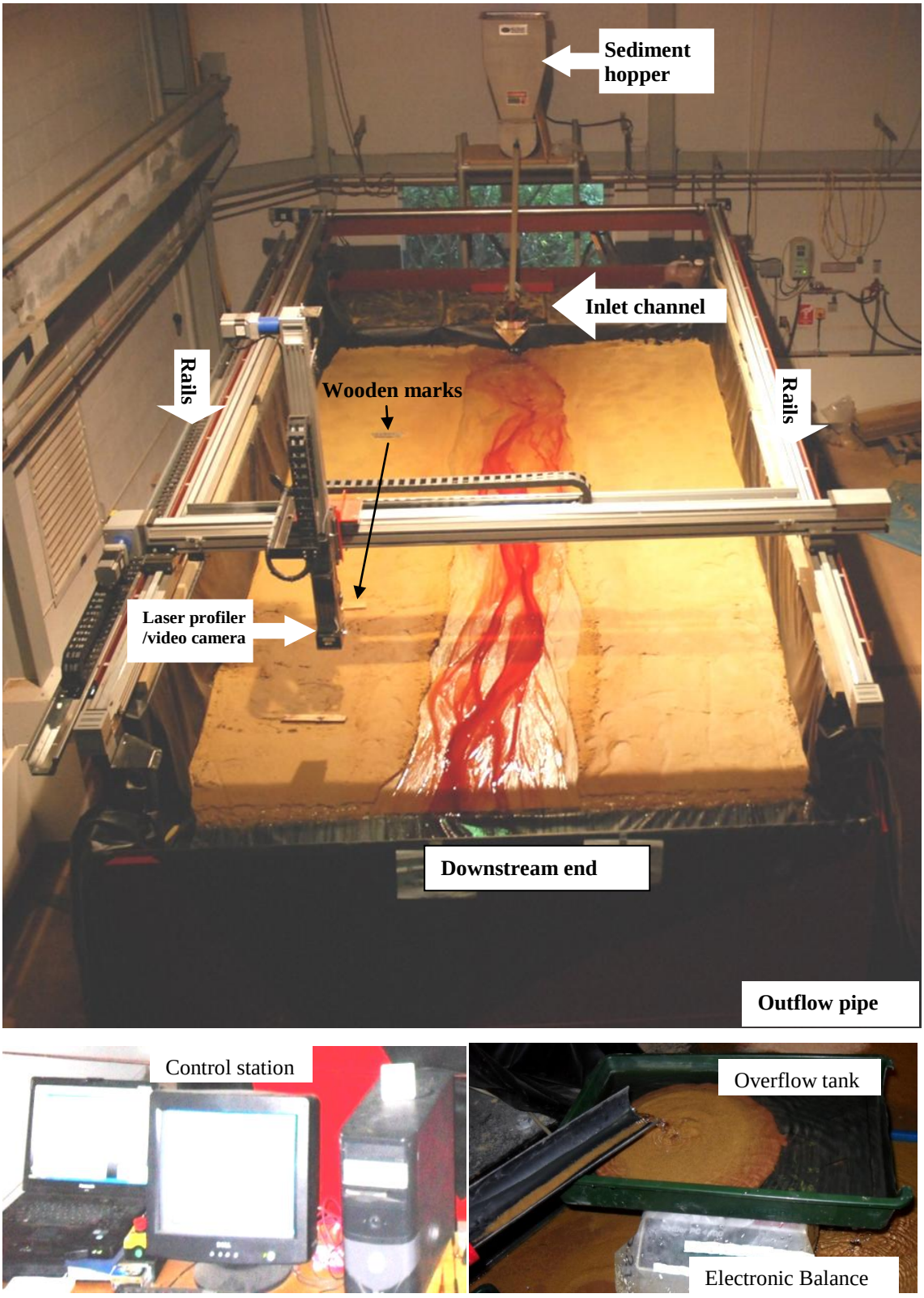


Figure 4-1 The Experimental apparatus

At the downstream end of the basin a plastic gutter conveyed both the liquid and sediment flux to a constant head overflow tank. The tank rested on a high precision laboratory scale (accuracy 0.1g) which was used to measure the mass of sediment and water at 5 minute intervals. These measurements were used to derive the cumulative mass of exported sediment. These data were used with observations of channel width at the downstream flume to derive sediment transport per unit river width. Neither sediment nor water is recirculated in the system.

### 4.3.Experimental Design

In most mobile bed physical modelling studies the focus is on a few crucial processes and conditions are defined to deliver representative values for the important hydraulic variables. Studies rarely attempt to simulate all flow and sediment transport processes. As discussed in the chapter 3, in case of formal physical modelling (Froude scale modelling), the primary task is to ensure that all the important forces and motions in the model and prototype are in the same proportion. The dimensionless numbers appropriate for the given flow situation should have the same value in the prototype and model.

Generally in undistorted Froude scale models, geometric similarity must be obeyed in all length parameters, slope, relative roughness ($y/d_{50}$) and Froude number (i.e. these should be the same in model and prototype) whereas in distorted models the horizontal scale is more than the vertical, and slope and Froude number are slightly exaggerated. As length scales are driven by the particle size, relative roughness ($y/d_{50}$) will stay the same and other parameters will be developed accordingly.

In micro-scale modelling, these formal similarities are rarely achieved. Some previous micro-scale models have used arbitrary combinations of parameters (Malverti *et al.*, 2008;Meunier and Métivier, 2003;Métivier and Meunier, 2003;Malverti *et al.*, 2007;Hong and Davies, 1979) and some others used highly exaggerated length scales (Davies *et al.*, 2003;Gaines and Maynord, 2001) with horizontal scale in excess of 3000 times the vertical scale. An important parameter which will help to establish if bed material transport is expected is the bed shear stress.

Kamphuis (1991) suggests that laboratory effects in physical models are analogous to problems in numerical models caused by numerical approximation to the equations, round-off and truncation errors, and computer speed, memory, and availability. As the prototype/model scale ratio increases, the consequence of scale effects also increases. Scaling effects are reasonably well understood for fixed bed models (Hudson *et al.*, 1979;Dalrymple, 1985). Nevertheless, scaling effects in the material used to represent sediment in a movable bed physical model are less well understood. Common scaling problems arise when a model is designed exclusively according to the Froude modelling condition or when the prototype grain size is diminutive. In those cases the size of bed materials will be reduced beyond acceptable limits. This presents a problem for sand bed prototypes because replacement of sand grains by model grains using a linear scale will result in use of particles with very different physical features (Struiksma, 1986). Moreover, the fine sediments that would be used are often cohesive, and the significant surface tension force can make them float on the fluid, and when used they can cause ripple formations on the bed that have no equivalents in gravel-bed rivers (Young and Warburton, 1996). For this reason model scales are usually guided by the geometric scale imposed by the given particle size (e.g. Ashmore, 1991b). Since the threshold value between cohesive and non-cohesive sediment is around 0.065mm (Hudson *et al.*, 1979;Dean, 1985), it is suggested that model grain size should not be less than 0.065mm and some studies have employed a higher threshold to ensure that the sand is loose and to avoid the above effects

Having elected to pursue a micro-scale modelling approach within the experimental apparatus, there are a series of model parameters that must be defined:

- Scaling – although formal similarities are not pursued, it is important to maximise the potential for comparison with natural analogues by careful consideration of scaling and definition of:
    - Length scale
    - Time Scale
- Boundary Conditions
    - Discharge
    - Sediment Supply

The final element of Experimental Design is the definition of scenarios to be explored. Each of these elements is outlined in the following sub-sections

### 4.3.1. Length and time scale calculations

Length-scale calculations are needed to determine the most appropriate grain-size to use during the experiments within the available experimental setup. According to Malverti *et al.*(2008), relationships for up-scaling of length and time parameters of a micro-scale experiment to natural rivers are given by the following ratios:

$$\frac{h_l}{h} = \frac{\Delta_l}{\Delta}\frac{l_l}{l} \quad \text{4-1}$$

$$\frac{X_l}{X} = \frac{l_l}{l} \quad \text{4-2}$$

$$\frac{t_l}{t} = \frac{{l_l}^2}{l^2}\frac{1-\lambda_l}{1-\lambda}\frac{D}{D_l} \quad \text{4-3}$$

$$\Delta_l = \frac{{R_l}^3 {d_l}^3 g {\theta_l}^3}{3\vartheta_l Q_l} \quad \text{4-4}$$

Where h denotes river bed elevation, Δ is threshold slope below which no sediment is transported; x is downstream distance, $l$ refers to characteristic length of the river channel the choice of which depends on the problem under consideration (it could be the length of a reach if one is to investigate the river profile at a more local scale), t is time, λ is the bed porosity and D is a diffusion coefficient. The subscript $l$ in all the equations refers to the micro-scale experiment and parameters without subscript are for the natural river. These equations were developed to address the issue of up-scaling the longitudinal profile development of a micro-scale channel to a natural river. Having said this, values of porosity for experimental micro-scale rivers and natural rivers lie within the same range; 0.35-0.4 for micro-scale river beds (Malverti *et al.*, 2008) and 0.15-0.35 for natural rivers (Frings *et al.*, 2008). This will mean the relationships for up-scaling (down-scaling) mainly depends on the characteristic length scale, the diffusion coefficient and the threshold slope (Malverti *et al.*, 2008). The length scale solely depends on the characteristic length of the river reach and the laboratory flume. This means for local problems of natural rivers, for which length typically ranges between 5 and 10 km, will have a length scale of about 1:1000 to 1:2000 on a 5m long laboratory flume.

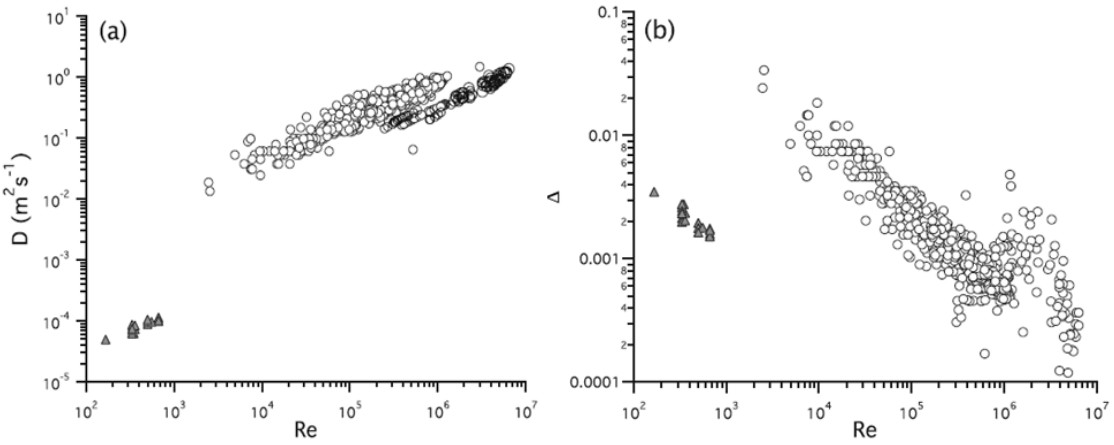


**Figure 4-2** **Typical values of (a) diffusion coefficient and( b) threshold slope as a function of Reynold's number for natural rivers (circle marks) whose median diameter is greater than 2mm and micro-scale experimental rivers (triangle marks). Taken from (Malverti *et al.*, 2008)**

Equation 4.4 is similar to a distorted physical model scale equation with ($l/l_l$) representing the horizontal scale, ($h/h_l$) as the vertical scale and ($\Delta/\Delta_l$) as distortion ratio. A distorted model will usually have larger horizontal scale than the vertical scale. This has the effect of lessening the required horizontal space while increasing slopes in the model. So the effects of having steeper slope on the sediment transport will also come as a result of distortion (details in section 3.3.3.1). There is no strict limit for the level of acceptable distortion in movable bed hydraulic models. Glazik (1984) put 1.5 as an acceptable level of distortion to provide adequate results for movable bed models whereas Suga (1973) used 5 in his experiments but recommended no distortion for studies related to scour depth. ASCE (2000) suggests a maximum limit of 6. Micro-scale rivers commonly use distortions ranging from 8 to 15 (Maynord, 2006). However, it is generally believed that distortion should be kept as low as possible to minimize scale effects. Figure 4-2 shows typical values of the threshold slope (related to distortion in this case) and diffusion coefficient for natural rivers from different environmental conditions and micro-scale experiments as a function of Reynold's number. Values of threshold slope ($\Delta$) for natural gravel-bed rivers varies, on average, from 0.0001 to 0.01. Laboratory experiments at a micro-scale have also shown that they have a similar range of threshold slope from 0.001 to 0.01, giving a range of variation of the threshold slope ratio $\Delta_L/\ \Delta$ between 1 and 10, which is within the commonly used level of distortion for micro-scale channels. This would suggest an order of magnitude estimate for the vertical scale ($h_l/h$) from equation 4.3, and hence an idea of model grain size by assuming vertical model scales guided by the geometric scale imposed by the

given particle size. Based on this, vertical scale will be in the range of 1:100 to 1:1000 for a 5 km length of river. Published data on grain-size distributions of gravel-bed rivers (e.g. Young and Warburton, 1996;Ashmore, 1991b) also informs the choice of order of magnitude of the model grain-size. Finally, the restrictions on the size range of sand that was available for purchase was considered. The final model grain size distribution is shown in Figure 4-3.

The other important consideration in physical modelling is time scaling. Malverti *et al.*(2008) used the following equations to estimate approximate time scales for natural and micro-scale channel to evolve:

$$t = (1 - \lambda) l^2 / D \qquad 4\text{-}5$$

$$t_L = (1 - \lambda_L) {l_L}^2 / D_L \qquad 4\text{-}6$$

Where t and $t_l$ represents the characteristic time scale for a natural river and experimental micro scale river to evolve. Equations 4.8 and 4.9 are applied directly for the experimental range and with typical values for the parameters taken from Figure 4-2. This means the experimental river with a net length of 4m (excluding the entrance and exit), porosity of 0.4 and diffusion coefficient $D_L$ of $10^{-4}$ evolves on a characteristic time scale of about 96000 s (~ 26 hours) and this is equivalent to a time scale of between a month and 55 years in natural rivers with only 5 km local reach length. Doubling the reach length will increase the characteristic time scale by four times, similar to the vertical scale of accretion or erosion noted by Yalin (1971). This difference in time scale is one reason for the keen interest in the use of micro-scale models (Malverti *et al.*, 2008) to explore longer-term morphological evolution.

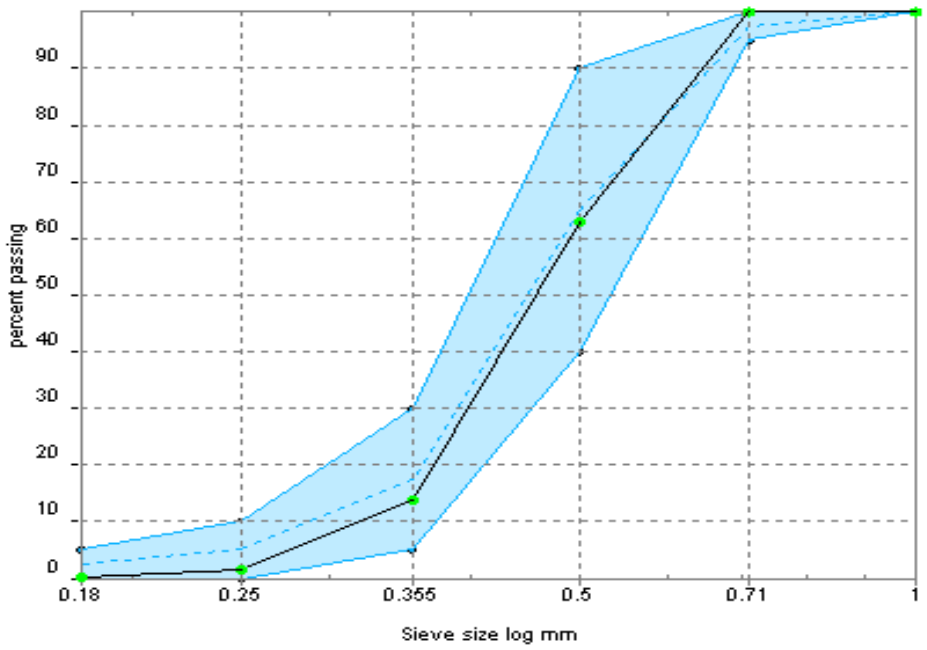


**Figure 4-3 Gradation curve of the sand used in the experimental runs**

### 4.3.2. Basis for water and sediment discharge calculations

The parameters for this project are calculated for sand with a grain size distribution varying from 0.25mm-0.71mm ($d_{50}$~0.47mm). The experimental sediment grain size and water discharge relationship is established mainly using the Shields theory (Shields *et al.*, 1936) for initiation of bed materials. As this study does not seek to simulate a particular river, there is no strict similarity between values of sediment feed rate and water discharge. Even if there is debate on the scatter of the data and the interpolation of the trend line in the original Shields diagram (Peakall *et al.*, 1996), research has shown that it is possible to create a completely movable bed for $\tau^*_c$ (critical shields parameter) more than 0.056. For example, as quoted in Glazik and Schinke (1986), results from Liebs (1942), under the assumption of specific gravity of 2.65, indicate that a Shields parameter of 0.03 represents "initial movement of single grains", 0.047 represents "initial, though slow, transformation of the bed, and 0.076 represents "beginning of vivid bed material movement". The selected critical bed shear stress will vary depending on the hydraulic conditions in the flume. So, to create a moderately moving bed for $d_{50}$ = 0.47mm, critical bed shear stress ($\tau_c$) values are chosen (for water at 20$^o$c) from the Shield's diagram (Shields *et al.*, 1936). If a given critical bed shear stress ($\tau_c$) for a particular average grain size is less than the applied bed shear stress then movement of the bed material is expected. Flow depth is then calculated

using the uniform flow approach and equivalent roughness is estimated using a Keulegan type roughness estimator. Based on this and a preliminary channel width of 0.2m, the threshold discharge is calculated. The channel dimension is chosen to just accommodate the imposed discharge and keep the influence of the flume walls to a minimum later in the experiment when the river braids and expands in width. This approach gives order of magnitude estimates of model parameters to be used under a specified condition of grain Reynolds number. Experimental discharge values are selected based on this reference and slightly refined based on prevailing experimental conditions and characteristics of the available water pump.

At the start of each experiment the sediment and water discharge rates were set to the predetermined values and held constant throughout the experiment, unless the experiment dictated otherwise. An estimate of the sediment feed rate to use in subsequent experiments was arrived at after a period of time during which the sediment collected in the overflow tank was monitored (Figure 4-4). The aim was to achieve and maintain a balance in feed and transport rate and to avoid long term aggradation at the entrance of the river channel. This experiment was carried out with a discharge of 3.5 l/min (0.0583 l/s) and gave an estimate of the amount of sediment transport to be expected in subsequent micro scale experiments. However, this does not imply that the channel is in absolute equilibrium as there was no long term monitoring of either longitudinal slope or channel configurations. There appeared to be a small amount of variation in sediment feed rate in the long term (hours) which proved to be very difficult to quantify. Accordingly, an effort was made to ensure that sediment feed was approximately constant by frequent checking of the feed rate and continual addition of sediment to the hopper to keep the level of sediment in the hopper constant.

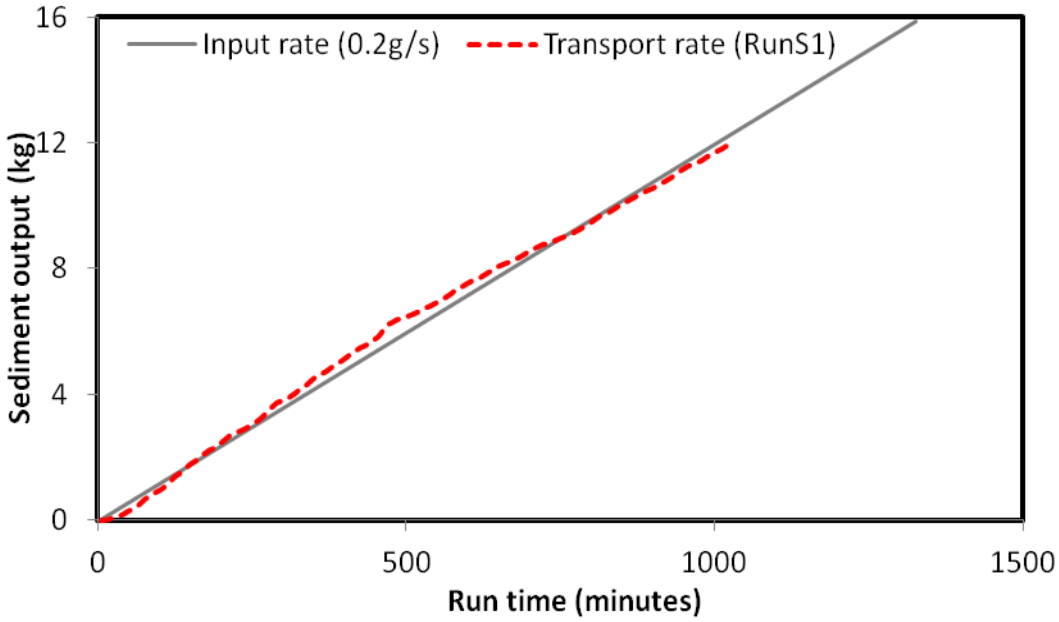


Figure 4-4 Cumulative sediment transport curve

### 4.3.3. Summary of model parameters

For this project, since the model is intended to be a generic one it is not really important to perfectly scale the length dimensions. However, the intention was to establish a relationship between different parameters with a highly exaggerated length scale like the one used by Davies et al.(2003), while keeping vertical distortion within acceptable limits. This relationship only helps to give an idea of the kind of Prototype Rivers to which the results can be applied or compared.

The tables below (Table 4-1 and Table 4-2) show a rough comparison of the values of some parameters used in the experiments in this study compared to previous Froude scale models, micro-scale models and natural rivers. The expectation is that by obeying gross scaling procedures some of the details of the modelling will in effect take care of themselves and at least give approximate similarity of process, because some of the scale free parameters of braided streams correlate strongly among themselves regardless of stream sizes (Howard et al., 1970).

**Table 4-1 Comparison between the typical range of parameters in Froude scale models, micro-scale models, and natural rivers (original table from Malverti *et al.* (2008) and modified for this study)**

| PARAMETERS | FROUDE SCALE MODELS | MICRO-SCALE MODELS | NATURAL RIVERS | THIS STUDY |
|---|---|---|---|---|
| **Flume length (m)** | **3-160** | **1-3** | **-** | **~5** |
| **Flume width (m)** | **1-4** | **0.05-2** | **-** | **2.7m** |
| **Channel width (m)** | **0.1-4** | **0.01-1** | **1-1000** | **0.1-1** |
| **Average flow velocity (m/s)** | **$10^{-1}$-1** | **0.05-0.5** | **0.1-4** | **0.1-0.2*** |
| **Y/d** | **4-$10^{5}$** | **1-40** | **10-$10^{5}$** | **1-36** |
| **$\rho_s/\rho$** | **2.5** | **2.5** | **2.7** | **2.65** |
| **Slope** | **2.$10^{-3}$-0.02** | **$10^{-4}$-0.05** | **$10^{-6}$-$10^{-2}$** | **0.035-0.05** |
| **$R_e$** | **$10^{3}$-$10^{6}$** | **100-500** | **$10^{4}$-$10^{7}$** | **>400**** |
| **$R_e$*** | | | **$10^{3}$-$10^{4}$** | **9-11.5** |
| **$W_e$** | | | **$10^{3}$-$10^{5}$** | |
| **$B_o$** | | | **$10^{5}$-$10^{7}$** | |
| **$F_r$** | **0.1-1** | **0.5-5** | **$10^{-2}$-1** | **0.74-1.4** |
| **$\tau_*$** | **0.1-1** | **0.01-0.8** | **$10^{-2}$-10** | **0.2-0.5** |
| **Discharge (l/min)** | | | | **2.0-4.0** |
| **Experiment duration** | **0.5-15 days** | **1hr-1week** | **50 years***** | **22-27hrs** |
| **sediment feed rate** | | | | **0.25 g/sec** |

* *velocity calculated by tracking the length travelled by dye (potassium permanganate) solution released at upstream and only represents velocity in the channel occupying most of the water. This is average flow velocity and some values are higher.*

** *Based on the estimated flow velocity and minimum flow depth of 2mm, the Reynold's number is more than 400. A minimum flow depth of 2mm is considered for analysis and anything less is thought to be wet surface held by surface tension.*

*** *Calculated for a reach of river 5 km long using equation 4.6.*

Table 4-2 Comparison of experimental parameters of this experiment with previous micro models

| **Researcher** | Water Discharge (**$Q_W$**) **(l/min)** | Sediment Discharge **$Q_S$ (g/min)** | **Apparatus Dimension (w*l) (m)** | **Study Area** | **Sediment type used and $D_{50}$ (µm)** | **Bed slope (%)** |
|---|---|---|---|---|---|---|
| Malverti *et al* (2008) | 0.1-2 | * | 0.05*0.9 | Braided Rivers | Glass beads (50) | 0.5-5.2 |
| Hong & Davies (1979) | 0.18-1.08 | 1.5-50 | 2*5 | Braided Rivers | Fine sand (170) | 4-10 |
| Malverti *et al* (2008) | 0.5-2.5 | * | 0.05*1 | River response to vertical offset | Glass beads (50-100) | 0.3-4 |
| Metivier & Meunier (2002) | 0.93-2.5 | 1.8-42 | 0.5*1 | Braided Rivers | Glass beads (500) | 3.3-9.2 |
| Davinroy *et al* (1996) | Hydrograph | No info. | Custom built | Sedimentation study of Mississippi River | Plastic urea | No info |
| Smith (1997) | 0.000083-0.00083 | No info | No info | Modelling high sinuosity meanders | Cornstarch, Rock, flour, Kaolinite (35) | No info |
| Davies *et al* (2007) | 0.25-0.5 | 4-6 | Scaled to 1:2500 | Alluvial fan | Fine silica sand (190) | 10 |
| ***This experiment*** | ***3.5*** | ***12*** | ***2.7*5*** | ***Braided Rivers*** | ***Fine sand (470)*** | ***5*** |

## 4.4.EXPERIMENTAL SCENARIOS

To achieve the study objectives, sets of mobile bed micro-scale experiments were designed based on the considerations outlined above. The sediment and water discharge for all the runs were determined from the previous sections and through testing in the trial experimental runs. Trial experiments were run for discharge of 2 l/min to 4 l/min, sediment output was monitored and the experiment with discharge of 3.5 l/min was selected (Table 4-3 and Figure 4-5). This selection is based on achievement of a balance between sediment input and output and to avoid channel aggradation at the inlet.

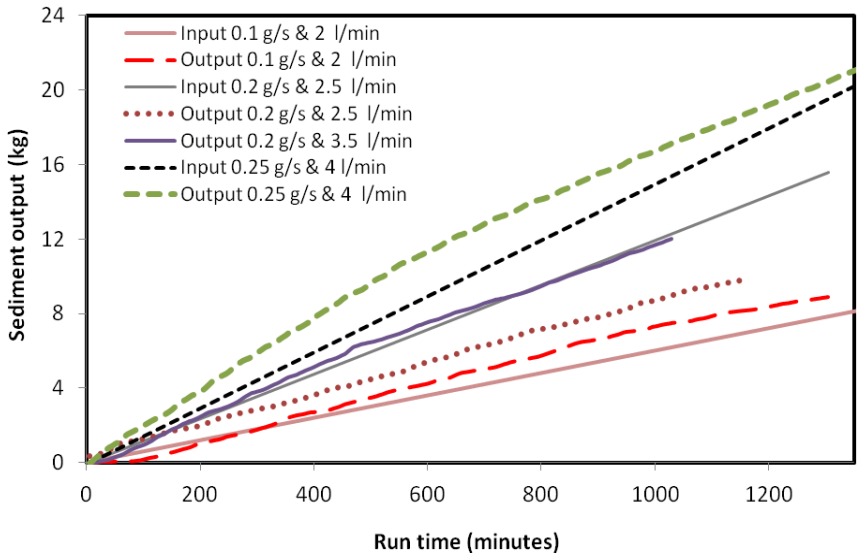


**Figure 4-5 Range of experimental discharges and sediment feed rates tested during trial experiments.**

**Table 4-3 Trial experimental scenarios explored.**

| No. | Sediment Feed rate (g/s) | Discharge (l/min) | Slope | Duration (min) |
|---|---|---|---|---|
| 1 | 0.1 | 2 | 5 | 1340 |
| 2 | 0.2 | 2.5 | 5 | 1140 |
| 3 | 0.2 | 3.5 | 5 | 1025 |
| 4 | 0.25 | 4 | 5 | 1340 |

The experimental setup (RunS1-S5) were formed at constant discharge and varying sediment input to induce successive scenarios of aggradation and degradation. Although a vast amount of research has been directed towards understanding braided rivers, we

still do not completely understand the relationship between changes in sediment load and braided channel morphology. From a practical perspective, investigating the effects of aggradation and degradation would also be desirable for many aspects. Typical examples includes interpreting or predicting channel responses to climate change, tectonic activity, land use or river management problems (Germanoski and Schumm, 1993).

Experiment RunS1 was run until no appreciable difference was observed in sediment feed and collection rate, in which case it could be assumed that the channel was in approximate equilibrium, though the channel itself was not monitored for changes in slope or elevation. In fact, the sediment output rate was never constant throughout experiments.

**Table 4-4 Sequence of Experimental series 1**

| Run | $Q_w$ (l/min) | $Q_s$ (g/s) | Duration (mins) | Number of x-sections in time t | Number of full bed scans | Number of sediment samples | Remark |
|---|---|---|---|---|---|---|---|
| **S1** | 3.5 | 0 | 1320 | 8 | 2 | 206 | Degradation |
| **S2** | 3.5 | 0.2 | 1620 | 9 | 3 | 265 | Aggradation |
| **S3** | 3.5 | 0 | 1320 | 7 | 2 | 236 | Degradation |
| **S3** | 3.5 | 0.2 | 1320 | 8 | 2 | 288 | Aggradation |
| **S5** | 3.5 | 0 | 1320 | 8 | 2 | 288 | Degradation |

## 4.5.REALISING THE EXPERIMENTAL DESIGN: EXPERIMENTAL PROCEDURE AND DATA COLLECTION

### 4.5.1. Initial conditions

The sand bed was prepared as follows. Before RunS1, the sand was gradually soaked and when fully saturated, the channel bed was relevelled and a central straight and flat channel of dimension 20 cm wide and 2 cm deep with flume longitudinal bed slope of 5% was cut into the sand bed. It was found difficult to make the sand bed perfectly horizontal at all locations though an utmost effort was put to do that. Furthermore, variation in Pre-RunS1 condition is unlikely to have exerted a significant

influence on channel formation in later Runs since they followed formation of a relatively stable channel and no re-flattening of the bed was undertaken. Flow was turned on and off frequently for cross section measurements.

With the exception of initial condition of RunS1, the river channel was self formed in the sedimentation tank under the imposed conditions of discharge, flume slope and bed material particle size RunS2 followed immediately after RunS1 without re-flattening the bed and all subsequent runs were initiated with the final topography of the preceding run.

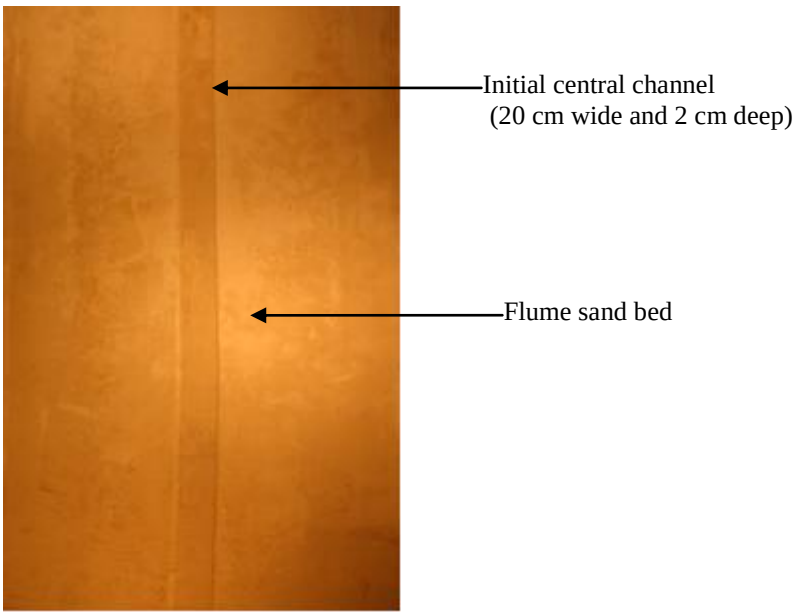


**Figure 4-6 Initial channel configuration of the experimental setup.**

### 4.5.2. Channel morphology and geometry

In order to establish the hydraulic geometry of the modelled river and quantify channel changes (channel fill or incision or lateral erosion) for the braided anabranches, a series of channel cross-sections were measured to obtain parameters required for further analysis and modelling. The parameters to be estimated include flow width, depth, bottom elevations, water surface slope and active width. Channel cross sections were measured at regular spatial and temporal intervals.

Channel cross sections were surveyed at 25 cm evenly spaced intervals every 3 hours. A single cross section survey at time 't' included measurement of 19 sections spaced at 25 cm intervals from the flume entrance (X=5000 mm) to downstream end (X=500 mm) in both a wet (inflow still running) and dry (inflow switched off) condition. A total of 760 cross sections were surveyed throughout the experimental series (dry and wet conditions counted as one survey). In each experimental run, the cross-section surveys were complemented by 2-3 high resolution surveys of bed topography and elevation recorded on a regular grid of 8 mm*2 mm (in the stream wise and transverse directions respectively). These allowed bed level variation to be monitored throughout the course of the experiment. Digital elevation models were generated to illustrate changes in bed elevation and channel planform resulting from changes in sediment feed. Quantitative comparison was then carried out between DEMs generated both within a single run and between different runs. Wherever possible, mean velocity measurements were made by releasing concentrated potassium permanganate solution from upstream and recording the time required to travel 1 m length of a channel. Small wooden marks were put in place at 1m interval along the flume (see Figure 4-1). Polystyrene beads were first considered for use in velocity measurements, but they tended to become grounded on the channel bed.

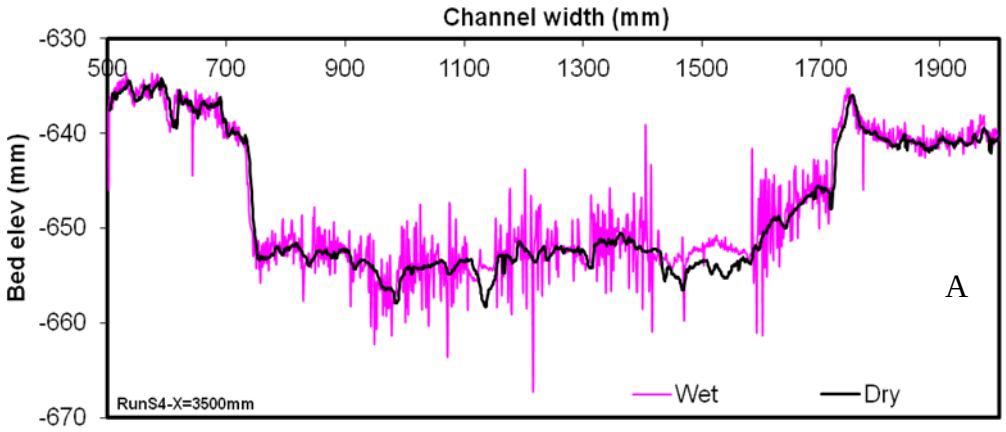

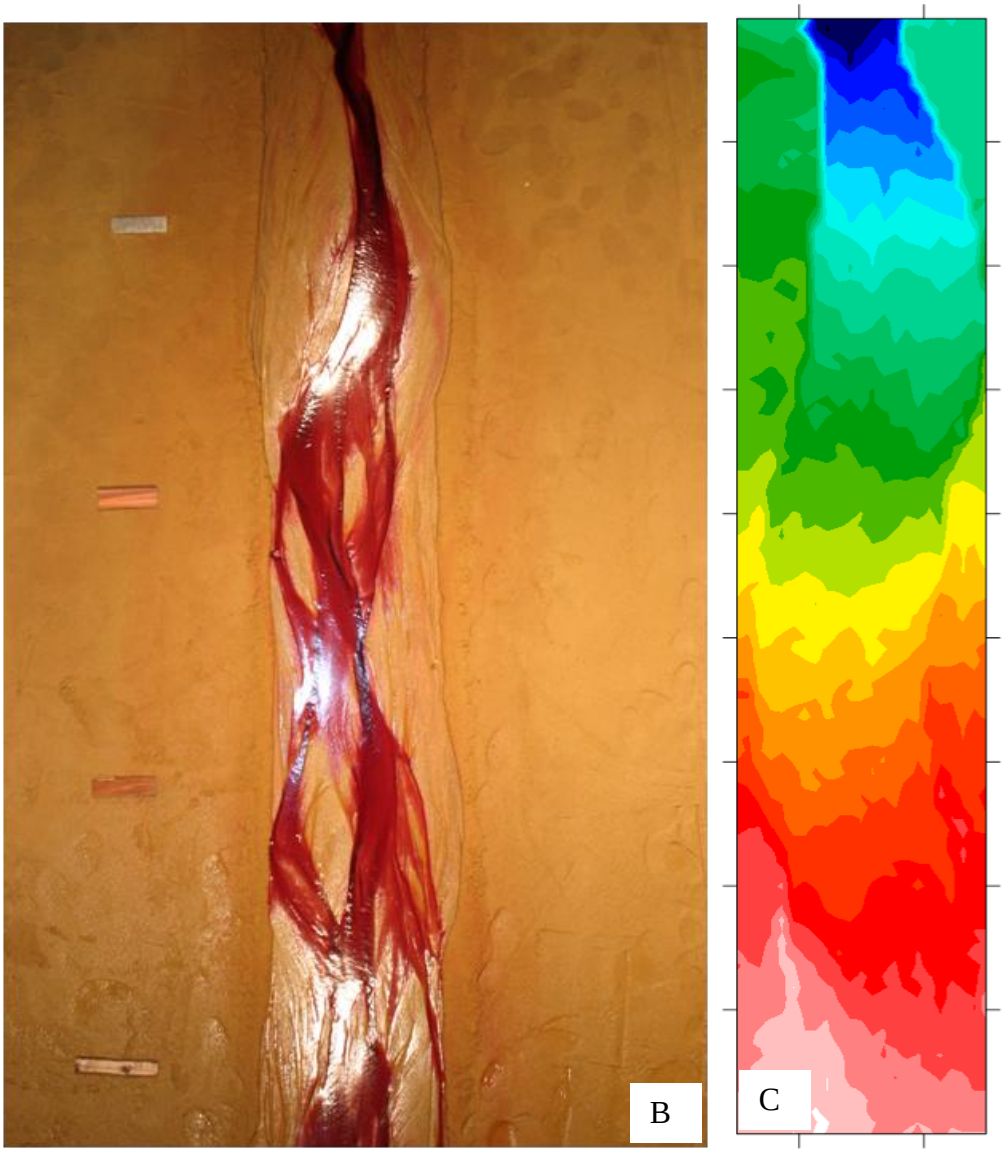


**Figure 4-7 Examples of data set collected from the experiments (A) Dry and wet channel cross sections; (B) Photograph taken from overhead; (C) DEM taken towards the middle of the 3rd experiment.**

During all the runs, the planmetric development of the channel was continuously monitored by photographs taken every 2 min using a digital camera mounted overhead. Photographs covered the whole length of the flume. However, it was found to be very difficult to get quantitative output from the photographs due to the shallowness of the flow. Since flow depth was in the order of a few millimetres in most parts of the channel (the highly degraded upstream reaches may reach a centimetre or even more sometimes) and the sand was ubiquitously fully saturated, it was very difficult to differentiate automatically the wet and dry parts from photographs. This limited the value of the photographs for investigating channel development and the identification of

the main mechanisms of braiding. Therefore, the photographs were used principally to assist interpretation of the measurements obtained using the laser. This was assisted by a digital video recorder mounted at the moving part of the robotic system providing a continuous record of cross sections as well as allowing identification of wet and dry parts of the channel.

### 4.5.3. Sediment Transport

During operation of an experimental run, water was injected by a pump at the upstream flume inlet with a constant discharge. At the outlet, sediment particles transported by the flow settled out in a constant water level overflow tank (Figure 4.1). The overflow tank rested on a high precision (0.1 g) laboratory scale and this was used to derive the sediment transport at the outlet of the tank every five minute. The sediment transport at the flume outlet was then determined using the following equation:

$$M_t = M_w - M_{ex} + M_s$$

$$M_{ex} = (M_s/\rho_s)\rho_w$$

$$\boldsymbol{M_s = (M_t - M_w)/(1 - (\rho_w/\rho_s)} \qquad \textbf{4-7}$$

$M_t$ = Mass at time‘t’

$M_w$ = Maximum mass of water

$M_s$ = Mass of sediment

$M_{ex}$ = Mass of water exported (displaced)

$\rho_s$ and $\rho_w$ = Density of sediment and water respectively.

The measurement tank and laboratory scale were calibrated to see if there was any kind of inherent mass fluctuation and to check if constant inflow and outflow secures a constant mass of the overflow tank in the long term. Data were collected after the tank was full and water had started spilling over the tank. This showed that there was only a very small fluctuation (in the order of 2 g) in the total mass of water collected every two minute.

Table 4-5 Calibration for mass fluctuations in sediment measurement tank

| | Q=2.5 l/min | Q=4 l/min |
|---|---|---|
| | Mass of Water(g) | Mass of Water(g) |
| 1 | 1888.7 | 1888.5 |
| 2 | 1886.7 | 1888.4 |
| 3 | 1887.7 | 1889.4 |
| 4 | 1889.7 | 1888.6 |
| 5 | 1889.2 | 1888.6 |
| 6 | 1888.8 | 1887.2 |
| 7 | 1886.8 | 1889.1 |
| 8 | 1886.9 | 1888.6 |
| 9 | 1886.8 | 1888.7 |
| 10 | 1889.1 | 1888.3 |
| 11 | 1889.2 | 1887.1 |
| 12 | 1889 | 1889.1 |
| 13 | 1889.2 | 1889.5 |
| 14 | 1886.8 | 1889.4 |
| 15 | 1887 | 1889.7 |
| 16 | 1889.9 | 1890.3 |
| 17 | 1888.8 | 1890.5 |
| 18 | 1883.8 | 1892 |
| 19 | 1886.3 | 1892 |

### 4.5.4. Additional Observations

Other than the data directly measured throughout the experiment, continuous qualitative observations of channel pattern evolution were made in all experiments. Moreover, continuous checking in the amount of water and sediment delivered to the experimental channels was done to make sure the prescribed amount is delivered to the channel.

### 4.5.5. Data Post-Processing

After the data was collected from the different experimental setups, it was processed in different ways. DEM and cross section data was imported to Excel and channel cross sections were plotted. A short Excel Macro program was developed to automate the process of plotting the different channel cross sections. In most of the cross section plots, it was observed that some points are clearly outliers, mostly in the

wet cross section plots. This was mainly due to the saturation of the sand and presence of very shallow water at some points even when the tap was closed. The effect was more severe close to the flume outlet where there was more water collected and insufficient time for water to drain through the outlet. A short Excel Macro was then developed to identify those outliers from the data. The outliers were then removed and the elevation value of a particular outlier point is replaced by the average of the preceding and following data points. Analysis of data was done mostly in Excel and distribution fitting in BestFit distribution fitting software. DEM was plotted using Global Mapper (Version 11) and Surfer (Version 10) was used to plot result data from the two-dimensional hydraulic model as will be described in chapter 7. Some DEM detrending calculations were also carried out in MATLAB.

### 4.6.SUMMARY

This chapter introduced the micro-scale physical model to be used in this project. A detailed explanation of the experimental design and the scaling considerations to be used in this research was given. The model is not scaled to a specific prototype and does not follow a formal framework of similitude consideration, hence it is generic. However, an utmost effort was put to ensure realistic representations of sediment grain size and water discharge in terms of capability to transport sediments and formation of important morphodynamic phenomena. Moreover, previous published data for the grain-size distributions of gravel-bed-rivers is considered for realistic representations of sediment grain-size. Five experimental scenarios were used in the final analysis; four of them follow directly from the previous experiment without re-flattening the bed. Water discharge was kept constant throughout the experiment whereas sediment feed from upstream was varied to induce scenarios of aggradation and degradation.

# 5. CHANGES IN SEDIMENT STORAGE AND CHANNEL MORPHOLOGY IN A MICRO-SCALE EXPERIMENTAL BRAIDED RIVER

## 5.1. INTRODUCTION

This chapter presents an assessment of the effects of varied sediment supply on sediment storage and channel morphology using output from the micro-scale experimental series of aggradation and degradation scenarios (RunS1-RunS5). First the various data sets collected throughout the experiment will be presented in a systematic manner followed by changes observed in sediment transport and channel morphology over the experimental series. This will be followed by investigation of changes in longitudinal profile and channel bed slope over the course of the experiments. The chapter concludes with a summary of the key findings and how this compares with the previous studies of braided river evolution.

## 5.2. DATASETS

### 5.2.1. Channel cross sections and Digital Elevation models

The experiments were all carried out in a sedimentation tank with a working length of 5 m and internal net width of 2.7 m (explained in chapter 4). The experiment was started with a channel located in the centre of the flume that was 20 cm wide and 2 cm deep. This channel was allowed to braid and expand in width laterally. No obstructions were observed from the walls of the flume in the development of a stable braided channel throughout the experiment. Channel cross sections were acquired at regular spatial and temporal intervals for both dry and wet conditions (explained in chapter 4). Moreover, a high resolution (8 mm in the stream wise and 2 mm in lateral direction) bed survey was conducted two to three times in an experiment and a digital elevation model generated. The flume gradient in the digital elevation models generated and presented in Figure 5-2 is removed and then they are detrended to illustrate lateral variation more clearly. Therefore, this figure does not show the true channel gradient.

### 5.2.2. Sediment transport data

Sediment transport data collected at the end of the flume at 5 minute interval are presented in Figure 5-1. Detailed statistical analysis of the sediment transport data will follow in section 5.3.1. There is some variation in the total number of sediment transport measurements collected at the outlet of the flume for each experiment since there is some difference in the experimental time for different experiments.

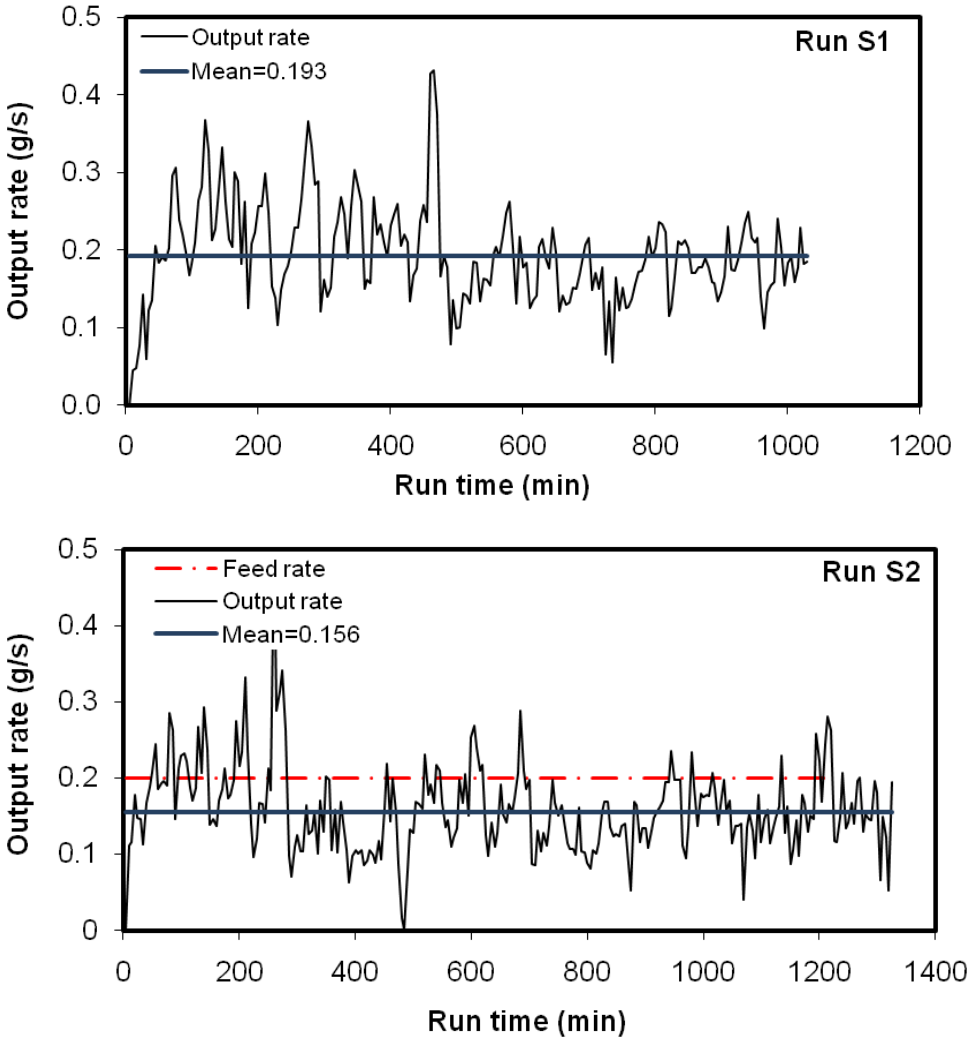

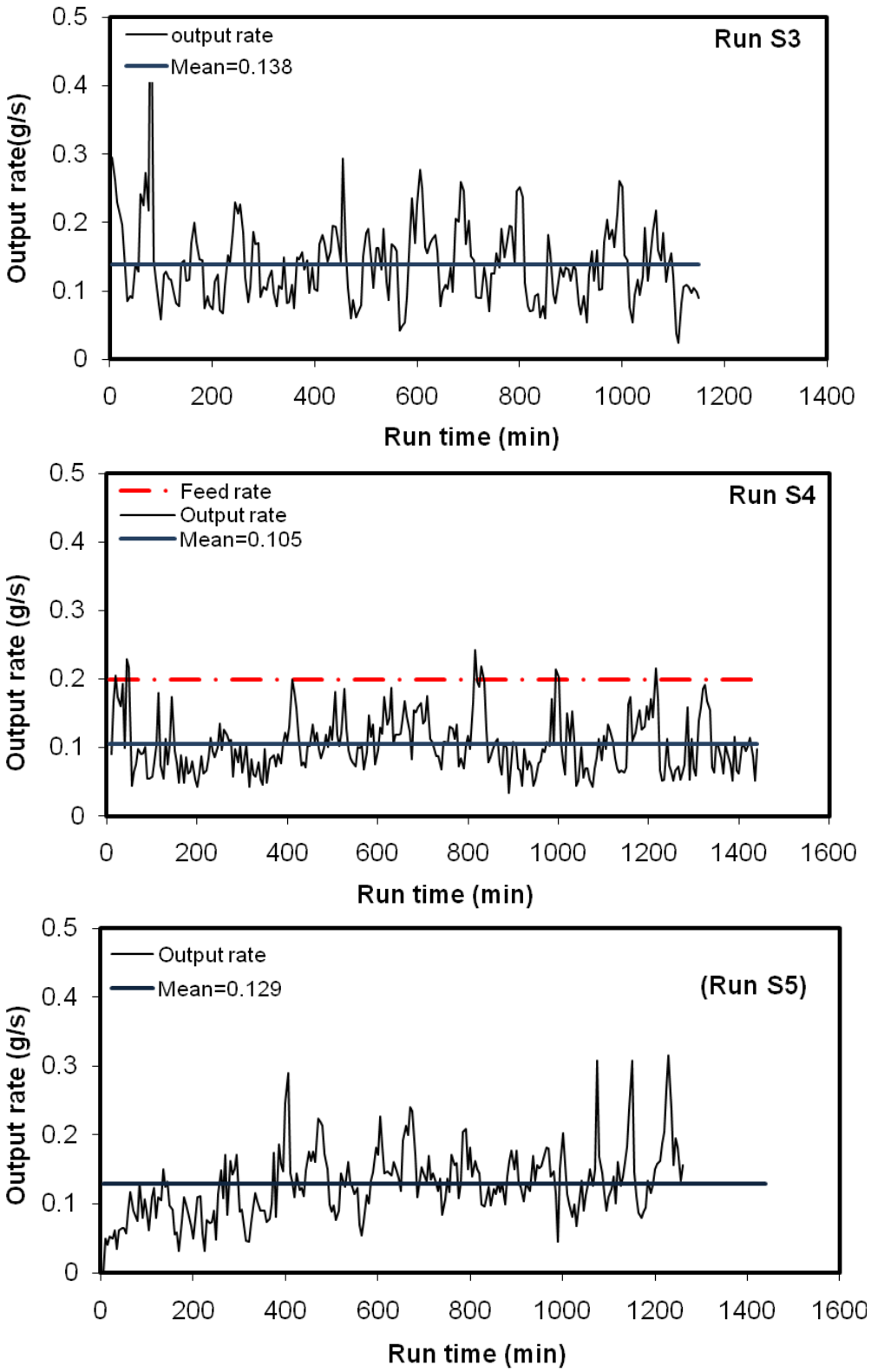


**Figure 5-1 Sediment transport as a function of time (RunS1, RunS2, RunS3, RunS4, RunS5). Time refers to the time elapsed since the start of the run.**

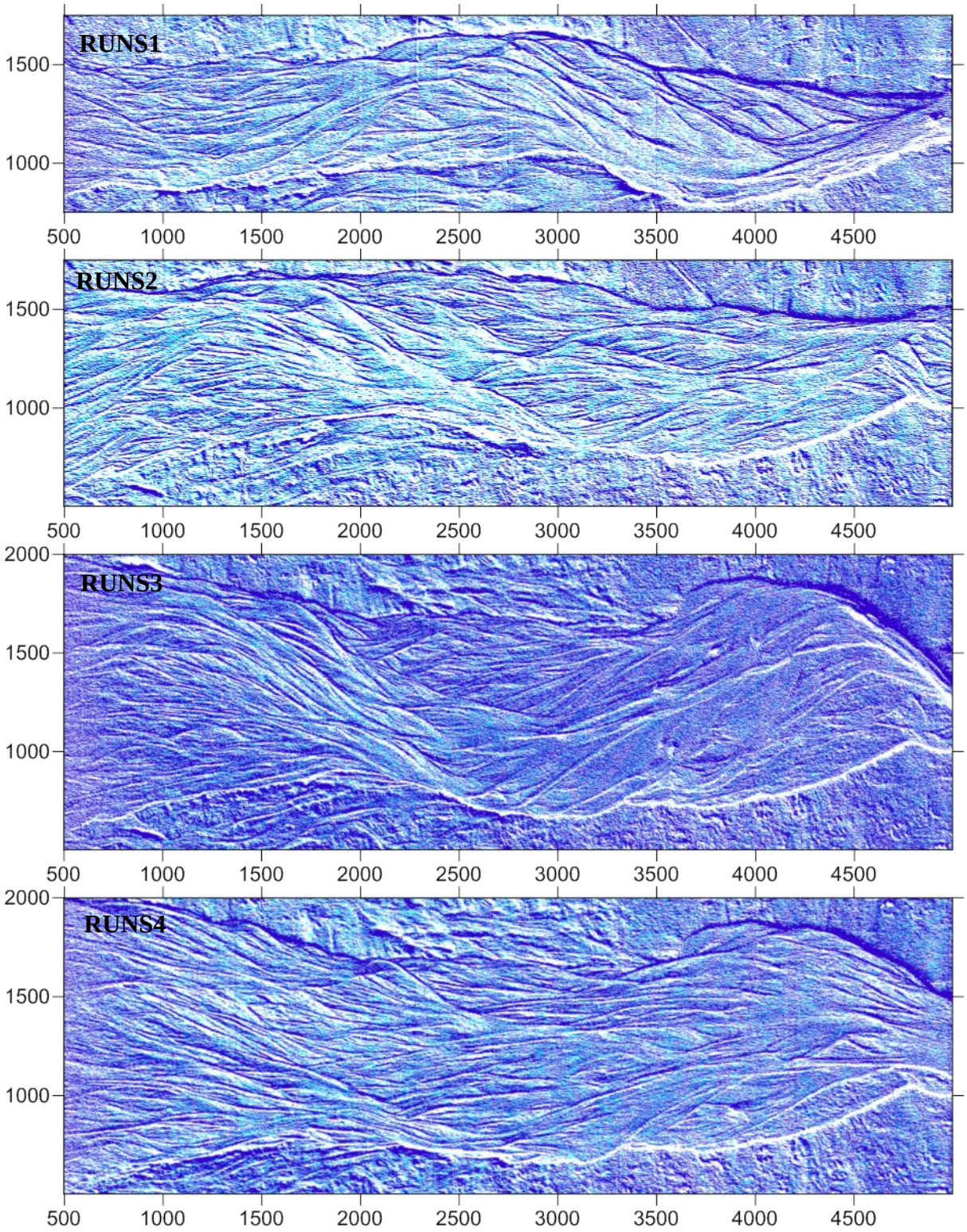
RUNS1
RUNS2
RUNS3
RUNS4
500
1000
1500
2000
2500
3000
3500
4000
4500

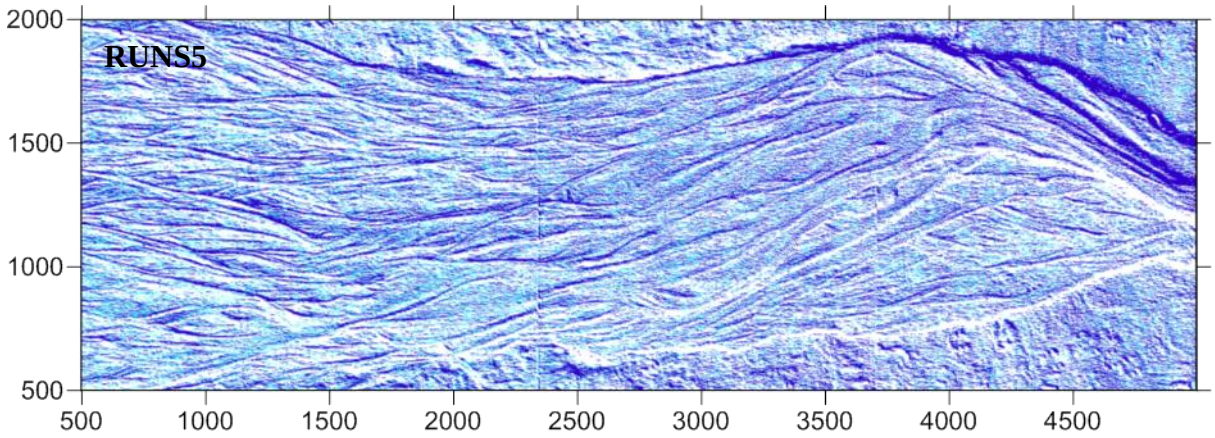

Figure 5-2 Detrended Digital Elevation models collected at the end of each experiment (flow is right to left)

## 5.3.RESULTS

### 5.3.1. Variability and Changes in sediment output and Channel storage

In this subsection quantitative and statistical description of the measured sediment output time series and channel storage is presented. A qualitative comparison has also been made with other experimental works.

Sediment transport measurements taken at the outlet of the flume are displayed in Figure 5-1. When sediment output was first measured during the period when a stable braided channel was being established, a time lag of about 50 min to 60 min was observed before the output rate began to increase. Once this occurred, sediment output immediately increased and the rate was never constant. For the remainder of the run, sediment output in RunS1 fluctuated with greater amplitude until approximately 500 min, after which it became relatively consistent with minor fluctuations. Excluding the initial phase, and based on the exponential fit in Figure 5-3, there seems to be a gradually decreasing average transport rate during the evolution of the channel network.

At the beginning of the first aggradation cycle (from 0 to 275 min in Figure 5-1, RunS2), the transport rate was generally higher than the transport rates observed in the later stages of the previous degradation run, with a mean of 0.205g/s, which was nearly equal to the sediment feed rate of 0.2 g/s and statistically indiscernible with the mean transport rate of RunS1 (samples within the same standard deviation). Channel storage

was almost constant during this time. However, as channel aggradation progressed, sediment outputs reduced gradually and channel storage suddenly stepped-up and began to increase continuously (Figure 5-4). Observation of the changes in the long profile and cross section of the main channel shows that at the beginning of the first aggradation cycle (S2), the sediment input was probably stored in the actively incised upstream reach (the section between 4 m and 5 m upstream of the flume outlet) (details can be referred in Figure 5-10 C, H, L). Around the middle of the flume, there was some erosion but this intensified further downstream close to the flume outlet (1m upstream of flume outlet). The mean sediment output rate for RunS2 excluding the first 275 min of the flume run was 0.148 g/s, which is well below the feed rate.

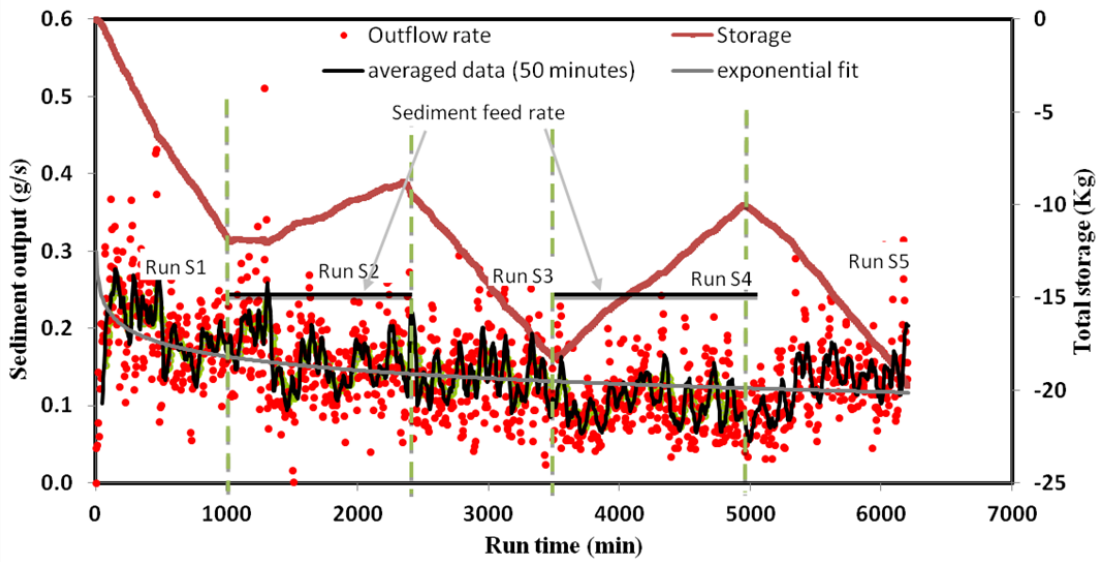


**Figure 5-3 Sediment transport as a function of time (all Runs)**

When sediment feed ceased during the second degradation run (S3), channel storage reduced abruptly. Similar sediment output continued despite cessation of sediment input at the upstream end of the flume. The mean output rate for RunS3 is 0.138 g/s, which is not very different from 0.148 g/s, as measured in RunS2 excluding its initial phase. With an increase in sediment feed again to 0.2 g/s (Figure 5-1, RunS4 and starting at 3500 min in Figure 5-3), sediment output reduced for the first 340 min. and varied with lesser amplitude having a mean of 0.094 g/s. When sediment feed continued, the output started to increase slightly with a mild fluctuation around a mean of about 0.105 g/s and standard deviation of 0.042 g/s. Moreover, as channel aggradation continued, sediment

storage increased at a steeper rate than during the previous aggradation cycle (RunS2). During the last degradation cycle (RunS5), similar sediment output continued for about 360 min (around 5300 min in Figure 5-3). The mean output rate in this period was 0.088 g/s. With continued degradation and cessation of sediment feed from upstream, a slight increase in sediment output is observed. The overall mean of this last degradation cycle is 0.129 g/s.

Overall, output rates decline progressively over runs S1 to S4 and then stabilizes or perhaps increase slightly in Runs5. Storage rates are poorly related to output, but strongly related to sediment feed (storage increases when sediment feed occurs and declines when the feed is stopped). Although the relations between sediment output and channel storage in RunS2 and RunS4 displayed similar styles, the magnitude and patterns of response differed early in the cycle. At the start of RunS2, when sediment feed was increased, storage was almost constant while output was steadily increasing. In RunS2, storage then increase steadily while output rates fluctuated around 0.15 g/s. When feed was stopped in RunS3, storage continuously decreased as output remained in a similar state as in the previous run. There is a large loss of storage volume of around 10,000 g during RunS3. In RunS4, storage increased greatly as a slight reduction in output was observed up to around 3900 min in Figure 5-3. After this time, sediment output remained fairly high until the end of this run even though storage continued to increase. The sediment storage in the second aggradation cycle (RunS4) increased at a much steeper rate than the first aggradation cycle (RunS2). This may be due to the fact that sediment storage may persist long after aggradational events and channel responses may be affected as a result of repeated cycles of aggradation and degradation (Madej *et al.*, 2009). At the beginning of RunS5, transport rates were the same as in RunS4, as storage declined and the channel bed started to degrade. This decline in storage continued up to the end of the run and transport rates also appeared to increase slightly towards the end of the experiment.

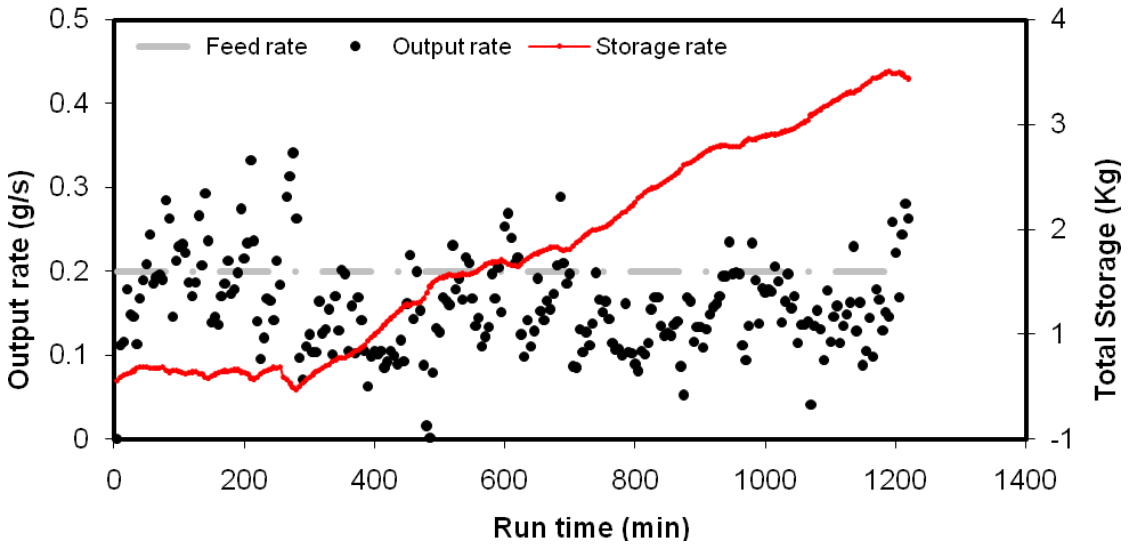


**Figure 5-4 Sediment output-storage relations for RunS2**

When sediment input ceased in the degradation runs, the channel actively incised and channel morphology changed to more of a single thread near the flume inlet and remained braided close to the outlet (details discussed in section 5.4.2). However, there was not significant variation between the mean sediment output rates for the degrading runs (S1, S3 & S5) and mean sediment output rates of aggradation runs (S2 and S4). This suggests that transport rates respond weakly to sediment supply variations and hence sediment transport appears to be more closely related to transport capacity than sediment supply. This is in agreement with flume experiments of Germanoski and Schumm (1993) but counter to the experiments of Madej *et al.* (2009), who observed high sediment output rates for aggradation runs when the sediment feed rate was high. In fact, the mean sediment output for the first aggradation cycle (S2) was higher than the next degradation cycle (S3).The sediment output rate was partly restored in the last degradation cycle (S5). There is also a tendency for transport rates to remain unchanged for some time despite a change in sediment supply conditions.

Temporal variability in bed load transport rates has been observed in various laboratory studies of braided river dynamics (Ashmore, 1988;Ashmore, 1991a;Hoey and Sutherland, 1991;Young and Davies, 1991;Warburton and Davies, 1994) and field studies e.g. (Griffiths, 1979;Goff and Ashmore, 1994). This temporal variability in sediment transport has been attributed to the downstream migration of bedforms at different temporal scales, migration of large bars or groups of bars and localized

incision (Ashmore, 1988;Hoey, 1992;Gomez *et al.*, 1989) and has often led to difficulty in measuring both total and local bed load transport in braided rivers e.g. (Bridge, 1993).

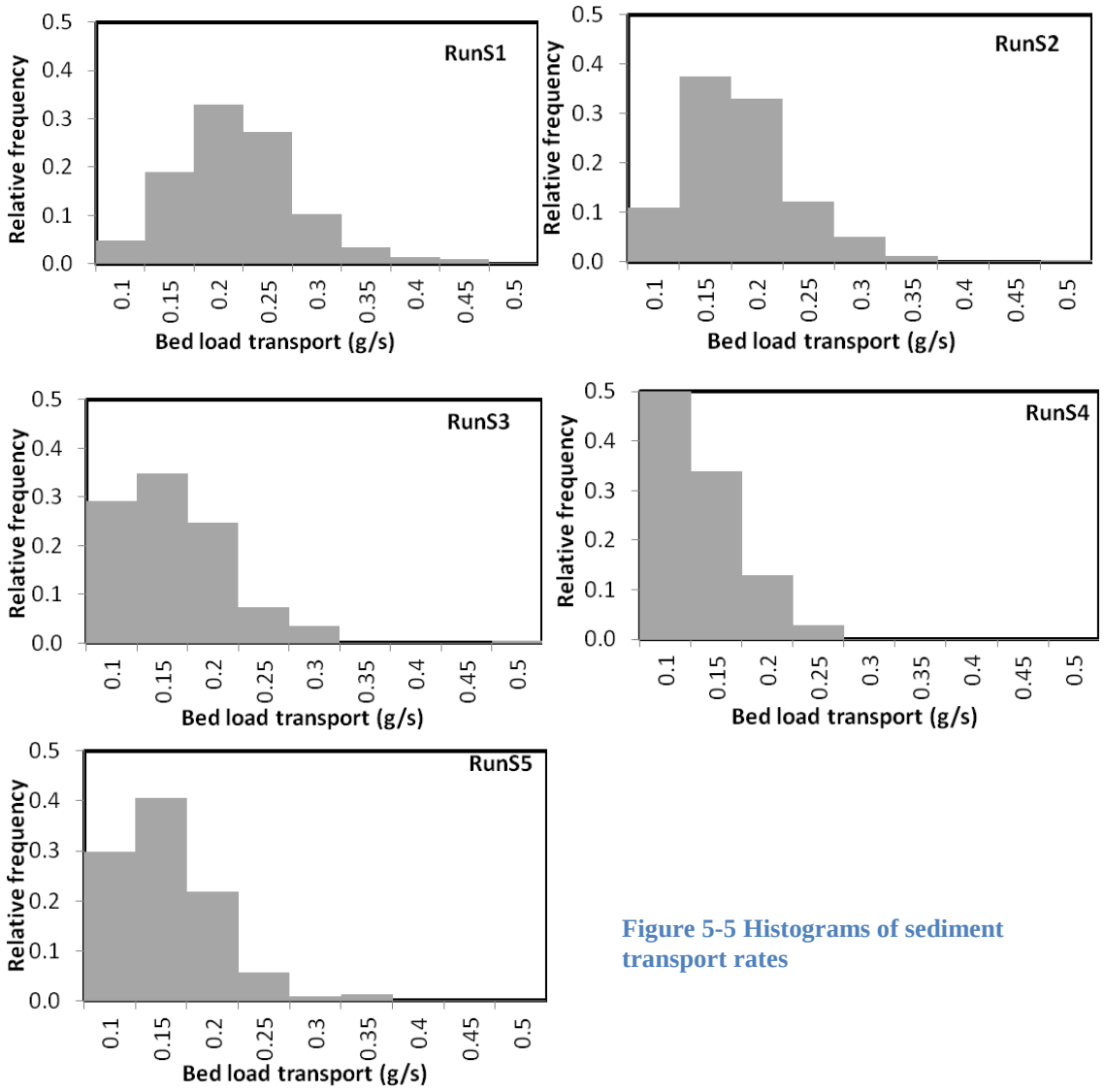


**Figure 5-5 Histograms of sediment transport rates**

The time series shown in Figure 5-1 confirm that bed load transport rates are highly variable and show a series of fluctuations. Although within-run transport rates sometimes vary from close to zero to just twice the mean rate, the extent of variability observed here is much lesser than in previous investigations e.g. (Hoey and Sutherland, 1991;Warburton and Davies, 1994;Bertoldi *et al.*, 2009;Ashmore, 1988). This is probably due to the fact that most previous investigators used much higher water discharge leading to higher transport capacities and hence greater potential for large scale bed incision or bank erosion. At smaller discharges (similar to the one used in this

experiment), the sediment transport capacity will be lower with less variability (Thmoas, 2003).

The original sediment transport rate time series is used to derive the histograms shown in Figure 5-5 to demonstrate the variation of bed load transport rate within each run. A close look at the histograms shows that they are slightly skewed towards the lower transport rates (S3, S4, and S5) with the exception of RunS1. RunS1 is almost symmetrical with most output values varying around the middle and dying off out near the tails. Mean transport rate decreases from RunS1 to S4 and is restored slightly during RunS5. Transport rates in RunS2 are heavily influenced by RunS1 in that more than 50 samples collected were all relatively high and close to the mean transport rate of RunS1, which changes the shape of the histogram. Excluding this initial phase, the shape of the histogram of RunS2 would have been very similar to the later runs.

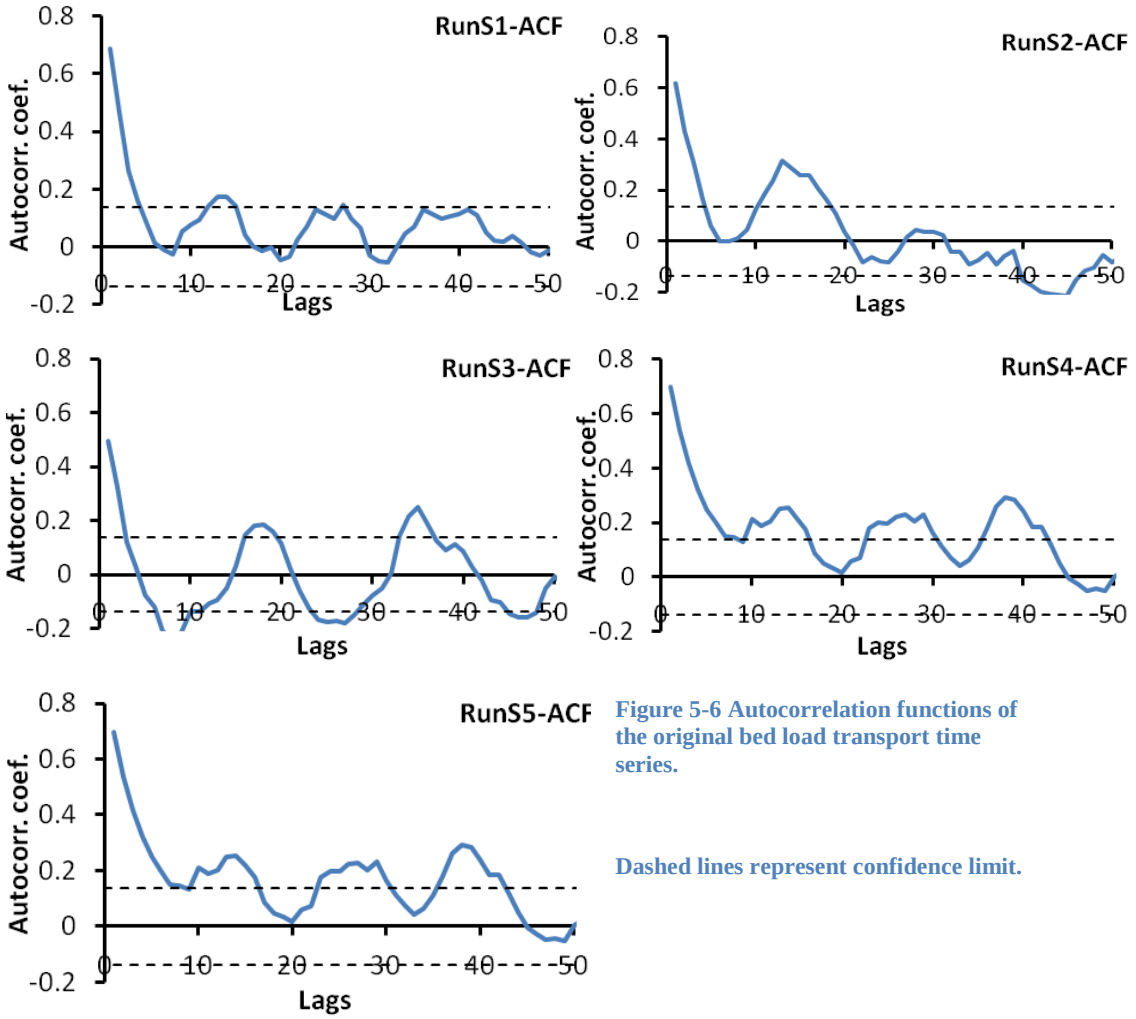


**Figure 5-6 Autocorrelation functions of the original bed load transport time series.**

**Dashed lines represent confidence limit.**

Similarity of sediment output rates over a period of time despite a changing input condition (as was observed in almost all of these experiments) is an indication of ‘’persistence’’ (a tendency for a system to remain in the same state from one observation to the next). This was found to be a very common characteristic of the bed load transport processes in braided river models (Warburton and Davies, 1994). The best way to describe this statistically is using an autocorrelation function, because visual assessment from the time series is too subjective. The autocorrelation function provides a measure of the correlation between transport rates in the series at positions separated by a time interval along the series. Autocorrelograms of the time series of bed load output rate shown in Figure 5-6 revels strong and positive autocorrelation with significant periodicity in the fluctuations of bed load transport rates. This is observed in almost all runs. The interpretation of this is that there is a greater persistence and some statistical dependency on the previous transport rates of the series as positive departure from the mean is followed by negative departure from the mean and vice versa. The frequency of periodicity varies between runs. However, a peak in the autocorrelation function at lags of about 1 hour is common to all runs. Periods ranging from 2 to 10 hours were observed in braided river models of (Ashmore, 1988).

Figure 5-7 shows the cumulative sediment output curves for the whole experimental series. They are indicators of sediment output histories for the whole duration of the flume runs. The sediment feed rate for Run S2 to S5 was selected based on an investigation of the cumulative sediment output curve of RunS1. Where data plots above the input line (dark line), sediment output is more than sediment input. This does not happen in any of the runs, although sediment output was nearly balanced by the input for the first 300 minutes of RunS2. An interesting point to note here is the deflection of the curve for RunS2 at around 300 minutes of the flume run and for RunS5 at around 400 minutes of flume run for this experiment. Warburton (1996) explained a downward deflection in cumulative transport curves (like RunS2) in terms of increased bed stability and the upward deflection (like RunS5) as representing large scale sediment pulses. These sediment pulses might be attributed to intrinsic controls or might be extrinsically driven as a result of sediment supply variations from upstream. However, it is very difficult to differentiate the source of such sediment pulses in this

experiment. Given that such a slight increase occurs within a few minutes of the cessation of sediment feed and transport rates usually show a tendency to remain in the same transport condition as earlier, pulses probably represent the effect of sediment supply variation from upstream.

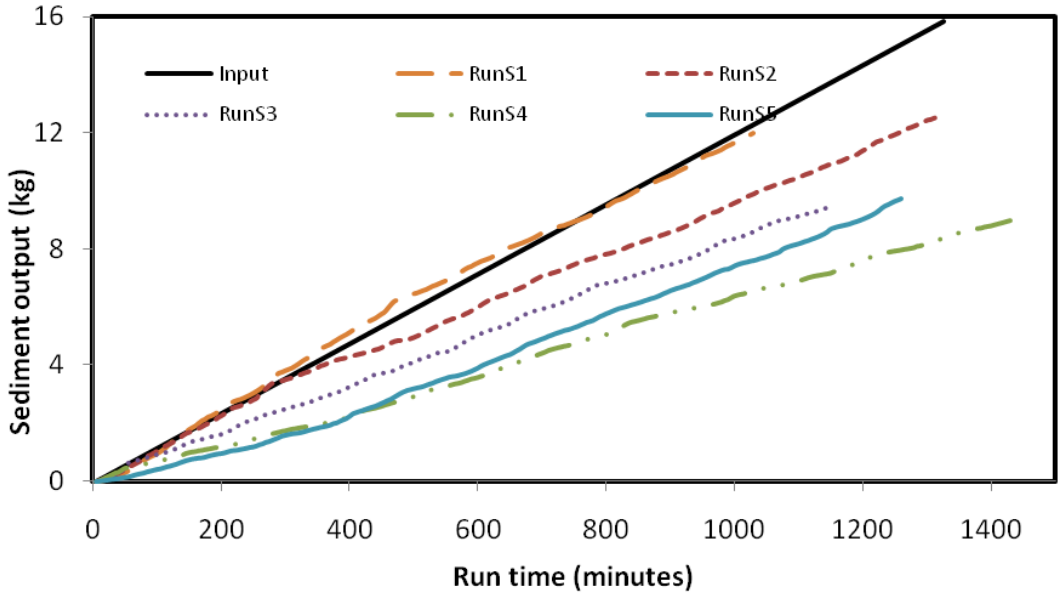


Figure 5-7 Cumulative sediment transport curve

### 5.3.2. Changes in channel pattern and morphology

Generally, aggradation or degradation of a river bed can occur as a result of natural or human induced processes that will ultimately result in changes in controlling variables, such as modification of water and sediment discharge. When this occurs the morphology of alluvial channels develops through spatially and temporally variable patterns of erosion, transport and deposition. This subsection will aim to describe the changes in channel pattern and morphology that occurred during the experiments as a result of changes in sediment supply from upstream.

The photographs taken at the end of each run shown in Figure 5-8 illustrate changes in channel planform during aggradational and degradational cycles. A range of channel morphological characteristics were quantified and are summarised in Table 5-2. Bed elevation changes were compared with the initial bed when the experiment was started. Channel bed slopes calculated from thalweg elevations extracted from the digital elevation model at the end of each run are also presented and compared. Fill and scour of the river channel is quantified using the bed relief index (BRI), which is calculated as

the difference between thalweg and bar surface elevations. The cross-channel bed relief index (CBRI) is defined here as the flume averaged bed relief index. In this experimental series the CBRI is calculated as the average difference between bar surface and thalweg elevations of 19 cross sections along the flume acquired at end of experiments.

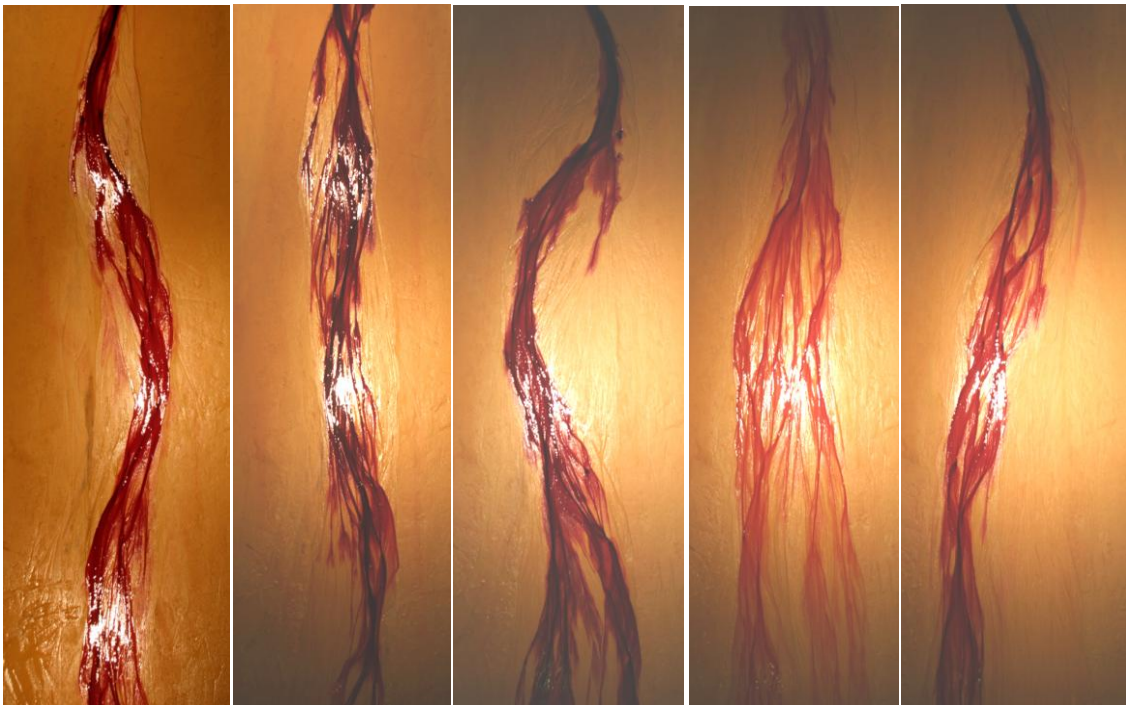

End of RunS1 End of RunS2 End of RunS3 End of RunS4 End of RunS5

**Figure 5-8 Photographs of channel pattern taken towards the end of each run**

An important characteristic of channel response to increased or decreased sediment load is that different portions of the channel may respond differently. Two zones can be identified in the experimental channel examined here: a degrading upstream channel that is the primary source of sediment, and an aggrading downstream part characterized by deposition of eroded sediment from upstream. Channel aggradation and subsequent degradation have been accommodated across the entire channel bed. The response times and mechanism of channel adjustment after disturbance depend on the magnitude of the imposed change and stream power available to effect changes (Knighton, 1998).

The braiding intensity is a basic morphological property of braided channels. While the occurrence of braiding has been extensively analysed theoretically and empirically,

there has been little discussion or quantitative analysis of the braiding intensity and its response to various controls. Several metrics of braiding intensity have been proposed and used in literature. For example, bar dimension and frequency (e.g. Rust, 1978;Brice, 1960;Brice, 1964;Germanoski and Schumm, 1993); the number of channels in a network (e.g. Howard *et al.*, 1970); and the total channel length in a given river length (e.g. Hong and Davies, 1979;Mosley, 1981). At present, channel count indices give the best combination of rapid measurement, precision and range of sources from which measurements can be reliably made (Egozi and Ashmore, 2008). Moreover, channel count indices and sinuosity are those most commonly used in correlating braided channel pattern with flow, stream power, sediment transport and morphology and in observing variations over time under experimental conditions (Mosley, 1983;Mosley, 1982;Ashmore, 1991a;Chew and Ashmore, 2001). Consequently, in this experiment, braiding index is defined as the number of wet channels per cross section.

Data collected from 19 cross sections were averaged spatially and temporally to characterize the network configuration. Through this averaging procedure mean values of the braid intensity parameter were obtained, which are representative of each run. The data in Figure 5-9 show an obvious pattern in aggradation and degradation experiments. Aggradation of the channel bed, as a result of sediment feed from upstream, changed the channel morphology in each aggrading channel by increasing the braiding index and widening the active channel itself. A visual comparison of the channels in Figure 5-8 also illustrates the increase in pattern complexity resulting from aggradation. This increase in channel complexity from aggradation is also reflected by a consistent increase in braiding index (Figure 5-9). The trend is consistent for transitions from RunS1 to RunS2 and then from RunS3 to runS4. Although each sequence of runs was carried out one after the other without re-flattening the bed (i.e., different gradients), the braiding index increased when sediment feed increased and decreased when sediment feed decreased.

Similar morphological changes have been reported to some sections of laboratory braided channels as a result of bed load pulses moving into the reach (Ashmore, 1991a). The magnitude of aggradation and degradation varied throughout the length of the flume, but it was greater near the flume entrance and there were minimal changes near

the outlet due to the fact that bed level is fixed at the downstream end, hence damping out any major elevation changes.

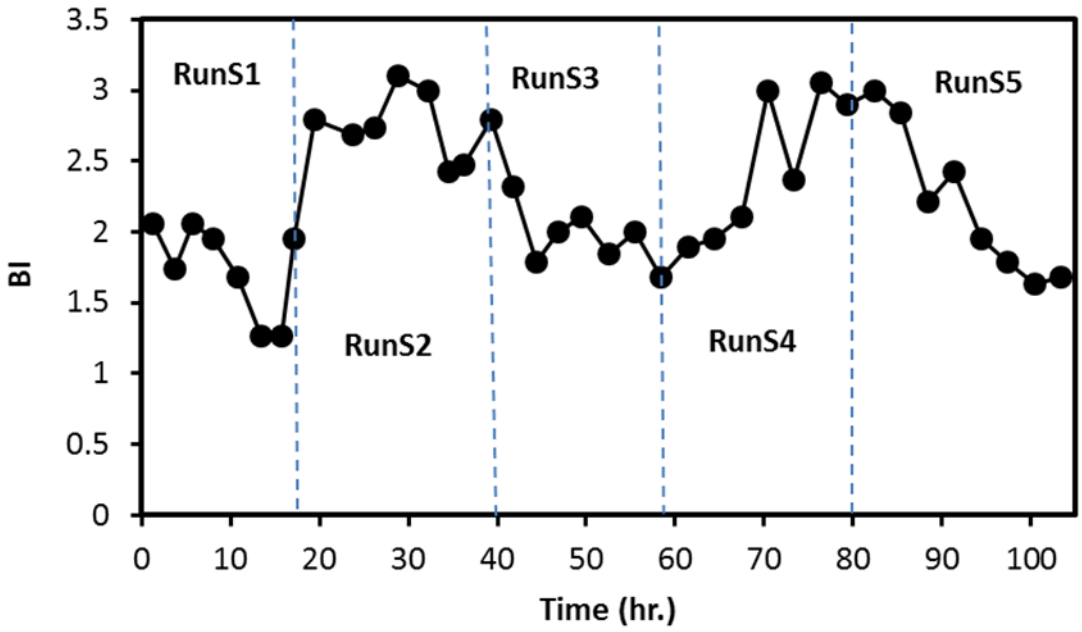


**Figure 5-9 Temporal variation of time averaged braiding intensity throughout the experiment.**

**Table 5-1 Channel Morphological characteristic of the experimental series**

| *Run* | *Bed load transport (g/s)* | | *Mean bed slope* | *Channel width (m)* | | *CBRI (mm)* |
|---|---|---|---|---|---|---|
| | Mean | Std. dev. | | Mean | Std. dev. | |
| S1 | 0.193 | 0.063 | 0.0227 | 0.59 | 0.07 | 20.1 |
| S2 | 0.156 | 0.058 | 0.0274 | 0.74 | 0.07 | 11.7 |
| S3 | 0.138 | 0.063 | 0.0252 | 0.49 | 0.1 | 19.4 |
| S4 | 0.105 | 0.042 | 0.0259 | 0.86 | 0.15 | 14.2 |
| S5 | 0.129 | 0.049 | 0.0203 | 0.54 | 0.13 | 26.1 |

Figure 5-10 shows typical cross-sectional profiles at various distances down the flume during all the runs and illustrates the changes that occurred throughout the experimental run, and how this varied with time. Generally, the further downstream the cross section is located, the less channel change in terms of degradation and aggradation occurred. Figure 5-10 (A, B, K) represents cross sections taken at the channel bed before sediment feed began and a braided channel had formed. Major changes in the first run include

considerable channel widening, degradation of the channel near the flume inlet and deposition of eroded materials in the channel midway down the flume. The channel were transformed to single-thread system in the upstream reach and remained braided in the downstream reach. This may be attributed to the fact that the amount of sediment supplied from the rapidly degrading and widened upstream reach resulted in an increase in sediment discharge downstream, where the channel was unable to transport all the sediment supplied to the reach. Consequently, despite the absence of sediment feed to the upstream end of the channel, the downstream part continued to aggrade.

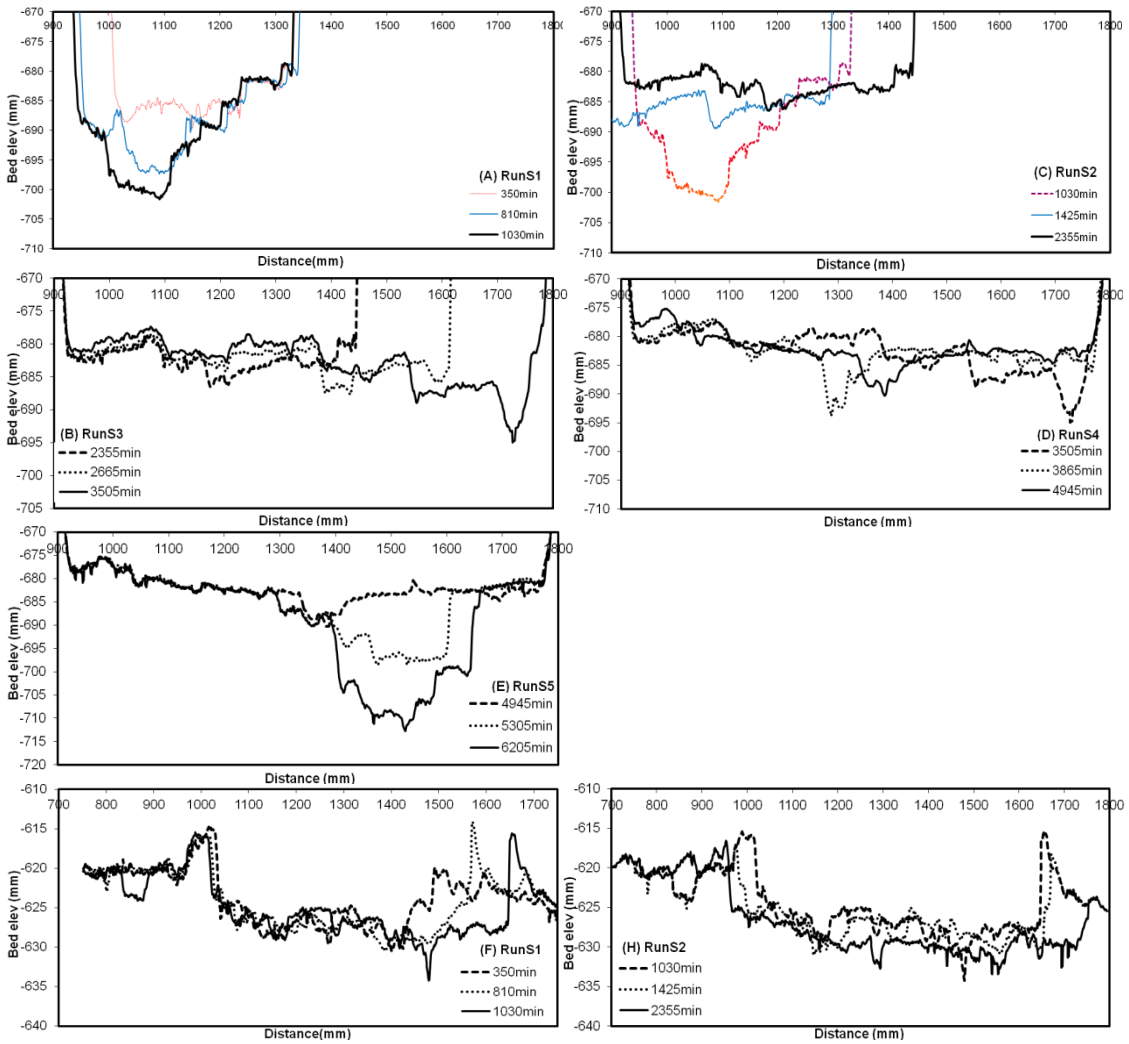

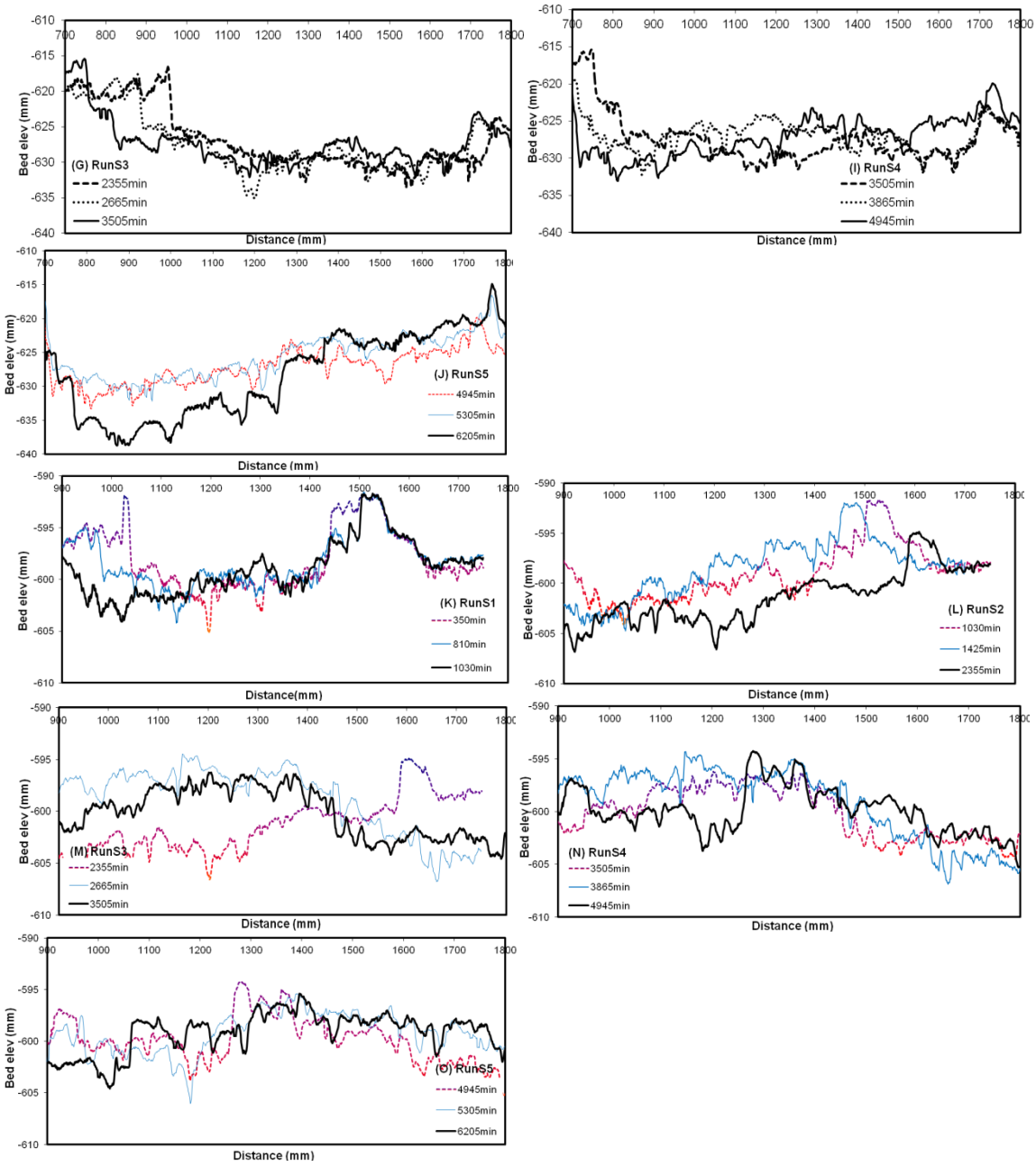


**Figure 5-10 Typical cross-sectional changes during aggradational and degradational runs in the flume, measured at 1000mm (K,L,M,N,O), 2500mm (F, G, H, I, J) and 4500mm (A,B, C, D, E) upstream of outlet.**

During the second run with sediment feed (RunS2), the thalweg and active channel bed filled at the upstream cross sections and the channel widened by more than 10cm (Figure 5-10C). Channel fill and widening midway down the flume at this time was insignificant (Figure 5-10D). Moreover, as can be seen from the plot of long profile evolution Figure 5-13, thalweg elevations in the downstream section remained well below elevations during the previous degradation run. Aggradation was greatest near the

inlet, associated with development of new braid bars which forced the flow into the channel banks and resulted in lateral erosion and an increase in overall channel width by more than 25% to 0.74 m. This value was more or less consistent throughout the length of the channel. The CBRI dropped from nearly 20.1 mm at the end of RunS1 to 11.7 mm because of deposition in the active flow channels apparently reducing the relief between channel beds and bar tops. This is in agreement with some studies (Hoey and Sutherland, 1991;Madej *et al.*, 2009) but different to the laboratory braided channel experiments of (Germanoski and Schumm, 1993). Germanoski and Schumm (1993) attributed the different responses measured between their experiment and those of others (e.g. (Hoey and Sutherland, 1991) as a reflection of different rates and magnitudes of aggradation. It is obvious that the bed relief index increases when a braided channel is degraded as a result of a rise in the difference between the incising channel bed and stable bar tops, but Germanoski and Schumm (1993) also illustrated that the greater number of braid bars that formed during their aggradation experiment contributed to an increase in BRI. They found that the bed relief index could increase if aggradation occurred over the entire cross section and produced new bars. The BRI may remain constant or decrease if aggradation is confined to the channel thalwegs. Germanoski and Schumm (1993) concluded that both aggradation and degradation can increase the BRI, although for different reasons.

During RunS3 (Figure 5-10, B, G and M) the main channel continued to migrate and shifted to the right in the upstream parts of the channel. By the end of the run, it had migrated by more than 35cm, while at the same time the thalweg deepened by more than 1cm close to the upstream end of the flume. Degradation appeared to have been concentrated in the upper reaches of the channel and terraces appeared to have formed. Towards the middle of the flume the channel migrated slightly to the left and the thalweg somewhat filled up. However, further downstream thalweg bed elevations remained below those in RunS2 for most of the reach. Mean morphologically active channel width, which is defined as the parts of the channel actively changing its elevation by erosion and deposition, declined and CBRI increased to almost pre-RunS2 conditions. As in the case of degradation in the first run, the channel here also experienced a transformation towards a single thread pattern in its upstream reach. More

than half the length of the channel remained braided in the downstream part of the flume.

Initially, the channel response to the second period of sediment feed was similar to that during the first, with a small amount of widening and minor channel fill (Figure 5-10, D, I and N). As sediment feed progressed, the channel completely filled in. A relatively large mid-channel bar formed near the middle of the flume (from 1000 mm- 2500 mm downstream the flume entrance), dividing the channel and hence the flow (sections with the mid-channel bar are indicated in Figure 5-11) and making the channel appear as an elongate fan structure. The CBRI declined from 19.4 mm at the beginning of RunS4 to 14.2 mm at the end of RunS4. The number of channels appeared to increase throughout the flume, although many of those channels were relatively narrow and shallow.

The most significant channel change occurred in RunS5. Incised channels formed on the true left of the flume towards the upstream end and on the true right towards the middle of the flume. The depth of incision in this channel decreased in the downstream direction as can be seen from the long profile evolution. Upstream the channel was actively incising (Figure 5-10I) and by the end of the experiment it had incised by more than 2cm. Mid-flume degradation appeared to be concentrated on the true right side of the channel with a reduced magnitude of about 1cm. However, further downstream channel changes did not appear to be very significant owing to the effects of the fixed bed elevation at the flume outlet. The CBRI rose to its highest value in the experiment of 26.1 mm. The channel bed slope was reduced significantly, but the mean sediment transport rate increased, although it remained smaller than in the corresponding degradation runs without sediment feed.

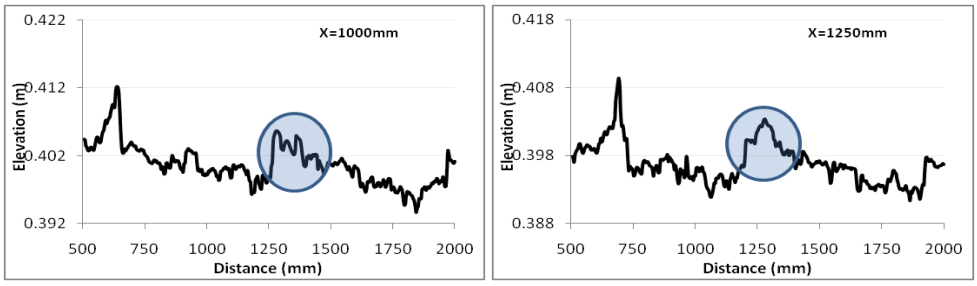

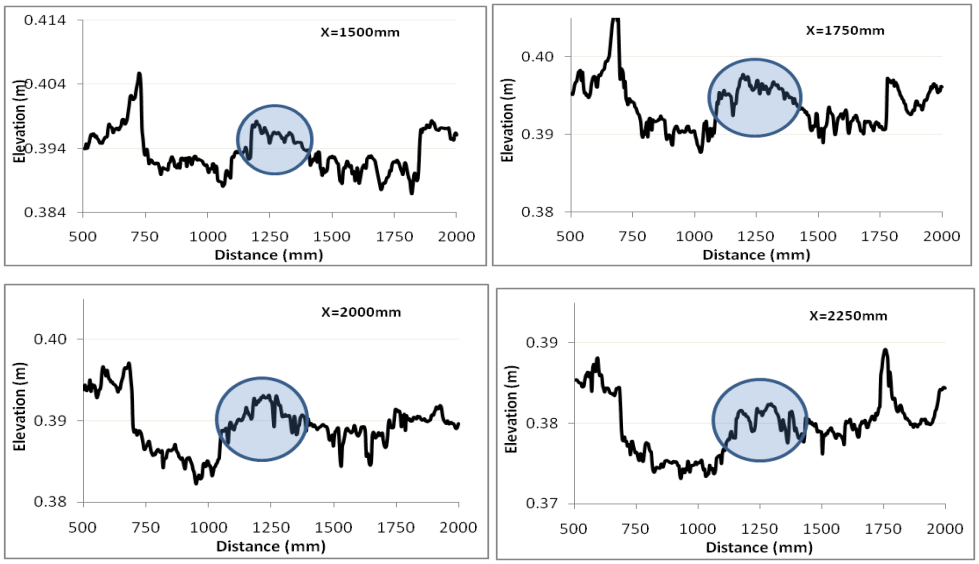


**Figure 5-11 Development of mid-channel bar towards the end of RunS4**

Differences in channel form exist between the five experimental runs, with the most noticeable changes occurring in the upstream one-third of the flume. Channel pattern in downstream areas remained similar for all the runs. In runs with sediment feed, cross section elevations clearly demonstrate the aggrading nature of the channels. In RunS2, the magnitude of aggradation varied from around 1.7 cm (measured close to flume inlet at X=4500 mm) to almost nothing (measured around mid-flume at X=2500 mm). Small amounts of degradation (about 0.6 cm) were measured close to the flume outlet at X=1000 mm. Overall, amounts of aggradation were almost three times as great as amounts of degradation. The trend was the same for the second aggradation cycle (RunS4) though with a lesser magnitude. The absence of sediment feed essentially reversed the trend. Most parts of the upstream flume reach were degraded; the highest degradation of around 3cm being for the last experiment (RunS5), measured at X=4500 mm. Further downstream changes were reduced in magnitude. The notable difference between RunS5 and RunS3 was that in RunS5 degradation was highest and continuous throughout the length of the flume except at the very downstream end. Moreover, degradation was concentrated over less than 50% of the channel bed occupied by flow. During aggradation runs, a greater proportion of the bed accommodated changes in sediment volume.

### 5.3.3. Variation in water surface slope between aggradation and degradation runs

Water surface slope is a key determinant of shear stress; because as slope increases boundary shear stress and bed material transport generally increase (Madej *et al.*, 2009). Water surface slope is often assumed to be constant when calculating and predicting sediment transport in rivers despite commonly being used as a substitute for energy gradient and its impact on sediment flux (Dingman, 1984). In the experiments described here it was very difficult to measure water surface elevation directly, primarily due to shallow flow depths. To overcome this problem, water surface widths were estimated during the experiment by surveying cross sections using the laser profiler twice; first, with the water supply to the flume turned off (i.e. with a dry bed); and second, with the water supply on (i.e. with a wet bed). Sections were spaced at 25 cm intervals along the flume. A video recorder was attached to the bottom of the laser profiler at the same time while measuring wet channel cross sections, and the footage was used to help to identify wet and dry parts of the channel. Once the starting point of the wet channel is identified, a constant water level is assumed and the water surface elevations are fixed along the flume and water surface slope is calculated. The method used is described in detail in chapter 6.

Figure 5-12 shows the variation in water surface slope during the aggradation and degradation scenarios. During the first experiment in which the braided channel formed without sediment feed, water surface slope decreased sharply to 0.0232 m/m from a value which was very close to 0.028 at the early start of the experiment. During most of RunS2, water surface slope increased steadily and shows a slight fluctuation, but attained a maximum value of 0.0291 m/m at around 36 hr, before declining again. Water surface slope decreased further when the sediment feed stopped. For the majority of RunS3, slope decreased continuously until an experimental time of around 60 hr. For most of the second aggradation cycle, the water surface slope was nearly constant, with limited variation around an average value of 0.0266 m/m. For the last degradation cycle, slope decreased sharply to 0.02 m/m at the end of the experiment.

Most of the changes in water surface slope were accommodated close to the entrance of the channel (from X=3500mm to X=5000mm) with some small changes observed (from

X=1500mm to X=2500mm). Run S5 (the last degradation cycle) provided an exception to this general observation. There was a significant reduction in water surface slope during the last degradation cycle that probably resulted in a reduction in overall mean sediment transport rate compared to that during the second degradation cycle (Table 5-1).

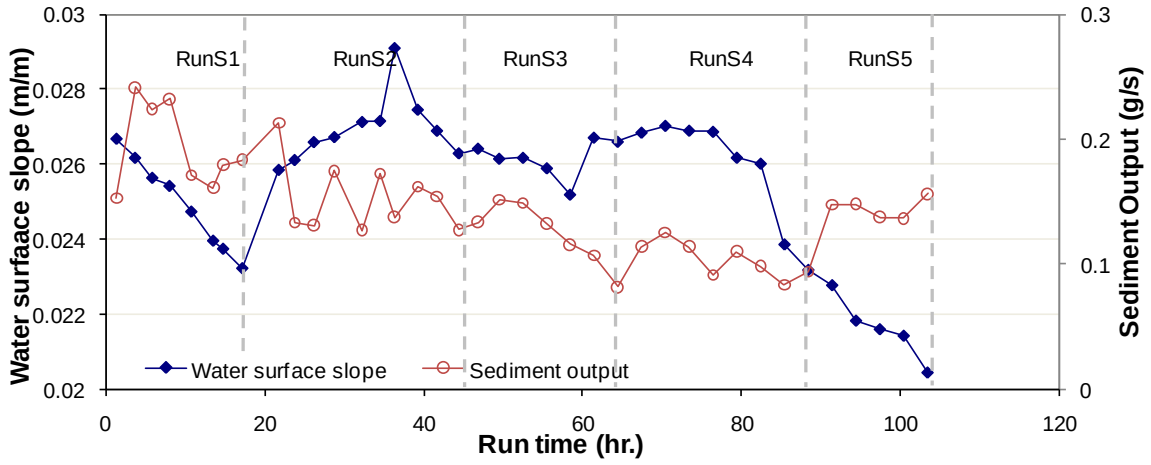


**Figure 5-12 Variation of mean water surface slope and sediment output at flume outlet**

As can be seen from Figure 5-12, there is no definite statistical relationship between total sediment discharge and water surface slope. Different amounts of total sediment discharge can be obtained at the same slope and different slopes can also produce the same sediment discharge. This is because sediment transport is also controlled by channel cross section geometry. Despite this, there is a positive relationship between the water surface slope and sediment transport during some runs (e.g. during RunS1, RunS3 and RunS4). For these 3 runs the coefficient of determination ($r^2$) between these variables was 0.33, 0.73, and 0.34 respectively.

### 5.3.4. Development of longitudinal profile and channel bed slope

Previous research has examined the effects of water discharge, the characteristics of river bed material, suspended or bed load discharge, the type of bedrock and other variables on the form of the longitudinal profile of a river and its evolutionary tendencies. In most of the studies, water discharge, river bed material grain size and sediment load are believed to be the most important controls on the shape of the profile

(R doane *et al.*, 2003). Other factors, (e.g. tributary channels, tectonic movements etc) play a secondary role and account for deviations from the general form of the profile (R doane *et al.*, 2003). This subsection will describe longitudinal profile evolution and change in channel bed slope during the flume experiments.

Figure 5-13 shows the development of the longitudinal profile throughout the course of the experiments. It is clear that defining a single channel thalweg is very difficult in braided rivers. This is due to the fact that there are a number of smaller channels that will make multiple thalwegs to exist. In this case the channel thalweg defined is the deepest section of the channel. The channels observed here typically exhibited convex upward profiles marked by several distinct inflections. The slope of the channel declined as the sediment feed rate ceased for RunS1, RunS5 and to some extent RunS3. Longitudinal profiles of rivers are most commonly concave upwards. However, many dryland rivers are either less concave than those located in humid temperate areas (Parsons and Abrahams, 2009) or upward convex (Schumm, 1961). This may be attributed to the fact that the ratio of sediment to stream flow often increases downstream due to transmission losses (Parsons and Abrahams, 2009). This means that sediment is transported by progressively less flow, leading river bed aggradation and development of convex profile. Likewise, when more sediment flows out of the reach than is fed in, the channel is forced to degrade. This transient period of degradation at the upstream boundary assisted by the transmission losses and inability of flow to transport sediment, will force the profile of the channel to be upward convex. In the current experiments, incision was very rapid and intense for degradation runs in the upstream part of the channel. Thus, even when sediment feed stopped, the downstream reach continued to aggrade because of continued delivery of sediment from the rapidly degrading reach in the upstream portion of the channel (Germanoski, 1993). This is probably what happened especially in RunS1, RunS3 and to a lesser extent in RunS5. Snow and Slingerland (1987) also modelled and analysed the effects of changes in water discharge, sediment discharge, sediment calibre on the long profile evolution of both sand and gravel beds by holding other variables constant. They observed that downstream variation in sediment discharge relative to flow discharge has strong potential to influence profile form and produce convex profiles.

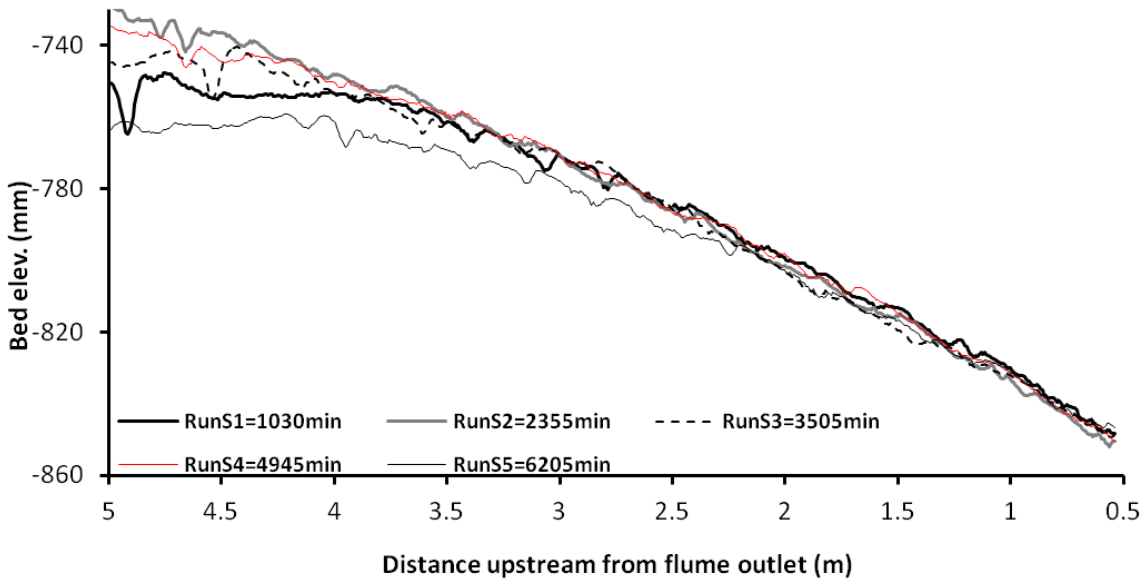


**Figure 5-13 Longitudinal profile of channel thalweg measured at the end of aggradation and degradation runs**

Fill and scour of the bed varied for short lengths of the flume during aggradation and degradation runs. Most changes were accommodated between the flume entrance and middle point. Changes in thalweg elevation from below 2.5 m to the outlet were very minor. During the first aggradation cycle (RunS2) bed elevation increased and most changes in elevations were accommodated at the entrance of the flume (from 3.5 m up to the inlet) while the rest of the flume exhibited little change. During all the degradation cycles, erosion largely contributed most of the changes in bed elevation especially from entrance to mid-flume. At the end of the final degradation cycle (RunS5), the bed elevation remained lower than the original for most of the flume length indicating that the channel is unable to recover from the disturbances (change in sediment supply).

The continued delivery of sediments from the actively incising upstream reach during the degradation experiments reduced the capacity of the channels to transport sediments further downstream. This caused bed elevations in the downstream portion of the channel to remain high although sediment feed has stopped (Figure 5-14). Examining the evolution of the longitudinal profile over the course of the experiment on Figure 5-14 two distinct areas can be noted (indicated by a dashed line in Figure 5-14A, B and C). Area 1 represents the section where the long profile of the degrading channel lies

completely below the following or previous aggrading channel (in most of the cases this is located close to entrance of the flume). Area 2 corresponds to the section where the long profile of the degrading channel lies above and/or below the next or previous aggradation phase. The two regions are separated by an inflection point: the point that separates the rapidly degraded upstream area from the braided downstream reach as reported in previous laboratory experiments (Germanoski and Schumm, 1993;Germanoski, 1993). This point also seems to migrate through time as illustrated in Figure 5-14. Initially, the division between the rapidly degrading upstream zone and the aggrading braided zone occurred close to the flume inlet (4m from the flume outlet as indicated in Figure 5-14A). The channel was then rapidly filled by sediments during the first phase of sediment feed. Intensive filling of this rapidly degraded zone has occurred for the first 500 min and after that only minor changes happened in this reach. The inflection point seems to move further downstream with cessation of sediment feed in RunS3, though it had only advanced not more than 50 cm from its former location (Figure 5-14 B). However, as the gradient continued to decrease in the upstream degrading zone (see upstream section of RunS5 in Figure 5-13) bed load transport also reduced (see section 5.3.2), leading to migration of the inflection point further downstream closer to the outlet. Very similar results have been reported by (Germanoski, 1993). In the experiments of (Germanoski, 1993) there is a clear trend that indicates the downstream migration of the inflection point as the channel continued to degrade. However, in this case it appears that phases of aggradation and degradation are alternating in the downstream section, with the exception of RunS1-S2, where in this case the long profile of RunS2 lies entirely above that of RunS1 below the inflection point (see Figure 5-14 D). This small difference between the results is due to the fact that (Germanoski, 1993) examined a continuously degrading channel whereas in this case continuous degradation is interrupted by supplying sediment and initiating aggradation in between degradation experiments. Moreover, there are certainly differences in controlling variables (water discharge, sediment feed rate and grain-size) between the two sets of experiments.

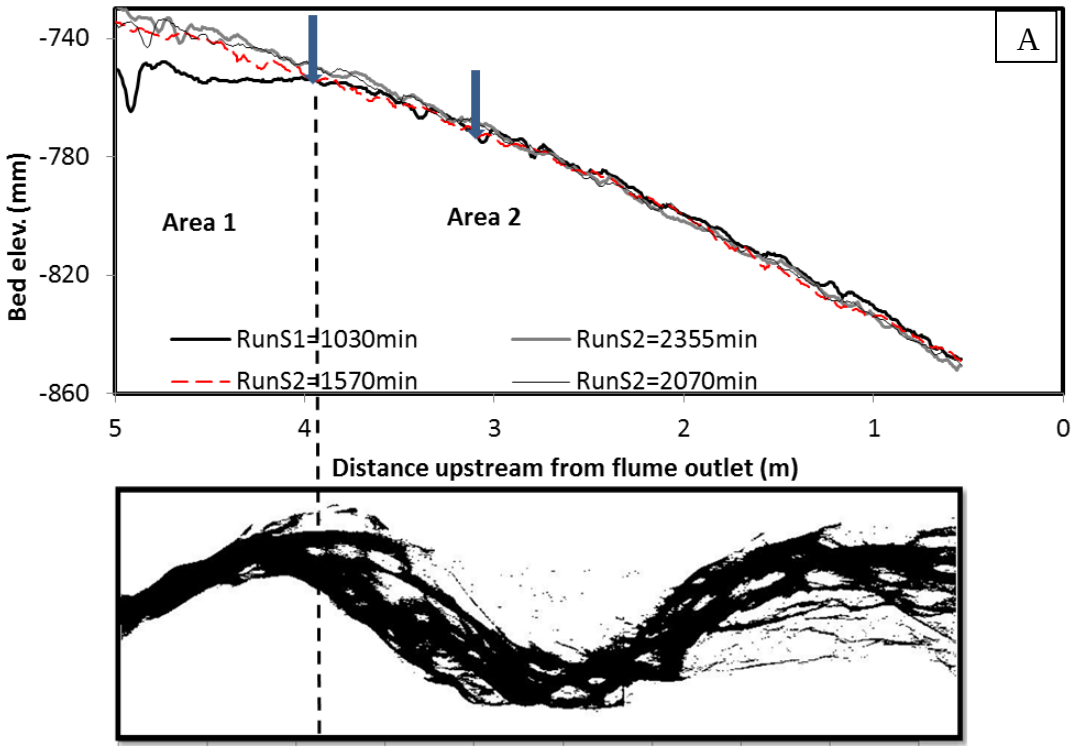
A
-740
-780
-820
-860
Bed elev. (mm)
Area 1
Area 2
RunS1=1030min
RunS2=2355min
RunS2=1570min
RunS2=2070min
5
4
3
2
1
0
Distance upstream from flume outlet (m)

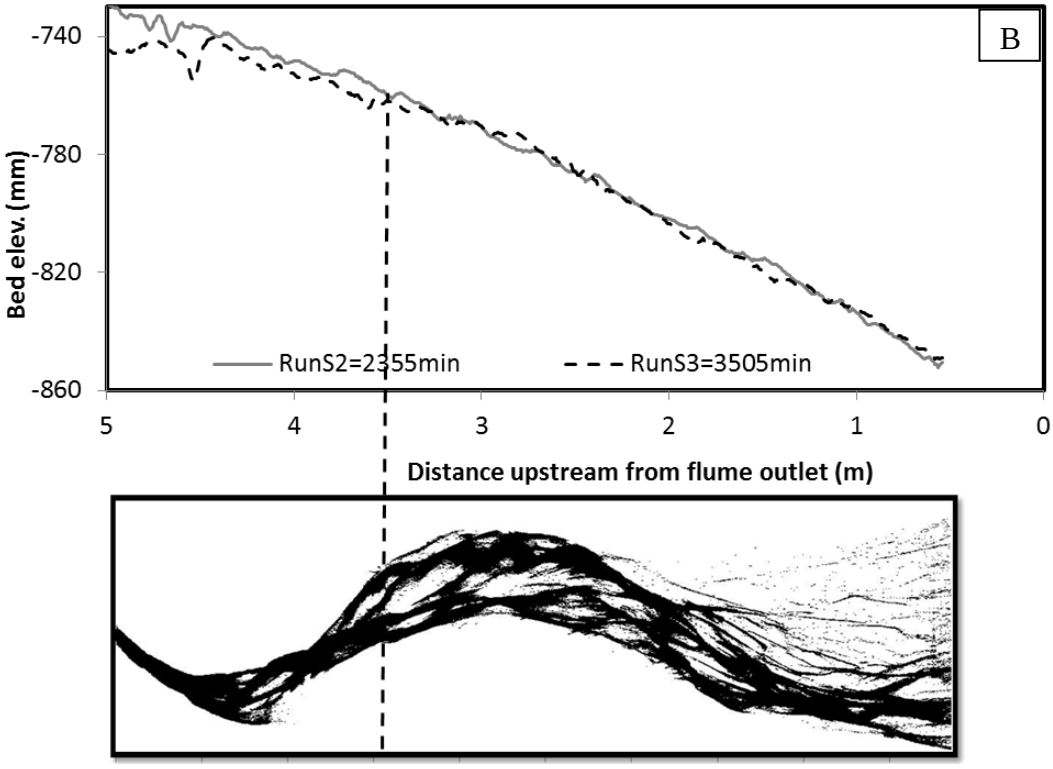
B
-740
-780
-820
-860
Bed elev. (mm)
RunS2=2355min
RunS3=3505min
5
4
3
2
1
0
Distance upstream from flume outlet (m)

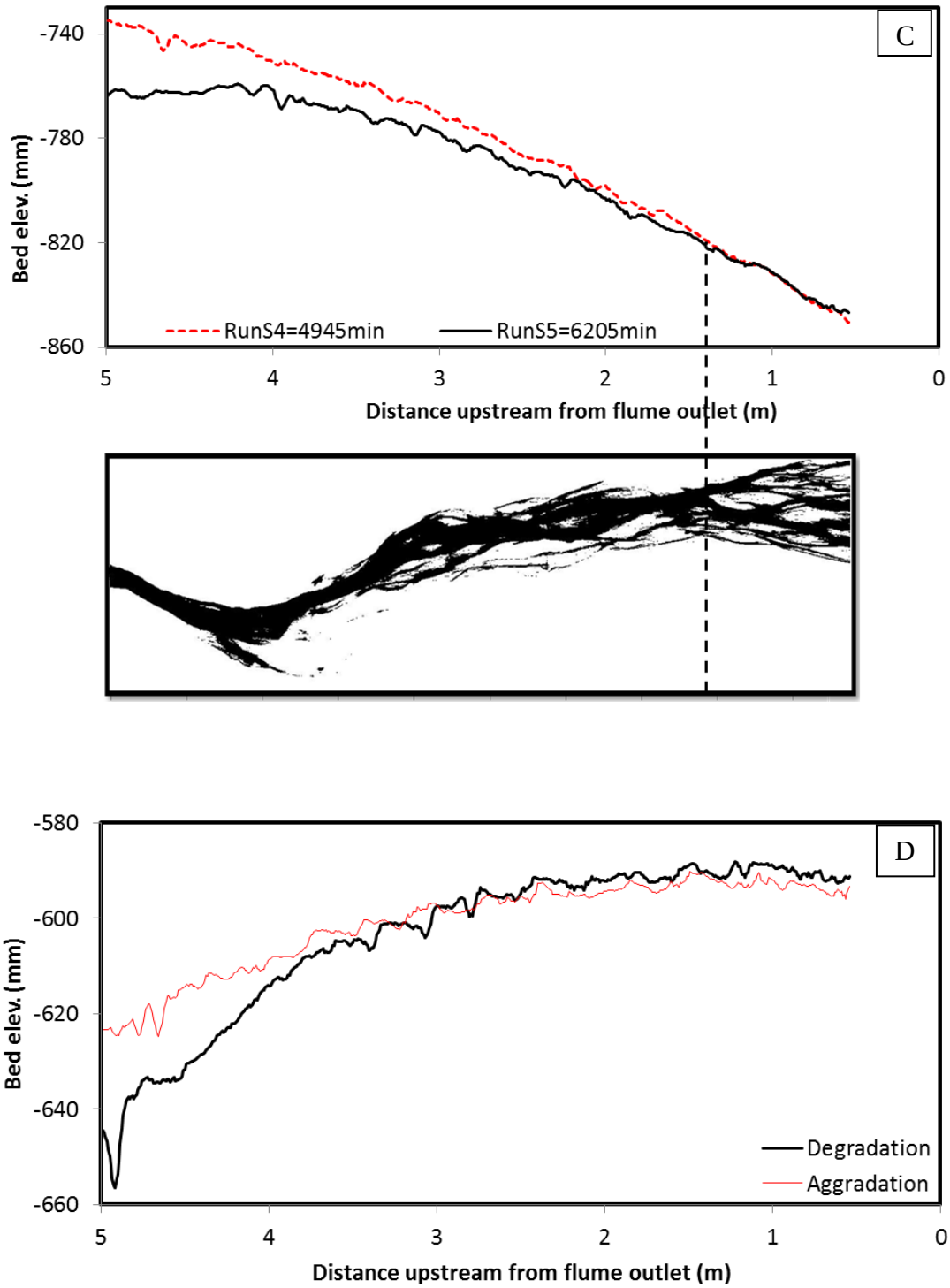


**Figure 5-14 Relationship between channel pattern and longitudinal slope and migration of inflection point**

In Figure 5-14D profiles are plotted relative to an arbitrary datum with the flume gradient removed to illustrate the inflection point more clearly. The profiles do not show the true channel gradient. It clearly shows the inflection point between the upstream degrading reaches and the downstream aggrading reaches in the degrading

channel. It suggests that degradation is rapid and high in the upstream reach and this has resulted in aggradation of the downstream reach.

Several researchers have studied relationship between channel pattern and longitudinal slope both quantitatively and qualitatively (Ackers and Charlton, 1970;Leopold and Wolman, 1957;Henderson, 1966;Lane, 1957;Osterkamp, 1978). Physical model studies have also been used in the past to demonstrate the existence of pattern thresholds related particularly to slope (Schumm and Khan, 1971). In general, for a certain discharge, braided streams are characterized by greater slopes than meandering streams. Different channel patterns can also occur at different sections of the same river depending on longitudinal slope and sediment characteristics. Lee and Henson (1977) observed an abrupt change in channel pattern of the Red river from non-braided to braided while in that same section the longitudinal slope doubled from 0.034% to 0.068%. Similarly, Leopold and Wolman (1957) also observed a change in channel pattern in Horse Creek from single thread to braided where the longitudinal slope changed from 0.0022 to 0.0073. In experimental series 1, channel bed slope is calculated from regression of thalweg elevations of cross sections taken every 8mm in the stream-wise direction. Furthermore, thalweg elevations of channel cross sections acquired at 25 cm longitudinal interval are also used to calculate temporal variation of longitudinal slope within an experiment. Channel slopes calculated by regression of thalweg elevations range in value between 0.020 and 0.027; the maximum being attained in the first aggradation cycle RunS2. Since bed elevation is fixed at the downstream end of the flume, significant increase in bed elevation occurred in the upstream end of the flume. For all degradation runs a break in slope occurred together with a change in channel pattern. This was greatest in RunS1 and RunS5. In RunS1 there was a significant change in slope (from 0.002 to 0.028) when the channel pattern changed from single thread to braided although it was only in the upstream 1m of the channel that this occurred (Figure 5-14A). In RunS3, however, the change in slope was reduced (from 0.0065 to 0.028) owing to interruption of degradation by sediment feed from upstream. Generally, absence of sediment feed and channel degradation throughout the experimental series was associated with the channel moving towards a single thread, meandering system (Figure 5-14) with milder slope close to the inlet. During periods of

sediment feed the slope of the channel was generally steeper and the pattern was braided.

The most abrupt change in gradient occurred in the area near the flume inlet or from 3.5 m to 5 m upstream of the flume outlet. When the upstream reach underwent a transition from braided to single-thread (RunS2 to RunS3), it experienced a reduction in longitudinal slope from 0.017 to 0.0065. When sediment feed was restarted in RunS4, the channel pattern in the same reach changed to braided and its longitudinal slope increased by more than double to 0.014 before finally attaining the minimum slope of 0.0046 in the course of the experimental run. In real terms, the increase in slope translates into aggradation and development of multiple threads at least for this experiment. In response to the cessation of sediment feed from upstream, transport capacity does not show a clear trend. Transport capacity appears to decrease in the first degradation cycle (S3) but it increases in the second degradation cycle (S5). However, there is vertical incision with different magnitude and channel migration through bank erosion in all degradation runs; both of which ultimately reduced the channel slope.

## 5.4.SUMMARY

There have been very few attempts to compare physical models and field prototypes at a more quantitative level, due to the complexities of braided rivers and difficulties encountered in investigations of full-sized braided river processes. So, most of the comparisons in this chapter are based on qualitative descriptions.

The morphological changes reported in this experimental series were mostly similar to those seen in previous laboratory studies of braided channels (e.g., (Ashmore, 1991a;Germanoski and Schumm, 1993;Hoey and Sutherland, 1991;Madej *et al.*, 2009;Germanoski, 1993). In most of these studies the braiding intensity, number of braid bars, pattern complexity and morphologically active braid plain width all increase when a channel experiences aggradation. The same relationship is recorded in this experiment. However, unlike other similar laboratory experiments the bar size observed here does not show significant differences between aggrading and degrading channels. Degradation essentially reversed the morphological changes associated with

aggradation. Initiation of degradation by stopping sediment feed resulted in vertical incision close to the flume inlet that sometimes extended to middle of the flume. Flow became concentrated into a single channel flanked by erosional terraces that ultimately left a greater proportion of the active channel exposed. This is the most prominent feature of the evolution of sand bed laboratory channels. However, the downstream portion of the channel did not degrade due to the resultant influx of sediment arriving from the actively incised reach upstream. This is also in agreement with the laboratory experiments of Germanoski (1993) and Germanoski and Schumm (1993). The experiments of Germanoski (1993) have also been compared with Ash Creek, a degrading ephemeral braided channel, on the east flank of the Mazatzal Mountains in central Arizona. The stream degraded due to a reduction in sediment delivery as a result of re-vegetation of the drainage basin. The channel responses to this reduction in sediment yield included incision progressing from upstream to downstream and continued aggradation downstream, maintaining the braided pattern. These trends are very similar to the laboratory experiments reported here.

In all cases, the degrading channels have experienced a transformation in channel pattern from braided to single thread in the upstream reach. However, the extent of the transformation varies between runs. In the first run (RunS1), only the first 1m reach near the flume inlet was clearly transformed to single thread. Despite similar conditions prevailing in the experiment (water discharge, sediment grain size and flume gradient) around 1.5 m and 2 m of the channel reach below the flume inlet were transformed to a single thread pattern in runs S3 and S5, respectively. Moreover, the channels in the upstream part of the flume became progressively narrower through time. This is an indicator of the fact that although the transformation towards a single thread channel was not completed in the series of runs, the ultimate consequence of continued degradation was evident from the trend.

The sediment output appeared to fluctuate substantially at constant discharge. Several irregular phases of transport intensity were observed in the time series, which statistical analysis confirmed to posses a strong periodicity and dependence on previous transport rates. There is no significant difference in the magnitude of the sediment transport rate

peaks for aggrading and degrading channels, but these peaks were higher in relative terms during degradation runs.

The quantitative analysis of experimental data presented in this chapter included the changes in channel morphology in aggradation and degradation runs, variability in sediment transport and patterns and development of long profile evolution over the course of the experimental run. The experimental work presented in this chapter has shown that despite the lack of dynamic similarity conditions and simplification of overall similarity criteria, fairly consistent results could be obtained which can be interprated in a generic sense. The similarity between the laboratory channels from this experiment and those previously investigated by different researchers with or without a field prototype utilizing the Froude modelling principle suggest that the laboratory channels are at least qualitatively transferable to the field. Chapter 7 will present the application of a two-dimensional hydraulic numerical model using the DEMs collected during the experiment and test the representations of flow depth and unit discharge simulated by this model against the characteristics derived from the experimental channels.

# 6. HYDRAULIC AND SEDIMENT TRANSPORT CHARACTERISTICS OF EXPERIMENTAL BRAIDED CHANNELS

## 6.1. INTRODUCTION

This chapter examines the hydraulic and sediment transport characteristics of the experimental braided channels. First, the method of analysis used to derive the hydraulic parameters will be presented. This will be followed by results outlining the prediction of sediment transport rates by conventional transport equations and using cross section averaged hydraulic parameters. The effect of cross stream flow variability on sediment transport will be addressed by incorporating lateral variations in the calculation of sediment transport. The sediment budget approach will be used to investigate downstream patterns of sediment transport rate. A gamma probability density function will be used to model shear stress variation in the experimental braided channels and relationships will be investigated between the gamma shape parameter, sediment transport rate and channel morphological parameters.

## 6.2. METHODS OF ANALYSIS

Continuous data were collected over the course of all experiments. The evolution of the channel was documented by a laser profiler (that records bed elevation information), a video camera attached to the section of the laser profiler (that records and helps to identify wet and dry parts of a cross section) and high resolution photography from overhead cameras (that records changes in channel pattern). An example from each run of such cross section measurements, made when the bed was in a dry and wet state, is given in Figure 6-1, which shows the wet and dry sections together. A combination of different methods has been used to identify wet and dry parts of the channel depending on the availability of data. Acquiring quantitative information on channel morphology and processes operating on the channel from the photographs was not possible. However, the photographs were used to identify the inundation extent at channel cross sections. This was facilitated with the addition of potassium permanganate for flow visualization. In addition to the topographic

information provided by the laser profiler, the video camera attached on the arm of the profiler recorded continuous images of the channel cross sections. Channel cross sections were surveyed in both dry and wet states. The video is then used to identify the wet and dry parts of the channel. Although the laser does not measure water level accurately, it shows a typical pattern at locations where there is water. Consequently, in sections of the channel where the bed is very wet or water is very shallow, there is a lot of scatter in laser measurements. In locations where there is flowing water or when the flow is deeper, the laser readings in wet and dry conditions are totally different and wet laser data is relatively noise free. In this case the laser elevations may represent the water surface elevations. This pattern was especially helpful for identifying wet and dry parts of the flume at the inlet where flow is concentrated in one or two channels. The following procedure was adopted to identify wet and dry parts of individual cross sections with video records. For a specified speed of the laser profiler, the time required to traverse 1m (which was a commonly used survey extent in the experiment) is known, and hence the number of points the laser would read per minute is also known (since elevation is recorded at 1mm intervals). For each cross section, the recorded video is played and the time required to arrive at the right and left sides of the channel in which water is flowing can be determined with reasonable accuracy. The bed elevation at these two locations is determined from dry channel cross section surveys.

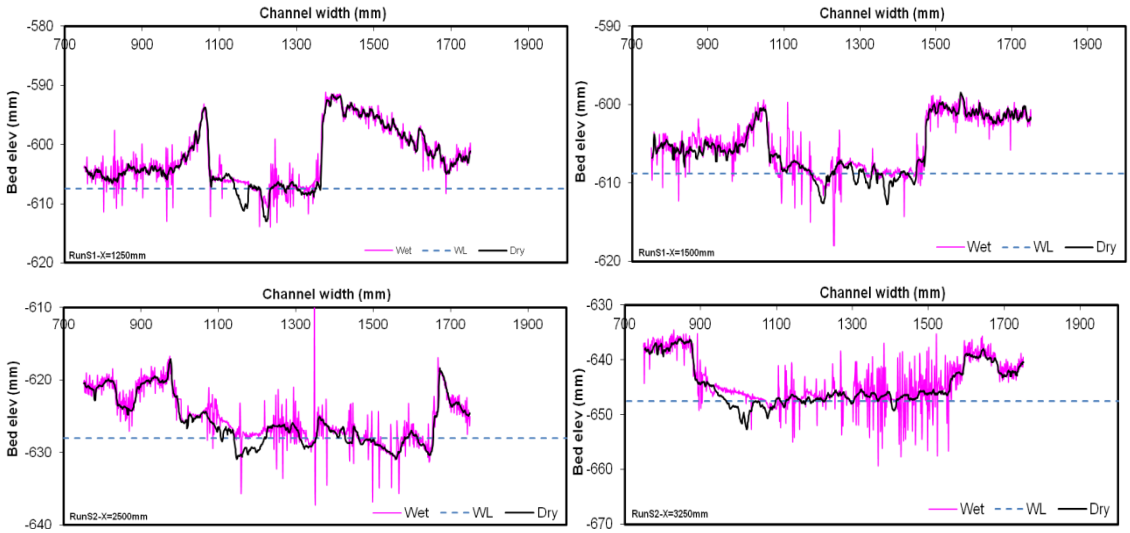

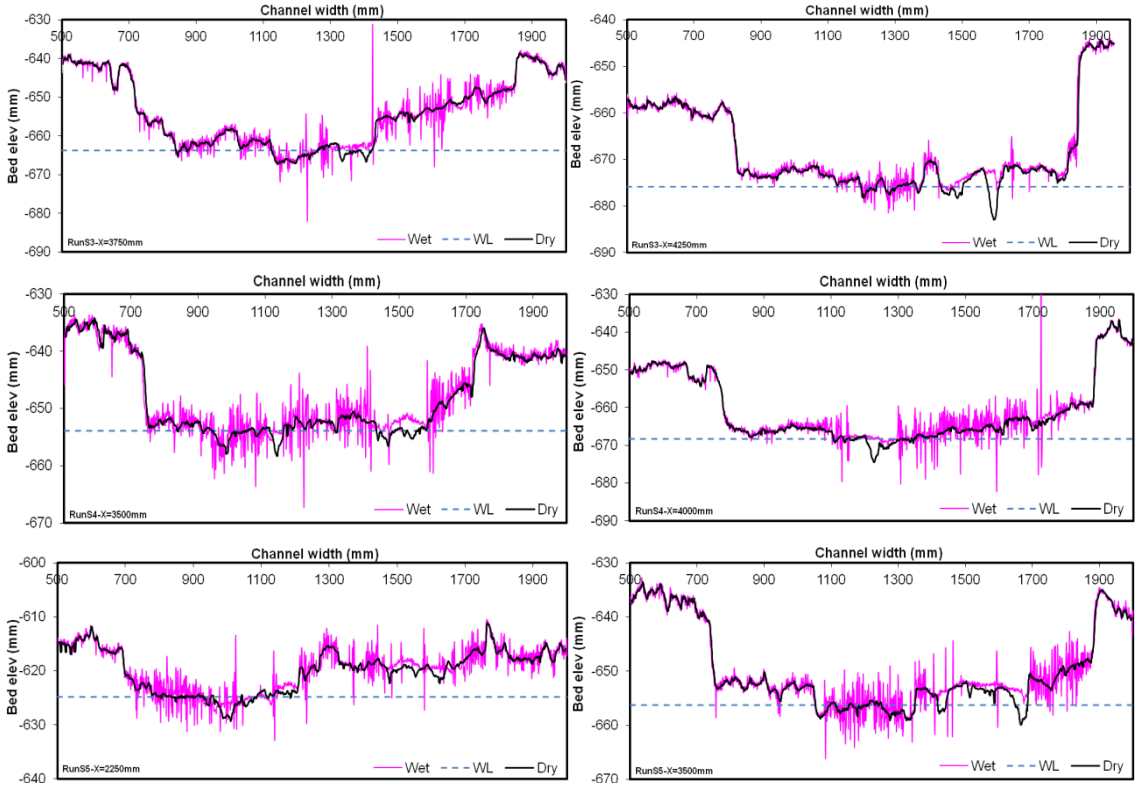


**Figure 6-1 Sample channel cross sections from each run with the dry (data surveyed when the channel is dry and filtered to exclude outliers), wet surveys and water level indicated by a dashed line**

At sections where a video record is not available, the photographs (taken at 2 minute intervals) and dry and wet channel cross sections were used together. The digital images were first geo-rectified manually using the flume X and Y coordinates (Geo-rectification is carried out using the software Global Mapper). Since the photographs cover the full extent of the flume (being similar in extent to the area covered by the laser) the margins of the photographs are given the start and end coordinates of the flume as surveyed by the laser in both the flume entrance and outlet. This was done so as to know the exact locations of channel cross sections surveyed by the laser, and match them with the photographs. Figure 6.2 to Figure 6-5 shows samples of rectified photographs used for this purpose, jointly presented with selected channel cross sections along with their location on the photographs. The horizontal and vertical grid lines superimposed on the photographs are drawn every 25 cm (for Figures 6-2, 6-4 and 6-5) and every 2cm (for Figure 6-3). These lines cover the whole length of the flume, but are cropped in the transverse direction to fit with the surveyed extent of the channel cross section. During identification of wet and dry areas, much finer grid lines (as fine as 1cm) were superimposed on photographs to locate the wet ends of the channel with a

reasonable accuracy. Once the start and end point of flowing water in the channel was identified from video records or digital photographs, the elevation of the two points are averaged and that elevation is taken to represent the water surface elevation that will be considered as constant over the cross section. The inundation extent of channel cross sections acquired by the above approach is further tuned manually by looking at each cross section.

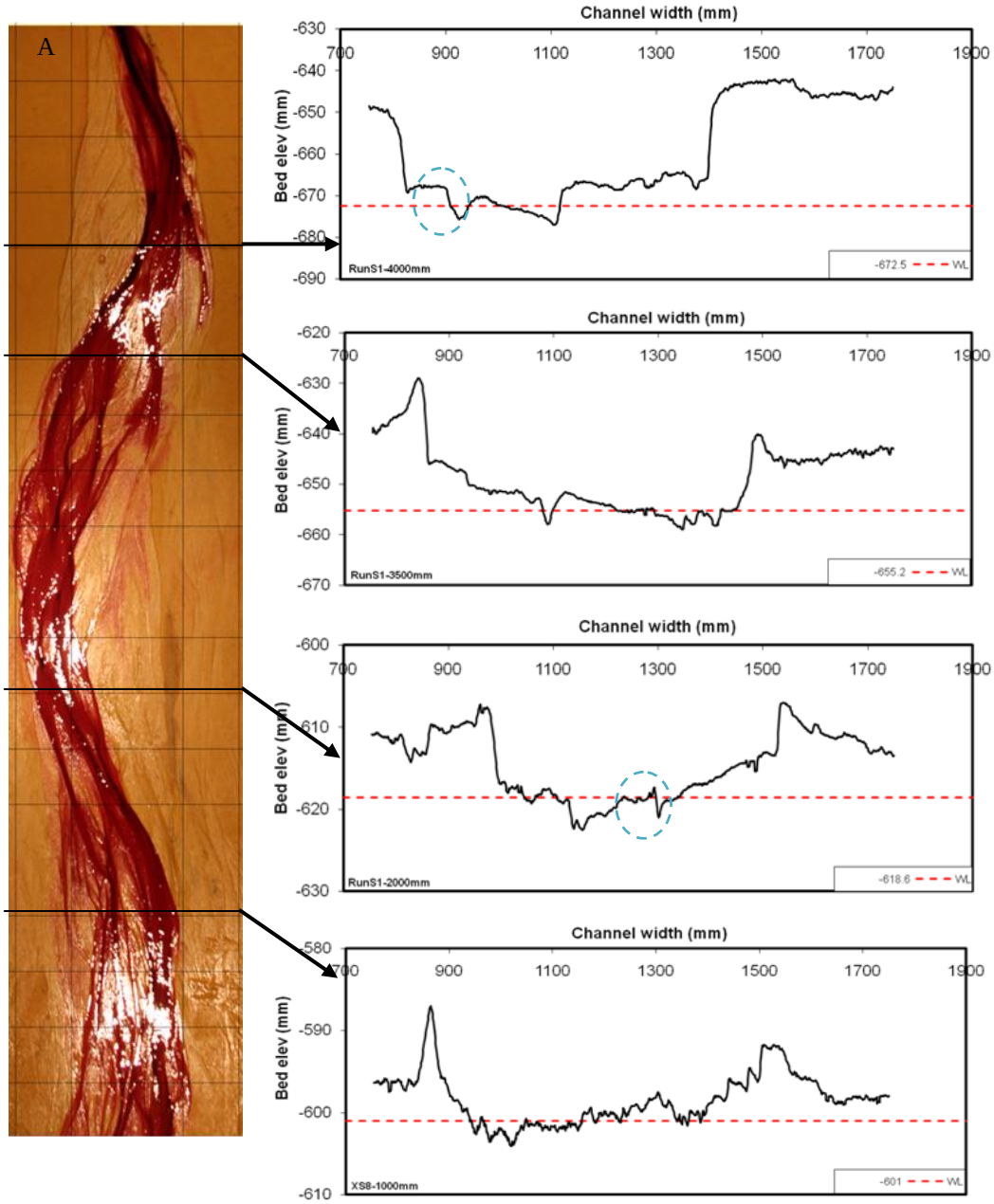


**Figure 6-2 Samples of geo-rectified photographs taken from overhead (End of RunS1); the number in the legend in each cross section represents the water level at that section. All the sections are being viewed looking downstream.**

This is done by visually inspecting the cross-sections for each time period to see if some parts of each section that have been identified as wet (assuming a constant water surface elevation across the section) might in fact have been dry. For sections that have more than one wet channel, the areas upstream and downstream were examined to make sure that the wet areas of each section appear to be connected. Where a small part of a section has been identified as wet but the same parts of the sections upstream and downstream are dry it's quite likely that the section between them is also dry. This is a reasonable assumption as cross sections are surveyed at relatively short distance interval of 25cm. Using this approach water levels were adjusted further and the number of wet channels in a cross section refined.

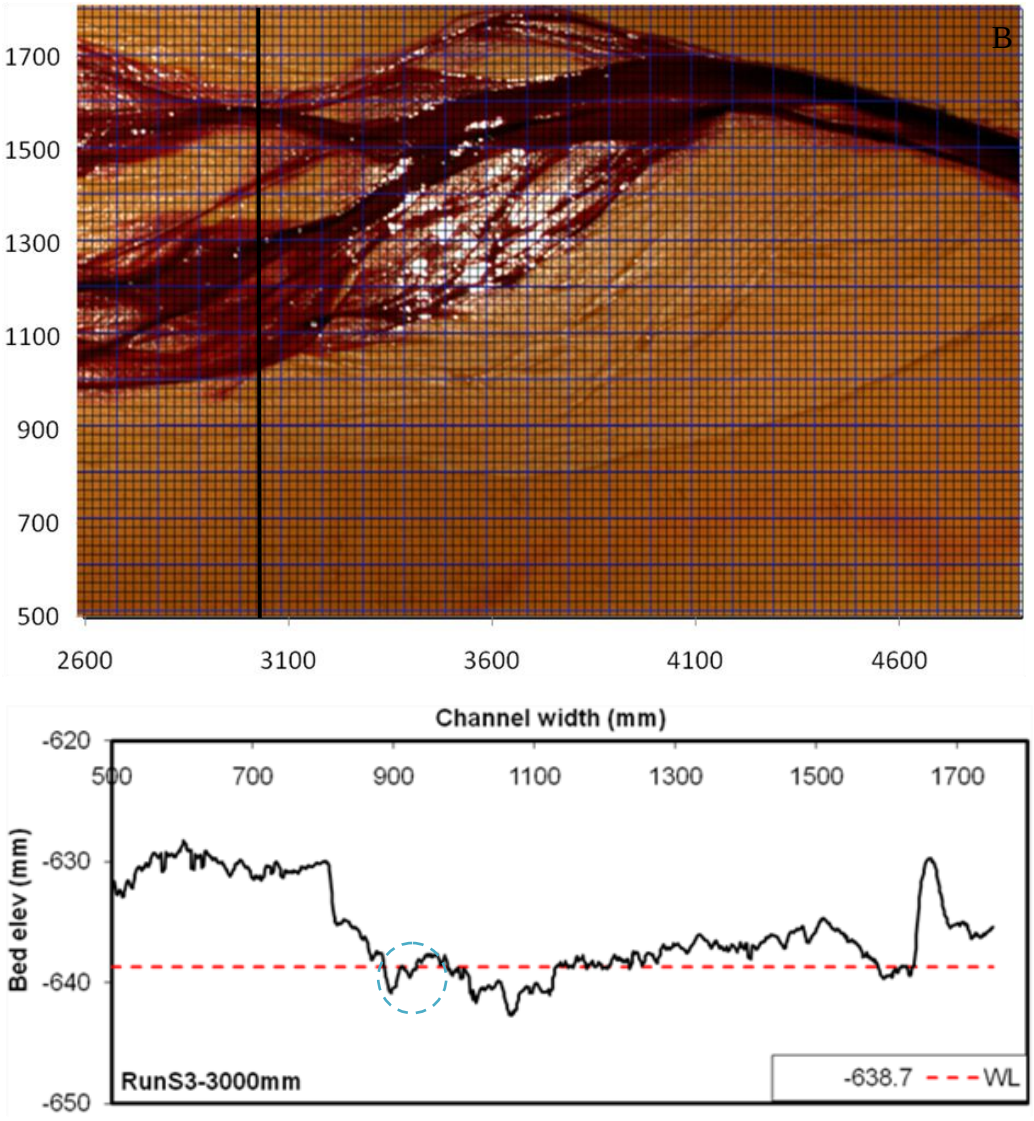


**Figure 6-3 Samples of geo-rectified photographs taken from overhead (RunS3); the number in the legend represents the water level at that section.**

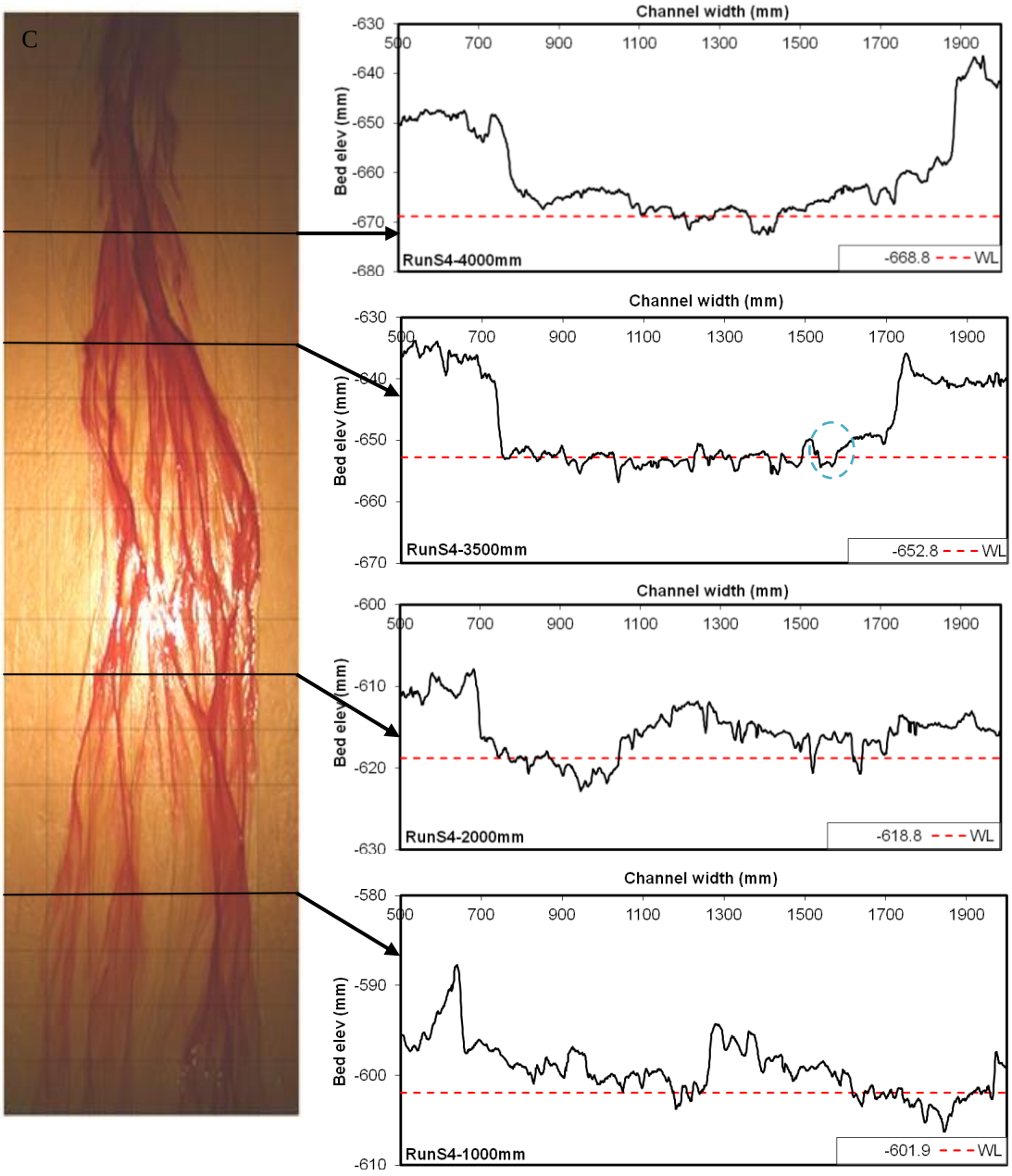


**Figure 6-4 Samples of geo-rectified photographs taken from overhead (End of RunS4); the number in the legend in each cross section represents the water level at that section. All the sections are being viewed looking downstream.**

The refining process was further assisted by the geo-rectified digital images taken from overhead. Some parts of the channel circled with dashed lines (in Figure 6-1) indicate parts of the section that were identified as wet according to the constant water surface elevation assumption, but might in fact be dry. These issues were identified by visual inspection of photographs and corrected before the final calculations were carried out.

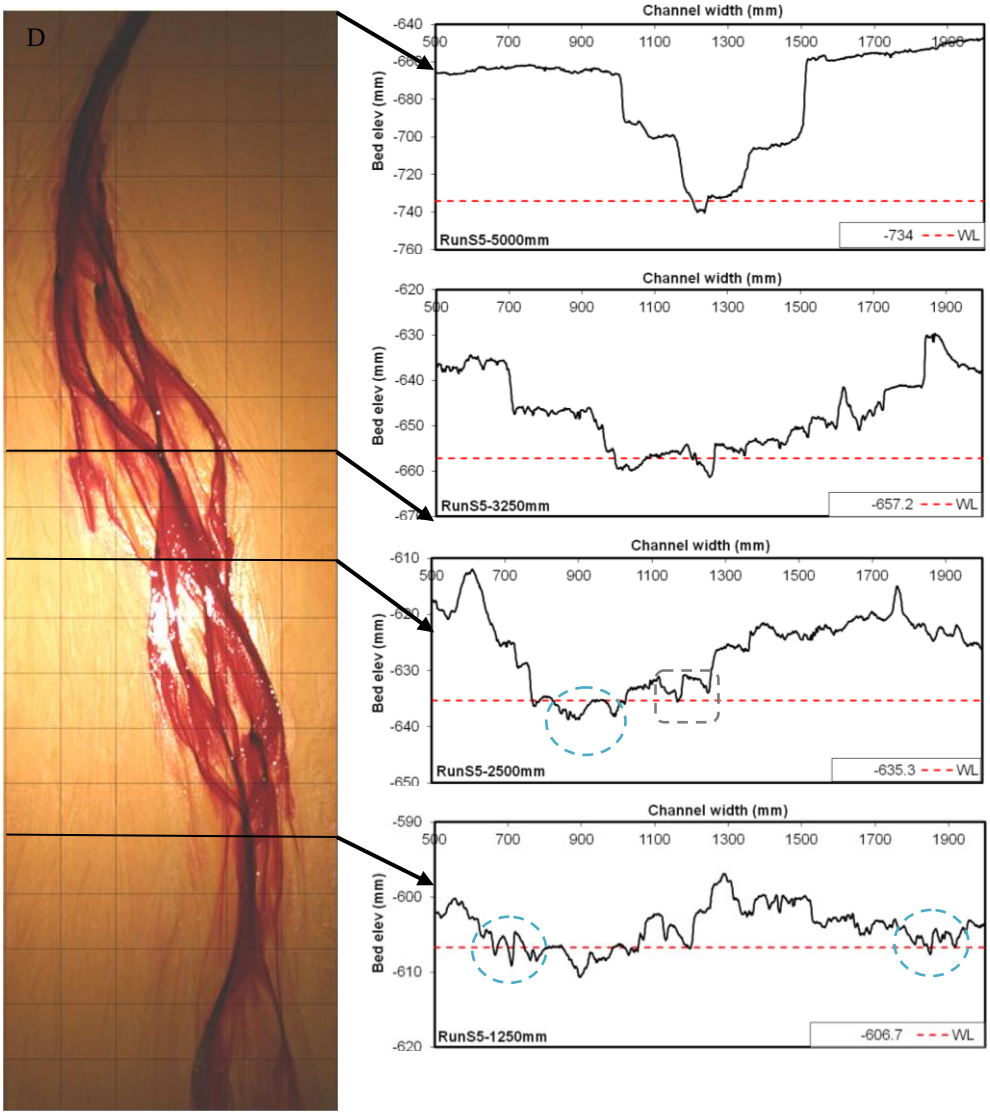


**Figure 6-5 Samples of geo-rectified photographs taken from overhead (End of RunS5) used to identify and refine wet parts of the channel; the number in the legend in each cross section represents the water level at that section. All the sections are being viewed looking downstream.**

Once the free surface level is known, flow depth at any point can be estimated as the difference between water surface elevation and bed elevation. Total water discharge and sediment transport capacity can then be determined based on a simple one dimensional numerical calculation using cross-section geometry alone, as proposed by (Bertoldi *et al.*, 2009). A key aim of carrying out these calculations is to allow a more detailed examination of the relationships between flow hydraulics and sediment transport during the experiments than is possible using the sediment transport data collected at the flume outlet.

The approach is more direct than some other models and has limited data requirements (it requires data on cross sectional geometry only). Moreover, it accounts for lateral variability in hydraulic parameters. The method works by dividing the cross section into a number of vertical panels and calculating water and sediment discharge assuming locally uniform flow. In this procedure, bed roughness is calculated by a Keulegan type roughness estimator using the water depth determined at each panel as the difference between the water surface elevation and the channel bed level. Water velocity is determined using a flow resistance equation and discharge is then estimated in each panel using the principle of continuity. The sediment transport rate within each panel can be calculated using a range of bedload transport equations. The total water and sediment discharge is calculated as the sum of the values in each panel.

Using the water surface elevation values derived from dry and wet cross section surveys with video records sometimes resulted in over estimation of the water discharge. To reduce this disparity, the water level was tuned iteratively using the Keulegan type resistance function until the sum of the panel discharges equals the known total discharge by varying the water surface elevation. Shear stress in each panel was estimated using the uniform flow approach and by assuming the same ($d_{50}$) grain size in each panel.

One simplifying assumption of the method is that the free water surface level is horizontal across the whole section, which is inaccurate as water level at a given discharge often differs between adjacent anabranches in a braided river (Zolezzi *et al.*, 2006;Bertoldi *et al.,* 2009) and some channels may not have significant flow even though they are at lower elevations than those conveying water. This also happened in some cross sections (an example is given in Figure 6-5 RunS5_XS-2500, where in this case water should actually be inside the dashed square). Every effort was made here to correct these errors using visual inspection of the adjusted images. The expectation is that the averaging of the estimated hydraulic and morphological parameters over a reach from multiple cross sections may balance the error due to non uniform water surface level. The same model was also used by Bertoldi *et al.* (2009) to compute sediment transport rates in braided networks and results were found to be satisfactory, when compared to observed values.

**Computation of flow and sediment transport**

Water depth at each panel is determined as the difference between the water surface elevation and the channel bed level (refer to Figure 6-6 below):

$$h = \left[Z_s - 0.5\left(\eta_{b,j} + \eta_{b,j+1}\right)\right] \quad \text{6-1}$$

The flow in each panel of the channel is computed using the Keulegan type resistance equation and the normal flow approximation. Local boundary shear stress is related to flow velocity using a drag law of the form:

$$V = \sqrt{\frac{\tau_o}{C_f}} \quad \text{6-2}$$

In the above equation V is mean flow velocity and $C_f$ is bed resistance coefficient. Reducing the relation for momentum conservation using the uniform flow approach with the drag law equation shown above yields:

$$V = \sqrt{\frac{g}{C_f}} h^{1/2} S^{1/2} \quad \text{6-3}$$

$$V = C_z \sqrt{g} \sqrt{hS} \quad \text{6-4}$$

$C_z$ is dimensionless Chezy resistance coefficient which is estimated using a Keulegan type resistance estimator:

$$C_z = \frac{1}{C_f} = \frac{A}{\kappa} ln\left[11\frac{h}{K_s}\right] \quad \text{6-5}$$

Where κ is the dimensionless Karman coefficient, which equals 0.4, $K_s$ is a roughness height characterizing the nature of the bed and A is a calibration coefficient. The continuity equation is then used to estimate discharge in each panel:

$$q = Vh \quad \text{6-6}$$

One of the simplest and most frequently used transport equations is the Meyer-Peter and Müller (1948) transport predictor. Though the equation captures only the basic physics of the transport problem, it has been used frequently to estimate rates of sediment transport (e.g., HEC, 1993; [289]Nicholas, 2000[7]) and was found to perform reasonably well by Gomez and Church (1989).

The general form of the Meyer-Peter-Muller equation reads as:

$$\frac{q_b}{\sqrt{Rgd_{50}^3}} = \begin{Bmatrix} K(\tau_* - \theta)^{3/2}, \tau_* \geq \theta \\ 0, \tau_* < \theta \end{Bmatrix} \quad 6\text{-}7$$

$$\theta = \tau_c/(\rho_s - \rho)gd_{50};\ \tau_* = \tau_o/(\rho_s - \rho)gd_{50};\ R = (\rho_s - \rho)/\rho$$

Where $q_b$ is the volumetric sediment transport per unit river width ($m^2/s$)

$d_{50}$ is the median grain-size

K is the numerical constant for the Meyer-Peter and Muller transport law

$\theta$ is threshold shields stress for the MPM transport law

$\tau_c$ is the critical shear stress for sediment entrainment

$\tau_o$, $\tau_*$ is the local bed shear stress and dimensionless Shields stress respectively.

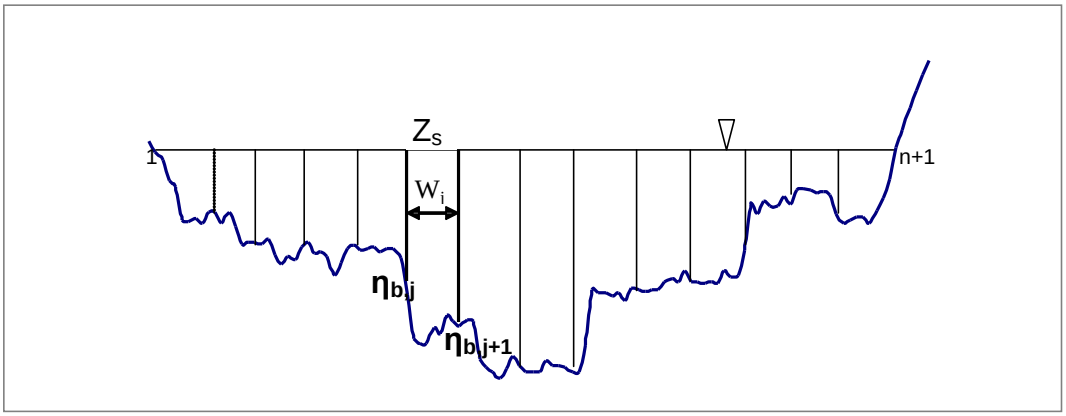


**Figure 6-6 Representation of channel cross section**

The total water and sediment discharge are calculated as the sum of the values in each panel

$$Q = \sum_{j=1}^{n} q_j \quad 6\text{-}8$$

$$Q_b = W_i \sum_{j=1}^{n} q_{b,j} \quad 6\text{-}9$$

Where $\eta_{b,j}$ = bed elevation at station j; and $W_i$ = distance between stations j and j+1; $Z_s$ = water surface elevation which is assumed to be constant across the whole section; Q = total water discharge; $Q_b$ = total volumetric sediment transport; $q_j$ = unit water discharge in $j^{th}$ sub panel; $q_{b,j}$ = sediment transport rate in sub panel j.

## 6.3. MEAN SEDIMENT TRANSPORT RATE AND EFFECT OF FLOW VARIABILITY

Prediction of sediment transport remains a significant problem in understanding braided river morphodynamics for engineering and geomorphic applications. This is mainly due to the complexity and instability of braided river morphology and consequent wide variations in transport rates (Ashmore, 1988;Gomez and Church, 1989;Hoey and Sutherland, 1991;Warburton and Davies, 1994). Despite more than a century of work on sediment transport, there exists no formulae that is capable of predicting bed load transport to a satisfactory level (Gomez and Church, 1989). Although transport rates can be estimated using standard bedload transport functions(Carson and Griffiths, 1987;Ashmore, 1988), there are lots of uncertainties in those equations related to the choice of formula and entrainment threshold. Moreover, those uncertainties are further amplified by the lateral variation in morphology, grain size and hydraulics of braided rivers.

A better understanding of the effect of lateral hydraulic variability on sediment transport can be obtained by calculating total sediment transport using both cross-section averaged and local hydraulic parameters. Most previous researchers have suggested that cross-section averaging of hydraulic parameters in applying standard bed load functions has a much more significant effect in braided rivers than single thread rivers (Carson and Griffiths, 1987;Paola, 1996;Nicholas, 2000;Ferguson, 2003;Bertoldi *et al.*, 2009). The actual bed load transport in braided rivers is thought to be several times greater than the one that can be estimated using cross-section averaged parameters. The worst case scenario for this underestimation is when the section averaged shear stress is less than the ‘assumed’ critical shear stress for sediment transport. This means no transport would be predicted in the channel. Ferguson (2003) also pointed out that underestimation of transport rates will be greater for low values of shear stress as this leads to underestimation of the average shear stress.

Having said this data collected during the experiments were used to compare two approaches of sediment transport computation. First sediment transport is computed by using cross section averaged hydraulic parameters and the Meyer-Peter and Muller transport equation, as described in the previous section. Second, sediment transport is

computed by accounting lateral hydraulic variability into consideration. Cross section averaged hydraulic parameters are determined by simple averaging of local flow depth values in each cross section as obtained using equation 6.1 above (i.e., averaging only over the wetted width). As flow strength may vary across a river because parts of a channel may be deeper than others, failure to allow for local spatial variability in flow strength may lead to underestimation of bedload fluxes (Ferguson, 2003). The measured time series of the sediment transport was used to calculate a mean (time-averaged) flux for each experiment. By this procedure an individual data point for the measured sediment transport rate is obtained as shown in Figure 6-7. For computing sediment transport rates, channel cross section measured at the outlet of the flume towards the end of an experiment is used to represent an individual data point in Figure 6-7. The variation between transport rates measured during the five experimental runs is very small, which makes it difficult to differentiate between different points when presented in a single graph. Due to this, each run is presented below in a separate graph (Figure 6-7).

To identify the most suitable values of the parameters "K" and "θ" for use in the MPM sediment transport equation (equation 6-7), a sensitivity analysis was carried out by comparing the sediment output measured at the flume outlet with the sediment transport predicted using the MPM transport equation and taking lateral flow variability into consideration. The value of the Shield's parameter is originally defined as 0.06, however a range of values from 0.01 to 0.1 have been used previously in the literature (Church, 1978;Williams, 1983). Values of the Shield's parameter ranging from 0.05 to 0.12 are considered for the sensitivity analysis in this case. Since both the measured and predicted sediment transport contains errors, the relationship between them can be expressed in the form (Webster, 1997):-

$$\boldsymbol{Y = A + BX + (y - Bx)} \qquad \textbf{6-10}$$

Where x and y are errors in the variables X and Y. Errors in the measurements and predictions were assumed to be proportional to the total variance in the respective dataset. In this case, the best-fit line through the X and Y data is termed the reduced major axis and has a gradient (B) given by the variance of the datasets:-

$$B = \sqrt{{\sigma_Y}^2 / {\sigma_X}^2} \qquad 6\text{-}11$$

Where $\sigma_X$ and $\sigma_Y$ are the standard deviation of the X and Y data.

**Table 6-1 Calculated values of B for a range of values of Shield's parameter (θ) and the numerical constant (K) in the MPM equation. Calculations here relate to where lateral variation is included.**

| | θ (Shield's Parameter) | | | | | | | |
|---|---|---|---|---|---|---|---|---|
| K values | **0.05** | **0.06** | **0.07** | **0.08** | **0.09** | **0.1** | **0.11** | **0.12** |
| **1.25** | 6.11 | 4.36 | 3.2 | 2.4 | 1.82 | 1.4 | 1.09 | 0.88 |
| **1.5** | 7.33 | 5.23 | 3.84 | 2.88 | 2.18 | 1.68 | 1.32 | 1.06 |
| **2** | 9.79 | 6.98 | 5.12 | 3.85 | 2.91 | 2.24 | 1.76 | 1.42 |
| **2.5** | 12.23 | 8.73 | 6.41 | 4.81 | 3.64 | 2.80 | 2.20 | 1.78 |

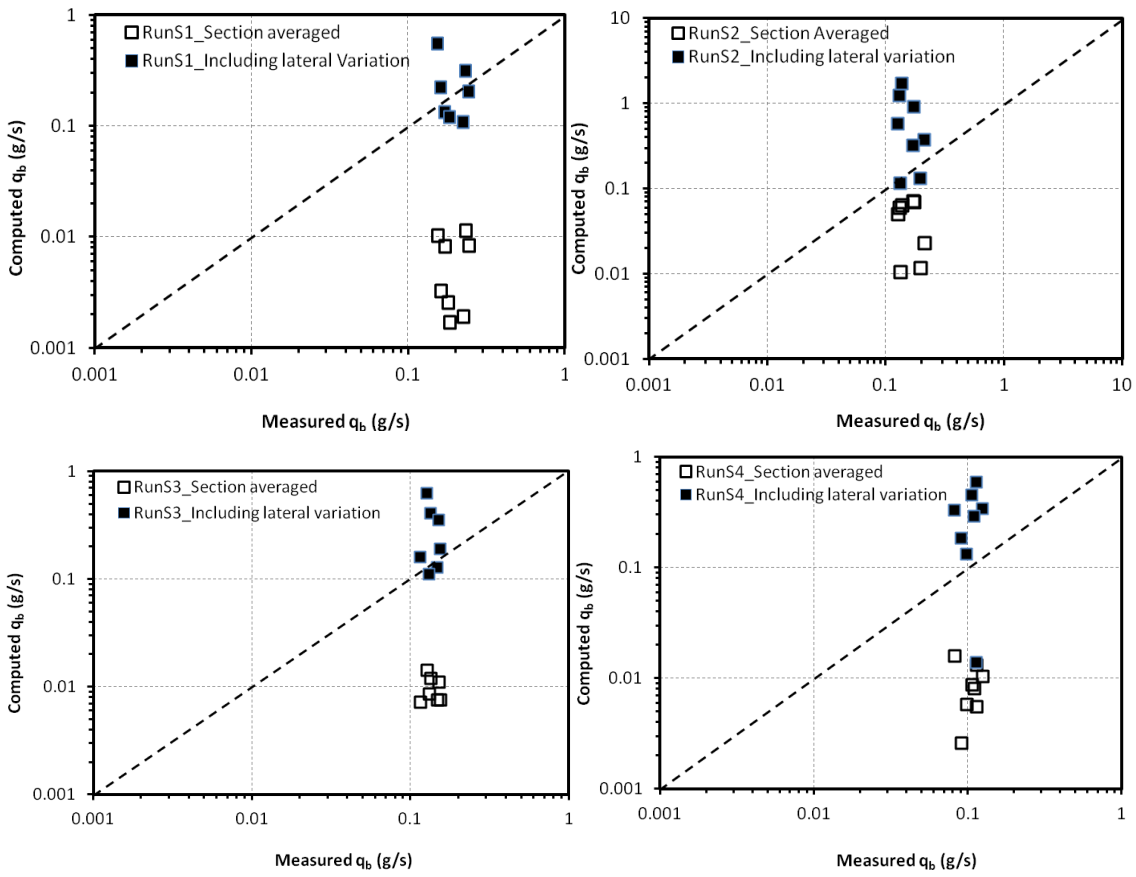

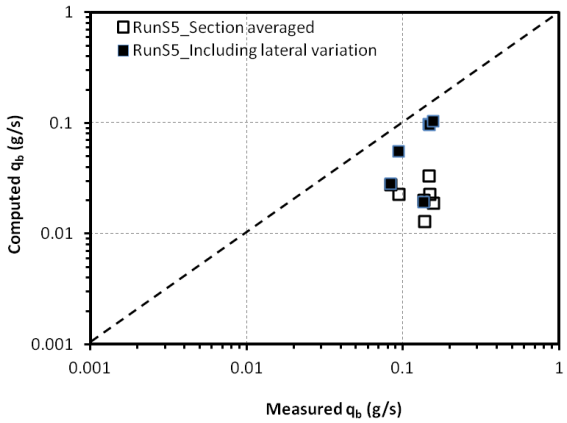


**Figure 6-7 Comparison of time averaged sediment transport values measured at the flume outlet and computed sediment transport rates using section averaged parameters (open symbols) and including lateral variation (closed symbols). Calculations are based on the Meyer-Peter-Muller equation.**

Best fit lines between measurements and model predictions suggest an optimum Shield's parameter (θ) value of around 0.11 and numerical constant in the MPM equation (α) of around 1.25 (Table 6-1). Those values of θ and α are calculated for sediment transport that are calculated by taking lateral flow variability into consideration. However, $r^2$ values are relatively lower (around 0.35). It appears that other combinations of θ and α might give a better value of B (e.g., θ=0.12 and α=1.5). However, a further increase in the Shield's parameter more than 0.11 would annul the sediment transport in some cross sections with visible transport. Due to this reason, value of α and θ that give a relatively better value of B are chosen. These coefficients for the Meyer-Peter and Muller transport equation obtained here are not uncommon in micro-scale models. Malverti *et al* (2008) obtained very similar parameters (α=0.67 and $\theta$=0.12). Moreover, $\theta$=0.11 is not very different from the critical Shields number (which is around 0.07) predicted from the Shields curve for the experimental average grain Reynolds number (around 14).

The computed sediment transport rate by including lateral variation seems a little overestimated in some of the cases of Figure 6-7 (closed symbols) although the method is believed to give a reasonable estimate and correct the effect due to cross section averaging. The result and discrepancy can be explained in different ways. The method is supposed to give a better estimate when multiple cross sections are considered and an average flux is calculated (Bertoldi *et al.*, 2009). This is mainly due the horizontal water level assumption which is known to be inaccurate especially in multi-thread channels

(Zolezzi *et al.*, 2006). The averaging of multiple cross sections is believed to cancel out the error in individual cross sections due to non-uniform water surface elevation and local variation in slope (Bertoldi *et al.*, 2009). The other problem is the definition of suitable reach average values for the dimensionless parameter called the critical Shields stress. Basically, an appropriate definition of critical Shields stress can be defined in two different ways: one is to fit the experimental data and extrapolate to a zero or low reference transport rate which depends on the extrapolation method and the particular reference transport value chosen. The other method is to provide a useful demarcation of a range below which the bed load transport rate is too low to be of interest. Accurate evaluation of a critical shear stress for a given channel configuration would require the direct measurement of flow depth or velocity. However, accurate measurements of those variables are not often available or are costly to obtain. Even with the availability of measured values, identifying the initiation of motion for particle sizes over a range of conditions and scenarios is very difficult. It must be done with considerable care and with knowledge of channel geometry and hydraulic conditions. In this experiment the critical shear stress is calculated as a calibration parameter to fit with the measured transport rate and also to avoid false zero transport conditions at some cross sections. This value is also in good agreement with the critical shear stress predicted from the Shields curve for the experimental conditions considered. A further increase in the critical shear stress would annul the sediment transport in some cross sections with visible transport. Another possible reason for overestimation of transport rates might be errors which cannot be avoided primarily due to inaccuracies in sediment output measurements.

It seems that the overestimation is much greater in the aggradation experiments (Figure 6-7 RunS2 and RunS4) as compared to the degradation experiments, although it is not surprising that transport rates are overestimated during aggradation runs. This is probably due to the fact that aggradation is associated with deposition and bar multiplication having numerous channels of varying width and depth and hence increased spatial variability in flow conditions as compared to degradation experiments. This will make the constant water level assumption more erroneous as the probability of including some channels without water and/or with no visible transport increases. In the

previous chapter (Chapter 5) it is also shown that during the aggradation runs, the sediment storage increases which implies that transport rates decline down the flume and upstream (feed) rate is 1.3 to 2 times the output rate. So, it is expected that the transport rates calculated throughout the flume to be higher than those measured at the outlet. Degrading channels are more or less transformed to single thread channels, for which the assumption of constant horizontal water surface would have little significant influence.

The critical shear stress evaluated above is directly applied to compute sediment transport without taking into account the actual geometry of the channel cross section and the consequent lateral distribution of bottom shear stress (i.e., by assuming an equivalent rectangular section). Doing this resulted in a huge underestimation and even zero transport in most sections. Indeed, the relative magnitude of underestimation is higher than those previously investigated (Paola, 1996;Nicholas, 2000;Ferguson, 2003;Carson and Griffiths, 1987;Hoey *et al.*, 2001) with below threshold shear stresses in much of the sections considered and consequently false zero values of sediment transport rates. This is indicator of the fact that simple width averaging over the full channel width and even over the wetted width (like the present case) severely underestimates the bedload flux in channels with substantial lateral variation in shear stress.

## 6.4. DOWNSTREAM VARIATIONS IN SEDIMENT TRANSPORT

Details on the distributed pattern or magnitude of erosion and deposition within a channel are desirable for different purposes. Moreover, establishing the relation between perturbations and magnitude of channel modifications and the sediment transport regime provides a means for evaluating the sensitivity of the channel to environmental changes and provides a tool for predicting the response to additional forcing. In this subsection an estimate of the longitudinal pattern of erosion and deposition along with the variation in sediment transport rate is provided using the sediment budget approach. The sediment budget approach reveals details of spatial and temporal channel change that other approaches do not. Since the underlying principle

relating sediment transport to morphologic change involves inter-survey comparison, useful information on rates and locations of morphologic change (erosion and deposition) can be derived as a consequence. The sediment budget approach has been used previously by some researchers to estimate bed load transport in natural rivers. It has also been used to determine the magnitude and dynamics of channel scour and fill along surveyed cross sections (Martin and Church, 1995). In this approach measured morphologic and bed topographic changes are related directly to sediment transport rates within the sediment budget framework. The basic equation for this approach can be expressed as:

$$\mathbf{V_o = V_i - (1 - \boldsymbol{p})\Delta V - V_d} \qquad \textbf{6-12}$$

Where $V_o$ is the volumetric sediment output;

$V_i$ is volumetric sediment input to the reach during some specified time period;

$V_d$ accounts for any kind of sediment removed from the system, for instance, by dredging;

$p$ is the term that accounts for the sediment porosity;

$\Delta V$ is the change in storage within the channel system.

The storage term is measured as the net difference between scour and fill of the channel bed and banks and is estimated from the difference between collected topographic survey data over the course of the experiment. The equation can further be reduced to a mean transport rate by dividing all terms by the time between successive surveys. This sediment budget approach can further be defined for any arbitrary length of channel smaller than the total flume length. Since detailed DEMs are available for this study, the flume is divided into 8 mm intervals in the downstream direction, allowing the transport rate to be estimated at any section down the flume. This approach is useful for illustrating the downstream variation of sediment transport along the flume.

The sediment budget approach presented here is based on topographic data collected at 8x2mm spatial resolution (longitudinal and lateral respectively). This resolution should be quite sufficient to capture the actual topographic variability that exists in the channels. The total volume of scour and fill in an interval, reach or cell is simply the product of the elevation change and the area under consideration. Then the individual

channel volumes are summed, giving the net scour or fill over the interval that is being considered.

$$\Delta A = \Sigma 0.5(\Delta Z_i + \Delta Z_{i+1}) d_{(i,i+1)} \quad \text{6-13}$$

$$\Delta V = \Sigma 0.5(\Delta A_j + \Delta A_{j+1}) L_{(j,j+1)} \quad \text{6-14}$$

Where i, i+1 represent two successive points on the survey line, $\Delta Z$ is the change in elevation between surveys, $\Delta A_j$ is the change in area at cross section j, $\Delta A_{j+1}$ is the change in area at the cross section upstream, d is the distance between the two points in a section and $L_{(j, j+1)}$ is the distance between the two cross sections. In some cases the area of bed surveyed with the profiler differs between surveys. This happens especially in RunS1 and RunS2. Initial surveys in RunS1 were limited to the central 1m width of the channel. In later runs the channel continues to braid and occupies a much wider area than in RunS1, requiring an equivalent survey extent. Performing calculations by simply cropping the wider area was found to result in significant underestimation and misinterpretation of transport rates, especially in RunS2. In those cases, two successive topographic datasets collected within a single run are considered for analysis, unlike in the other experiments where DEMs collected at the end of the previous run and during the next run are considered. This approach does not represent the transport variability in the whole run but only part of it. This does however have the advantage that it reduces the time bias due to the use of longer inter-survey period. One assumption of the sediment budget technique is that there is no compensating scour and fill between successive surveys. As the inter-survey time increases, the possibility of undetected changes will also increase.

Figure 6-8 shows the measured volumetric change in sediment storage along the flume from RunS1 up to RunS5 based on repeated DEM measurements and displays an alternating pattern of erosional and depositional lengths of channel. However, because the sediment budget is based on the DEM differencing approach, local and complex patterns of erosion and deposition at each cross-section are not displayed, but rather net changes. Previous researchers (Martin and Church, 1995;Lane and Richards, 1997) have demonstrated that estimates of volumetric changes in sediment storage determined

using topographic survey data may include some error, however, consistent patterns of change, across several individual cross sections and temporally throughout different inter-survey intervals (Figure 6-9) suggest that such errors do not affect the gross stream-wise patterns of erosion and deposition. Erosion dominated most parts of the channel for experiments without sediment feed (Run S1, S3 & S5). This is probably the result of the flow being confined in a single channel with high erosive power. It is also due to lateral channel shifting (e.g., RunS3 as explained in chapter 5).

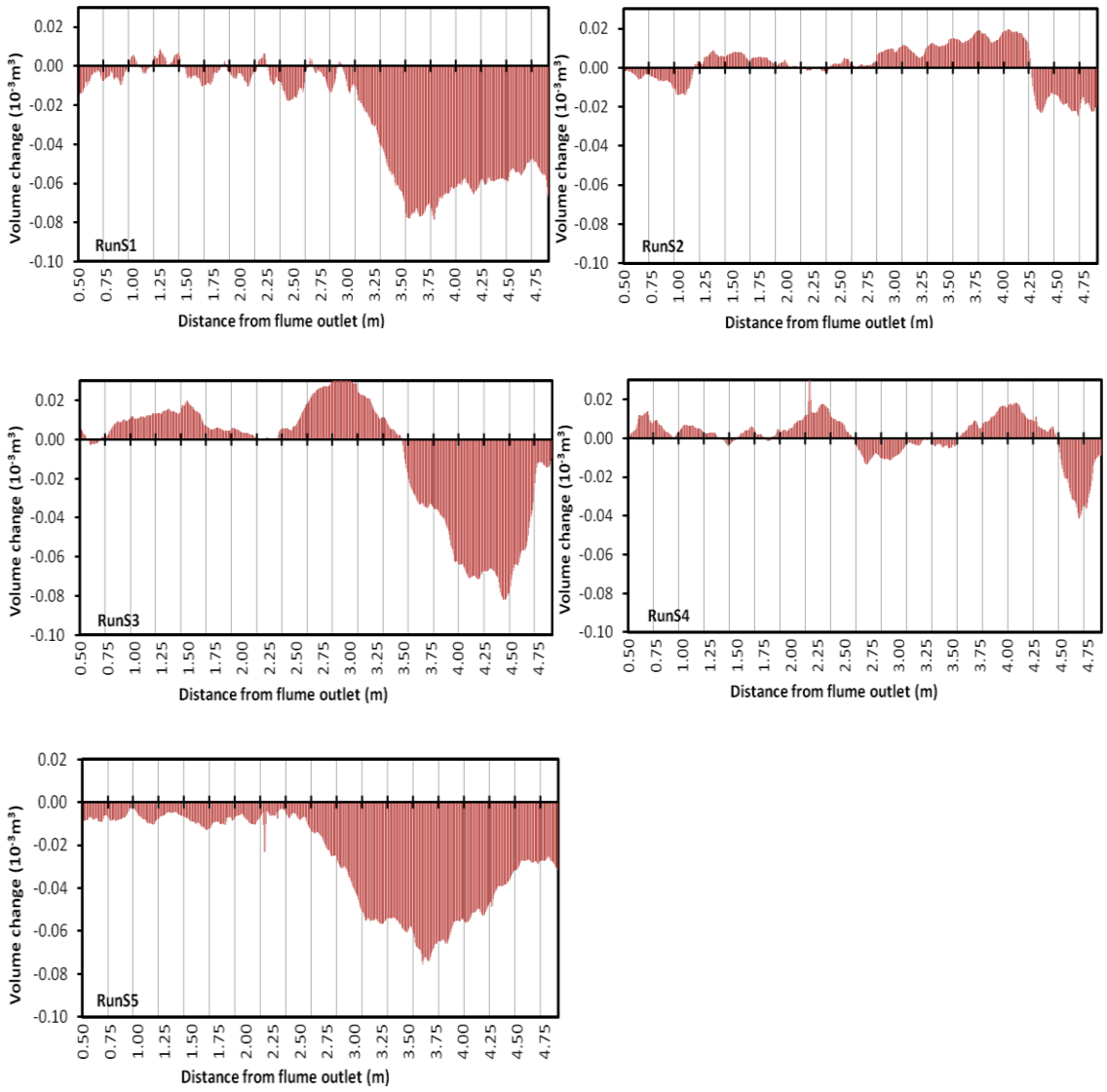


**Figure 6-8 Distributed patterns of volumetric erosion and deposition along the flume**

The downstream parts of the channel (downstream of 2.5m from flume inlet) show minimal volumetric changes. This is in agreement with the morphological changes reported in chapter 5.

The sediment budget analysis and the DEMs analysed are summarized in

Table 6-2. For comparison and to provide insight into the temporal distribution of channel change, a direct difference of DEMs collected at the end of experiments is compared with summation of DEMs collected in between each experiment. The sediment budget should satisfy the mass continuity since the inter-survey budgets are simply sub-components of the full experimental period. Patterns of erosion and deposition are also shown in Figure 6-9. Adding the net changes from the inter survey periods (shown in bold in

Table 6-2) produces the same result as the direct difference between the start and end of an experiment. For instance, up to 0.01478 $m^3$ of sediment was eroded (with 0.00027 $m^3$deposited), resulting in 0.0145 $m^3$ net degradation in RunS1. Adding the net changes from the inter survey periods ((Original-RunS1_DEM1) + (RunS1_DEM1-RunS1_DEM2)) produces the same result as the direct difference from (Original-RunS1_DEM2), thus the basic continuity equation for mass flux is satisfied. The sum of cut and fill volumes for inter survey periods is not presented for RunS3, mainly because the survey extent is different for this run and this would result in underestimation and misinterpretation of erosion and deposition patterns and volumes. Figure 6-9 shows that the spatial patterns of erosion and sedimentation do not remain constant over time. This figure also demonstrates some interesting channel changes. During degrading experiments, the rate of channel change declines with time, reflecting an increasingly stable channel morphology. Figure 6-9 (A and D) explains this. In both figures there are no significant channel changes beyond mid flume part (2.5m to flume outlet) after DEM 1 was surveyed, which is almost 10-12 hours after the start of each experiment. Moreover, there is a huge reduction in the volume of erosion at the flume entrance, especially in RunS5. This is not the case in the aggrading experiments.

If all the variables in equation 6-11 above are measured over a finite time then the equation becomes (Martin and Church, 1995),

$$Q_0 = Q_i - (1-p)\Delta V/\Delta t \qquad 6\text{-}15$$

Where $Q_i$ is the volumetric transport into a reach per unit time ($\Delta t$), $p$ is porosity of the sediment, $Q_o$ is the volumetric transport out of a reach per unit time and $\Delta t$ is the time between surveys. The above equation could be used to estimate ''minimum'' rates of sediment transport. To use the above equation, one transport rate must be known or be estimated to extend calculation along the river. In this case the transport rate measured at the flume outlet is used. However, generally transport rates estimated in this way are prone to errors and have to be used with caution.

**Table 6-2 Volumetric changes of erosion and deposition between each experiment**

| Survey Period | Cut Volume ($m^3$) | Fill Volume ($m^3$) | Net Volume ($m^3$) |
|---|---|---|---|
| Original-RunS1_DEM1 | -0.00848 | 0.0002 | -0.00828 |
| (RunS1_DEM1)-(RunS1_DEM2) | -0.00654 | 0.00031 | -0.00623 |
| **(Original)-(RunS1_DEM2)** | **-0.01478** | **0.00027** | **-0.01451** |
| (RunS2_DEM1-RunS2_DEM2) | -0.00204 | 0.003044 | 0.00101 |
| (RunS2_DEM2-RunS2_DEM3) | -0.00451 | 0.000144 | -0.00436 |
| **(RunS2_DEM3-RunS2_DEM1)** | **-0.00486** | **0.001505** | **-0.00336** |
| (RunS3_DEM2-RunS4_DEM1) | -0.00555 | 0.000304 | -0.00525 |
| (RunS4_DEM1-RunS4_DEM2) | $-6*10^{-6}$ | 0.005864 | 0.00586 |
| **(RunS4_DEM2-RunS3_DEM2)** | **-0.00204** | **0.00265** | **0.00061** |
| (RunS4_DEM2-RunS5_DEM1) | -0.01253 | 0 | -0.01253 |
| (RunS5_DEM1-RunS5_DEM2) | -0.00304 | 0.000421 | -0.00261 |
| **(RunS5_DEM2-RunS4_DEM2)** | **-0.01515** | **0** | **-0.01515** |

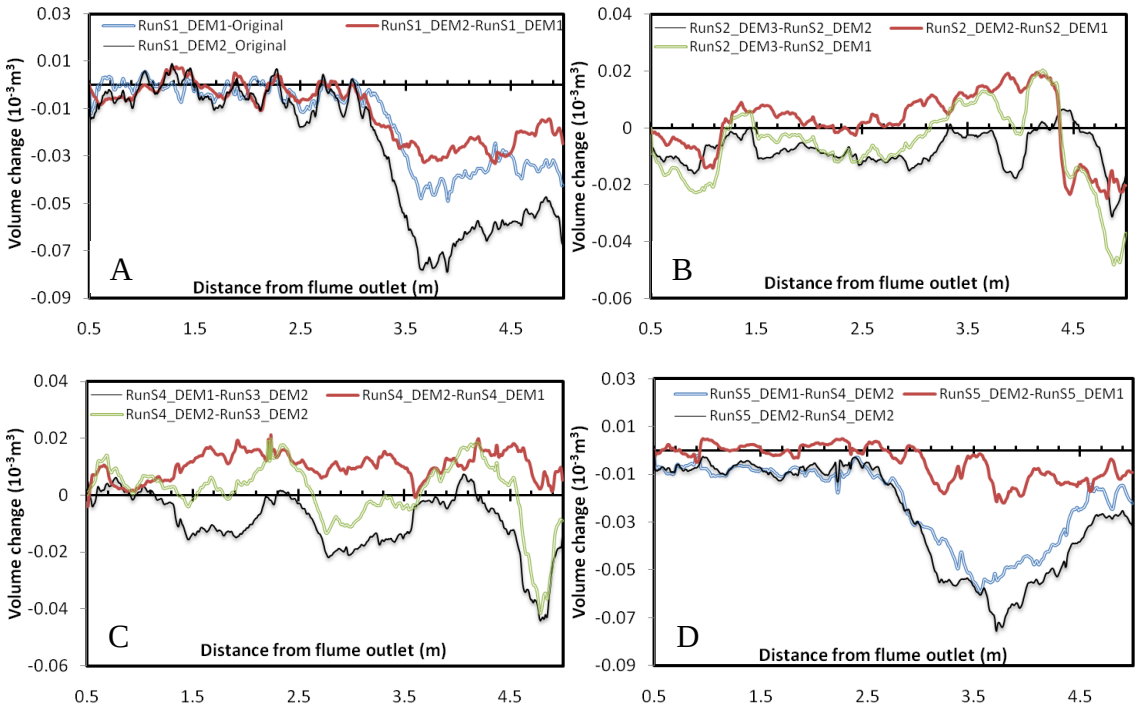


Figure 6-9 Patterns of erosion and deposition during inter survey periods

Figure 6-10 shows the downstream pattern of sediment transport obtained from the sediment budget approach. The transport rate increases fairly steadily from the flume inlet towards the outlet for the first 1.5 to 2 m in degradation runs (RunS1, RunS3 and RunS5), while the aggradation runs show that the transport rates are relatively uniform in the downstream direction.

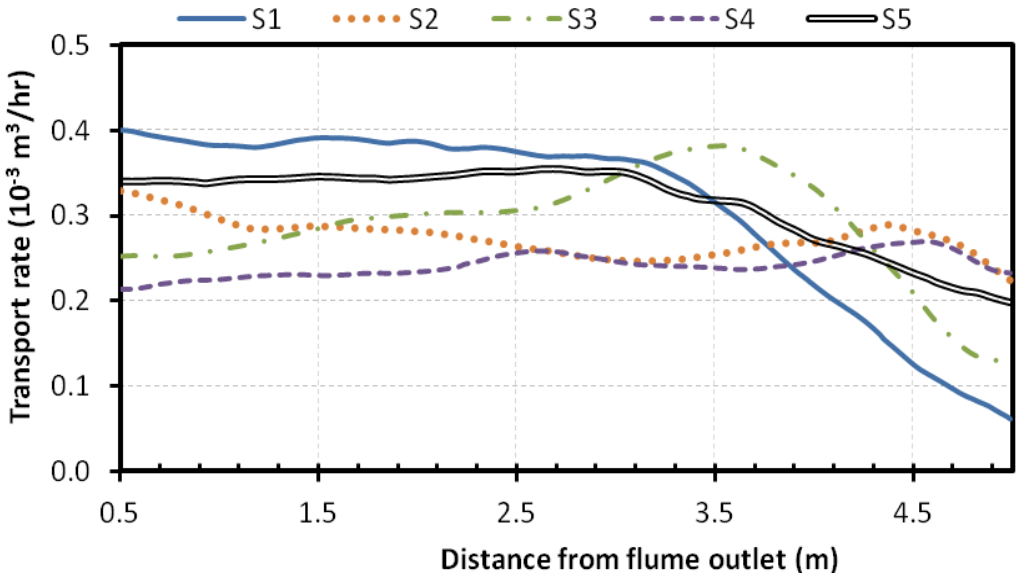


Figure 6-10 Downstream variation of sediment transport rate through the experimentals

The patterns of erosion and deposition at inter-survey periods shown in Figure 6-9 illustrates that erosion and deposition largely occur in distinct zones, reducing the effects of compensating scour and fill in storage and transport estimates. This provides some confidence in transport rates estimated by the DEM differencing and sediment budget approach, particularly given that the spatial resolution of the dataset is high. Based on this assumption that these transport rates are reliable, an attempt is made below to compare the downstream patterns of sediment transport estimated from sediment budget approach with the transport estimates of the Meyer-Peter-Muller equation made in the previous section. Figure 6-11 illustrates that transport rates calculated by the Meyer-Peter-Muller (MPM) formula are generally greater than values of the transport rates obtained by the sediment budget (SB) approach, and that the level of disparity between the results is almost the same between different experiments. The MPM equation also does not appear to capture the more complex downstream pattern evident from the sediment budget transport estimate.

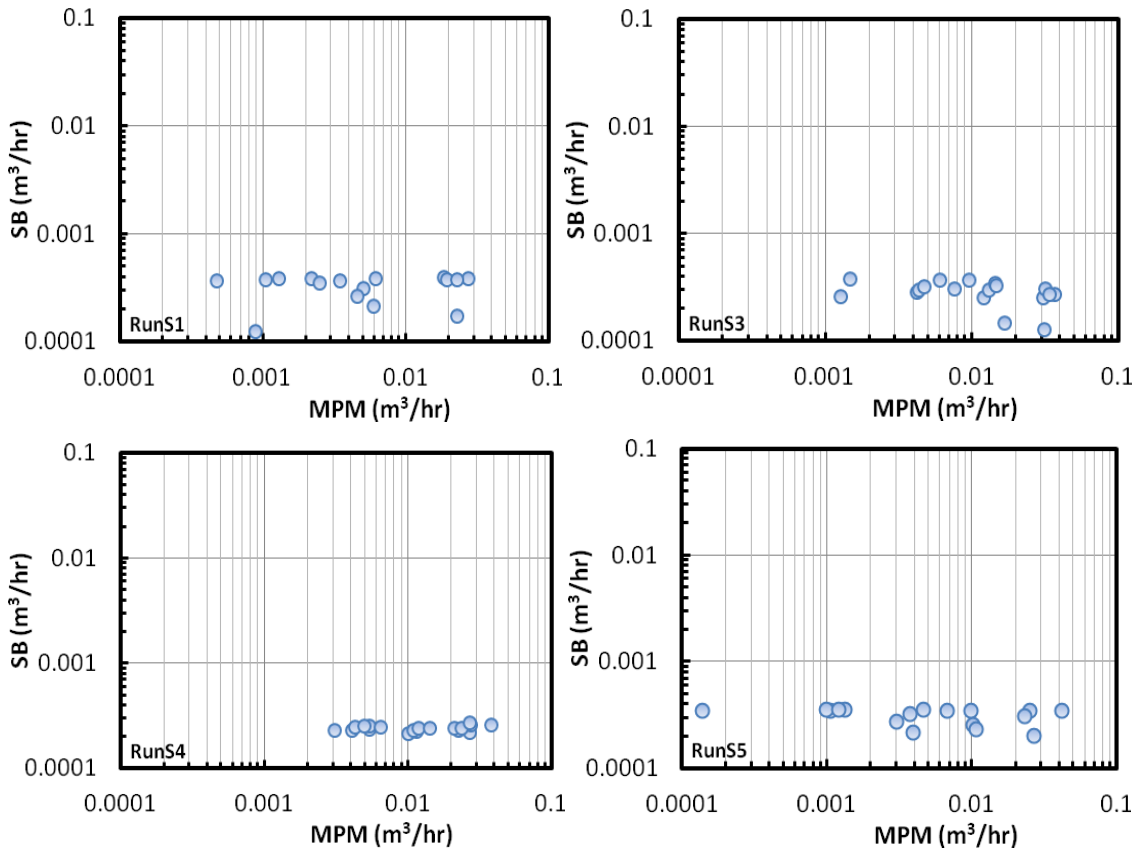


**Figure 6-11 Comparison of sediment transport rates estimated from sediment budget and MPM equation at different sections along the flume. All sections at 25 cm interval along the flume taken towards the end of each experimental run are considered.**

Although other sources of errors in transport predictions based on the MPM equation and the sediment budget approach may be important, varying the value of dimensionless critical Shields parameter and hence the critical shear stress for initiation of transport provides interesting insight into the possibility that transport predictions of the MPM can thereby become more compatible with the sediment budget approach. The dimensionless shields parameter value is related to critical shear stress for entrainment of sediment transport by the following equation and is a basic element in most sediment transport equations:

$$\tau_c = \theta(\rho_s - \rho)gd_{50} \qquad 6\text{-}16$$

Where $\tau_c$ is critical shear stress for sediment entrainment, $\theta$ is dimensionless critical Shields stress, $\rho_s$ and $\rho$ are the sediment and fluid density and $d_{50}$ is the median sediment particle size. The value of dimensionless critical Shields stress depends on many factors including bed structure and configuration and hydraulic geometry. Shields (1936) originally defined this coefficient to be 0.06, however, a range of values from 0.01 to 0.1 have been previously used in literature (Church, 1978;Williams, 1983). The value of Shields stress used in this study, (0.11) is a little larger than that obtained in other flume studies, especially Whipple *et al.* (1998). This value was determined based on the fit between sediment transport measured at the flume outlet and calculated transport at a cross-section 10 cm from the flume outlet. A similar value of critical shear stress has been used in previous micro-scale modelling by Malverti *et al* (2008). Sensitivity analyses were undertaken for the MPM formula by employing different dimensionless shield's values. A slight increase in shield's parameter from 0.11 to 0.15 and hence an increase in critical shear stress brings some of the transport estimates closer to estimates of the sediment budget approach (Figure 6-12). However, as explained in section 6.3, the results become unrealistic as zero transport is predicted in most sections. When the shield's parameter is reduced from 0.11 to 0.07, transport estimates increase and over prediction of values based on the sediment budget approach becomes worse (Figure 6-12). Overall, results indicate that transport rates are over predicted by the MPM formula as compared to the sediment budget approach.

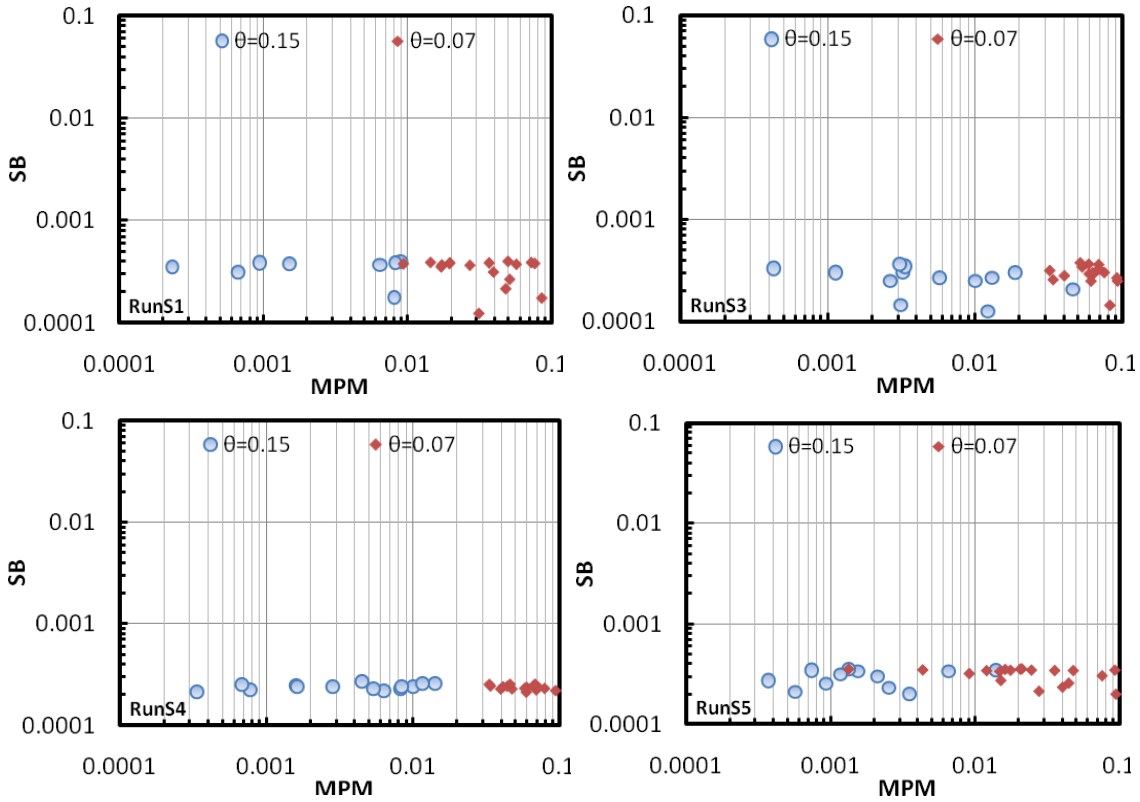


**Figure 6-12 Sensitivity of MPM transport estimates for Shield's parameter at different sections along the flume (the different points represent the different sections along the flume).**

The MPM equation used in the comparison of Figure 6-11 and 6-12 takes into consideration the lateral hydraulic variability at each cross section. Those figures are indicator of the fact that although this method (the panel method) is believed to avoid the underestimation of sediment transport estimates resulting from width averaging, there might also be a risk of overestimation. This overestimation, although to a lesser extent, is variable longitudinally. As noted in Ferguson (2003), underestimation/overestimation by a constant factor would not be a great problem since it would affect only the pace of aggradation or degradation. However, when this overestimation is not by a constant factor, it will affect the longitudinal pattern of change in bed elevation. This will have implications for one dimensional sediment transport models and might distort the overall pattern of sediment transport and channel bed elevations.

## 6.5. HYDRAULIC CHARACTERISTICS OF THE EXPERIMENTAL CHANNELS

This section discusses the hydraulic characteristics of the experimental braided channels. The main focus of this section is the investigation of frequency distributions of shear stress for the experimental channels. The variation of the shape of the distribution of shear stress is examined for situations in which the channel is aggrading and degrading. The relationship between the distribution shape and indices of bed topography variability, braiding intensity and sediment transport rate are investigated.

### 6.5.1. Frequency distributions of hydraulic variables

Applications of stochastic theories to shear stress have been reported in the literature. These studies have shown that a probability density function can be used to approximate the flow depth or bed shear stress distribution. For example, Paola (1996) outlined a model of flow and bed load transport by braided channels and incorporated the effects of spatial variability in braided river hydraulics by modelling the resulting boundary shear stress distribution using a gamma probability density function. Nicholas (2000) extended Paola's approach and assumed the boundary shear stress at a cross section to be a product of spatial variations in flow depth where the later is quantified by fitting normalized flow depth for a given water level and cross section to a gamma probability density function. Later Ferguson (2003) assumed a uniform probability density function and developed a general analytical insight into the effect of incorporating cross sectional variance in shear stress into bed load calculations. This approach is further investigated in this chapter by extracting data from the experimental channels and employing the gamma probability density function. As noted by Paola *et al.* (1999), it may not be practical to collect enough individual stress measurements to specify the stress PDF and model lateral variation directly. Instead, an estimate of the statistics of the stress distribution can be derived by using the flow depth and applying a reach averaged shear stress equation of the form:

$$\tau_o = \rho g h S_o \qquad \text{6-17}$$

Where $\tau_o$ is the bed shear stress, h is the flow depth and $S_o$ is the longitudinal bed slope.

The following general procedure is followed for data collected at each cross section. Local shear stress is calculated using the approach described in section 6.2 and equation 6.17. These stresses are then non-dimensionlized using the cross section mean value. The dataset is then filtered to exclude zeros. The filtered dataset is fitted to a gamma probability density function. Data for each cross section set is fitted to a gamma distribution independently of data collected at other sections. This was carried out for each experimental run using the software ‘’BestFit’. The parameters of the gamma PDF are also estimated. The program determines a first guess of the PDF parameters using maximum likelihood estimators (MLE) of the observed experimental dataset. Parameters are further optimized using a non-linear least square iterative routine (Levenberg-Marquardt method) that aims to improve the goodness-of-fit statistics from the first guess of all parameters. In this method the first order parameters, which are obtained earlier by the maximum likelihood estimators of the gamma distribution, are varied and optimized in an attempt to improve the goodness-of-fit.

Boundary shear stress data determined at each point within each cross section using the reach averaged equation (equation 6.17) were merged and fitted to a two parameter gamma distribution of the form:

$$f(\tau_*, \alpha, \beta) = \frac{\alpha^{\alpha} {\tau_*}^{\alpha-1} e^{-\tau_*/\beta}}{\beta^{\alpha}\Gamma(\alpha)} \qquad \textbf{6-18}$$

Where $\tau_* = \tau_0/\tau$ is normalized shear stress (local shear stress divided by mean shear stress), α is the gamma distribution shape parameter (proportional to the width of the stress distribution), β is the scale parameter determined by the mean shear stress τ and Γ(α) is the standard gamma function. Because inclusion of the scale parameter (β) does not change the shape of the shear stress distribution (Siegrist, 2001), most discussions in this chapter only concentrate on the variation of the shape parameter α with channel aggradation and degradation. α is a non-dimensional measure of the width of the distribution. It is equal to the inverse square of the coefficient of variation (standard deviation to mean). It gives some additional information than simply using the standard deviation of the distribution of depth or shear stress. This is due to the fact that the

sediment transport is not only affected by the lateral variability of hydraulic parameters but also by the mean hydraulic parameter.

Figure 6-13 shows examples of PDFs fitted to estimated shear stress data. It can be seen that the data fit equation 6.18 fairly well. These data also indicate that the spatial variation in shear stress declined when the sediment feed was stopped and the channel degraded (overall value of α is higher). There has been no previous direct investigation of the relationship between the gamma shape parameter (α) and channel aggradation and degradation. However, Paola (1996) and Nicholas (2000) have identified the relationship between discharge and the gamma shape parameter. Nicholas (2000) fitted gamma distribution to normalized flow depth estimates based on cross-section bed topography for the Waimakariri River, New Zealand. Paola (1996) employed the hydraulic data of Mosley (1982) and estimated the distribution of shear stress in the braided Ohau River, New Zealand. Both studies investigated the relationship between the shape parameter and discharge, and observed an increase in the value of α as discharge increases. Noting that as discharge increases the bed topography will be drowned out, with reduced spatial variation in flow depth (which is also the outcome of degradation), the result is consistent with those previous investigations. This also illustrates that micro-scale models are capable of generating bed topography that promotes frequency distributions of shear stress that are similar to those observed in natural braided rivers.

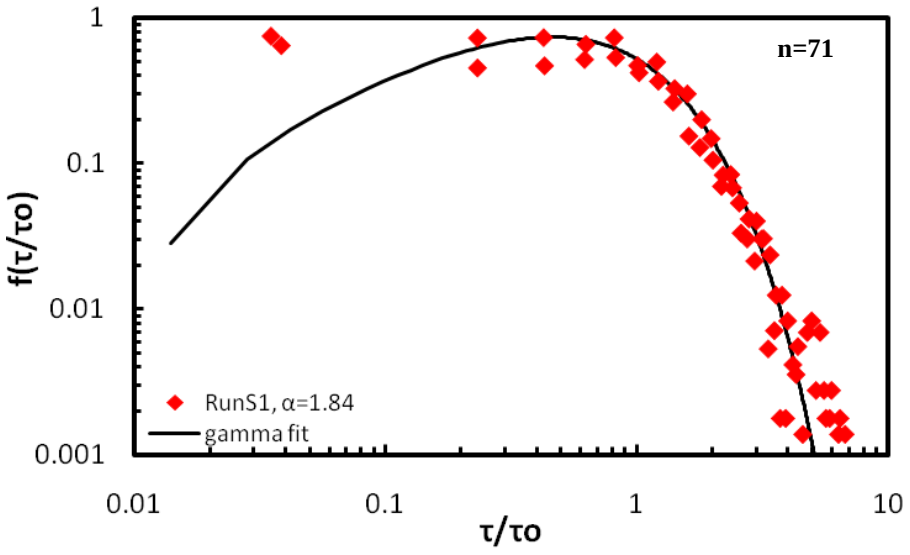

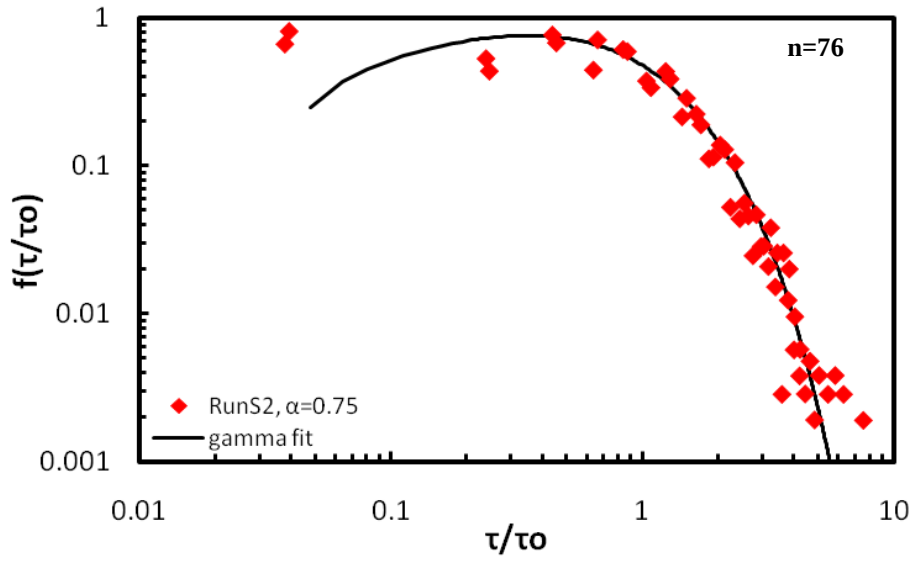
n=76
RunS2, α=0.75
gamma fit
f(τ/τo)
τ/τo
1
0.1
0.01
0.001
0.01
0.1
1
10

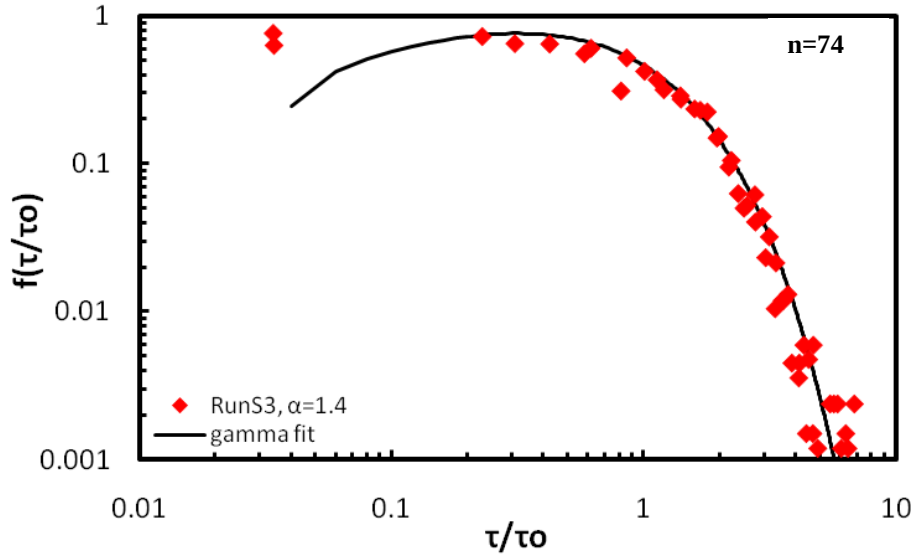
n=74
RunS3, α=1.4
gamma fit
f(τ/τo)
τ/τo
1
0.1
0.01
0.001
0.01
0.1
1
10

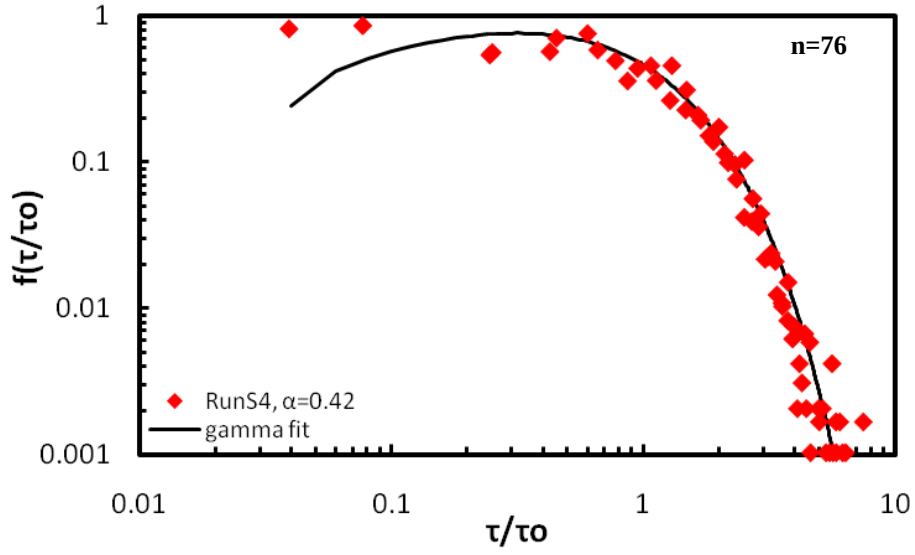
n=76
RunS4, α=0.42
gamma fit
f(τ/τo)
τ/τo
1
0.1
0.01
0.001
0.01
0.1
1
10

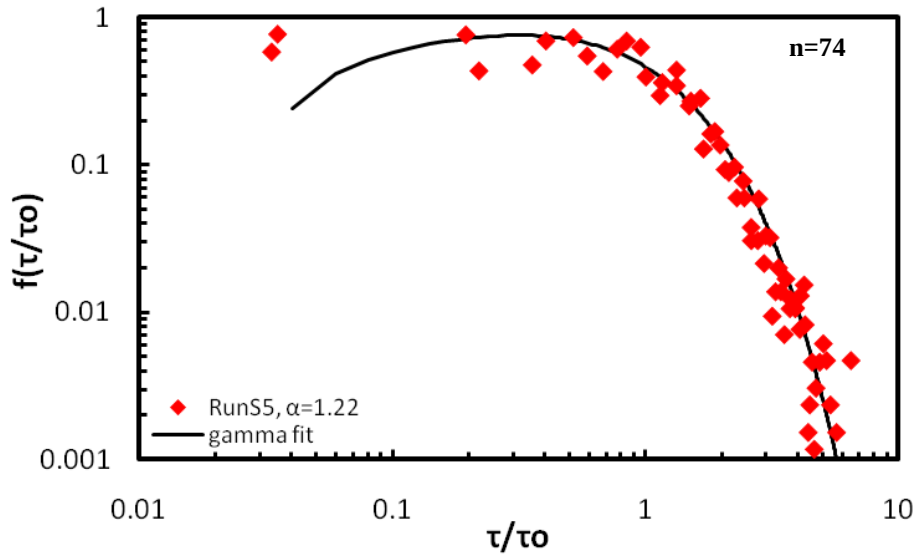


**Figure 6-13 Gamma probability density function fitted to dimensionless shear stress distribution for aggradation and degradation experiments ($\tau$ is local shear stress and $\tau_o$ is flume averaged shear stress in this case). Each graph shows shear stress data from different sections in a single run merged together. N in each graph represents number of observations.**

It is also interesting aspect to examine how the gamma shape parameter changes with aggradation and degradation of individual cross sections. Information on how alpha changes during aggradation and degradation could be very valuable for making sediment transport calculations where channels are not in equilibrium.

Channel cross-sections were surveyed as the experiment progresses at regular intervals. A general assessment was carried out of how the shape parameter varies with aggradation or degradation of individual sections. Figure 6-14 shows cross sections and respective values of shape parameters at the flume inlet where changes in incision and fill are greatest. Also shown are changes at the midpoint of the flume and near the flume outlet where there are minimal changes in bed topography. In those figures different vertical scales have been used to assist in visualizing the complex bed topographies as the level of degradation varies at different parts of the flume. The horizontal lines at X=4000mm shows the water level as obtained from the constant water level assumption.

The first two cross sections (X=4500 and X=4000mm) are those close to the flume inlet and show a typical pattern of channel change when flow is confined to a smaller portion of the flume. Both are indicative of the fact that as the channel degrades, flow is confined to a smaller portion of the flume leading to reduced flow variability and hence

a high shape parameter value. For instance, at X=4000mm from the flume outlet, at the end of RunS1, flow was limited to the small central portion of the channel and characterized by drowned bed topography. Consequently, this section is associated with the highest value of the shape parameter. As sediment feed started in RunS2, part of the channel bed filled and widened. This promoted increased flow variability and lowered the shape parameter value.

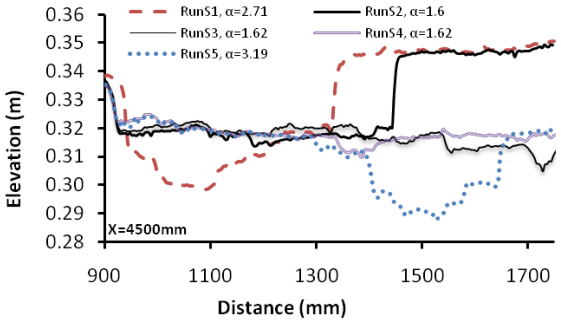


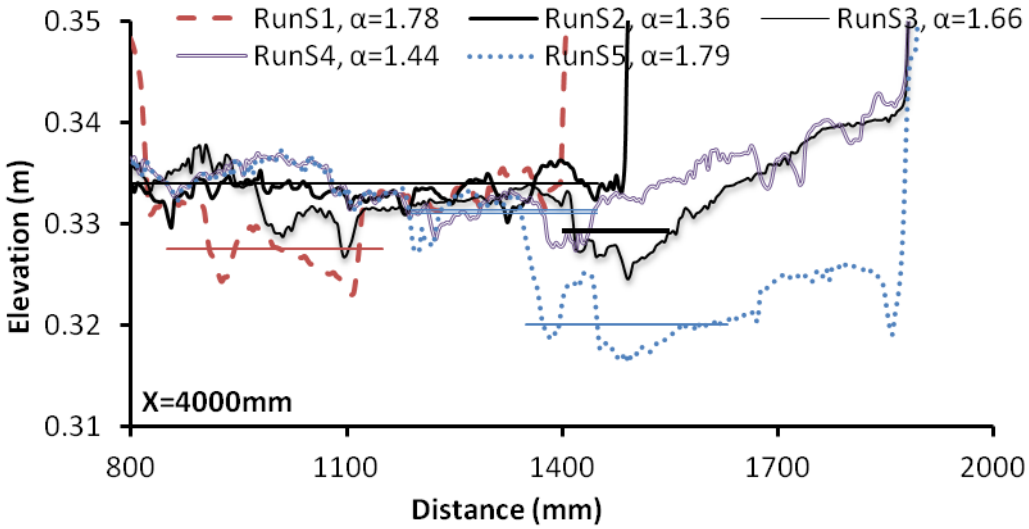


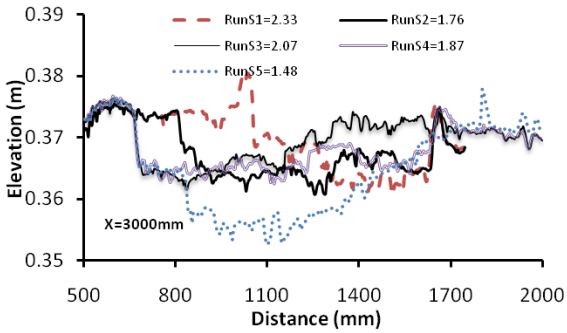


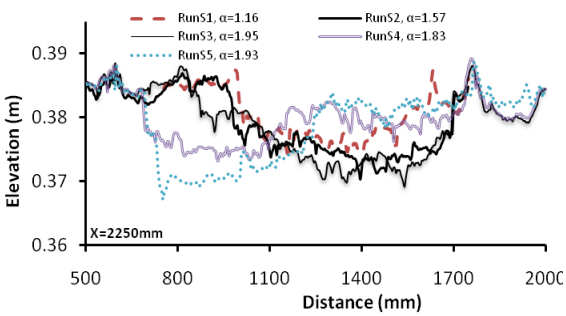

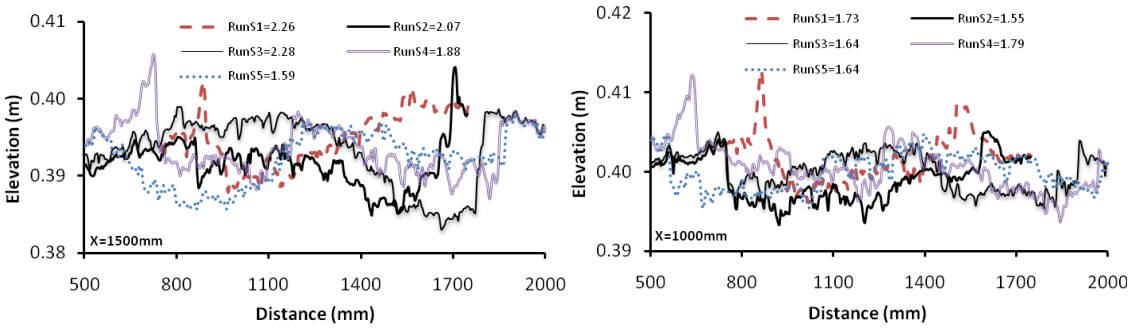


**Figure 6-14 Characteristic of aggraded and degraded cross sections (sections taken towards the end of each run)**

In RunS3, sediment feed ceased and the channel migrated to the left with flow apparently occupying two main channels. The channel was eroded (although to a lesser extent than previously) and the shape parameter remained high, but well below that in RunS1. When sediment feed began again (in RunS4) the channel filled slightly and widened, leading to a shape parameter value equivalent to that in RunS2. The final run (RunS5) is characterized entirely by intense erosion, with flow concentrated in one main channel. The shape parameter increased again to a value equivalent to that seen in RunS1. The other channel cross sections show similar behaviour. This systematic difference between the values of the shape parameter α and changes in bed topography for aggraded and degraded cross sections suggest that a relationship might exist between the shape parameter and an index that expresses the local variability of channel bed elevation (e.g., as described by the standard deviation of bed elevations) or a morphological parameter (for instance, areal erosion or deposition rate) The first of these relationship (between indices of local variability of channel bed elevations described by the standard deviation and 'α') is investigated in this chapter. An attempt will then be made to examine the latter in chapter 7 using model derived hydraulic parameters. Figure 6-15 shows relationship between bed elevation variability and α for each experimental run using data collected at different times during the experiments.

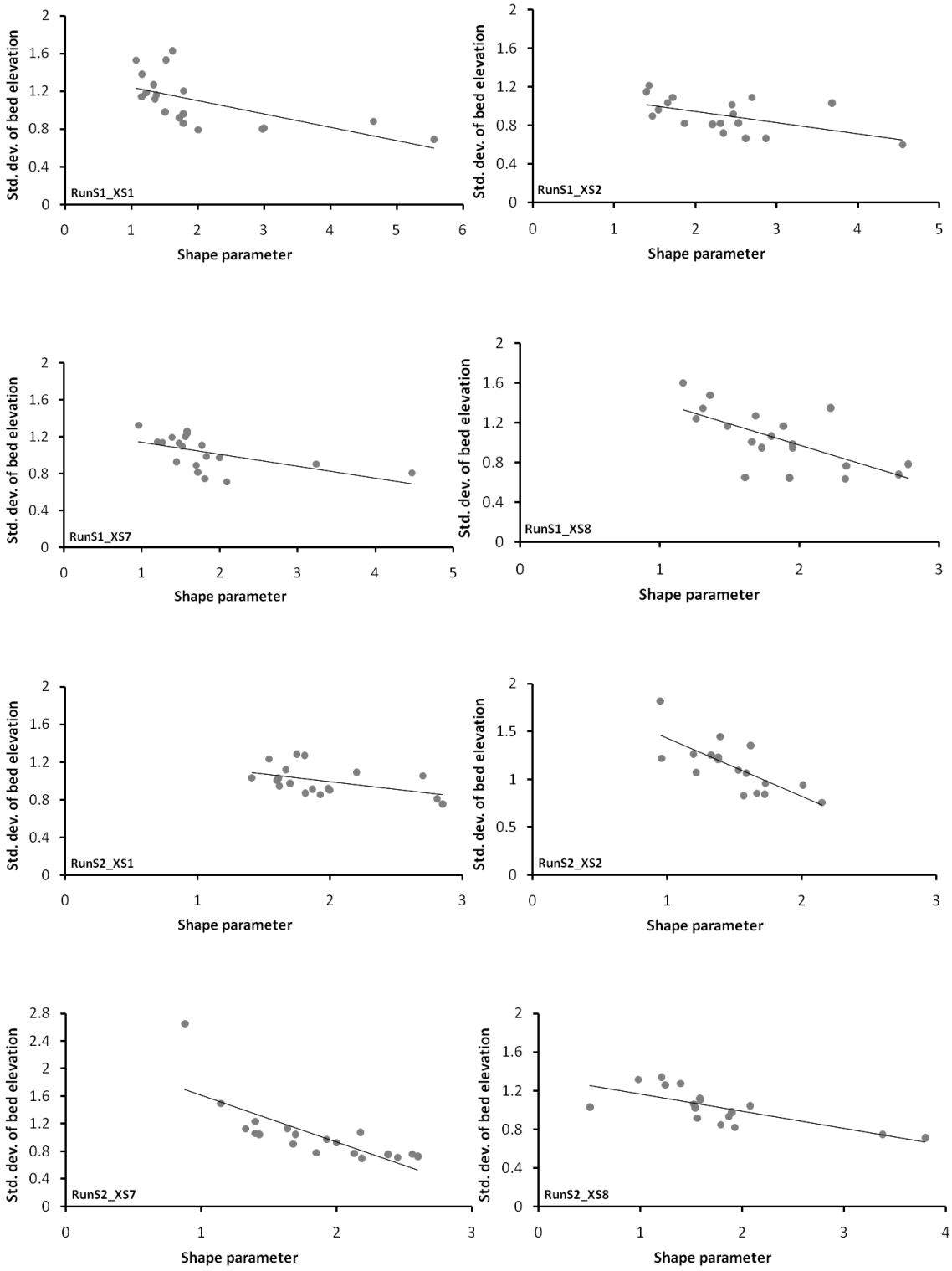
Std. dev. of bed elevation
Shape parameter
RunS1_XS1
RunS1_XS2
RunS1_XS7
RunS1_XS8
RunS2_XS1
RunS2_XS2
RunS2_XS7
RunS2_XS8

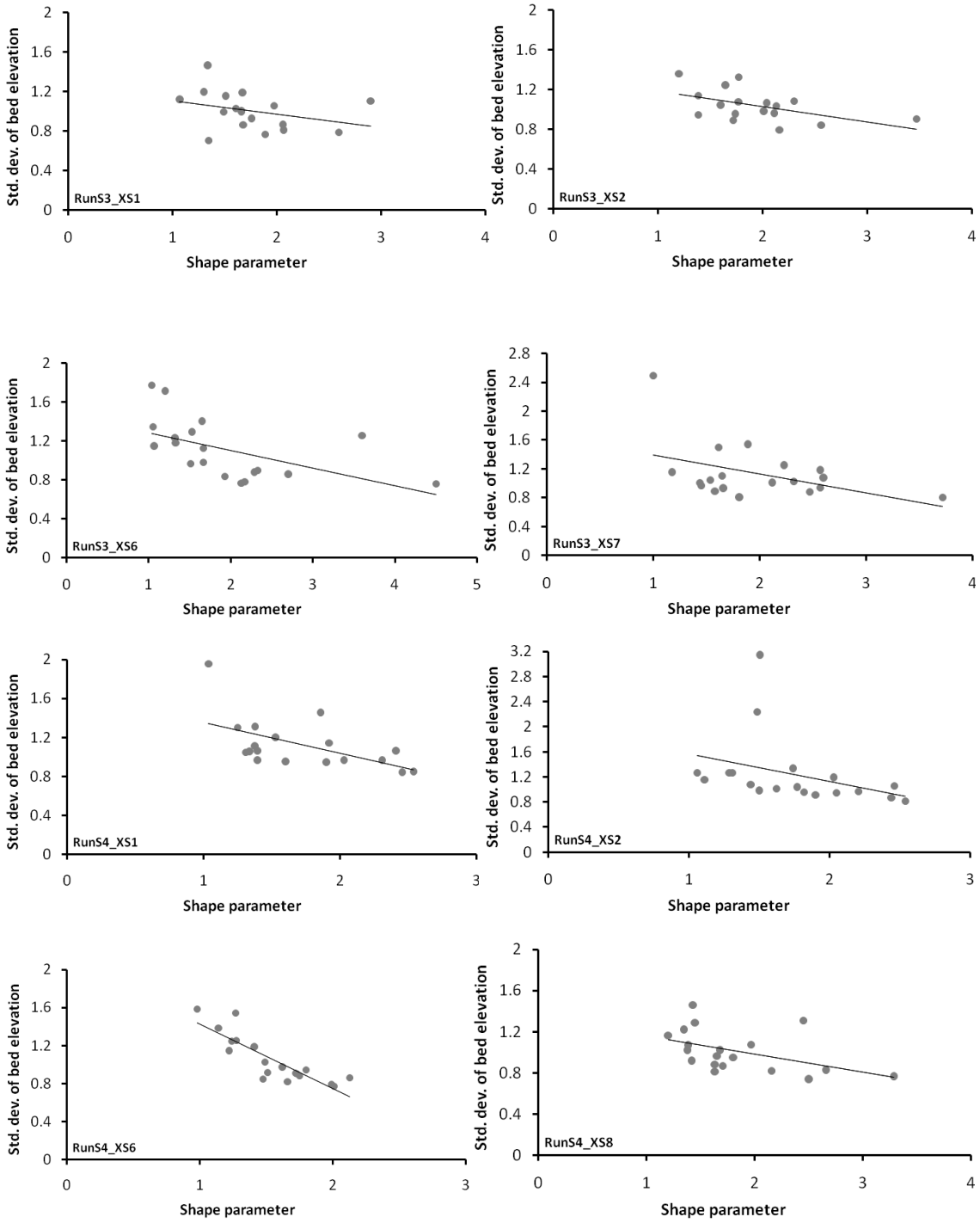
Std. dev. of bed elevation
Shape parameter
RunS3_XS1
RunS3_XS2
RunS3_XS6
RunS3_XS7
RunS4_XS1
RunS4_XS2
RunS4_XS6
RunS4_XS8

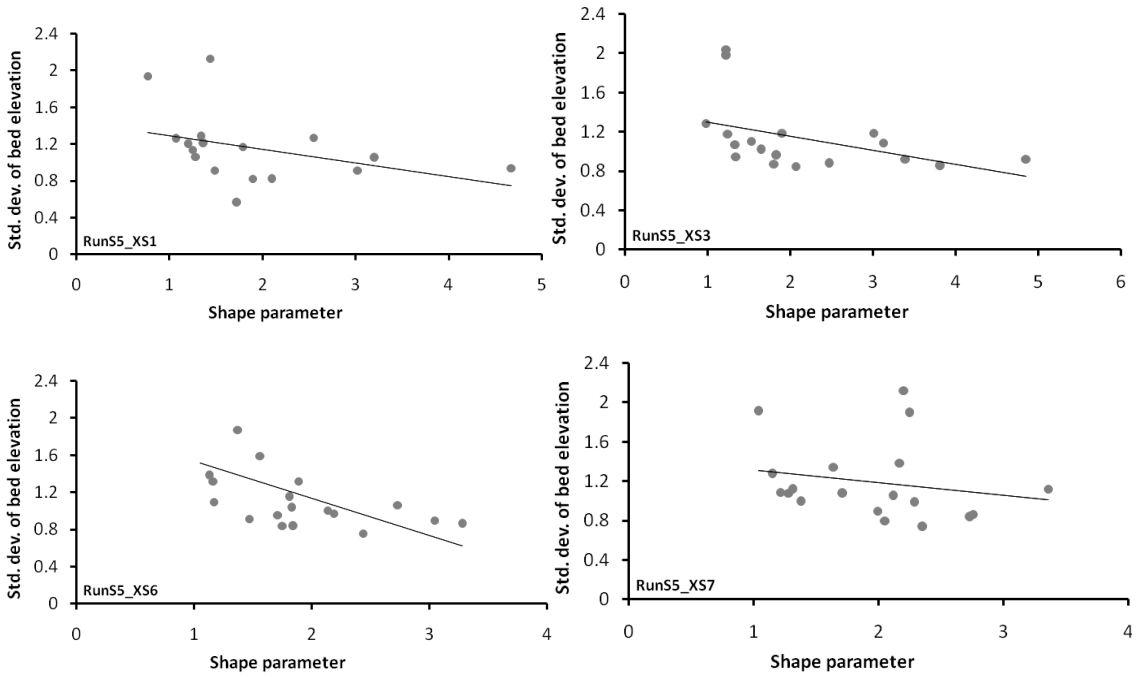


**Figure 6-15 Variation of standard deviation of channel bed elevation with shape parameter 'α' (Std. dev is in mm and only channel bed elevations with flow depth more than zero are considered)**

Graphs on Figure 6-15 are shown for four different times during experiments selected randomly towards the start and end of an experiment. However, it should be noted that these relationships are consistent with data collected at other times. The standard deviation of channel bed elevations was calculated for sections of the bed where there is flow at the time of the survey (i.e. wet areas only). Although the points are scattered in some of the graphs, the downward trend is consistent in all of them. As the variability in channel bed elevations decreases, the shape parameter value increases. The meaning is clear. A reduction in standard deviation of channel bed elevation is an indicator of the fact that spatial variations in bed elevation (and consequently flow depth) is less, and/or that bed topography has been drowned out (since only the wet section of the channel is considered). Higher values of 'α' are an indicator of reduced spatial variability in bed topography (as shown in Figure 6-13 and Figure 6-14). At-a-station variability of the relationship between standard deviation of channel bed elevations and gamma shape parameter 'α' also shows the same pattern. Some examples of such relationships are presented in Figure 6-16 for the inlet, middle and outlet of the flume. The pattern is more consistent and the points are closer to each other.

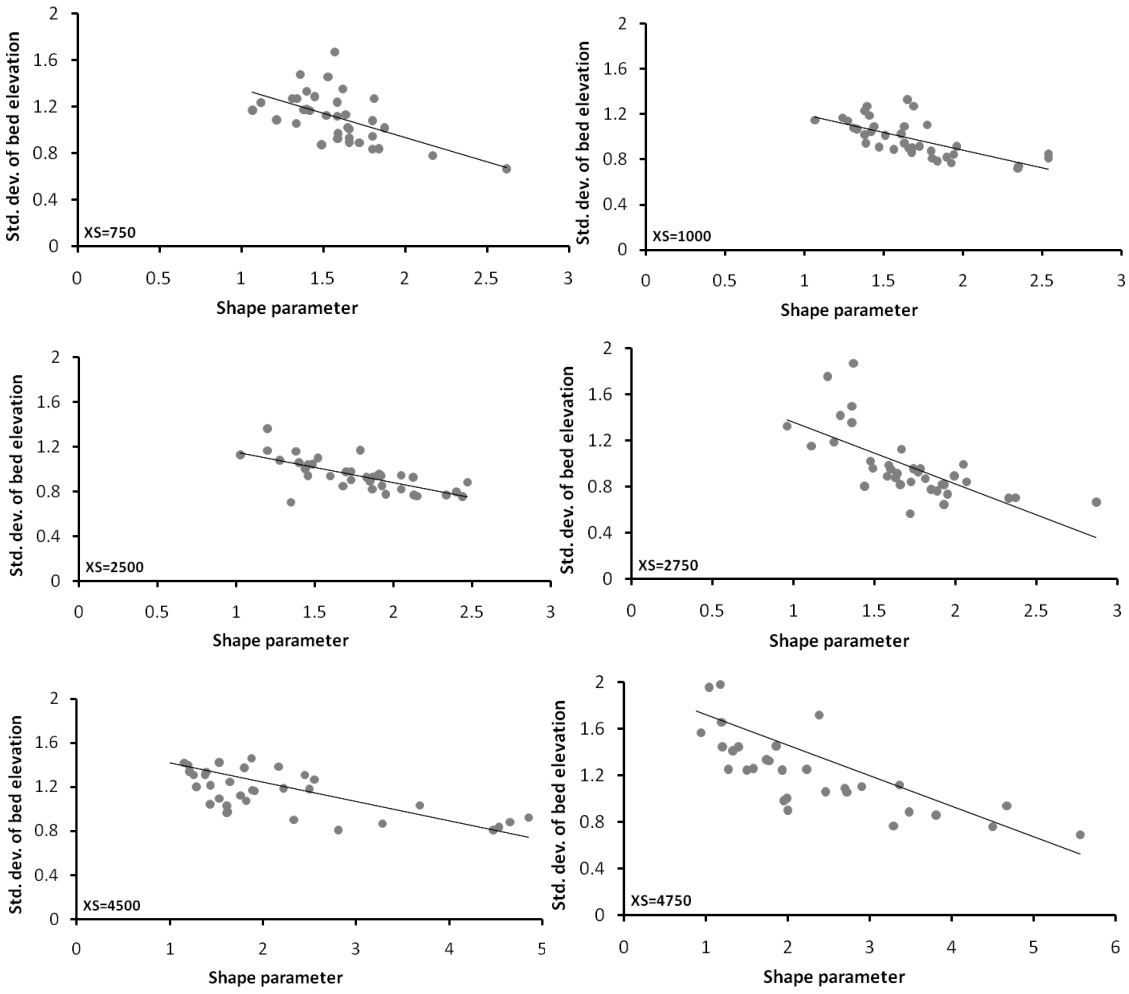


**Figure 6-16 At-A-Station variation between standard deviation of channel bed elevation and shape parameter**

## 6.6. STABLE GAMMA PARAMETERS IN AGGRADING AND DEGRADING CHANNELS

Shape parameters obtained by fitting individual cross-section data to gamma probability density functions were averaged for the whole reach and this procedure was repeated for each survey and for all aggradation and degradation experiments. It appears from Figure 6-17 that the sediment balance within the system has a role in determining the shape parameter. There is a tendency for the shape parameter to increase as the sediment feed to the system has ceased and the channel is degrading. This is similar to the proposition by Tunnicliffe *et al.* (2010) associating higher shape parameter values for the braided Waitaki River in New Zealand with channel degradation and vegetation expansion following dam construction upstream. However, the overall stress distribution shown by those plots is a composite of the various channel morphologies

present in the system. The figure also shows that there is a stable mean shape parameter that emerges from the different morphological features of aggrading and degrading braided channel. The term ‘stable mean’ in this sense is to say that the parameters are averaged for the whole reach with different morphological settings (since the flume entrance of some 50-100cm is mostly single thread and the rest is braided with different characteristics and braiding intensities) and the mean parameter values are almost stable (they are all in the range of 1.6-1.7 for experiments with sediment feed and 1.8-2.2 for experiments without sediment feed). Reach mean values of the shape parameter for an aggrading channel are limited to a maximum of 3.1 with a mean of 1.63 and standard deviation of 0.12 whereas for degrading cases, maximum values of up to 10.3 occur and the mean value is 1.92 and standard deviation of 0.33. Stable mean shape parameters for the braided Waiau and Waitaki rivers in New Zealand are in the order of 1.84 and 2.38 (J. Tunnicliffe, 2010).

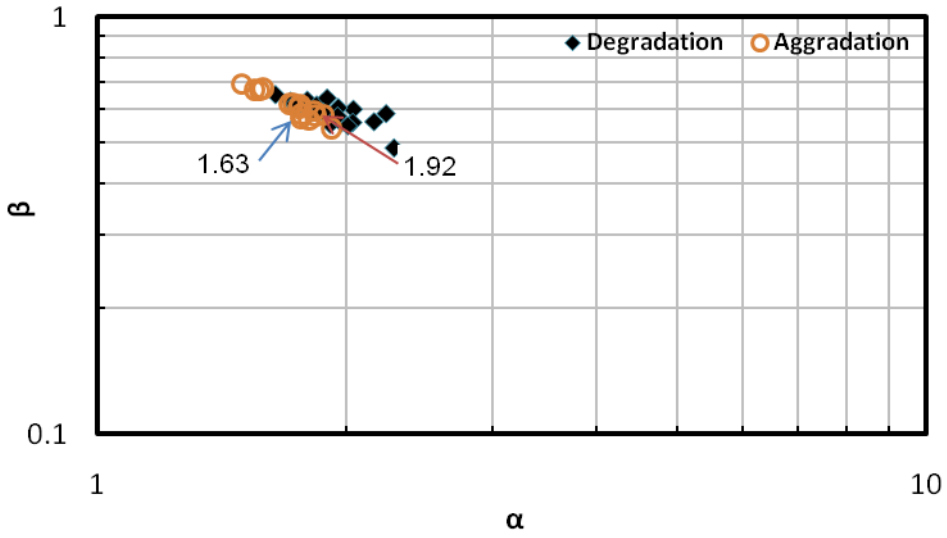


**Figure 6-17 Stable mean shape parameters for aggrading and degrading experimental runs**

Stream wise variations in channel characteristics (e.g. slope, width, braid intensity and particle size) control sediment transport and other morphological changes (Carson and Griffiths, 1989;Nicholas, 2000). Longitudinal variations in the values of the time averaged gamma distribution shape parameter, which controls the width of the stress distribution, is shown in Figure 6-18. A general trend in the variation of the shape parameter is not easily recognizable. However, higher values of ‘α’ are observed close to the inlet for RunS1, S3 and S5 (all degradation runs), where the channel is incising

and almost single threaded with smaller spatial variability. This effect is not limited to the flume inlet, but it is more acute close to the area of maximum degradation. Values for RunS2 and RunS4 (aggradation runs) at the same location are much smaller. This occurs because aggradation is associated with channel multiplication and bar deposition leading to higher spatial variability and hence lower 'α' values. Further downstream there is very small variation in 'α'. Nevertheless in most of the cases, channel cross-sections in the degradation runs possess higher 'α' values than the cross sections in the aggrading runs (Figure 6-18). Near the flume outlet there is a tendency for α to converge to a constant value. This might be due to the presence of a downstream weir at the flume outlet which tends to minimize any variation in downstream bed elevation and minimize changes in channel cross-section shape.

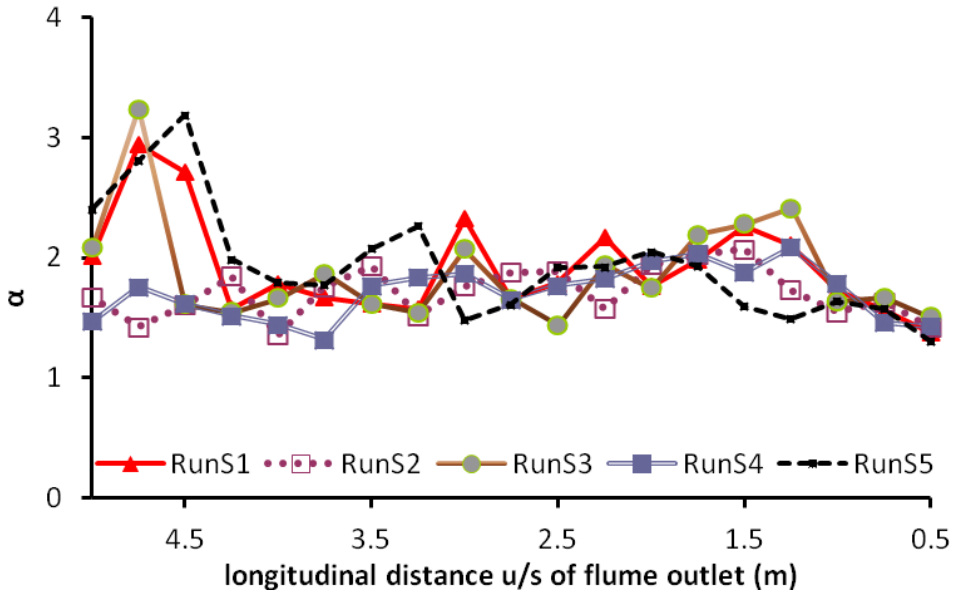


Figure 6-18 Longitudinal variation of time averaged shape parameter

## 6.7. RELATIONSHIP BETWEEN SEDIMENT TRANSPORT AND BRAIDING INTENSITY

Despite the progress made in relating sediment transport to hydraulic variables using conventional equilibrium sediment transport equations, the role played by channel pattern indices (e.g. braiding intensity) on sediment transport rates remains unclear. It has been reported by previous researchers that an increase in braiding intensity promotes high rates of sediment transport by enhancing topographic variability across the channel (Nicholas, 2000;Warburton and Davies, 1994). However, some argue that

as the channel gets more braided or experiences aggradation, the sediment transport rate decreases (Hoey and Sutherland, 1991). Laboratory flume experiments by Ashmore (1988) and Davies and Lee (1988) also suggested that a reduction in braiding intensity is associated with increased sediment transport for equilibrium braided streams.

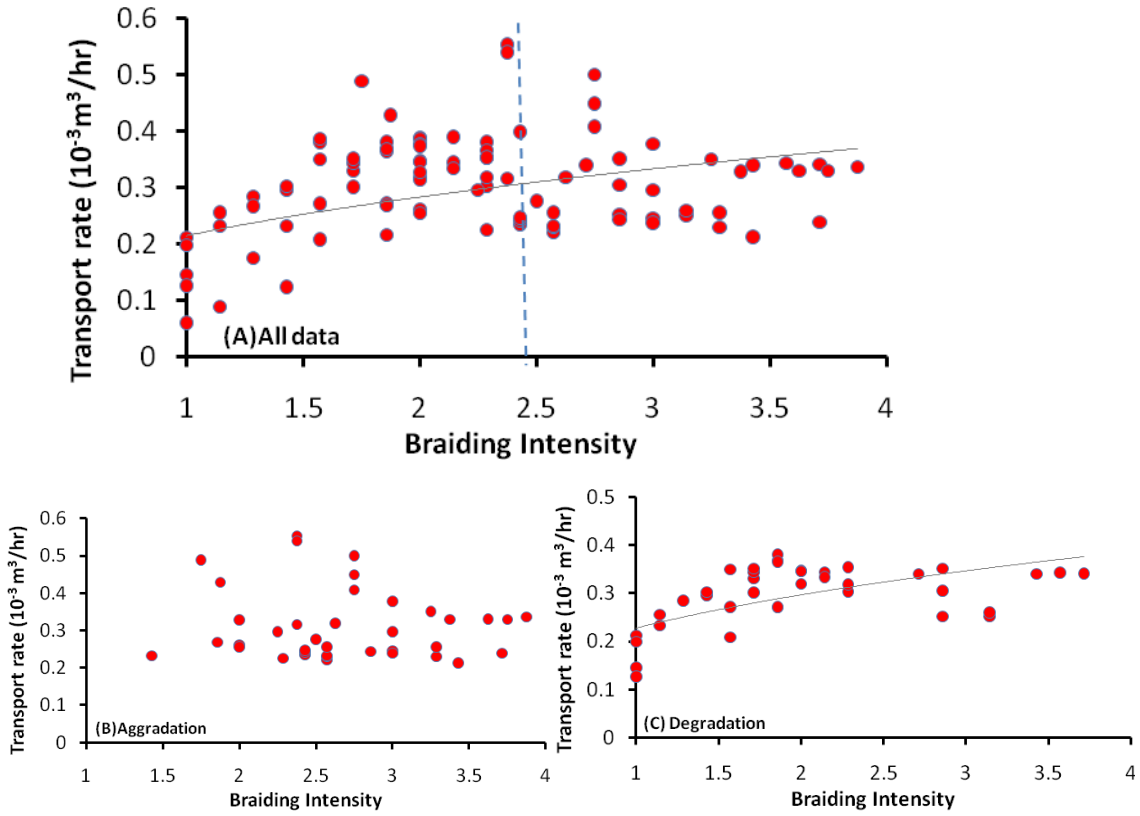


**Figure 6-19 Relationship between sediment transport rates and time averaged braiding intensity: a) all data; b) aggradation experiments: c) degradation experiments. Logarithmic trend lines are fitted to the dataset.**

Figure 6-19 illustrates the relationship between sediment transport rates acquired from the sediment budget approach utilizing DEMs obtained at the start and end of experiments, and estimates of the time averaged braiding intensity. It can be seen from Figure 6-19a that an overall positive relationship appear to exist. However, the data points show much scatter and seem to posses two different patterns for low and high braid intensities (separated by the dashed line). The data can be split into two groups based on sediment feed to see whether the process of stream braiding due to increased sediment supply results in an increase in sediment transport, thus enabling the increased load to be conveyed. During channel aggradation (i.e. during periods of sediment feed to the flume), an increase in braiding intensity seems to reduce the transport rates

slightly (Figure 6-19b). This is probably due to the formation of a number of smaller channels of varying width and depth that ultimately divide the flow (hence most of the channels will have smaller flow depth) and do not all contribute to sediment transport. Those channels that transport sediment may not be able to contribute significantly because flows are typically wider and shallower than during periods of bed degradation. The laboratory investigations of Ashmore (1991) and Ashmore (2001) have also shown that the active braiding index (based on the number of individual channels that transport sediment) is often much lower than the total braiding index (based on channels that convey discharge). A typical logarithmic relationship exists between braiding intensity and transport rate for the degradation runs (Figure 6-19c). As braiding intensity increases, transport rate also increases. However, transport rate does not appear to increase continuously (or at the same rate) as braiding intensity. There seems to exist a threshold up to which, an increase in braiding intensity leads to an increase in transport rate. Beyond that threshold, transport rates either remain constant or decrease with an increase in braiding intensity. In case of degradation it is clear that most of the variation changes in a narrow window of the braiding intensity between 1 and 1.5. This indicates that as the channel is becoming single thread or with less braiding intensity, it has more transport capacity than when it becomes highly braided. This seems to conform well to the finding from the aggradation runs in (Figure 6-19b). In aggrading braided rivers a number of smaller channels may be formed especially when there is sediment feed from upstream and it is likely that this threshold will be exceeded. This leads to division of flow by those channels and a reduction in transporting capacity, depending on other factors such as channel width, depth, slope and particle size.

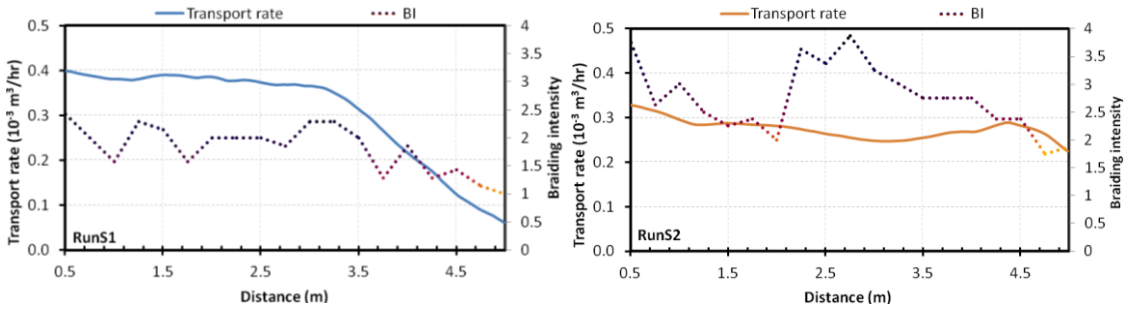

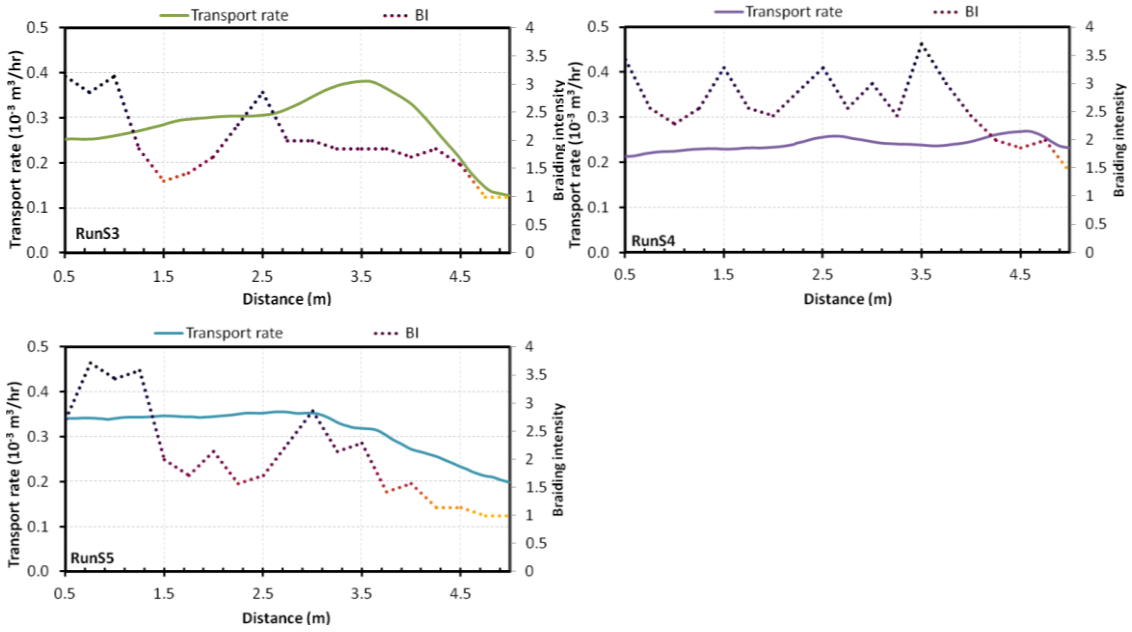


**Figure 6-20 Longitudinal pattern of transport rate and time averaged braid intensity**

The relationship shown in Figure 6-19a, b and c are supported further by the relationships between the longitudinal pattern of transport rate with braid intensity shown in Figure 6-20. The pattern of transport rate and braiding intensity in RunS1 is clear. Both parameters increase over the length of the flume. However, the braid intensity does not exceed 2.5. In RunS2, the pattern remains the same as RunS1 close to the flume inlet. But, a further increase in braiding around the middle of the flume slightly reduces transport rates. When braiding intensity decreased again around the flume outlet, transport rates increases slightly. The general trend close to the flume inlet in RunS3 is not very different from RunS1, although transport rates after mid flume appear to decline slightly in the downstream direction. The braid intensity in RunS2 fluctuated with an average value of around 2. In RunS4, the trend close to flume inlet is the same as RunS1 and RunS2. Braiding intensity increased in the middle of the flume and fluctuated at an average value of more than 2.5 up to the end of the flume. This fluctuation in braiding intensity resulted in a slight reduction or a constant rate of transport intensity all along the flume. An increase in braiding intensity above the average does not result in an increase in transport rate. Overall, these figures suggest that an increase in braiding intensity beyond a certain threshold does not necessarily increase sediment transport rates. It may even reduce the transport rate.

## 6.8. RELATIONSHIP BETWEEN BRAIDING INTENSITY AND SHAPE PARAMETER α

Stochastic approaches to bed load prediction are hindered by the requirement for a large number of measurements of channel morphology in order to derive the input parameters of the distribution. This channel morphology data either does not exist for large braided rivers or is very costly to collect. Having said this, several previous studies have tried to identify a relationship between channel morphology and the characteristics of frequency distributions of hydraulic variables (Nicholas, 2000;Nicholas, 2003;Paola, 1996). Nicholas (2000) showed both longitudinal (grain size and braid-plain width) and stage related variations in the gamma distribution shape parameter. An investigation of the existence of such relationships for the experimental data is carried out in a systematic manner below by examining temporal variations in the gamma distribution shape parameter for cross sections located near the inlet, outlet and mid-flume area. Following this, the relationship between the alpha parameter and the braiding index is examined over the course of the experiment.

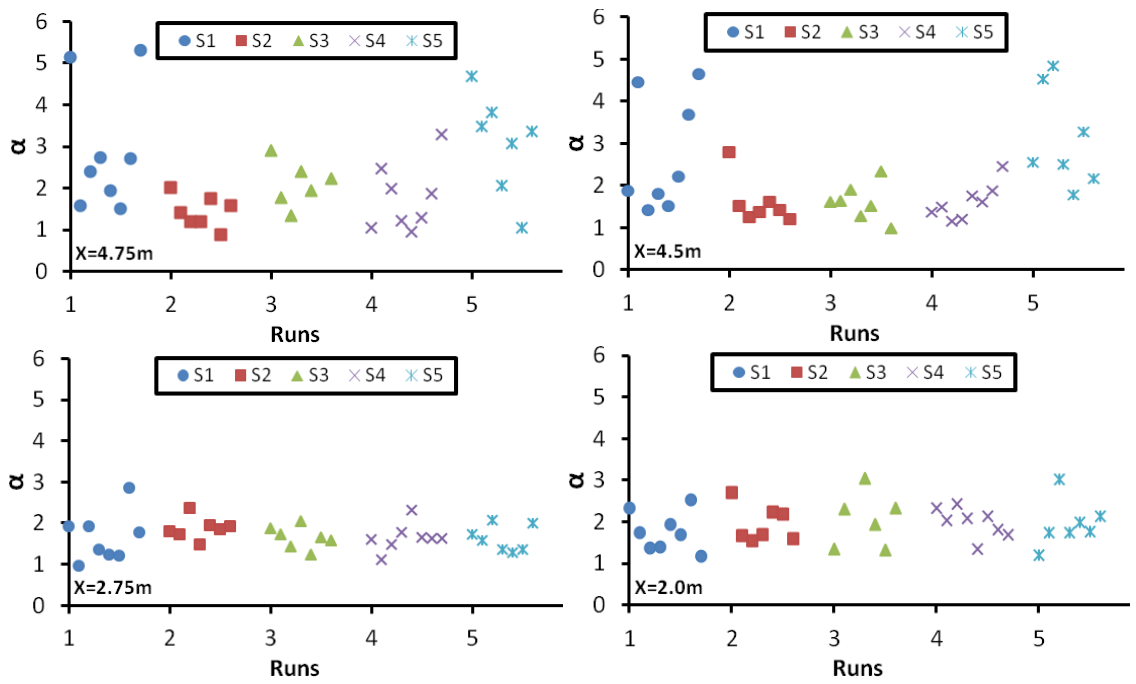

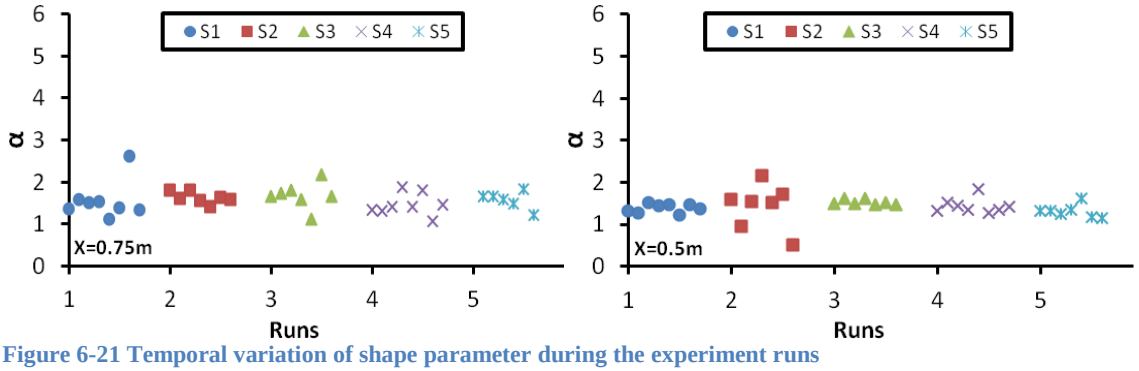


Figure 6-21 Temporal variation of shape parameter during the experiment runs

Figure 6-21 shows the temporal variation of the gamma distribution shape parameter (α) fitted to distributions of shear stress, calculated from flow depth, for representative cross sections over the experimental period. A typical trend is evident in the values of α near the flume inlet (at X=4.75m and 4.5m). High values of α are observed for RunS1, RunS5 and to some extent RunS3 (nearly 50% of the values are greater than the overall section mean). In contrast, very few of the values are greater than the overall section mean for runs without sediment feed (RunS2 and RunS4). This is a reflection of the fact that the channel tends to be single threaded in the absence of sediment feed and flow is characterized by reduced variability. This effect is acute near the flume inlet. The mean value of α changes little over the course of the experiment around the middle of the flume (X=2m and X=2.75m) and values of α appear to vary slightly around the overall section mean. Quantitatively, nearly half of the 'α' values are greater than the overall section mean in both degradation and aggradation experiments. This is possibly a result of the fact that the continued delivery of sediments from the actively incising upstream reaches during the degradation experiments has kept the middle part of the flume braided, as is the case during the aggradation experiments. The range of α value around the flume outlet is less (X=0.75m and X=0.5m) indicating absence of significant cross sectional change because of the downstream weir. These differences between the spatial and temporal values of α near inlet, middle and outlet of the flume suggest that a relationship may exist between the shape parameter and channel pattern indices (e.g. braiding intensity). This relationship is further investigated in greater detail by examining the spatial variation of braiding intensity versus alpha (α) parameter.

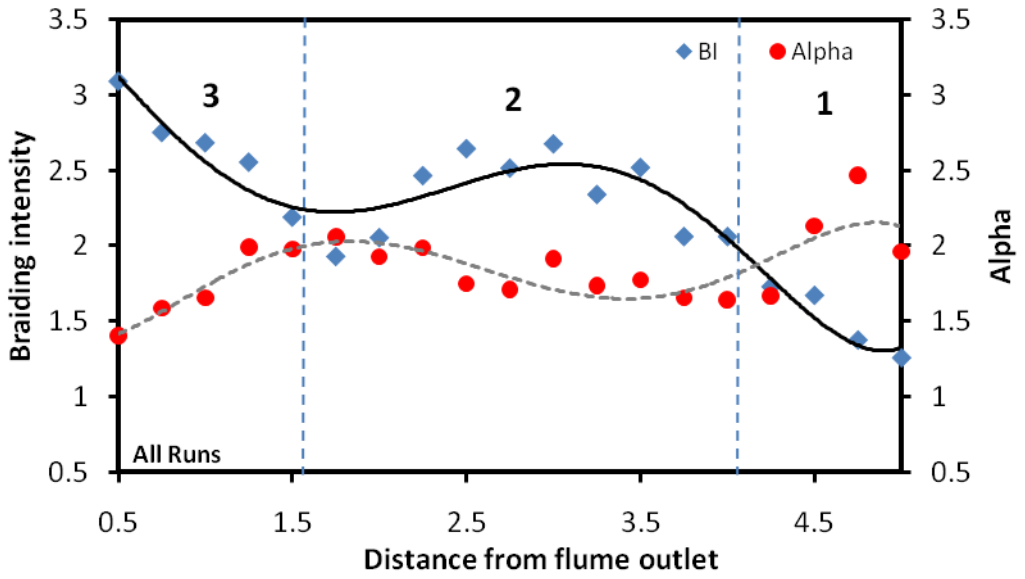


**Figure 6-22 Longitudinal variation of time averaged alpha and Braiding intensity**

In order to characterize the relationship between channel configuration and flow characteristics, parameters were averaged in time over the course of the experiment. Through this double averaging procedure an overall mean value of the parameters is obtained. Figure 6-22 illustrates how the time averaged braiding intensity and time averaged shape parameter varies throughout the experimental period over the whole length of the flume. A clear trend is evident in this figure. Both parameters exhibit complex non linear patterns. Because of this, the relationship is investigated by dividing the flume into three parts. Region 1 represents parts of the channel close to the flume inlet. This part of the channel is characterized by active incision and filling during degradation and aggradation respectively. Effects of degradation seem to be more acute than effects of aggradation. Due to this, fewer channels exists in this part of the flume leading to less spatial variability in flow depth, drowned bed topography and hence higher α values. Part 2 represents the channel in the middle of the flume. As explained in chapter 5, channel widening and narrowing is the most important change in this part of the channel, and changes in bed elevation are not significant. However, the overall average number of channels (for all runs) in this section does not show much spatial variation. Due to this, spatial variations in braiding intensity are small, though individual values are still high. Values of the shape parameter are smaller than those of part 1, but difference between individual values are very small. Part 3 is the downstream

section of the flume close to the outlet. The presence of a downstream weir prevented large changes in bed elevation, but a number of smaller channels did form in this region. Braiding was more intense in this part leading to low α values indicating greater spatial variability.

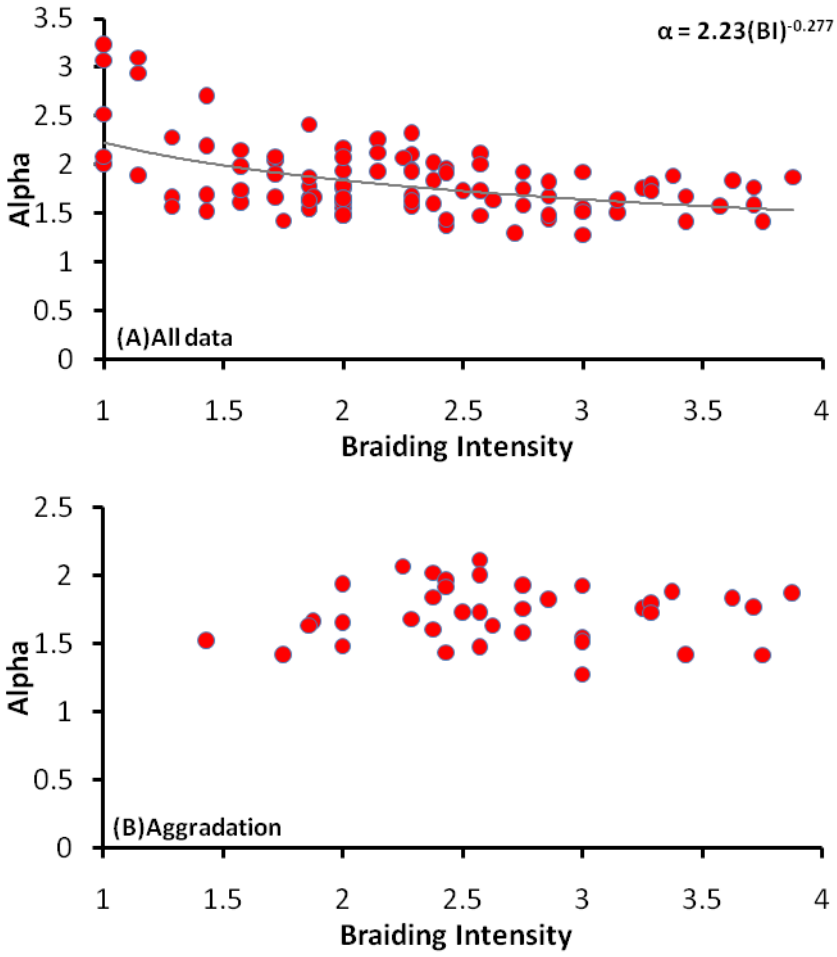

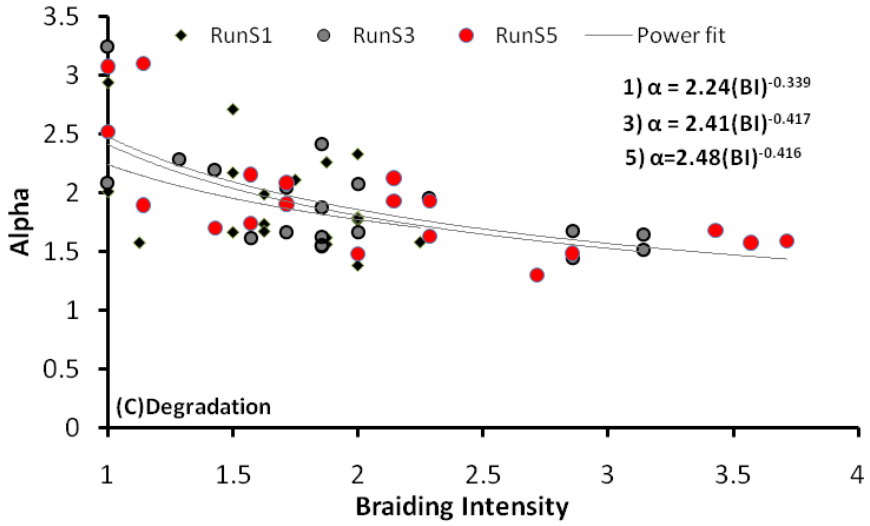


Figure 6-23 Relationship between braiding intensity and alpha

Figure 6-23 illustrates the relationship between gamma distribution shape parameter and braiding intensity. However, this relationship does not appear to be strong and there is much scatter in the data. Overall, an increase in braiding intensity leads to a decrease in the value of α, indicating greater spatial variability in bed topography. This is generally the case as an increase in braiding intensity means an increase in the number of channels, probably of varying width and depth, resulting in an increase in the variability of flow depth and hence shear stress among these channels. Braiding intensity correlates well with the shape parameter for degradation experiments (but less clearly for aggradation experiments). In each set of degradation experiments, the data show a similar trend and a least square regression yields very similar power relationships (with exponents -0.339, -0.417 and -0.416) between braiding intensity and shape parameter.

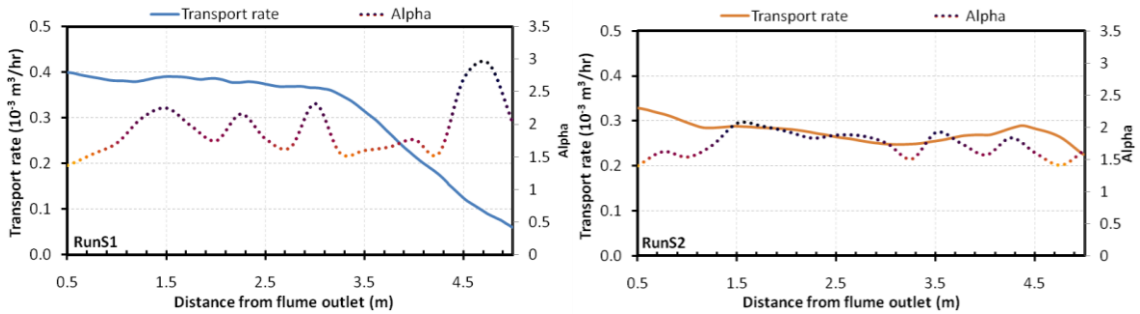

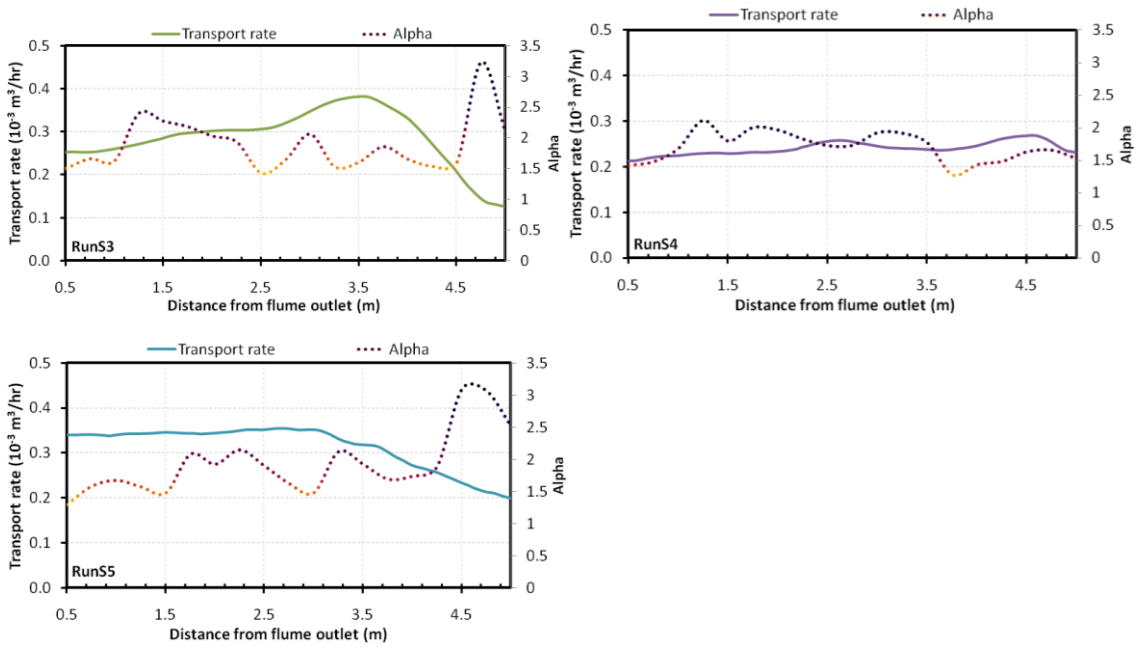


Figure 6-24 Longitudinal variation of sediment transport rate and shape parameter

Figure 6-24 illustrates the relationship between time averaged shape parameter α and longitudinal variation in sediment transport along the flume. Identification of a simple relationship between transport rates derived using the sediment budget approach and the shape parameter α is not possible. However, it is likely that longitudinal variation in sediment transport is controlled by, along with other factors, the degree of variability exhibited by bed topography across a section (Nicholas, 2000). In all graphs of Figure 6-24 the longitudinal pattern of variation between transport rate and the shape parameter 'α' is consistent. At the flume inlet for degradation runs (RunS1, S3 and S5), values of shape parameter 'α' remains high but decreases significantly in a very short length of the flume. At the same location, the transport rate was low and steadily increasing. This is probably because the inlet of the flume is characterized by active erosion and flow was confined in a single channel with apparently less flow variability and hence high 'α' values. There were very minor fluctuation in both transport rate and shape parameter along the flume for the aggradation runs (RunS2 and S4).

## 6.9. RELATIONSHIP BETWEEN CHANNEL WIDTH TO DEPTH RATIO AND SHAPE PARAMETER α

One of the most widely used measures of river channel shape is the width to depth ratio, or its inverse, form ratio, which was presented by Gilbert and Murphy (1914). The main reason for the popularity of the width to depth ratio is that it has been found to correlate satisfactorily with perimeter sediment characteristics under a wide range of conditions (Schumm, 1960). For example, Schumm (1960) showed that width to depth ratio is negatively correlated with the silt-clay content of perimeter sediments (an index of bank shear strength and erodibility). Based on this, an attempt was made to develop a relationship between the width to depth ratio and the gamma shape parameter α for the experimental channels. Width, in this case, is calculated as the total water surface width and depth as mean flow depth. Establishment of a general relationship based on the dataset for the whole flume was feasible, due to the fact that there is a lot of scatter in the data. Different approaches to grouping and analysing the dataset were considered. Initially, data were grouped based on thresholds of width to depth ratio. In this case, points were very much scattered and did not appear to show any kind of relationship. So, data were grouped by cross-section and a unique relationship between wdith:depth ratio and alpha was established for each cross-section. Parameter values from these relationships were then averaged to establish a single overall relationship. This averaged relationship was then applied at each cross-section and tested. Figure 6-25 shows the relationship between channel width to depth ratio and the gamma shape parameter α for each cross section along the flume.

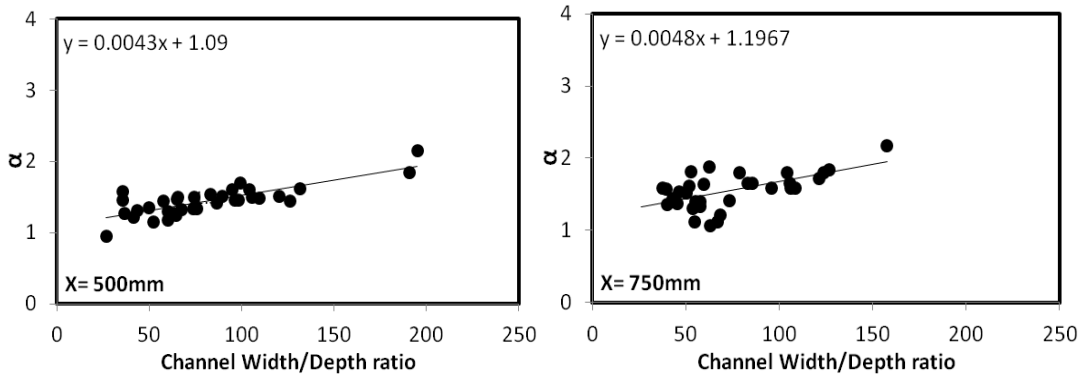

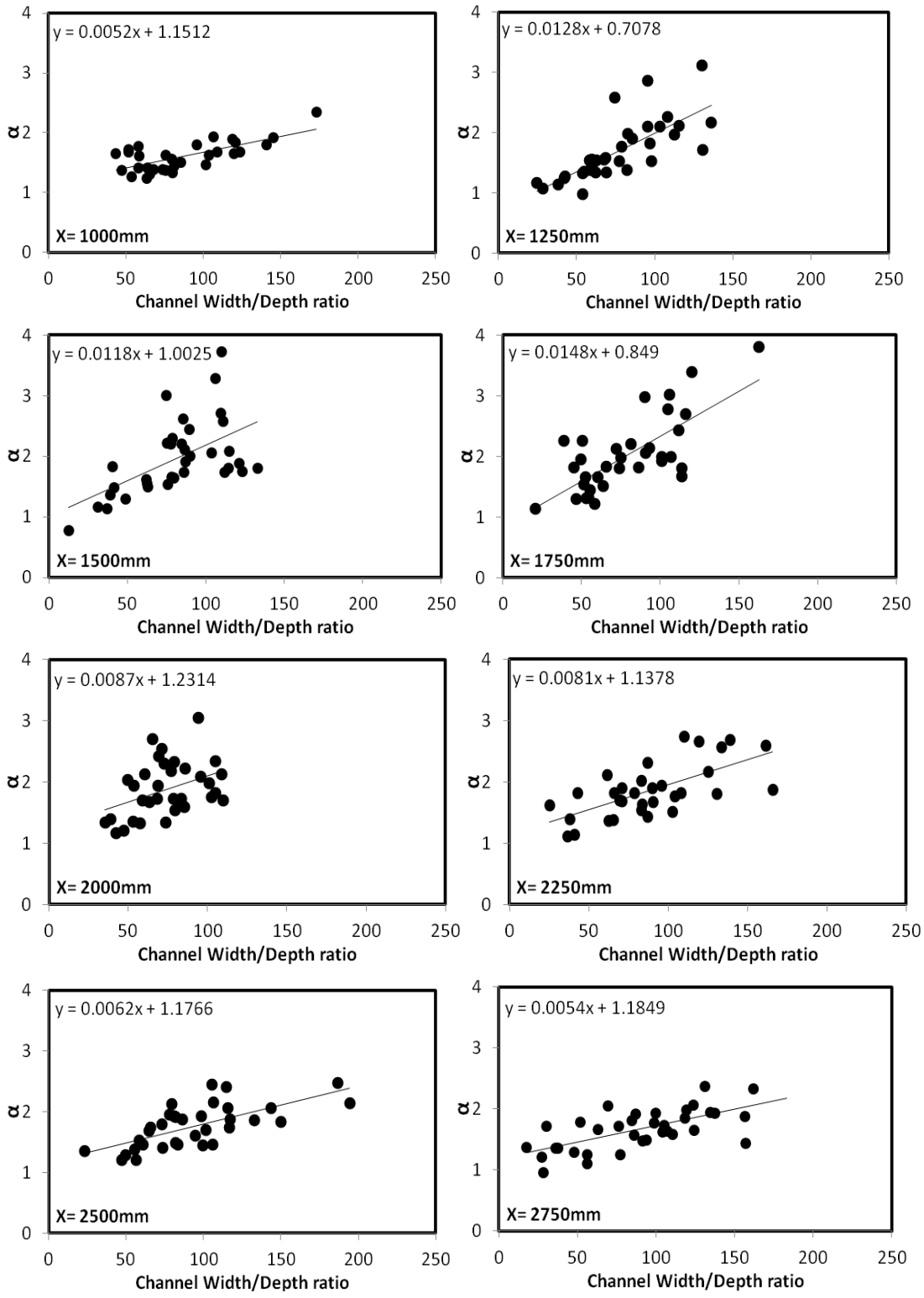
y = 0.0052x + 1.1512
X= 1000mm
y = 0.0128x + 0.7078
X= 1250mm
y = 0.0118x + 1.0025
X= 1500mm
y = 0.0148x + 0.849
X= 1750mm
y = 0.0087x + 1.2314
X= 2000mm
y = 0.0081x + 1.1378
X= 2250mm
y = 0.0062x + 1.1766
X= 2500mm
y = 0.0054x + 1.1849
X= 2750mm
α
Channel Width/Depth ratio
0
50
100
150
200
250
1
2
3
4

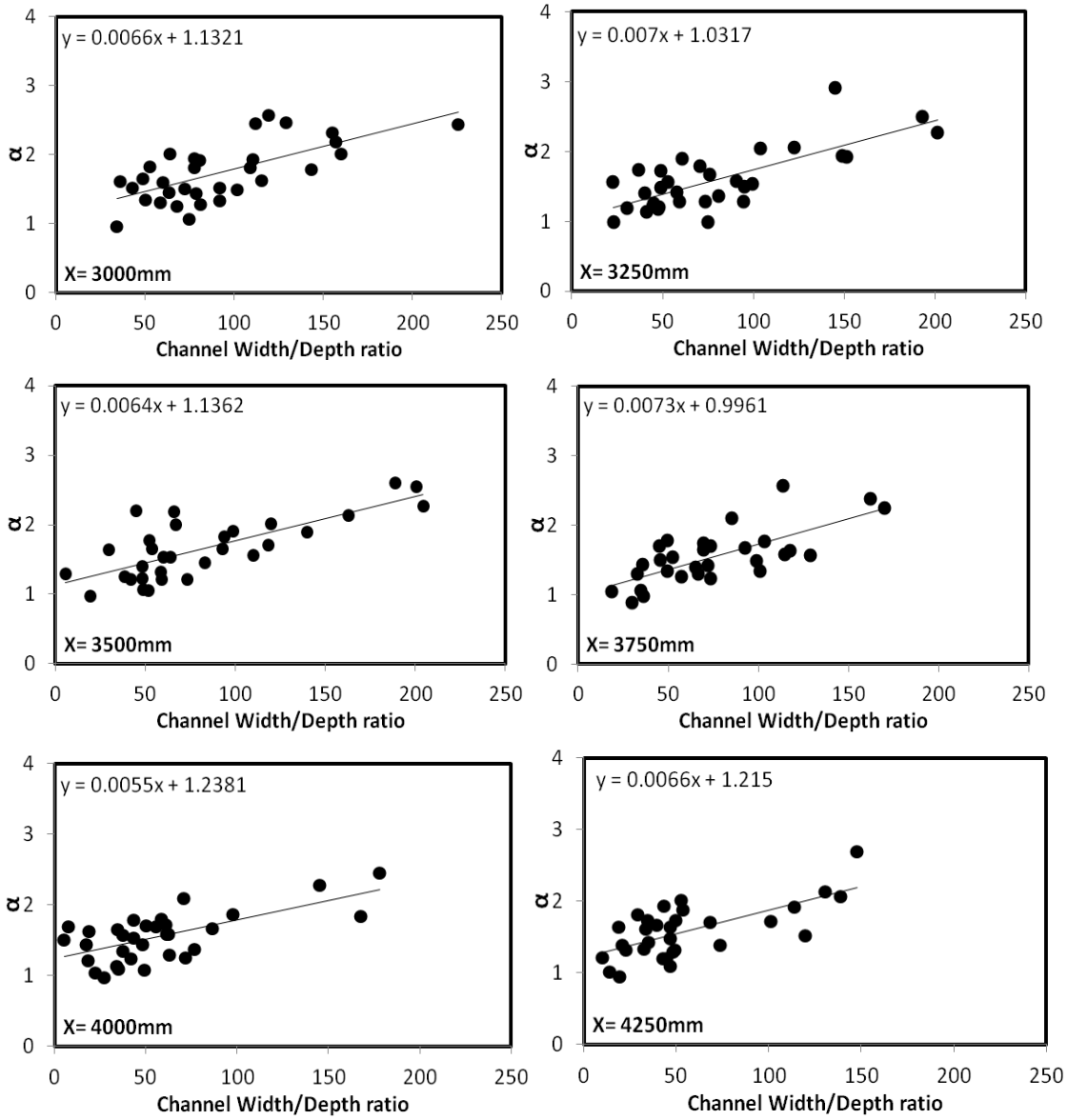


**Figure 6-25 Relationship between channel width to depth ratio and gamma shape parameter (α) at each cross section**

Figure 6-25 shows that although there is a lot of scatter in the dataset, most cross sections do have very similar equations for the relationship between channel width to depth ratio and α. However, all the equations from different cross sections in Figure 6-25 appears to be counter to the idea that alpha will increase at higher flows (greater depths). It appears that there is a slight dependency of alpha on flow depth. In all the equations generated from each cross section along the flume, the slope of the regression line is low indicating the fact that there is a weak dependency of α value on channel width to depth ratio. This means at high values of width to depth ratio (which is

characteristics of Braided rivers), alpha values do not increase significantly. Moreover, Paola (1996) has observed a weak tendency for α to increase with discharge for Ohau River and due to this Paola has considered the value of α to be constant. Nicholas (2000) also noticed that longitudinal trends in shape parameter α are more marked at peak discharges than mean annual flow for the case of Waimakariri River. In this case, experimental runs were carried out for much smaller, constant discharges. This may explain why the trends in Figure 6-25 appear counter to the idea that α will increase at higher flows.

A systematic variation does not appear to exist in the equations (in the constant term and the intercept) along the flume. Consequently, the equations from each cross section were averaged and a unique relationship that may be applied to the whole flume is established. The equation established by averaging all equations along the flume is:

$$\alpha = 0.00935\left(W/h\right) + 1.0035 \qquad 6\text{-}19$$

Where W is the total water surface width and h is mean flow depth. This equation (equation 6-19) is then directly applied to each cross section and its validity is tested by comparing it with α values generated by fitting shear stress data to a gamma PDF at individual cross sections.

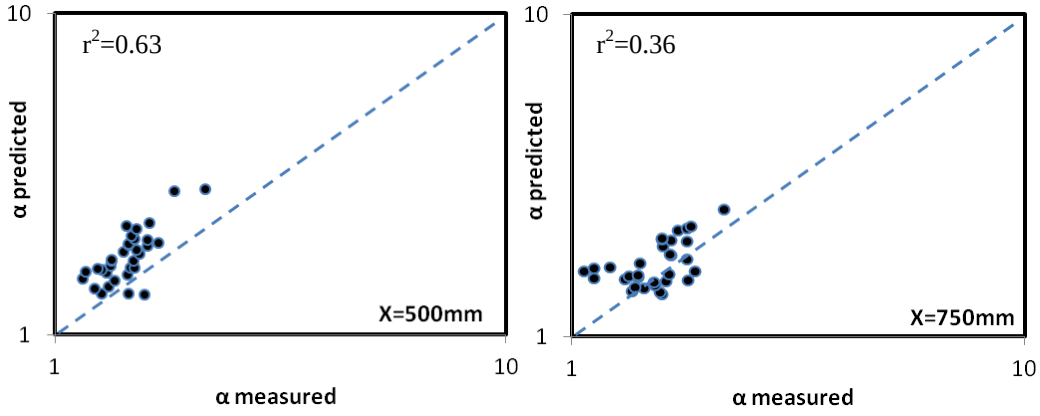

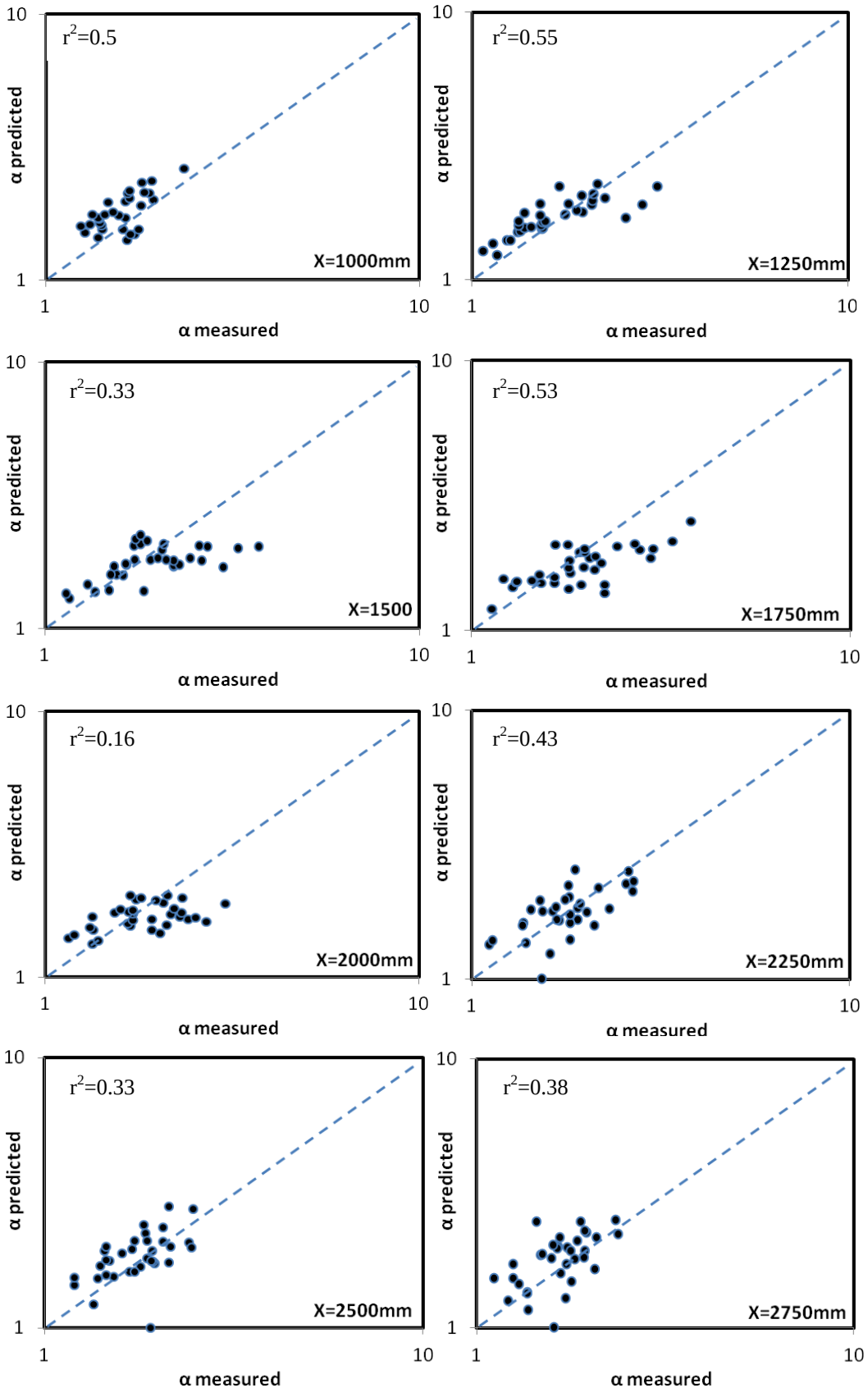
r²=0.5
X=1000mm
r²=0.55
X=1250mm
r²=0.33
X=1500
r²=0.53
X=1750mm
r²=0.16
X=2000mm
r²=0.43
X=2250mm
r²=0.33
X=2500mm
r²=0.38
X=2750mm
α predicted
α measured
10
1

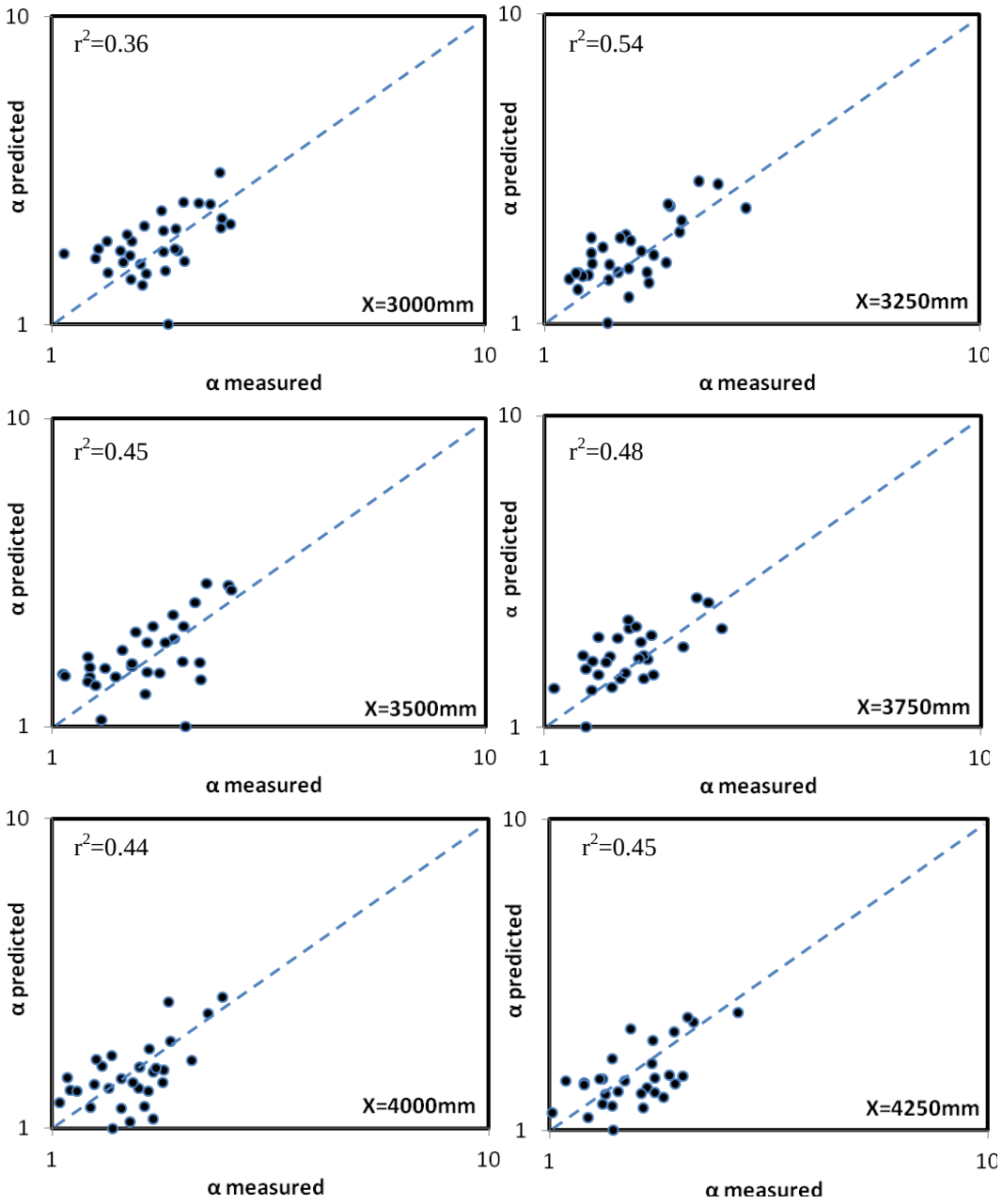


**Figure 6-26 Relationship between α values obtained by fitting shear stress from each cross section to a gamma PDF (α measured) to α values obtained by equation 6-19 (α predicted)**

Figure 6-26 shows the relationship between α values obtained by fitting shear stress data from each cross section to gamma PDF (α measured) and α values obtained by using equation 6-19 (α predicted). Although coefficients of determination values are relatively low at some cross-sections, the average $r^2$ value of nearly 0.55 suggests that equation 6-19 has some potential for predicting alpha for use in sediment transport calculations. Differences between α measured and α predicted can be attributed to a wide range of sources of error and uncertainty in the two. For example, a simple average of different

equations along the flume is taken to develop equation 6-19 (α predicted), although there appears to be some wide variations at some sections around mid-flume. In addition to these sources of error, some uncertainty exists in the accuracy of the way flow depth is predicted and shear stress is calculated, which is described in section 6.2. Despite this, the consistency between α measured and α predicted suggests that the equation can provide a first-order estimate of α values when other topographic information is unavailable.

## 6.10. SUMMARY

Measured total sediment transport rates (time averaged) were compared to the predictions of the Meyer-Peter-Muller equation (MPM) using surveyed topographic cross sections and cross-section averaged hydraulic parameters. Sediment transport rates predicted by the Meyer-Peter-Muller transport equation and cross section averaged hydraulic parameters substantially under-predict actual transport rates. This is consistent with previous investigations demonstrating the significant influence of transverse variability of hydraulic parameters in controlling and predicting sediment transport rates in braided channels. Computation of the transport rates using the measured topographic cross sections shows good agreement with the measured values even-though the critical Shields value is estimated as a calibration parameter. Estimates of volumetric changes in sediment storage determined using topographic survey data show consistent patterns of change, across several individual cross sections and temporally throughout different inter-survey intervals. This suggests that some sources of errors (e.g., compensating scour and fill) do not affect the gross stream-wise patterns of erosion and deposition. Transport rates determined using the sediment budget approach generally capture the overall transport pattern in aggrading and degrading channels. Mean transport rates estimated by the sediment budget approach generally are 30 to 70 times the mean transport rates determined from the equation of MPM for the case when flow variability is ignored in the MPM calculations. Varying the critical Shields parameter does not have a significant influence on the disparity of the two estimates.

Frequency distributions of shear stress were shown to fit gamma distributions. This is consistent with several other studies (Nicholas, 2000;Paola, 1996). Gamma probability

distributions fitted to shear stress data for aggrading and degrading experimental channels reveal that the former posses lower alpha values, indicating greater variation in flow depth and shear stress distribution. This may be because the aggrading channels are wider and more braided, so that flow depths are shallower and more variable. More generally, shape parameter (α) values decrease in the downstream direction indicating greater spatial variability in bed topography, although for the middle part of the flume (from 1.5m to 3.5m) variations in 'α' are small. In contrast, braiding intensity increases in the downstream direction. As with the shape parameter (α), the braiding intensity shows little variation around the middle of the flume. Maxima in braiding intensity and minima in shape parameter values occur around the flume outlet. In contrast, minima in braiding intensity and maxima in shape parameter values occur at the flume entrance. Averaging of the gamma shape parameter 'α' values for the whole channel seems to yield a stable value that emerges from aggrading and degrading braided channels.

A relationship exists between braiding intensity and sediment transport for the experimental braided channels. Earlier investigators have reported that an increase in braiding intensity may promote higher rates of sediment transport (Nicholas, 2000;Warburton and Davies, 1994) as a result of increased spatial variability in flow depth and shear stress. However, Ashmore (1988) and Hoey and Sutherland (1991) argue that sediment transport rate decreases as braiding increases. Results from the experimental braided channels reported here reveal that sediment transport increased with braiding intensity. However, there seems to exist a threshold, beyond which, an increase in braiding intensity does not increase sediment transport and it may even reduce transport rates. This may be because of the division of flow by the channels formed as a result of increase in braiding intensity, and hence increased flow width and lower mean shear stress. This will reduce the amount of flow to be conveyed by the ''active'' part of the channel. A relationship between channel shape index (width to depth ratio) and the gamma PDF shape parameter is established based on data from each cross section of the experimental channels. These relationships clearly show a slightly increasing trend of α with channel width to depth ratio.

The experimental work presented here offers a unique opportunity to observe in detail the spatial and temporal changes that occur on the gamma shape parameter as channels

evolve due to aggradation and degradation. The next chapter will attempt to compare these experimental results with results obtained using a two dimensional hydraulic numerical model. Model derived flow depth and shear stress will be fitted to the two-parameter gamma probability density function and temporal and spatial patterns of shape parameter will be investigated.

# 7. APPLICATION OF TWO DIMENSIONAL HYDRAULIC MODEL TO THE EXPERIMENTAL CHANNELS

## 7.1. INTRODUCTION

Numerical models are known to provide the basis for understanding the hydrodynamic and geomorphic conditions in rivers and estuaries and are a valuable tool for solving complex problems in river engineering and geomorphology.

In this chapter the experimental data from this project will be used to generate flow depth and shear stress predictions from a two-dimensional hydraulic model. The aim of this is to attempt to gain a better understanding of the controls on the shear stress distribution in the experimental channels and its influence on sediment transport and channel evolution. The chapter begins with an explanation of the equations used in the model and methods used to discretize them. This will be followed by application of the model using the data from the physical model experimental runs.

## 7.2. DESCRIPTION OF THE TWO-DIMENSIONAL HYDRAULIC MODEL

The model is a two-dimensional hydraulic model which solves the depth-averaged shallow-water form of the Navier-Stokes equation in conservative form. The model uses a Godunov-type finite volume method. This method balances all the fluxes entering and leaving each cell, using explicit time integration. Accuracy of second-order is attained through variable extrapolation approach based on van Leer's Monotonic Upstream Schemes for Conservation Laws (MUSCL) (Van Leer, 1977) and a simple but robust approximate HLL solver due to (Harten *et al.*, 1983). Modern finite volume schemes of the Godunov type achieve higher than first-order accuracy by reconstructing the cell interface data from cell centre values and using flux or slope limiters to preserve monotonicity (Mingham and Causon, 1998). The model equations can be expressed in conservative law form as:

$$\partial \mathbf{U}/\partial \mathbf{t} + \partial \mathbf{F}/\partial \mathbf{x} + \partial \mathbf{G}/\partial \mathbf{y} = \mathbf{S} \qquad \textbf{7-1}$$

Where:

$$\mathbf{U} = \begin{pmatrix} \Phi \\ \Phi u \\ \Phi v \end{pmatrix}; \quad \mathbf{F} = \begin{pmatrix} \Phi \mathrm{u} \\ \Phi u^2 + \Phi^2/2 \\ \Phi uv \end{pmatrix}; \qquad \mathbf{G} = \begin{pmatrix} \Phi v \\ \Phi uv \\ \Phi v^2 + \Phi^2/2 \end{pmatrix}$$

And where $\Phi = gh; h = \text{water depth}$; $g$= acceleration due to gravity; $u$ and $v$ = depth averaged velocity components in the *x*- and *y*- directions; **F** and **G** = convective fluxes in the *x*- and *y*- direction; and **S** = vector of source terms, which would normally include bed slope, friction losses, and Coriolis forces as well as turbulent transport effects.

The assumptions made in deriving these equations and within the solution procedure make the model applicable to steady or unsteady flow simulations. Flow regimes can also be subcritical or supercritical as well as gradually varying or discontinuous flow. The data required to run the model consists mainly of topographic data (DEM) describing the channel geometry, boundary conditions, channel-bed roughness coefficients (Chezy) and turbulent diffusivity constant. Bathymetry data were collected in the form of XYZ coordinates at 8mm stream-wise resolution. These DEMs were interpolated to construct 4x4mm resolution DEMs using a bi-linear interpolation. The bi-linear interpolation method uses the values of four surrounding cells of the input DEM to calculate an interpolated value for each cell in the output DEM.

The typical means of applying boundary conditions in the model is to define the discharge at the upstream boundary, which is represented with a piecewise linear hydrograph, and the slope at the downstream boundary. So, at the upstream reach of the channel the total discharge was specified as an input to the model. The downstream boundary condition in the model is set equal to the average bed slope for the channel as a whole.

To avoid computational difficulties associated with very shallow flow, the model requires a minimum flow depth for momentum calculations to be specified. Based on

this minimum depth the model handles the problem of some areas being wet while others are dry and transitions between the two. In this study the effect of the minimum flow depth for momentum calculations is also investigated by varying its value in the simulation and fixing other variables that influence model output like roughness parameters $R_c$ and $R_d$.

Accurate representation of resistance is essential in modelling shallow water flows and sediment transport. Previous researchers used different roughness estimators for similar studies; some derived the value of roughness from standard text books (e.g.Chow, 1959) and others by relating roughness coefficients to bed sediment grain size using the Strickler (1923) relationship. They often calibrate roughness coefficients to reconcile modelling outputs with measurements (Cao and Carling, 2002). Alluvial channels are subject to considerable difference in sediment transport rates that will give rise to significant differences in roughness, hence the roughness cannot be assumed to be fixed. The roughness does at least vary between the main channel and flood plains. The two-dimensional model used in this study uses a Keulegan type roughness estimator of the form:

$$C = R_c\left[log\left(Y/R_d\right)\right] \qquad 7\text{-}2$$

Where $R_d$ is the effective roughness height, a value of which is usually required when the Keulegan or Strickler equation is specified and $R_c$ is calibration parameter. It is a better descriptor of resistance than indices such as Manning's n because it tends to remain constant over a wider range of flow depths than does n (Steffler and Blackburn, 2002). There is no table of generally accepted values for the effective roughness as there are for Manning's n values. For resistance due primarily to bed material roughness, a starting estimate of this parameter can be taken as 1-3 times the largest grain diameter (Steffler and Blackburn, 2002) and calibration to observed water surface elevations gives the final values. In this study $R_d$ was initially set to be equal to the minimum flow depth for momentum calculations, which is nearly equal to the diameter of the mean grain size $d_{50}$ ($1.06d_{50}$). This is done so as to get a smooth, continuous and non-negative resistance value for any flow depth. $R_d$ values greater than the minimum flow depth set in the model for momentum calculations would result in negative roughness at some

locations where flow depth is shallower, which is unrealistic. $R_c$ is used as a calibration constant. A number of model runs were conducted, each using a different value of $R_c$ and $R_d$. Depth predictions for each model run were compared with measurements of flow depth obtained at 25 cm intervals across different cross sections within the flume. On the basis of this comparison between measured and predicted flow depths, optimal values of $R_c$ and $R_d$ were identified.

The experimental discharge was 0.000058 $m^3s^{-1}$. When the channel was degrading the upstream inlet section was approximately single threaded with more than 95% of the flow confined within it. When the channel was aggrading it was fully braided. The results of the model were tested for a range of experimental conditions using DEMs collected from the aggradation and degradation experiments. Data collected from each experimental run were used to calculate distributed patterns of flow depth (mm) at each section for comparison with the predictions of the two-dimensional hydraulic model. The initial condition for all model runs was a dry channel bed with total water discharge specified at the upstream model boundary. The flow pattern in the experimental channel was allowed to develop until a steady-state solution was obtained, which takes in the order of 35 to 40 hours depending on the complexity of the DEM. A final solution was considered to have been obtained when the inflow and outflow discharges had been equal to each other for at least 8 hours. The degree to which the two-dimensional model is able to replicate the measurements from the experiment is assessed below.

## 7.3. MODEL CALIBRATION AND SENSITIVITY ANALYSIS

The results of the model were examined first for a range of parameters and roughness values in order to compare predicted with observed flow depths. This was done using flow depth data obtained at 25 cm intervals across 19 cross sections within the experimental reach. In the experimental runs, water surface elevation was estimated using a survey of each dry channel cross section followed immediately by a survey of the wet channel cross section. A video camera was attached near the bottom of the laser profiler during traversing (explained in chapter 6). The drawbacks and suitability of this approach are dealt with in chapter 6. The distributed patterns of depth obtained from

these data will be used for comparison with the prediction of the two dimensional hydraulic model.

To identify the most suitable values of the parameters '$R_d$' and '$R_c$' for use in the two-dimensional hydraulic model, a sensitivity analysis was carried out by comparing flow depths measured during the experimental runs with the flow depths predicted using the hydraulic model. The initial value of the roughness parameter '$R_d$' was selected with the aim of obtaining continuous non-negative resistance values for all flow depths as explained in section 7.2. Values of the roughness parameter ranging from 0.0001 to 0.0005 were considered in the sensitivity analysis.

Since both the measured and predicted flow depth values contain errors, the relationship between them can be expressed in the form:

$$\boldsymbol{M = A + BE + (m - Be)} \qquad \textbf{7-3}$$

Where M and E are model predictions and measurements from experiments, respectively, and m and e are errors in the variables M and E. Errors in measurements and predictions were assumed to be proportional to the total variance in the respective dataset (see Webster, 1997)). In this case, the best fit line through the M and E dataset is termed the reduced major axis and has a gradient (B) given by the variance of the dataset:

$$\boldsymbol{B = \sqrt{\sigma_M^2 / \sigma_E^2}} \qquad \textbf{7-4}$$

Where $\sigma_M$ and $\sigma_E$ are the standard deviation of the model predicted and experimental dataset.

Table 7-1 outlines the statistical relationships between the model predictions and measurements of flow depth. The data used in the analysis is carefully selected to represent the flume entrance, middle part and flume outlet. Data from different cross sections representing inlet, middle and outlet of the flume were pooled together. It appeared from Table 7-1that the coefficient of determination for relationships between the predicted and measured flow depths is relatively insensitive to changes in either the roughness parameter ($R_d$) or the calibration constant ($R_c$). In all cases there is a strong positive relationship between model results and measurements. However, the slope of

the best fit line (B) shows some changes with roughness. When the value of the effective roughness is reduced, the slope of the best fit line (B) approaches 1 and this effect is stronger at high values of resistance (high $R_c$).

**Table 7-1 Results of sensitivity analysis for different values of effective roughness $R_d$**

| $R_c$ | Roughness values $R_d$ | | |
|---|---|---|---|
| | 0.0005 | 0.0003 | 0.0001 |
| 24 | $r^2$ =0.81 | 0.81 | 0.81 |
| | B = 1.36 | 1.23 | 1.14 |
| 15 | $r^2$ = 0.83 | 0.83 | 0.83 |
| | B = 1.32 | 1.29 | 1.24 |
| 5 | $r^2$ = 0.80 | 0.81 | 0.82 |
| | B =1.46 | 1.43 | 1.39 |

**Table 7-2 Results of sensitivity analysis at individual sections. Table A (flume inlet), table B and C (mid flume) and table D (flume outlet)**

| Table A | Roughness values $R_d$ | | |
|---|---|---|---|
| $R_c$ | 0.0005 | 0.0003 | 0.0001 |
| | $r^2$ = 0.54 | 0.63 | 0.74 |
| 24 | B = 1.18 | 1.12 | 0.96 |
| | $r^2$ = 0.72 | 0.72 | 0.73 |
| 15 | B = 1.37 | 1.3 | 1.13 |
| | $r^2$ = 0.66 | 0.68 | 0.69 |
| 5 | B = 1.66 | 1.6 | 1.5 |

| Table B | Roughness values $R_d$ | | |
|---|---|---|---|
| $R_c$ | 0.0005 | 0.0003 | 0.0001 |
| | $r^2$ = 0.51 | 0.8 | 0.9 |
| 24 | B = 1.38 | 1.16 | 1.1 |
| | $r^2$ = 0.72 | 0.72 | 0.91 |
| 15 | B = 1.23 | 1.21 | 1.16 |
| | $r^2$ = 0.84 | 0.85 | 0.86 |
| 5 | B = 1.34 | 1.34 | 1.33 |

| Table C | Roughness values $R_d$ | | |
|---|---|---|---|
| $R_c$ | 0.0005 | 0.0003 | 0.0001 |
| 24 | $r^2$ = 0.56 | 0.82 | 0.84 |
| | B = 1.50 | 1.26 | 1.16 |
| 15 | $r^2$ = 0.85 | 0.86 | 0.84 |
| | B = 1.35 | 1.29 | 1.25 |
| 5 | $r^2$ = 0.88 | 0.88 | 0.88 |
| | B = 1.29 | 1.29 | 1.29 |

| Table D | Roughness values $R_d$ | | |
|---|---|---|---|
| $R_c$ | 0.0005 | 0.0003 | 0.0001 |
| 24 | $r^2$ = 0.91 | 0.84 | 0.82 |
| | B = 1.33 | 1.32 | 1.25 |
| 15 | $r^2$ = 0.85 | 0.85 | 0.85 |
| | B = 1.38 | 1.36 | 1.33 |
| 5 | $r^2$ = 0.84 | 0.84 | 0.84 |
| | B = 1.44 | 1.44 | 1.43 |

In contrast, comparison of the coefficient of determination for relationships between measurements and predictions at individual sections representing flume outlet, mid-flume and flume inlet highlights significant variations with changes in both the roughness value $R_d$ and the constant $R_c$ (Table 7-2). As shown in Table 7-2 most sections show an increase in the coefficient of determination as the effective roughness decreases, although at lower resistance (lower values of $R_c$) this effect is slightly weaker. The improvement in model performance (based on values of $r^2$ and B) is different for different sections of the flume. At the flume inlet, best fit lines between measurements and model predictions suggest an optimum roughness value between 0.0003 and 0.0001 but lower values of roughness for middle and outlet of the flume (all achieved at higher values of $R_c$. see Table 7-2). This appears to show that some improvement in model performance can be achieved by using spatially variable roughness. Having said this, although an optimum value of the roughness value for which B equals exactly one is not achieved, it is clear that all parts of the flume show improvement (although at a different rate) in model performance at lower values of roughness. This suggests that the use of a constant roughness value, $R_d$, in all sections of the flume does not introduce significant errors in the performance of the model. This is probably due to the narrow grain-size distribution used in the experiment.

Flow depth in each cell must be greater than the minimum flow depth specified in the model in order for water to be routed in that cell. Consequently, higher values of the minimum flow depth parameter ($h_{min}$) lead to flow occurring over a smaller proportion of the channel. Having said this, simulations in which the minimum flow depth parameter was varied ($h_{min}$=0.0002, 0.0003, 0.0005 m) while using constant values of

$R_d$ and $R_c$, showed that the minimum flow depth parameter has a very small effect on model performance. Results from model simulations carried out for $h_{min}$=0.0002 m and 0.0003 m (for $R_d$=0.0001m and $R_c$=5) are shown in Figure 7-1 at X=5000mm and X=2500mm. These plots highlight considerable overlap between model predictions obtained for different values of $h_{min}$.

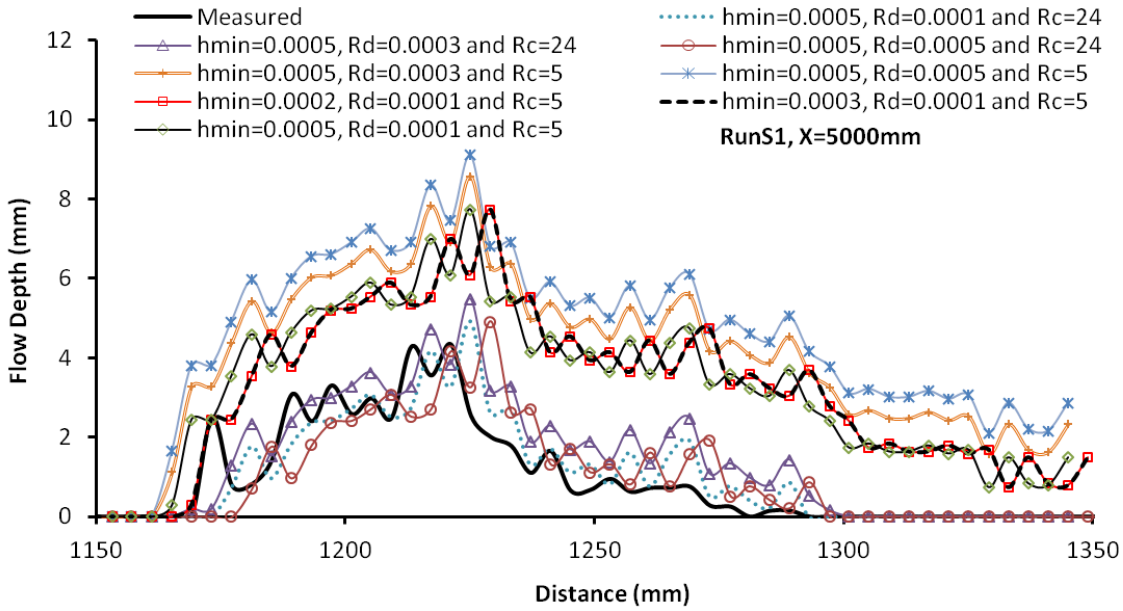


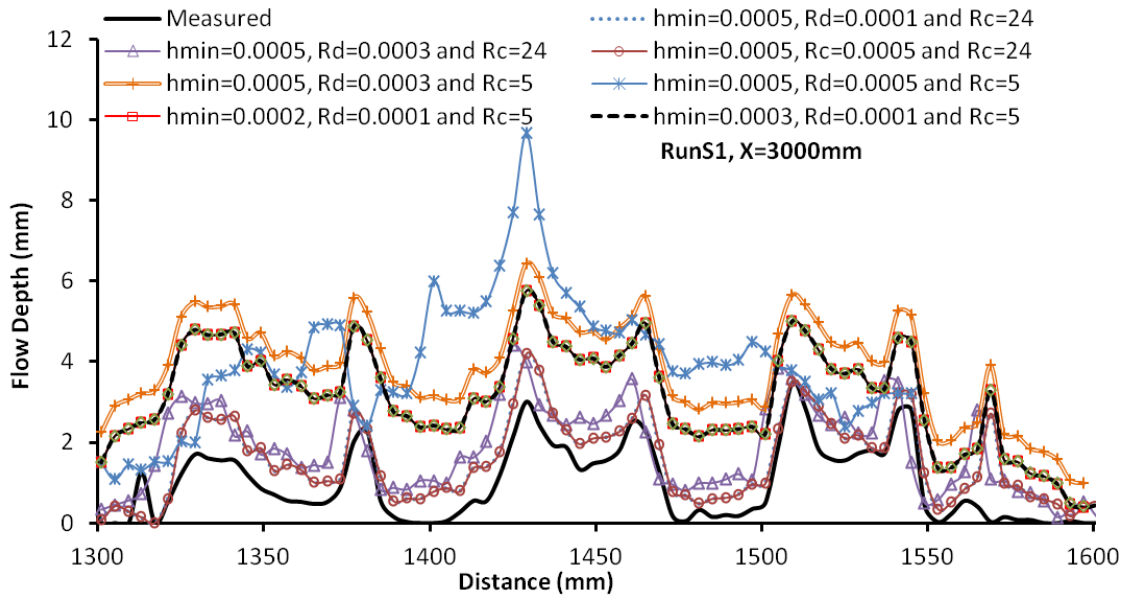

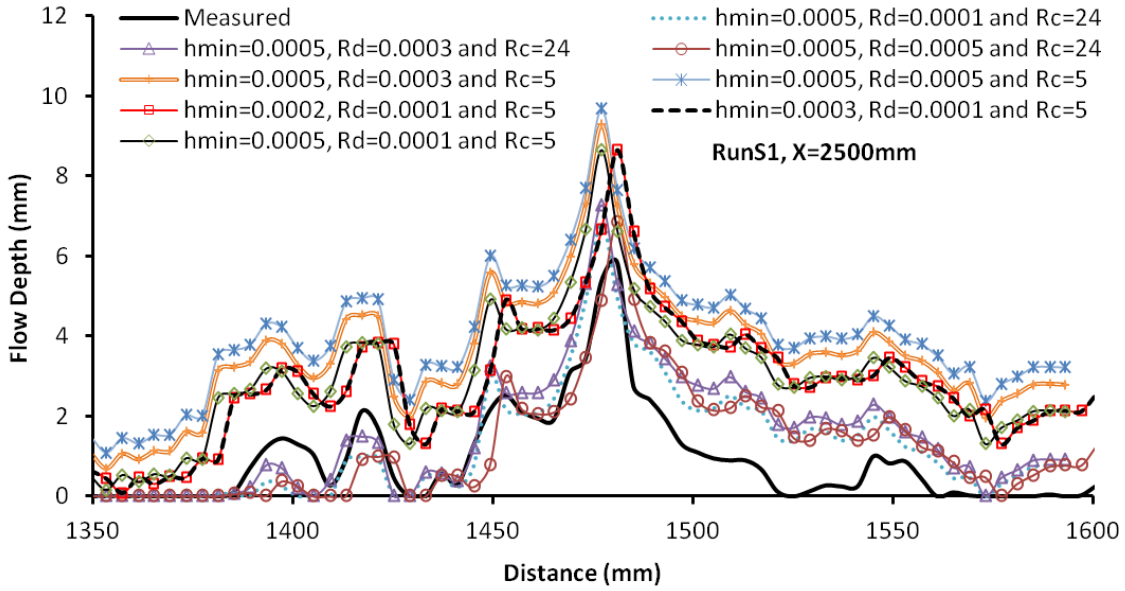


**Figure 7-1 The calibration process and effect of the minimum flow depth parameter $h_{min}$, the roughness depth $R_d$ and the roughness coefficient $R_c$.**

## 7.4. SPATIAL REPRESENTATION OF MODELLING RESULTS

The model performance can be assessed by considering and comparing the distributed patterns of flow depth predicted by this model with the experimental data obtained at individual cross sections. Representative cross sections are selected to include a range of section shapes and flow patterns (e.g., symmetrical, asymmetrical and sections divided by channel bars). Sections are selected from different experimental runs (with and without sediment feed) as this leads to different cross-section shapes and flow patterns.

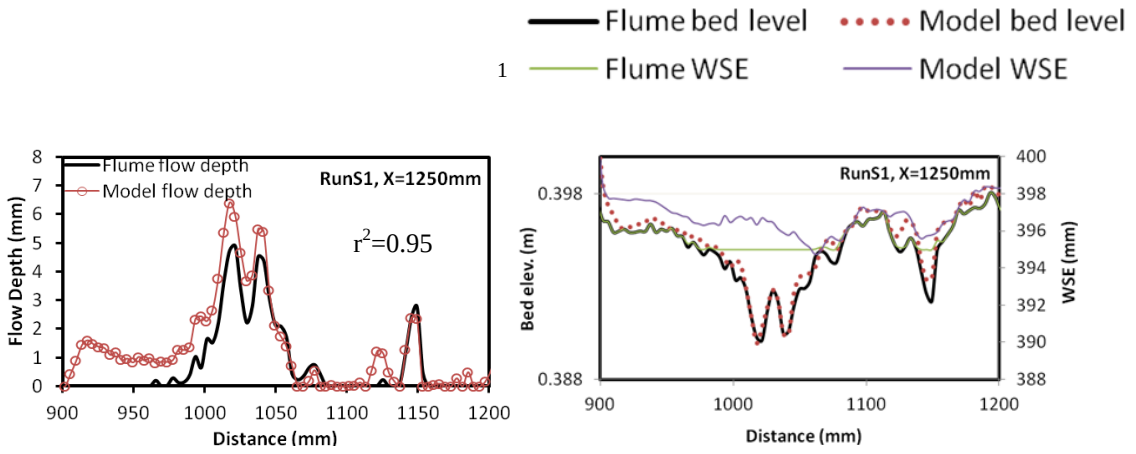


[1] WSE refers to water surface elevation. The key is for the figures in the right hand side.

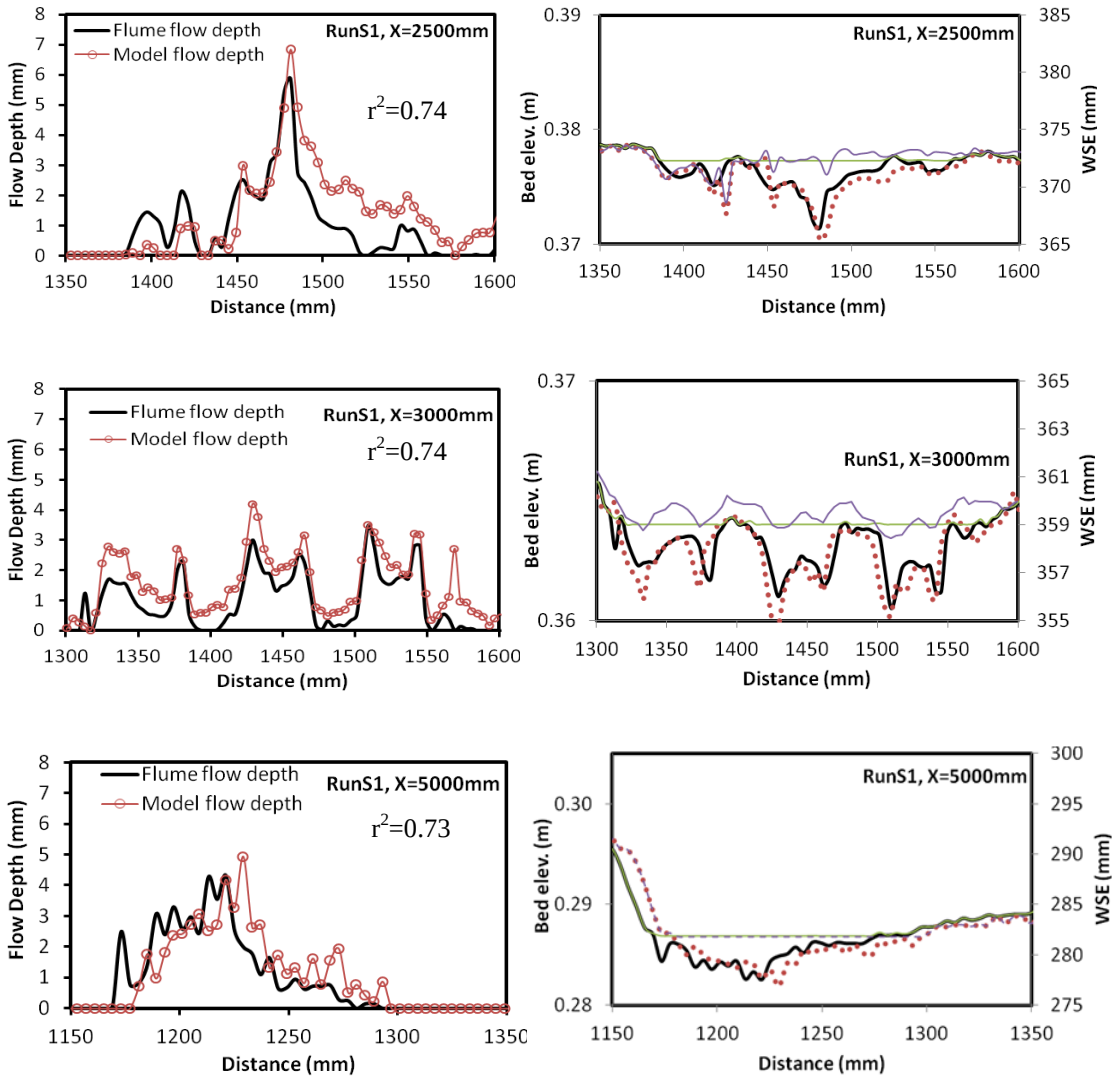


Figure 7-2 Comparison of distributed patterns of flow depth at various for cross sections (RunS1)

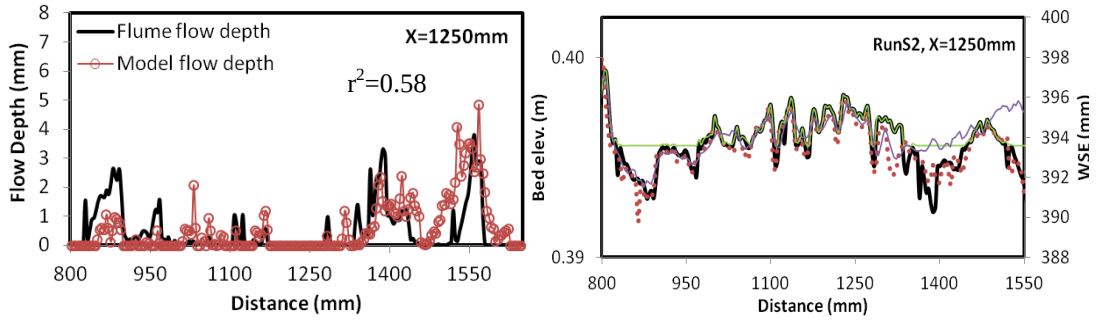

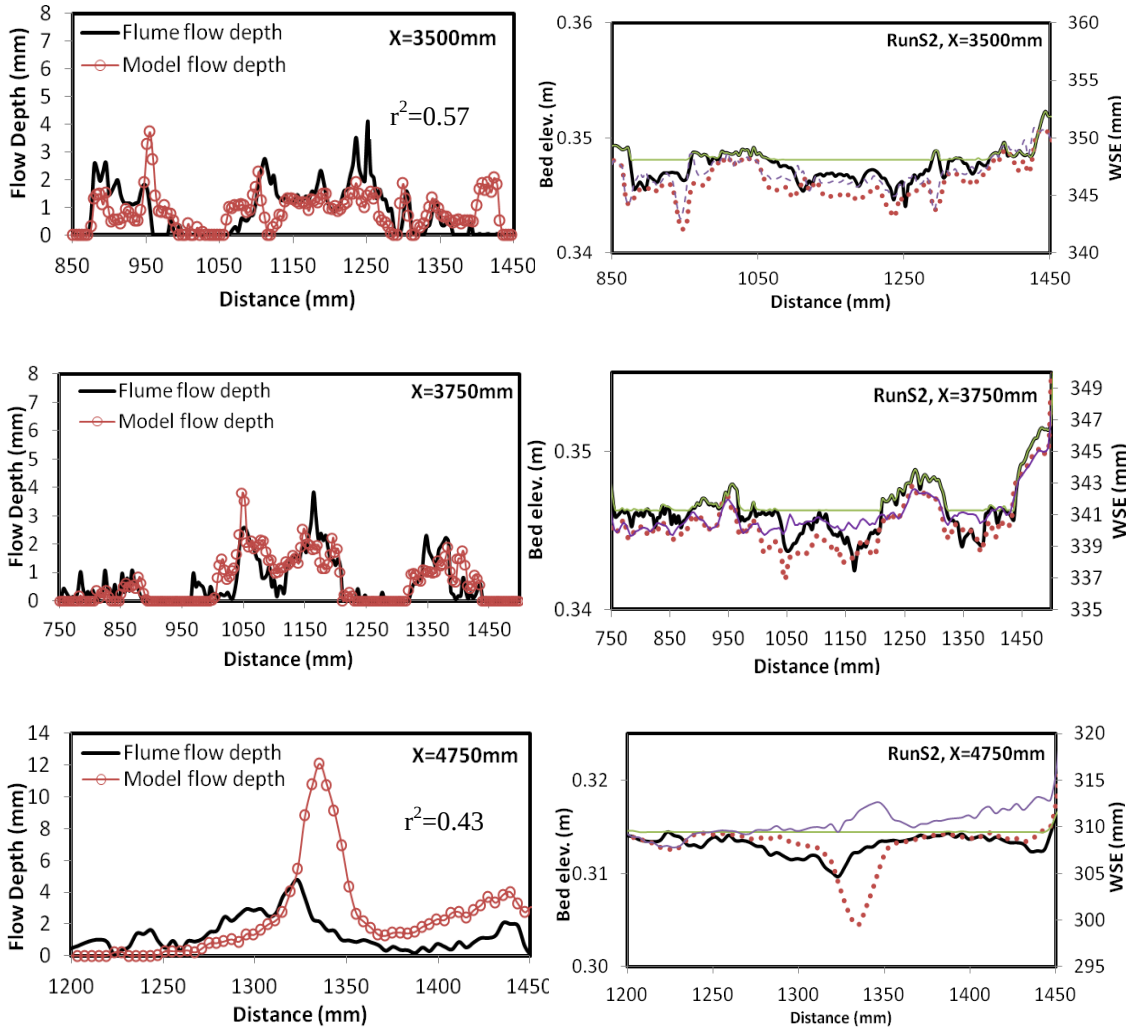


**Figure 7-3 Comparison of distributed patterns of flow depth at various cross sections (RunS2)**

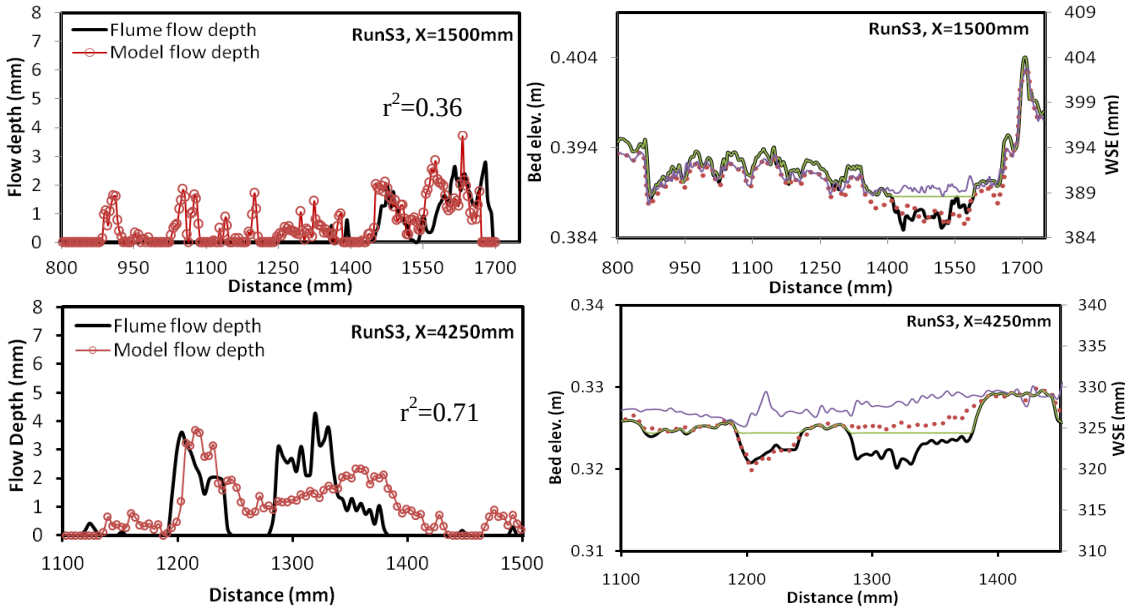

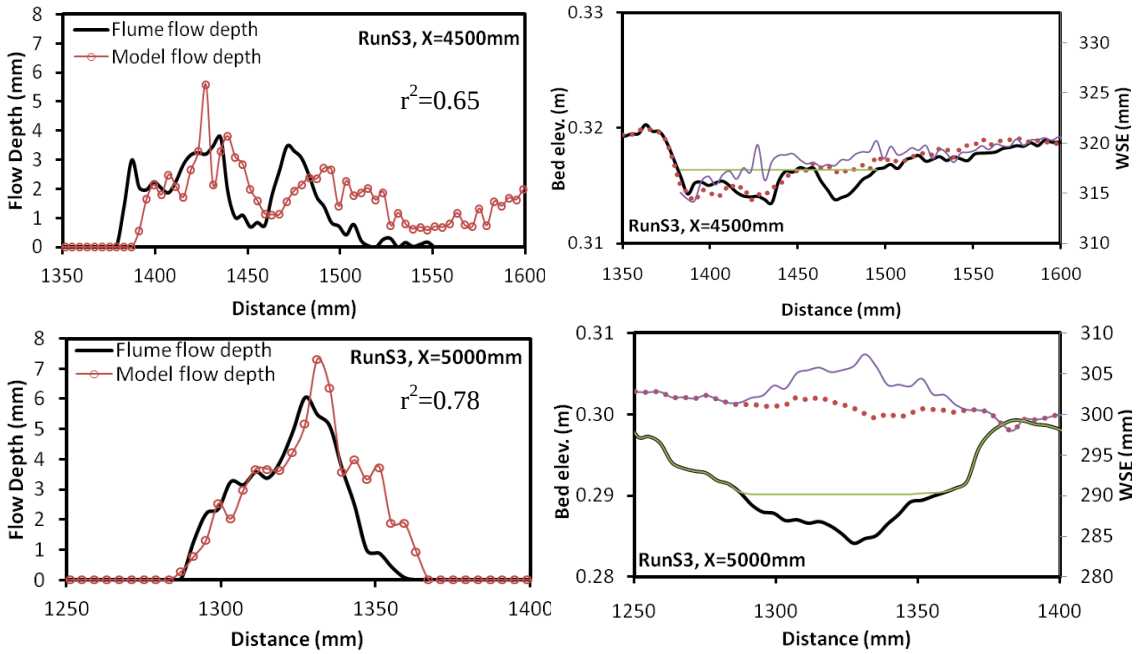


Figure 7-4 Comparison of distributed patterns of flow depth at various cross sections (RunS3)

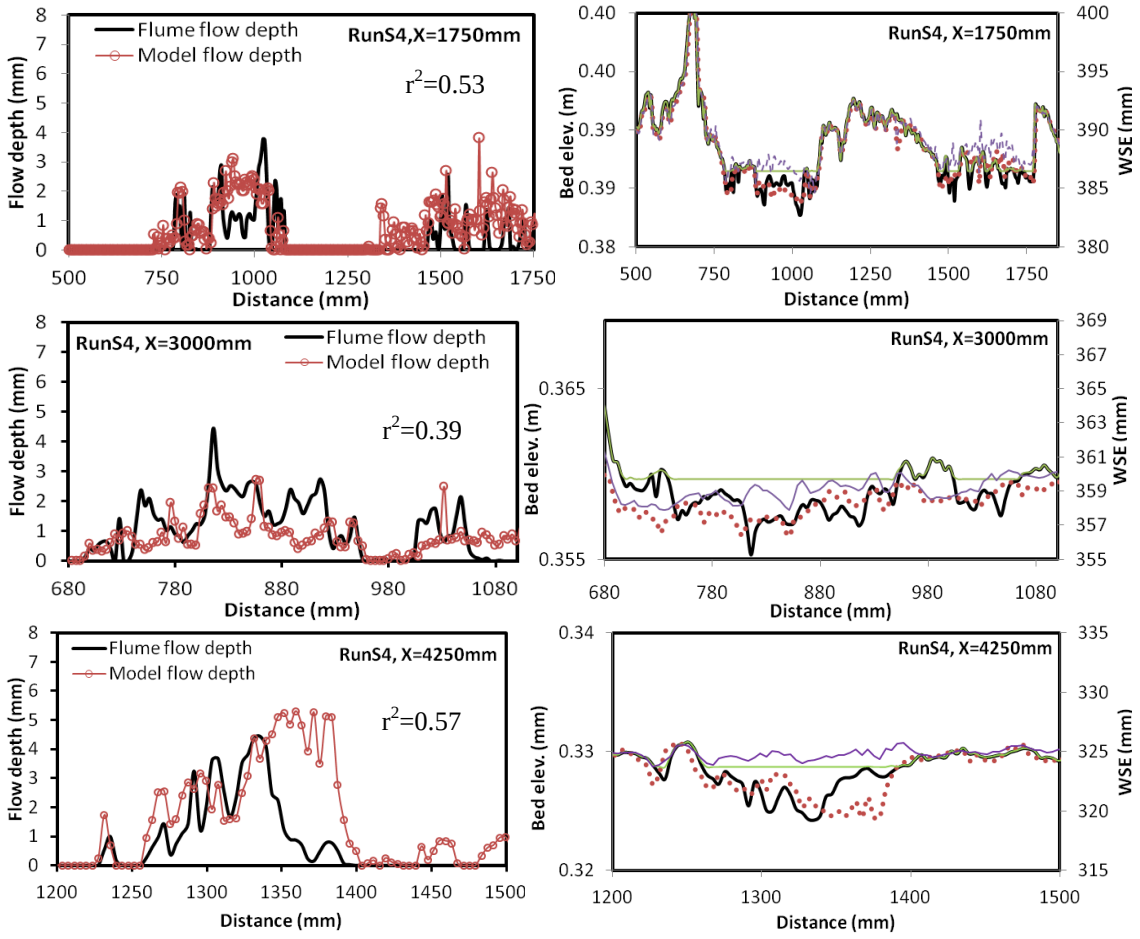

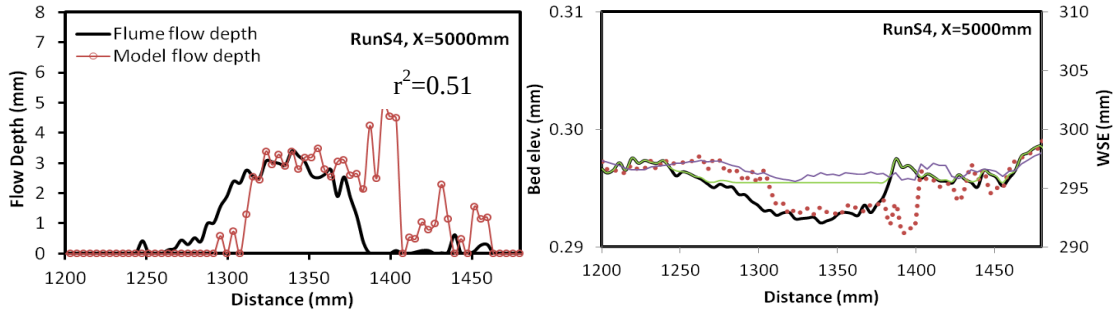


Figure 7-5 Comparison of distributed patterns of flow depth at various cross sections (RunS4)

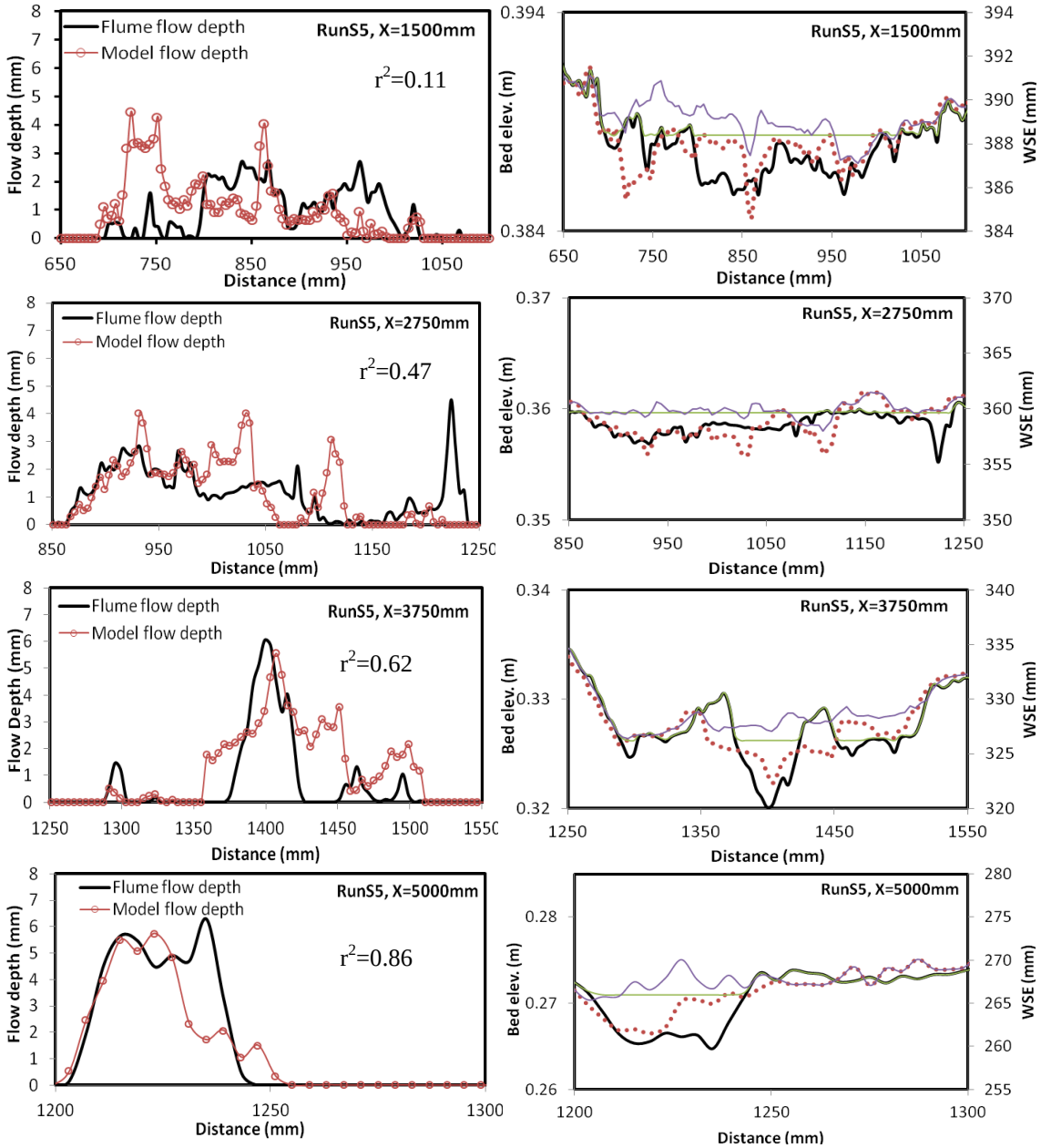


Figure 7-6 Comparison of distributed patterns of flow depth at various cross sections (RunS5)

Figure 7-2 to Figure 7-6 show the measured and predicted patterns of flow depth at different representative cross sections taken from the DEMs acquired from the experimental runs. The cross sections are taken to represent the experimental plot from the upstream, middle and downstream parts of the flume. Differences between the model predictions and the measured data can be attributed to different sources of errors. However, the comparison should first be seen by taking the following two points into account. First, the measured depths assume a constant water surface elevation, which is not always true; particularly for cross-sections that contains multiple channels. In multi-thread channels some parts may not convey water at all even if they are at a lower elevation than others (Zolezzi *et al.*, 2006). This means that the accuracy of the estimated water level depends to a great extent on the shape of the cross-section. The more complex the cross-section is, the less accurate the result will be. The second reason is that there is a significant difference between the bed elevation of some parts of cross sections used in the two dimensional model compared to the flume (measured) cross-sections. This is because the DEMs used in the two dimensional model were collected a short time after the wet and dry surveys of the individual sections for which flow depths have been 'measured'. Erosion and/or deposition in some parts of the channel leads to inevitable differences between measured cross sections and the DEMs used in the model simulations. Moreover, cross-section bed elevations are measured at a mm resolution, whereas the DEM used in the two-dimensional model has a 4mm grid resolution. This means that the 'measured' cross-sections capture considerably more detail than the model DEM in addition to which the DEM will be smoother due to the bilinear interpolation method used to resample the DEM, which averages neighbouring elevation values together. It is very difficult to quantify the contribution of each error source. However, the limited accuracy of predictions in some sections is clearly a result of differences in bed elevation between the 'measured' cross-sections and the equivalent sections extracted from the DEM.

Overall the results demonstrate that the model is reproducing the broad systematic variations in flow depth within cross sections. The coefficient of determination for relationships between measured and predicted depths is shown in each graph. Where the measured and the DEM extracted cross-sections match over most of the channel, the

coefficient of determination is higher (e.g. RunS1 X=1250, X=3000 & X=5000; RunS5 X=5000). However, in places where there are large differences in cross-section shape between the two, the coefficient of determination is lower (e.g. RunS4, X=4250; RunS2 X=4750; RunS5 X=1500). In most cases, the deviation between the measured and simulated flow depths is very small unless there is significant change in bed elevation, especially when the section is simple and without channel bars. At locations where there is a change in bed elevation, there appears a sudden increase or decrease in flow depth (see sections RunS2X=4750; RunS3X=4500; RunS4, X=4250 & X=5000). This suggests that the main element triggering the changes in predicted and simulated flow depth values is the difference between the bed elevations of the DEM extracted and measured channel cross-sections. The correspondence between modelled and observed flow depth values is perhaps weaker in aggradation runs than in degradation runs. This probably reflected the greater complexity of flow patterns due to the formation of a number of shallower and narrower channels everywhere. The modelled water surface elevation does not appear to be constant across most of the sections, although it typically varies by only a few millimetres and appears exaggerated by the vertical scaling used in the figures. Moreover, maximum lateral water surface slopes are in the same order of magnitude as the average longitudinal bed slope, which is plausible. This lateral variability in water surface elevation is probably the result of the shallow flows, high Froude numbers and high form roughness of the bed topography.

Figure 7-7 shows the simulated flow depths within the flume channels for the various experimental conditions. During experiments with sediment feed, it can be seen that a number of smaller channels were formed throughout the flume and there is an increase in the area of more uniform and shallow flow.

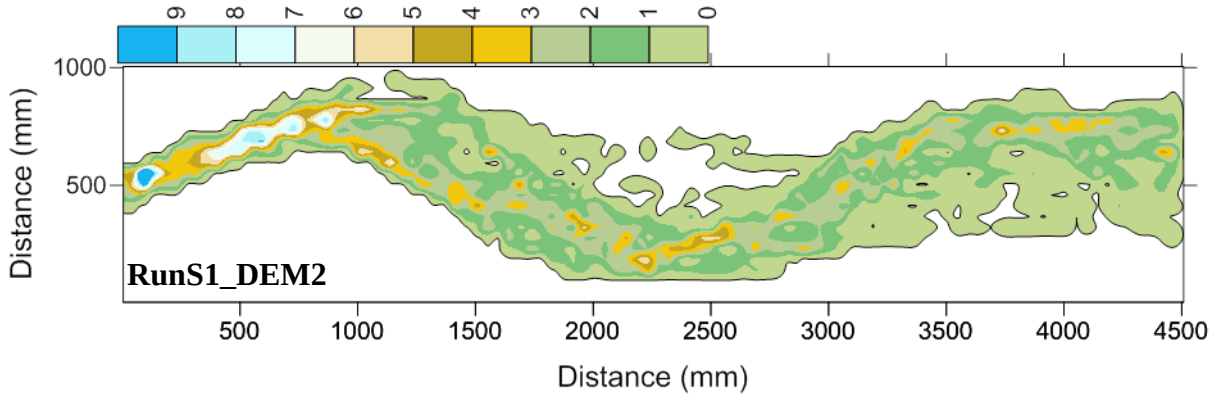
9 8 7 6 5 4 3 2 1 0
1000
500
Distance (mm)
RunS1_DEM2
500 1000 1500 2000 2500 3000 3500 4000 4500
Distance (mm)

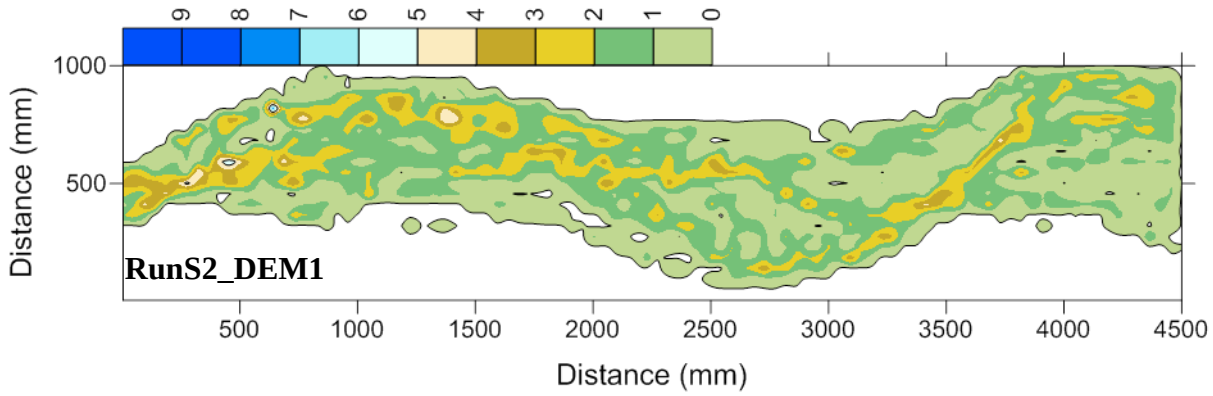
9 8 7 6 5 4 3 2 1 0
1000
500
Distance (mm)
RunS2_DEM1
500 1000 1500 2000 2500 3000 3500 4000 4500
Distance (mm)

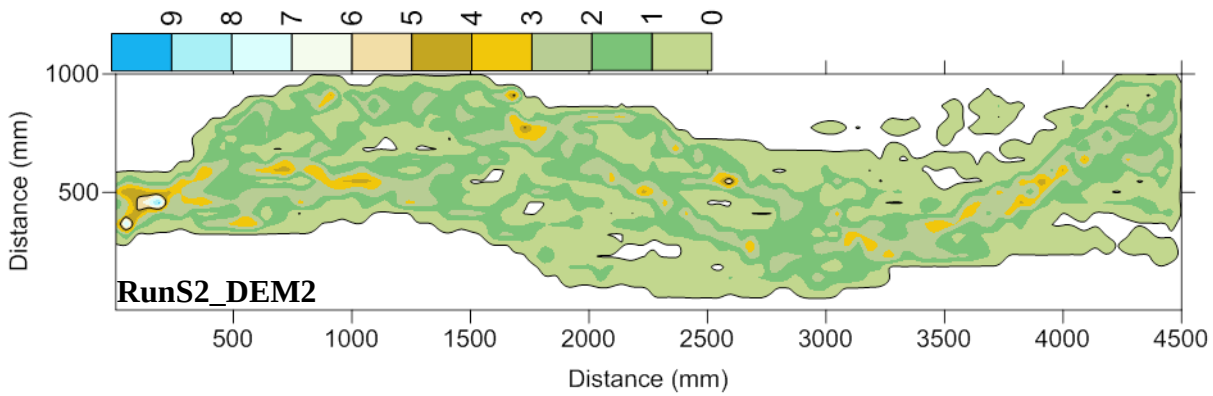
9 8 7 6 5 4 3 2 1 0
1000
500
Distance (mm)
RunS2_DEM2
500 1000 1500 2000 2500 3000 3500 4000 4500
Distance (mm)

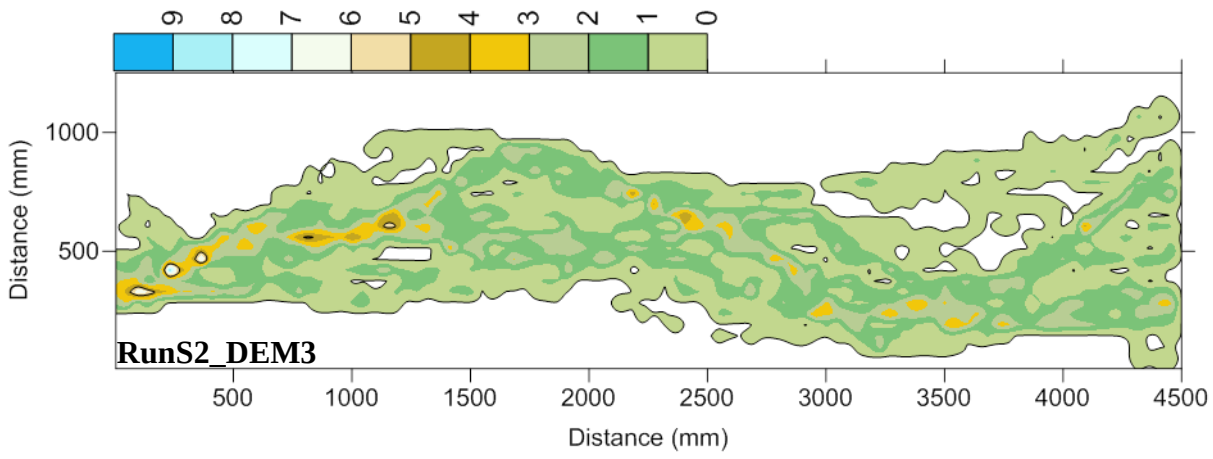
9 8 7 6 5 4 3 2 1 0
1000
500
Distance (mm)
RunS2_DEM3
500 1000 1500 2000 2500 3000 3500 4000 4500
Distance (mm)

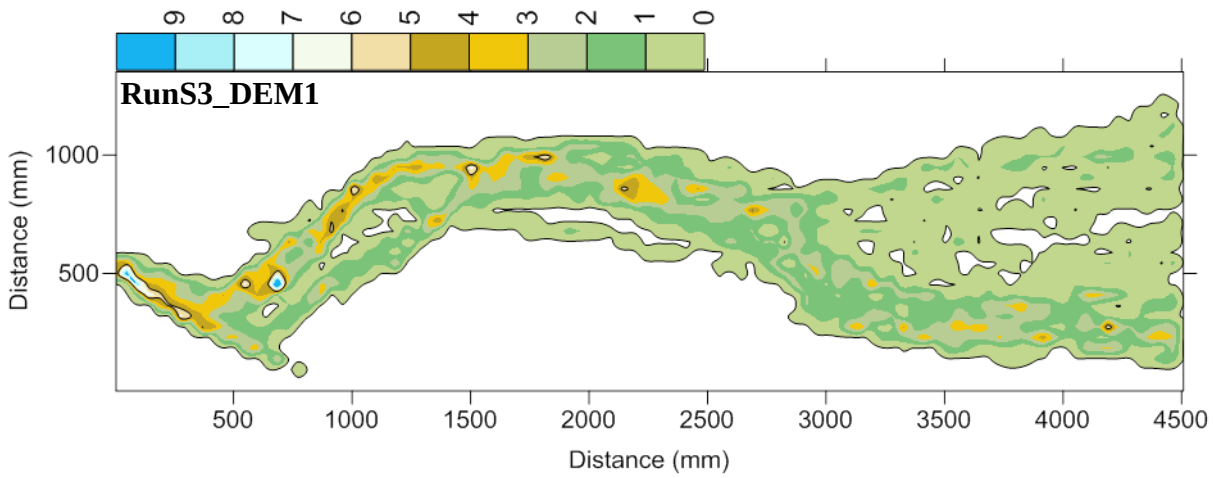
9 8 7 6 5 4 3 2 1 0
RunS3_DEM1
Distance (mm)
1000
500
500 1000 1500 2000 2500 3000 3500 4000 4500
Distance (mm)

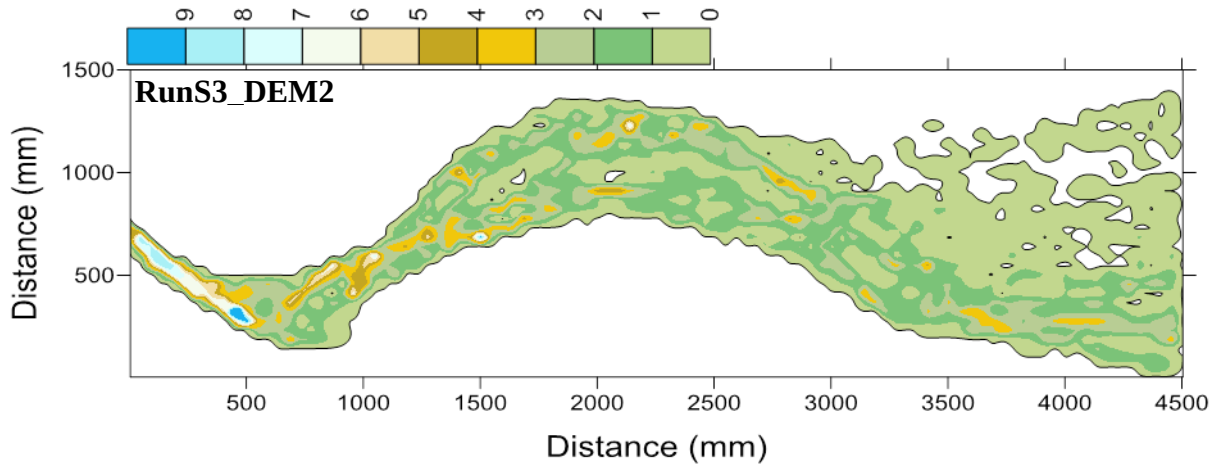
9 8 7 6 5 4 3 2 1 0
RunS3_DEM2
Distance (mm)
1500
1000
500
500 1000 1500 2000 2500 3000 3500 4000 4500
Distance (mm)

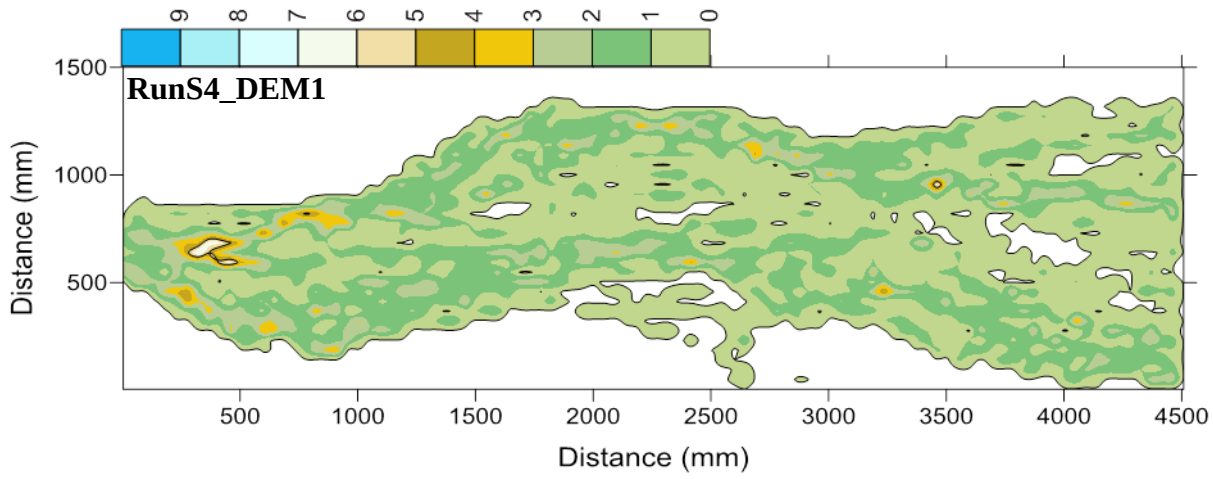
9 8 7 6 5 4 3 2 1 0
RunS4_DEM1
Distance (mm)
1500
1000
500
500 1000 1500 2000 2500 3000 3500 4000 4500
Distance (mm)

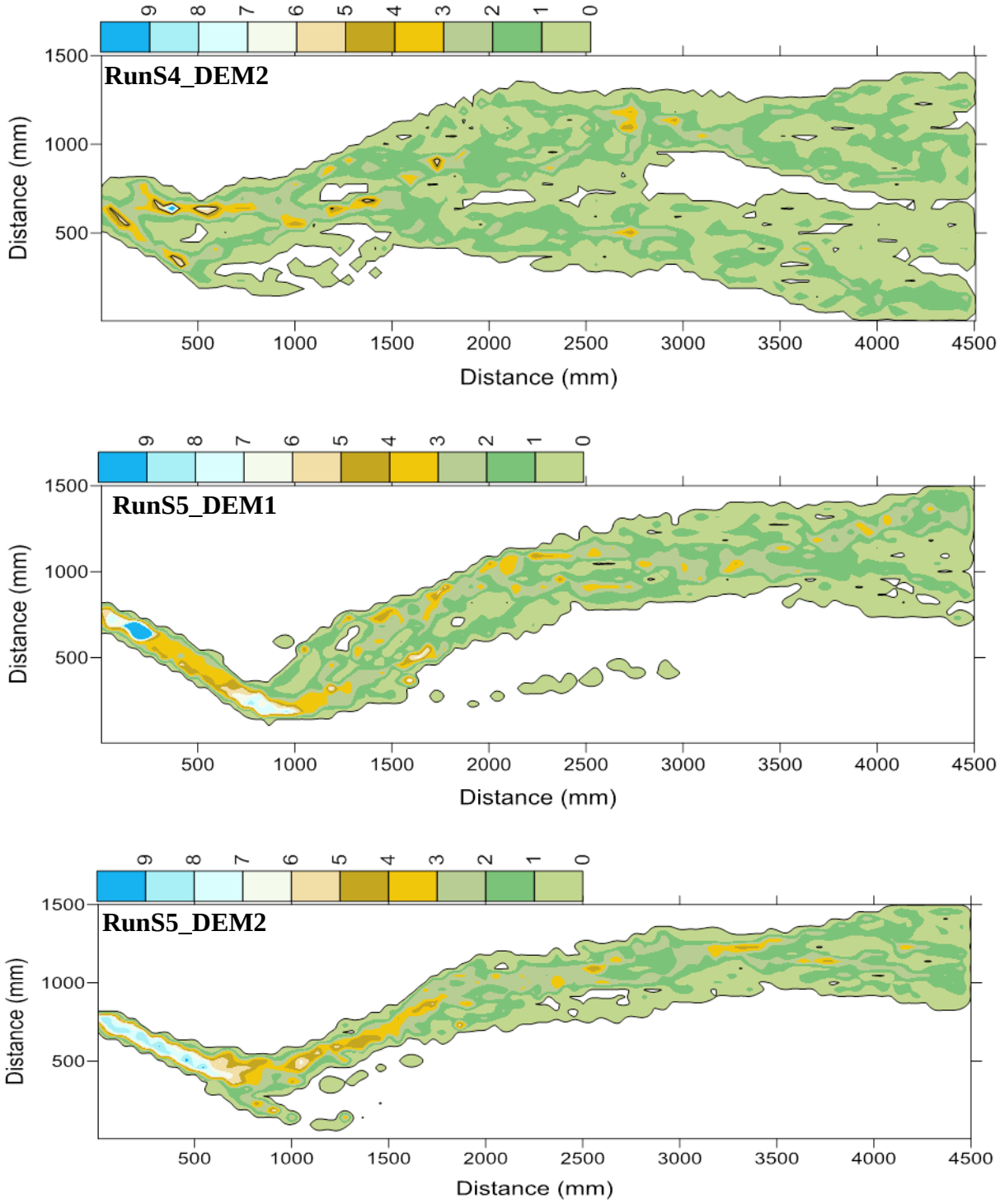


**Figure 7-7 Simulated patterns of flow depth for the experimental runs. In the depth scale above each figure flow depth is represented in mm. (difference in vertical scale indicates the surveyed extent as the channel braids.)**

It is evident from Figure 7-7 and Figure 7-8 that highly braided and wide sedimentation zones are associated with experiments with sediment feed whereas the narrow and single thread channels are produced when the sediment feed has ceased. At the

beginning of the simulation (RunS1_DEM2 in Figure 7-7 and 7.8), as suggested in chapter 5, the channel upstream tends to become single threaded with flow confined to the central portion of the channel, whilst the downstream section of the channel remains braided. After the start of the sediment feed in RunS2, it can be seen that an irregular braided pattern starts to be developed and this irregular pattern remains for the whole duration of RunS2. Since there was no change in other boundary conditions in the experiment, it is clear that this change in channel pattern is entirely a result of more sediment supply to the channel system. The channel has again evolved to become narrow and less braided in upstream areas while remaining braided in the downstream section in RunS3, but not as highly braided as in the case of RunS2. The channel continues to evolve and in RunS4 it has reached maximum braided state. As stated in chapter 5, the development of a mid-channel bar is also evident from the plot of RunS4_DEM2. In the same plot, it is also clear that the upstream part of the channel is distinctly narrow where flow is concentrated in one or two channels, whereas the downstream part of the channel is highly braided. In RunS5 the channel has evolved into a narrow, low sinuosity and less braided channel. Most parts of the channel were transformed towards a single thread with flow confined to only one channel.

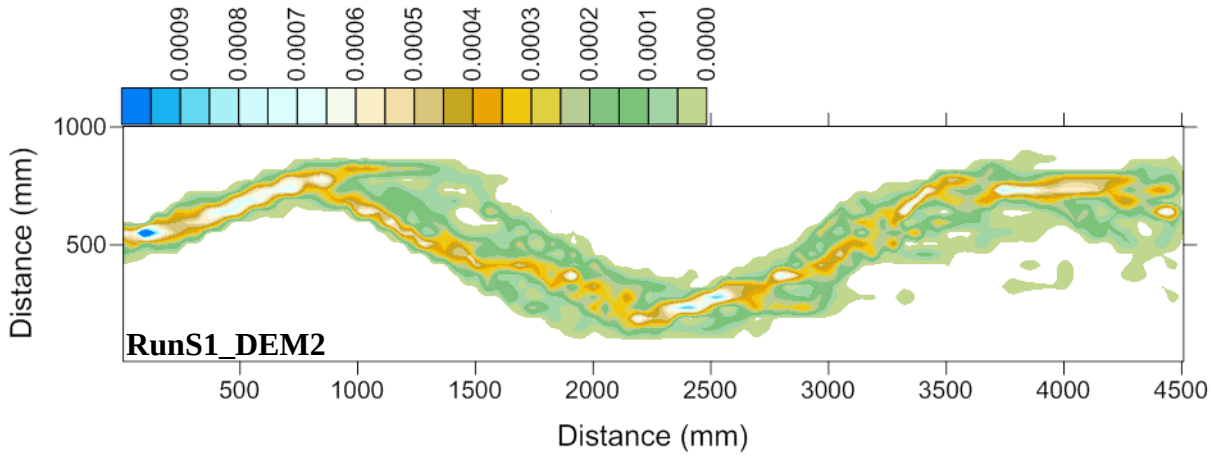

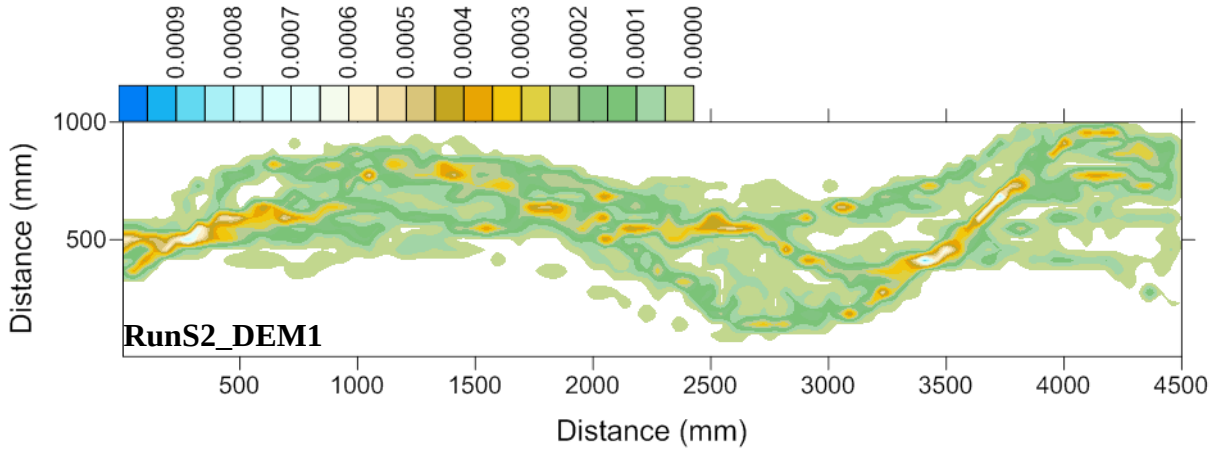
0.0009
0.0008
0.0007
0.0006
0.0005
0.0004
0.0003
0.0002
0.0001
0.0000
Distance (mm)
1000
500
RunS2_DEM1
500
1000
1500
2000
2500
3000
3500
4000
4500
Distance (mm)

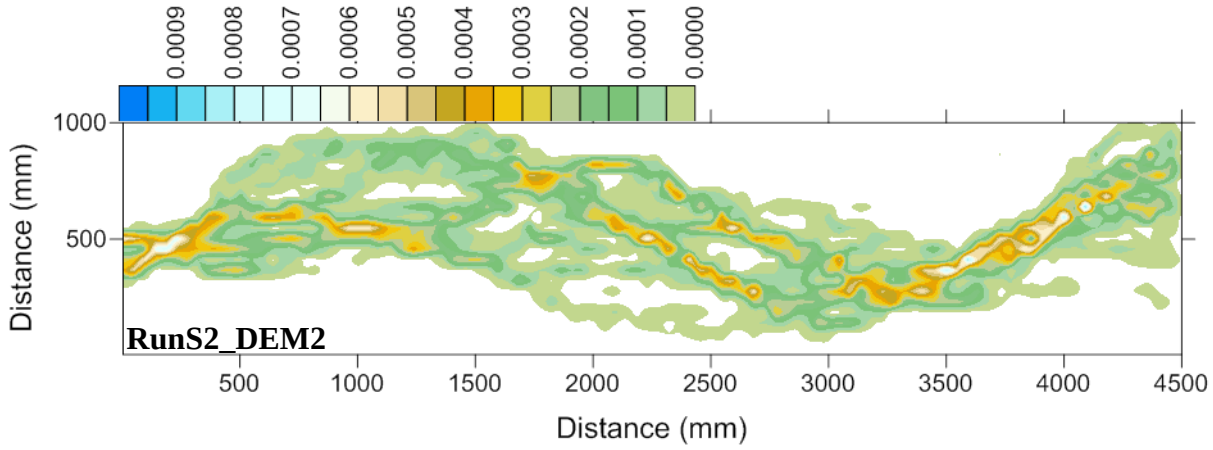
0.0009
0.0008
0.0007
0.0006
0.0005
0.0004
0.0003
0.0002
0.0001
0.0000
Distance (mm)
1000
500
RunS2_DEM2
500
1000
1500
2000
2500
3000
3500
4000
4500
Distance (mm)

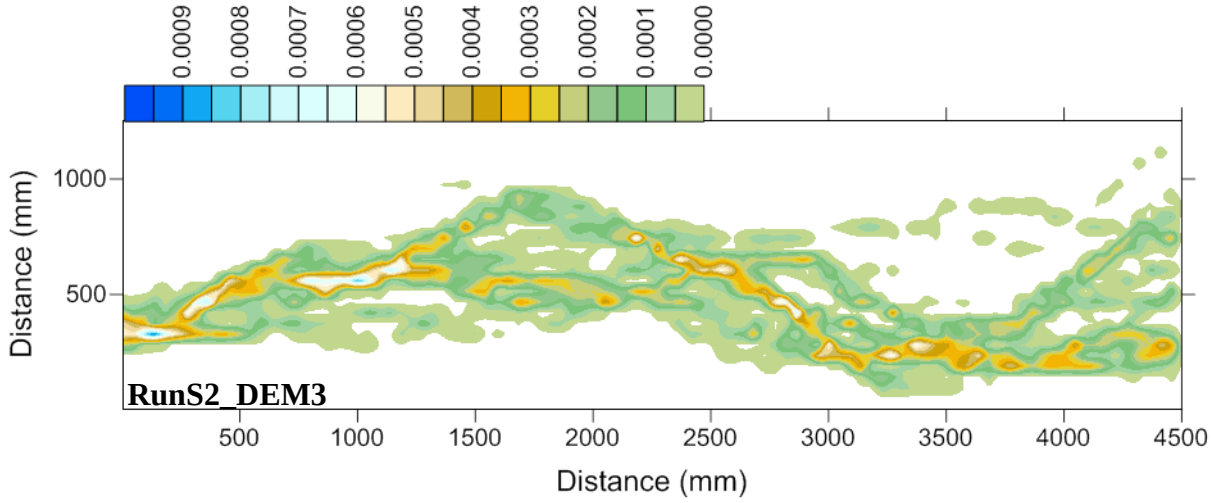
0.0009
0.0008
0.0007
0.0006
0.0005
0.0004
0.0003
0.0002
0.0001
0.0000
Distance (mm)
1000
500
RunS2_DEM3
500
1000
1500
2000
2500
3000
3500
4000
4500
Distance (mm)

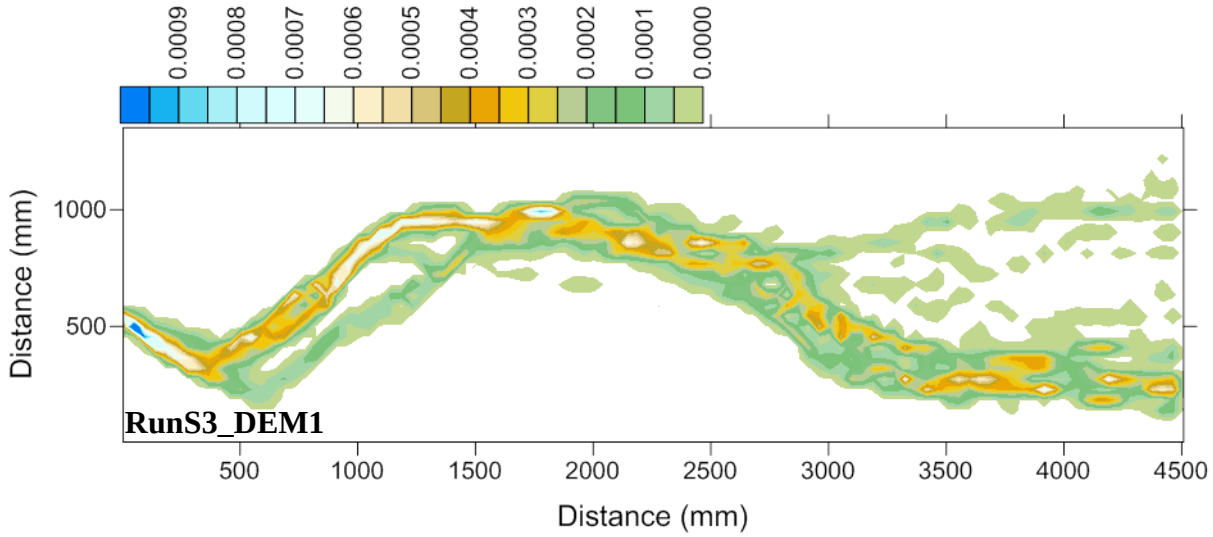
0.0009
0.0008
0.0007
0.0006
0.0005
0.0004
0.0003
0.0002
0.0001
0.0000
Distance (mm)
1000
500
RunS3_DEM1
500
1000
1500
2000
2500
3000
3500
4000
4500
Distance (mm)

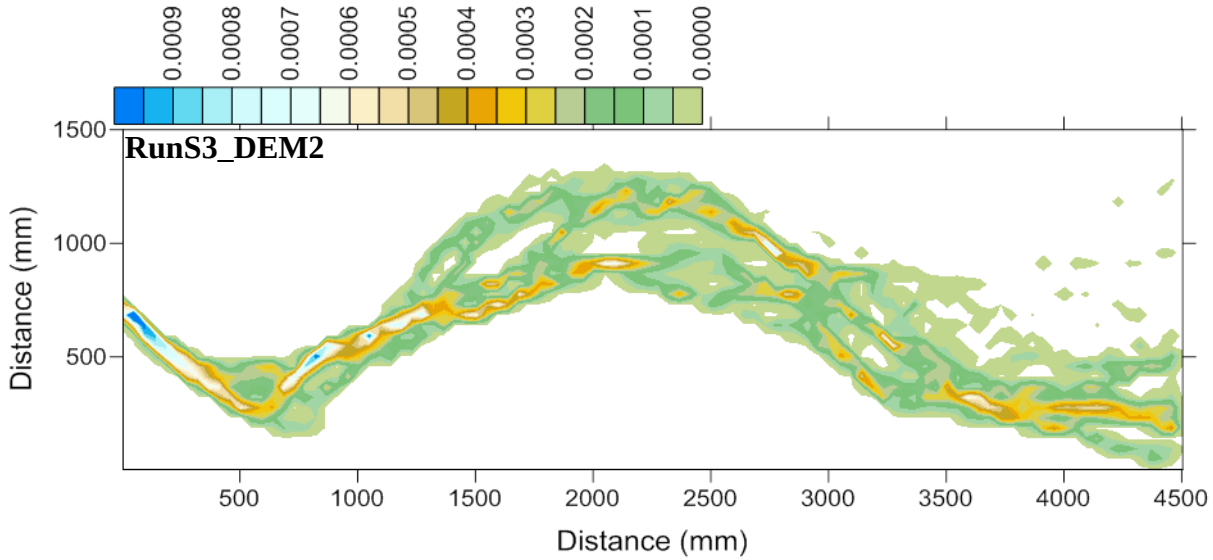
0.0009
0.0008
0.0007
0.0006
0.0005
0.0004
0.0003
0.0002
0.0001
0.0000
1500
RunS3_DEM2
Distance (mm)
1000
500
500
1000
1500
2000
2500
3000
3500
4000
4500
Distance (mm)

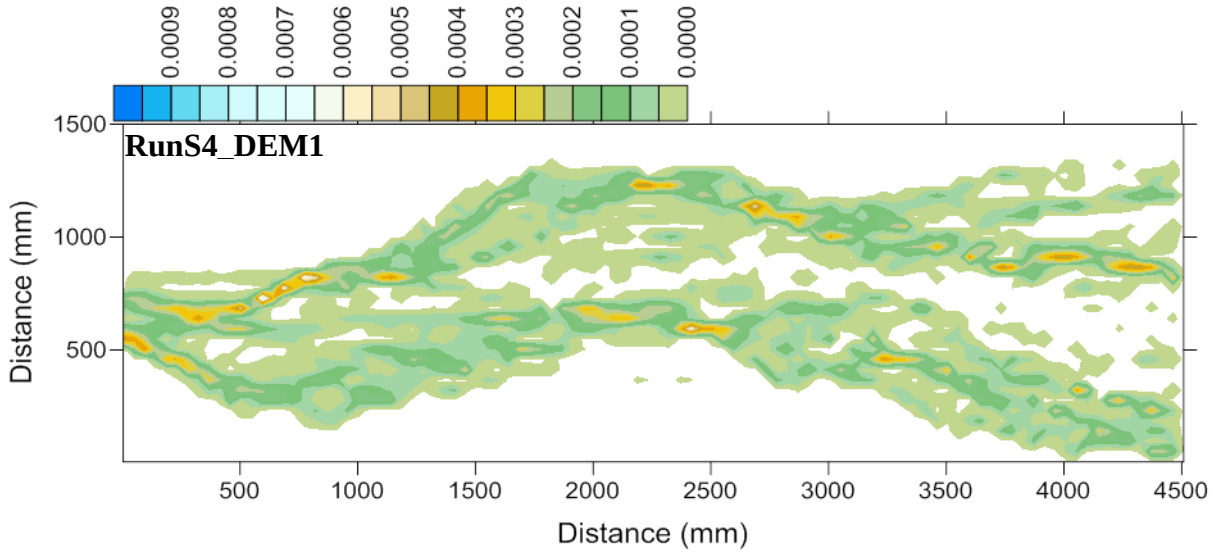
0.0009
0.0008
0.0007
0.0006
0.0005
0.0004
0.0003
0.0002
0.0001
0.0000
1500
RunS4_DEM1
Distance (mm)
1000
500
500
1000
1500
2000
2500
3000
3500
4000
4500
Distance (mm)

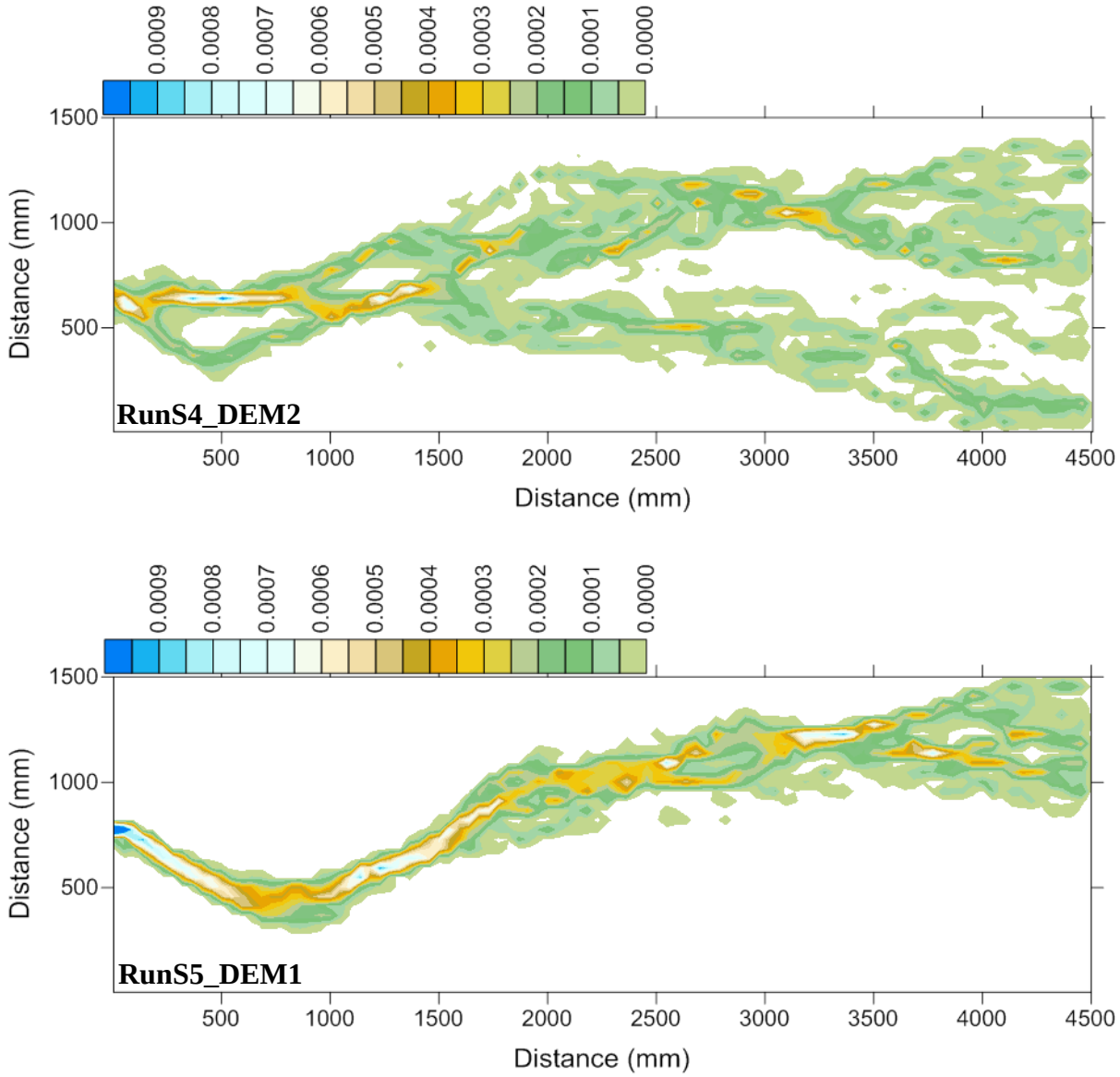


**Figure 7-8 Simulated patterns of unit discharge for the experimental runs. Unit discharge scale found above each figure is represented by $m^2/s$.**

Figure 7-9 shows the total water surface width determined from the experimental channels taken towards the end of each experiment. It is clear that in the upstream part of the channel, flow was confined and total water surface width is much smaller in degradation runs than aggradation runs. However, in the downstream parts of the flume, a number of smaller and shallower channels were formed in almost all runs and the difference in total water surface width between the aggradation and degradation runs is not as large as in the upstream part of the flume. An attempt was made to compare measured and simulated water surface width, although the shallow flows made identification of dry areas and areas with flowing water difficult. Consequently, the total

water surface width calculated by assuming constant water surface elevation is compared with the total water surface width obtained from the two-dimensional hydraulic model. Figure 7-10 shows the comparison between flume and model water surface width. Generally the fit between flume and model water surface width is good, especially in terms of the downstream trend and average widths for different runs. However, there are some large differences particularly for the case of RunS2 and RunS4. This is probably due to the fact that a number of smaller and shallower channels were formed during experiments with sediment feed (RunS2 and RunS4) that further complicates the constant water level assumption. Consequently, channels that do not convey water may be included in the calculation of the total water surface width, although some refinement was carried out to rectify this error. The photos in chapter 5 (Figure 5.8) are also indicative of the fact that flow width in the flume does not fluctuate in the way that it does in some graphs (e.g., in RunS2). Table 7-3 shows a statistical comparison of flume and model water surface widths.

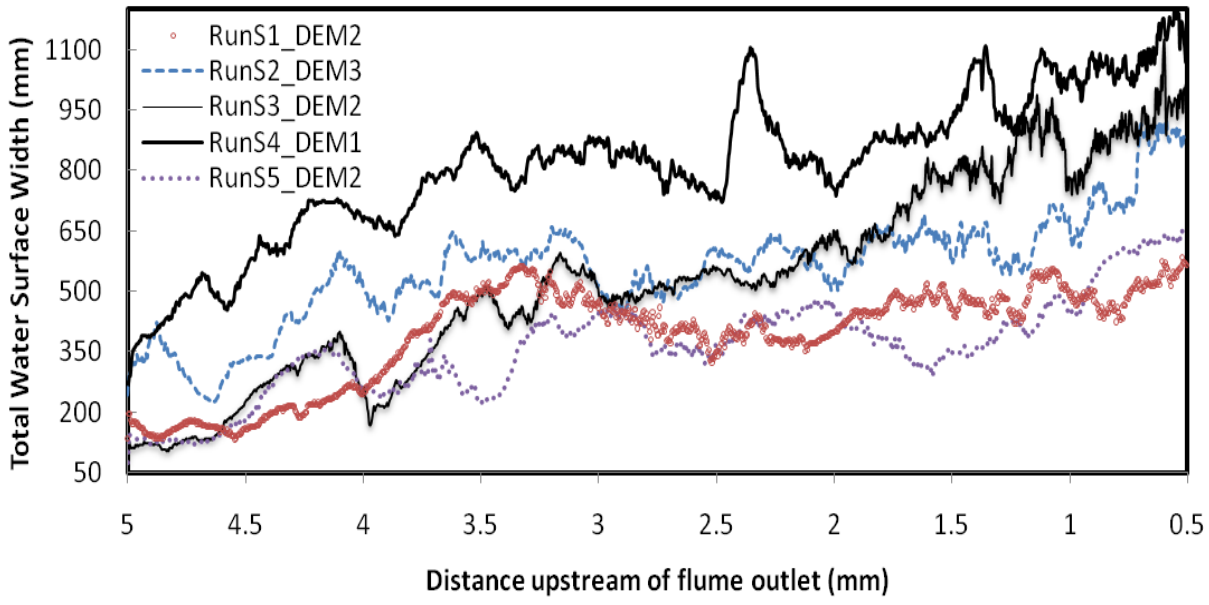


**Figure 7-9 Total simulated water surface width at the end of each experiment.**

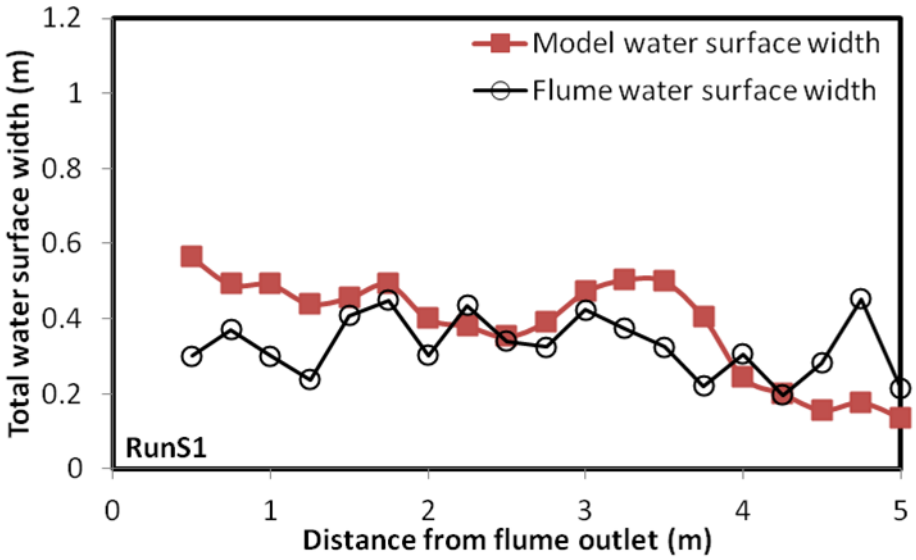
Model water surface width
Flume water surface width
Total water surface width (m)
RunS1
Distance from flume outlet (m)

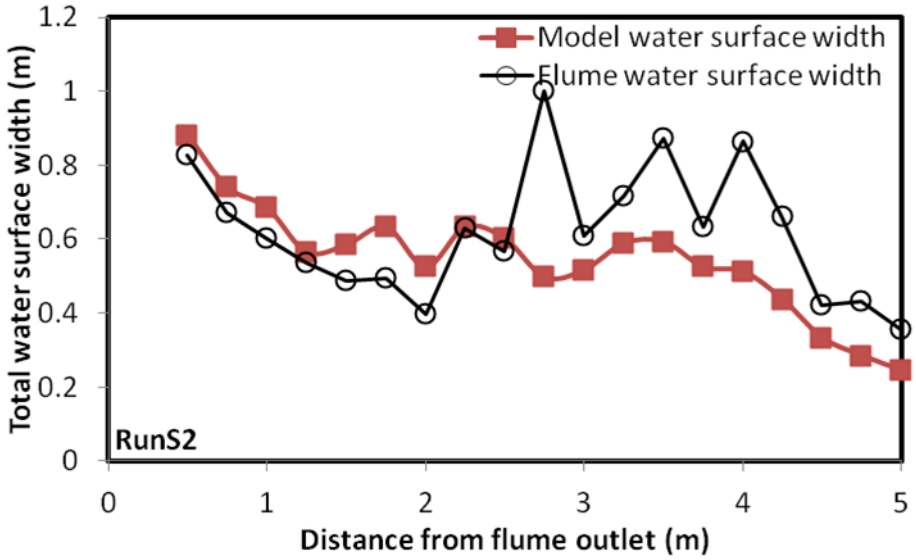
Model water surface width
Flume water surface width
Total water surface width (m)
RunS2
Distance from flume outlet (m)

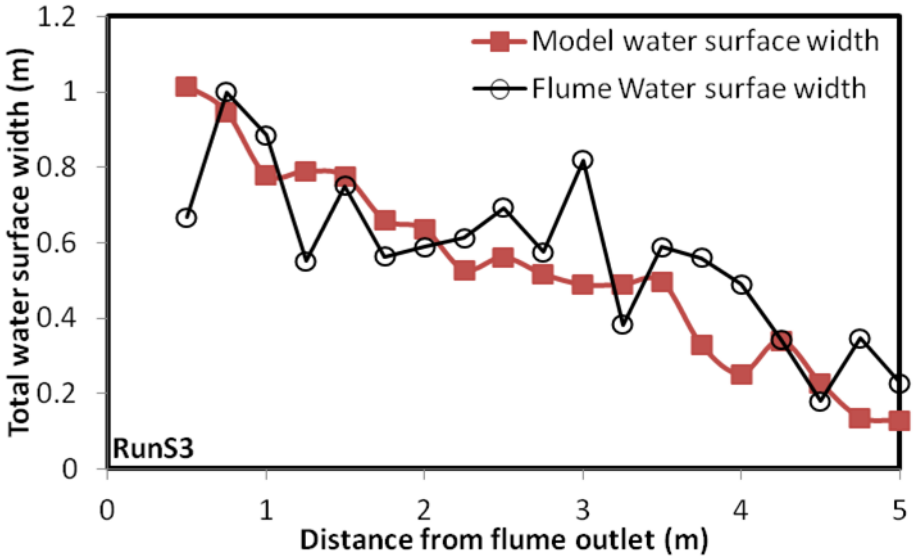
Model water surface width
Flume Water surfae width
Total water surface width (m)
RunS3
Distance from flume outlet (m)

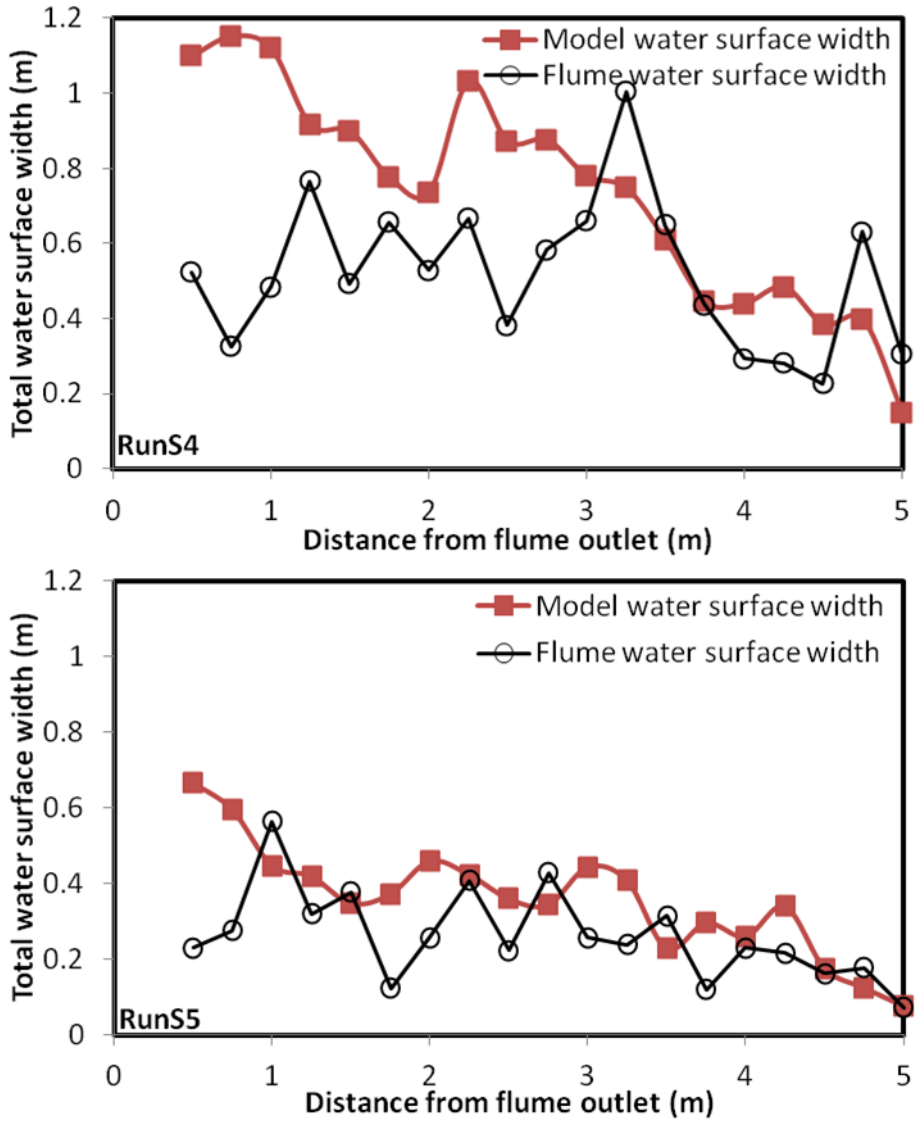


Figure 7-10 Comparison of flume and model total water surface width

Table 7-3 Statistical comparison of flume and model water surface width (WSW)

| Experiments | | Flume WSW | Model WSW |
|---|---|---|---|
| RunS1 | Mean | 0.32 | 0.38 |
| | SD | 0.08 | 0.13 |
| RunS2 | Mean | 0.62 | 0.55 |
| | SD | 0.18 | 0.15 |
| RunS3 | Mean | 0.57 | 0.53 |
| | SD | 0.21 | 0.26 |
| RunS4 | Mean | 0.52 | 0.73 |
| | SD | 0.19 | 0.28 |
| RunS5 | Mean | 0.26 | 0.35 |
| | SD | 0.12 | 0.15 |

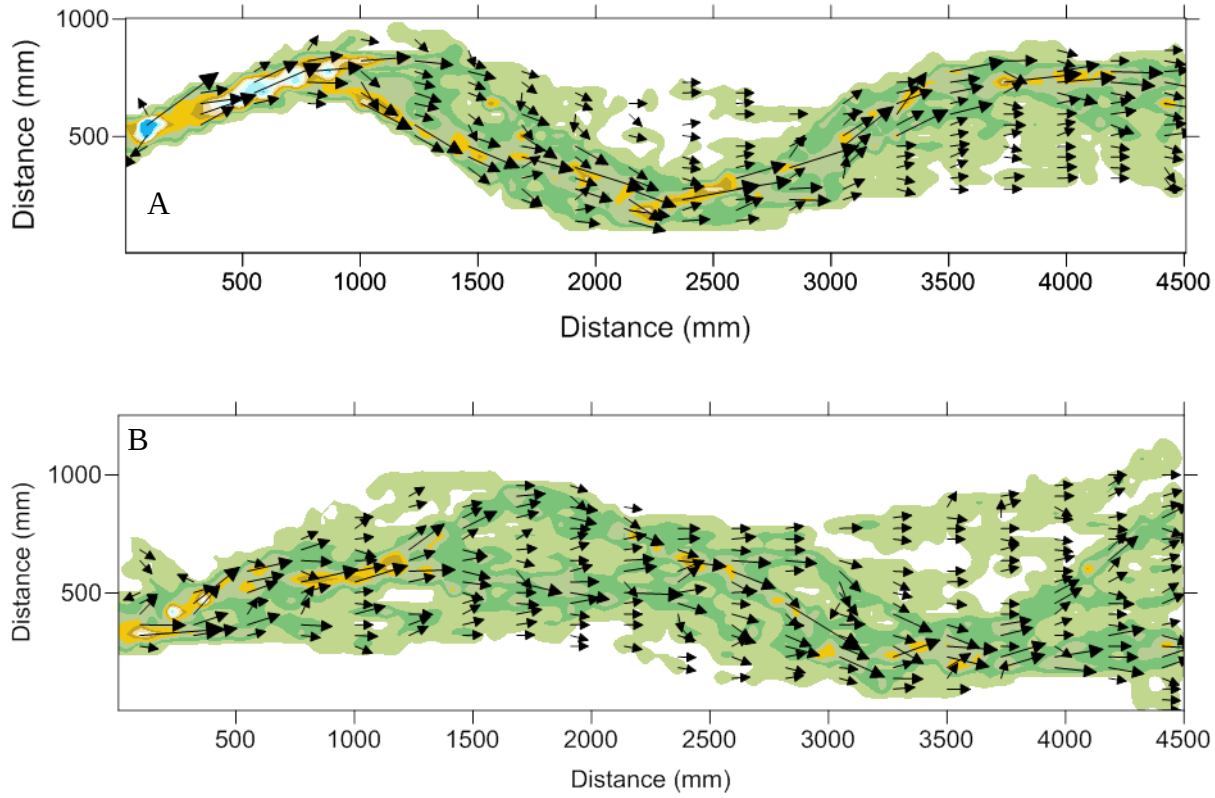


**Figure 7-11 Unit discharge vectors for RunS1, maximum unit discharge 0.0033 m2/s (A) and RunS2, maximum unit discharge 0.0013 m2/s (B); Shading corresponds to depth solutions and arrow corresponds to unit discharge vectors. Vectors scaled based on magnitude.**

The issues highlighted by Figure 7-7 and Figure 7-8 are further illustrated by the unit discharge vector distributions shown in Figure 7-11 (A and B). It can be seen that flow is split into a number of smaller flow channels for RunS2 whereas flow is predominantly confined into a single channel for RunS1.

Figure 7-12 shows the relationship between measured and simulated average water surface elevations over the entire experiment. The diagram illustrates that good agreement exists between the simulated and measured water surface elevation in most of the area. However, there is a consistent discrepancy in the observed and simulated water surface elevation at the flume entrance when the channel is degrading. This can be attributed to different factors. It is shown in chapter 5 that the upstream part of the channel actively degraded when the sediment feed ceased. During this period of intensive degradation, channel banks in the upstream part of the flume were rather vertical and steep. This creates a difficulty in accurate observation of the water surface

elevation using the dry and wet cross-sectional surveys and digital photographs. Moreover, in most of the cases modelled flow depths tend to be higher than measured flow depths. There is also a difference in the bed elevations of the surveyed cross-sections and the sections extracted from the DEM that results in differences between measured and predicted flow depths. This effect is most acute in the upstream part of the flume (especially for the DEMs obtained when the channel is degrading) as flow was confined to a single channel. In the downstream parts of the flume, however, this effect is distributed between a number of smaller channels.

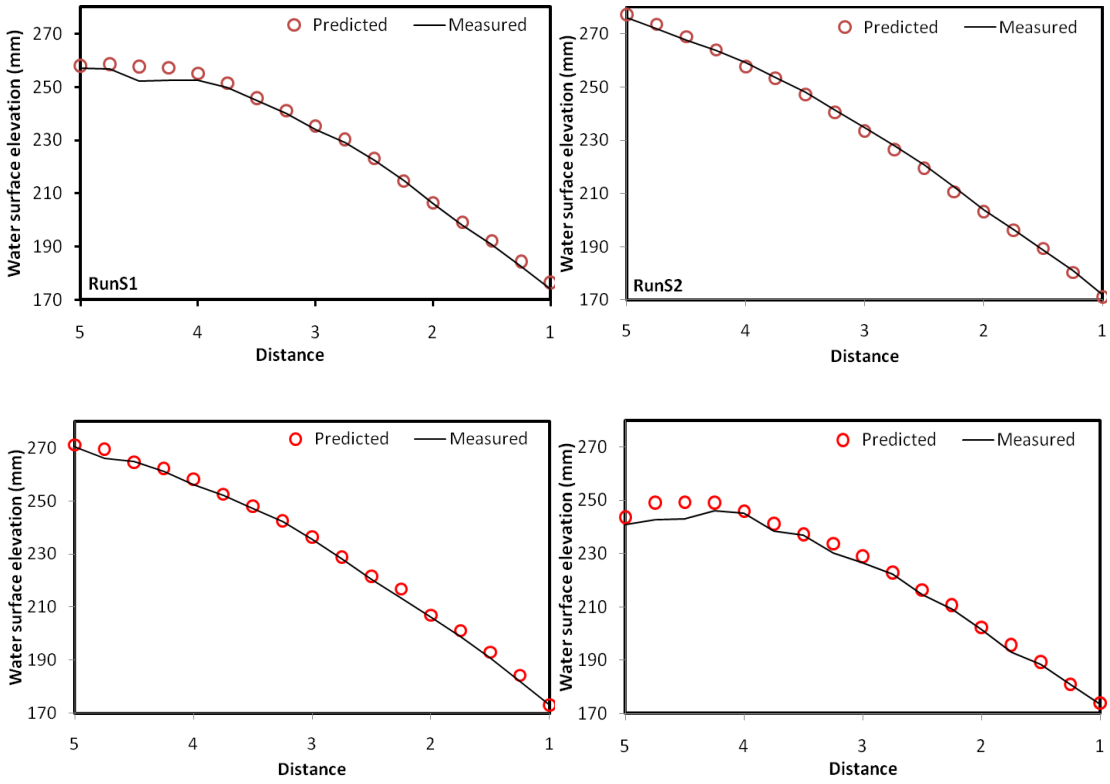


Figure 7-12 Average water surface elevation along the flume (RunS1, RunS2, RunS4, RunS5)

## 7.5. SHEAR STRESS DISTRIBUTION

The most popular method of computing shear stress in river studies is the reach-averaged bed shear stress (Babaeyan-Koopaei *et al.*, 2002), in which case, the boundary shear stress distribution is often assumed to be proportional to the local flow depth. This total boundary shear stress τ is quantified using the equation commonly referred to as ‘’the depth-slope product’’:

$$\tau = \rho g Y S_o \qquad 7\text{-}5$$

This approach also provides a means of incorporating the effects of spatial variability in shear stress if data on local flow depth estimates are present. However, the spatial variability in boundary shear stress is also a function of variability in the local energy slope (which is replaced by the mean longitudinal bed slope in equation 7-5) and by variability in roughness (Nicholas, 2000). An assessment of the importance of local variability in energy slope in shear stress prediction can be made using the results of the two-dimensional hydraulic model simulations. In fact, Figure 7-2 to Figure 7-6 show significant spatial variability in local flow depth that in turn may result in variability in local energy slope. This suggests that equation 7-5 may not provide reliable point estimates of local boundary shear stress. However, as extremes of flow depth are compensated by local energy slope (high flow depth with low energy slope as in scour pools, and low flow depth with high energy slope as in bar margins) (Nicholas, 2000), these local variations may average and the depth-slope product may remain a useful tool for examining shear stress distributions in rivers.

In the two-dimensional hydraulic model applied in this study, the shear stress is calculated using equations 7.6-7.8:

$$\tau_y = 9810 \left({q_x}/{YC}\right)^2 \qquad 7\text{-}6$$

$$\tau_y = 9810 \left({q_y}/{YC}\right)^2 \qquad 7\text{-}7$$

$$\tau = \sqrt{{\tau_x}^2 + {\tau_y}^2} \qquad 7\text{-}8$$

Where in the above equation $\tau_x$ and $\tau_y$ are bed shear stress in the x and y direction and $q_x$ and $q_y$ are unit discharge in x and y direction, Y is flow depth and C is the Chezy roughness coefficient.

A comparison of the shear stress frequency distributions derived using the two-dimensional hydraulic model with those estimated using the 1D reach averaged equation (equation 7.5) using model predicted flow depth is carried out here and results are plotted in Figure 7-13. The longitudinal profile of the channel clearly shows that the profile does not have a constant slope throughout. Consequently, in calculating the reach averaged shear stress the local bed slope obtained by dividing the whole reach

into a number of sections is used. In this case, the shear stress calculated using the two approaches at different cross sections is merged together to depict the overall differences between different runs. This is because in many cases there were significant changes in bed elevation between the measured cross-sections and cross-sections extracted from the DEMs. As a result, it will not be possible to determine if the difference in shear stress is due to differences in topography or variability in energy slope. Despite this, some sections exhibit no significant differences in bed elevation. Shear stress distributions at these locations will be considered later.

The results in Figure 7-13 are consistent for all runs. The overall mean shear stresses are roughly comparable implying that a reasonable estimate of the mean shear stress can be found using the conventional reach averaged equation (equation 7.5). Since local shear stress varies across a section, transport rates calculated using the overall mean shear stress will not equal the sum of the local transport rates, as shown in chapter 6. However, as the overall mean shear stress provides a useful index of flow strength, this comparison suggests a good level of confidence in using the reach averaged one-dimensional equation, for which data can easily be collected from cross sectional surveys. Shear stress distributions are similar in the low shear tails, except for a few runs, although this is less important as the contribution of low shear values to sediment transport and channel morphology is not significant. However, there appear to be some important differences for some runs, especially in the high shear tails. The effect of this difference in shear stress is not straightforward to determine but according to (Ferguson, 2003) the high shear discrepancies have important implications for sediment transport as bed load sediment transport increases with shear stress. Most conventional sediment transport equations use the excess shear stress $(\tau-\tau_c)^n$ as a parameter. Based on this it is likely that bed load transport will increase by an amount dependant on the relationship between $\tau$ and $\tau_c$.

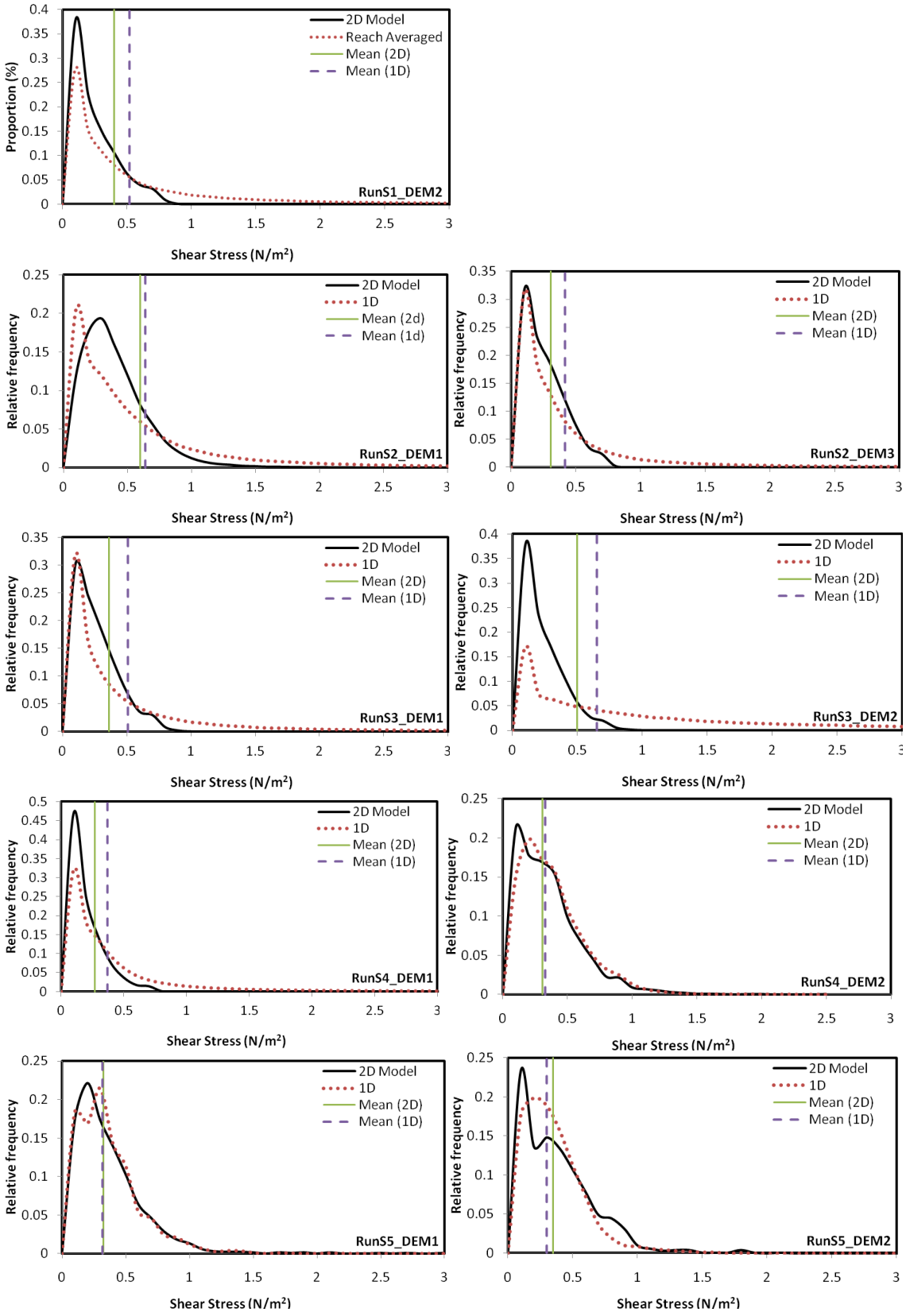


**Figure 7-13 Comparison of shear stress distribution in the experimental runs using the 1D reach averaged formulation and two-dimensional hydraulic modelling (the vertical axis indicates the relative frequency)**

To investigate the contribution of variability in local water surface slope to variability in boundary shear stress, cross-sections are considered below where the measured and DEM extracted sections have no notable differences in bed elevation (there still exist some differences in bed elevation although they are small). The cross-sections below are complex with substantial local variability in water surface elevation making them suitable for examining the influence of variability in local water surface slope on shear stress prediction.

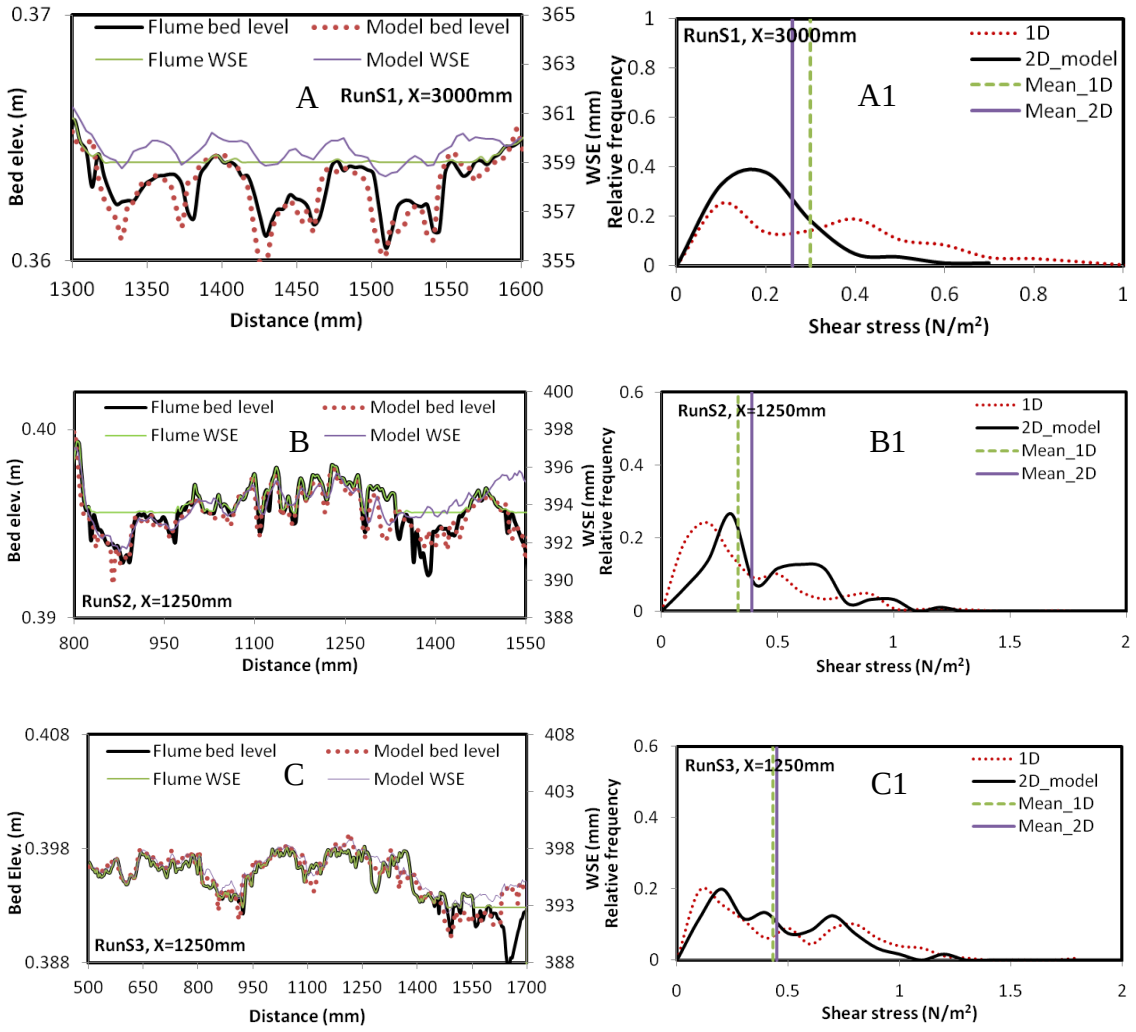

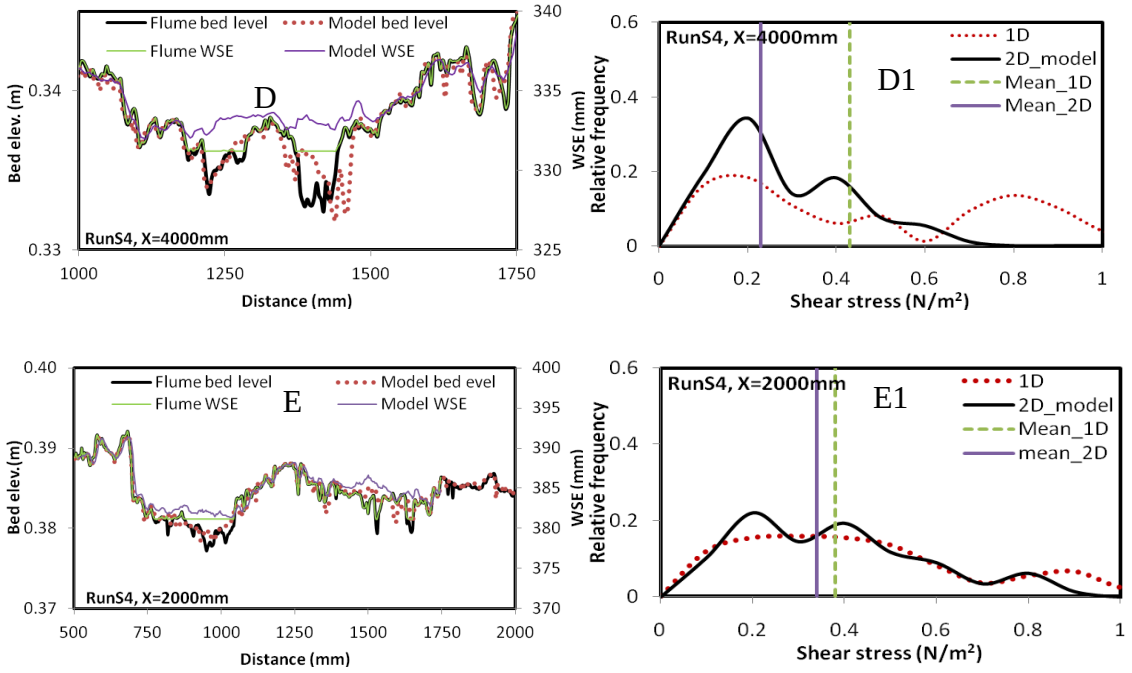


**Figure 7-14 Comparison of measured and modelled shear stress for matching cross sections**

Despite substantial variation in local water surface elevation in most of the sections, the boundary shear stress distribution determined using local depths and mean channel slope yielded a mean within 10% of that determined for the same data using local predictions of both depth and energy slope except for the case of Figure 7-14D. The variance of the modelled shear stress distribution, however, shows significant variation in some cases as compared to that calculated for the mean channel slope. There are still some differences in bed elevation of these channel cross-sections. The advantage of allowing for variable water surface slope in calculating shear stress and then sediment transport is less important in perennial gravel bed streams, although it is important in arid zones where floods are flashy (Meirovich *et al.*, 1998). Moreover, sediment transport rate may range over several orders of magnitude at any given level of shear stress (Reid and Laronne, 1995), which indicates the fact that there is considerable uncertainty in bedload prediction as a result of the combined influence of a number of factors that more than match any effects brought about by relatively smaller changes in water surface slope (Meirovich *et al.*, 1998). Table 7-4 shows a statistical comparison of shear stress predicted using measured and two-dimensional modelled flow parameters.

Some uncertainty exists in the accuracy of shear stresses determined using equations 7-6 to 7-8. Reasons for this can be attributed to poor process representation inherent in

such a depth-averaged approach (depth averaging of a three-dimensional flow field) and spatial variation of relative roughness due to variations in flow depth and bed sediment size (Lane *et al.*, 1999), although the latter has been shown to have limited effect in this case. Despite the limitations in the two-dimensional flow modelling, the overall trend between the shear stresses computed using the two approaches suggests that the two-dimensional modelling approach has considerable potential as a tool for quantifying the reach scale hydraulic characteristics of braided rivers.

**Table 7-4 Calculated values of mean and standard deviation (SD) of shear stresses predicted using measured and two-dimensional modelled flow parameters (unit is in $N/m^2$). FBE and MBE refer to flume and model bed elevations.**

| | ***A*** | ***B*** | ***C*** | ***D*** | ***E*** |
|---|---|---|---|---|---|
| Mean 1D | 0.3 | 0.33 | 0.43 | 0.43 | 0.34 |
| Mean 2D | 0.34 | 0.39 | 0.45 | 0.23 | 0.38 |
| SD of τ 1D | 0.22 | 0.29 | 0.34 | 0.31 | 0.24 |
| SD of τ 2D | 0.26 | 0.23 | 0.39 | 0.15 | 0.26 |
| SD FBE (mm) | 4.9 | 3.05 | 2.18 | 9.07 | 3.1 |
| SD MBE (mm) | 4.85 | 3.0 | 2.02 | 8.99 | 2.97 |

## 7.6. FREQUENCY DISTRIBUTION OF MODELLED FLOW VARIABLES

Previous researchers have applied stochastic theories to model braided river characteristics. These studies have involved: (1) derivation of probability density functions to approximate the number of channels and their dimensions from which bedload is calculated as the sum of transport in individual channels in a cross section (Pickup and Higgins, 1979); (2) estimation of the PDF for transport rate in an individual anabranch and applying this to anabranch numbers and widths (Hoey *et al.*, 2001); (3) application of gamma PDFs of normalized shear stress or depth in a reach irrespective of the location or dimensions of particular anabranch (Ferguson, 2003;Steffler and Blackburn, 2002); and (4) application of a uniform distribution function to model the

effect of cross-sectional variance in shear stress in sediment transport calculations (Ferguson, 2003).

In this study the patterns of modelled normalized shear stress are examined by applying the gamma probability density function. The gamma probability density function is determined by fitting distributed patterns of hydraulic parameters (in this case shear stress) to an equation of the form (equation7-9). The resulting PDF is described by a shape parameter (α), which is an indicator of the width of the stress distribution:

$$\mathbf{f(\tau_o; \alpha, \beta) = \frac{\alpha^{\alpha} \tau_*^{\alpha-1} e^{-\tau_*/\beta}}{\beta^{\alpha} \Gamma(\alpha)}} \qquad \mathbf{7\text{-}9}$$

where $\tau^*=\tau_o/\tau$ (local stress non-dimensionalised by the mean shear stress), α is the gamma distribution shape parameter (proportional to the width of the stress distribution), β is the scale parameter determined by the mean shear stress τ, and Γ (α) is the standard gamma function. Shear stress distributions obtained from the results of two dimensional hydraulic model simulations were fitted to a PDF of the form given by this equation. Modelled shear stresses from different cross-sections were merged together and the resulting dataset was normalized by the merged data average to investigate the overall fit with the gamma probability density function. Statistical parameters were calculated using equal interval (equal width) binning by splitting the whole range of data into intervals with equal size. Figure 7-15 shows examples of PDFs fitted to estimated shear stress data. It can be seen that the data fit equation 7-9 fairly well, although the modelled shear stresses contains some high shear values. However, those high shear values have relatively very low frequency. These data also indicate that the spatial variation in shear stress declined when the sediment feed was stopped and the channel degraded (the value of α is greater in runs S1, S3 and S5).

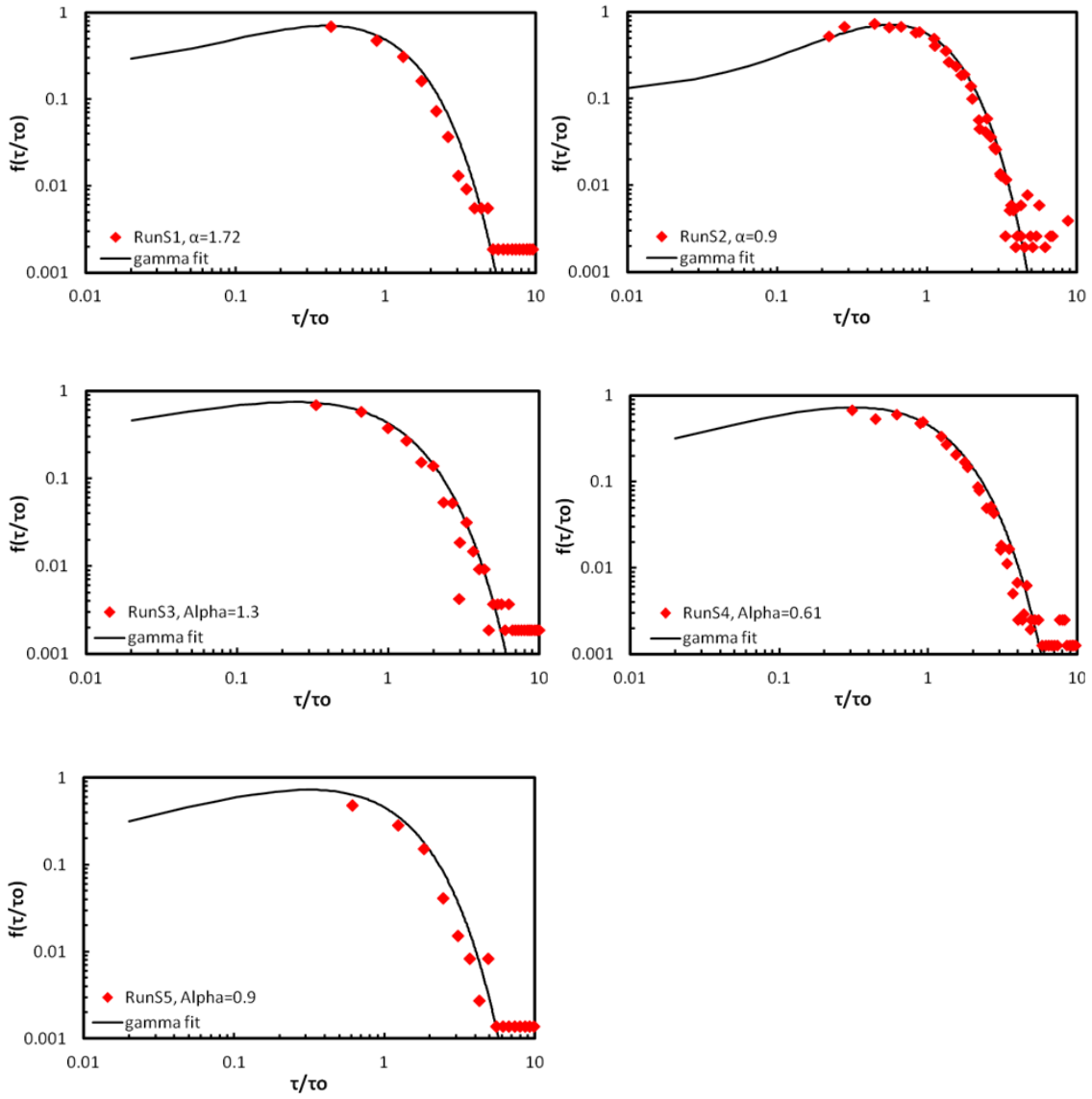


**Figure 7-15 Gamma probability density function fitted to modelled and dimensionless shear stress distribution for aggradation and degradation experiments (τ is local shear stress and τo is flume averaged shear stress in this case).**

Longitudinal trends in the shape parameter (α) determined by fitting the shear stresses obtained using the two dimensional hydraulic flow model to equation 7-9 are compared below to equivalent α values obtained using the measured local flow depth and mean water surface slope. In the two-dimensional hydraulic model, shear stress is determined using equations 7.6 to 7.8 and data for each cross section along the flume is extracted, normalized using the cross-section mean shear, and fitted to the gamma probability density function. For this comparison the data obtained at the end of each experiment is used. Results are plotted in Figure 7-16.

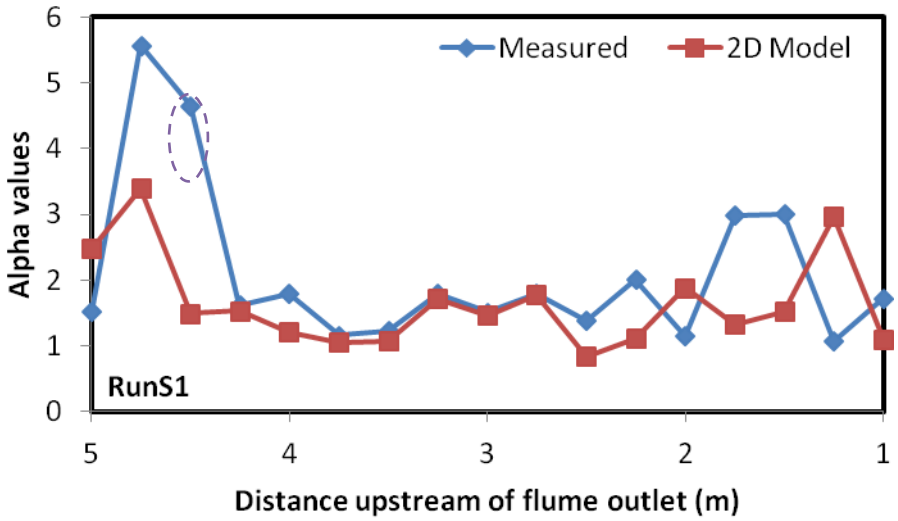
Measured
2D Model
Alpha values
RunS1
Distance upstream of flume outlet (m)

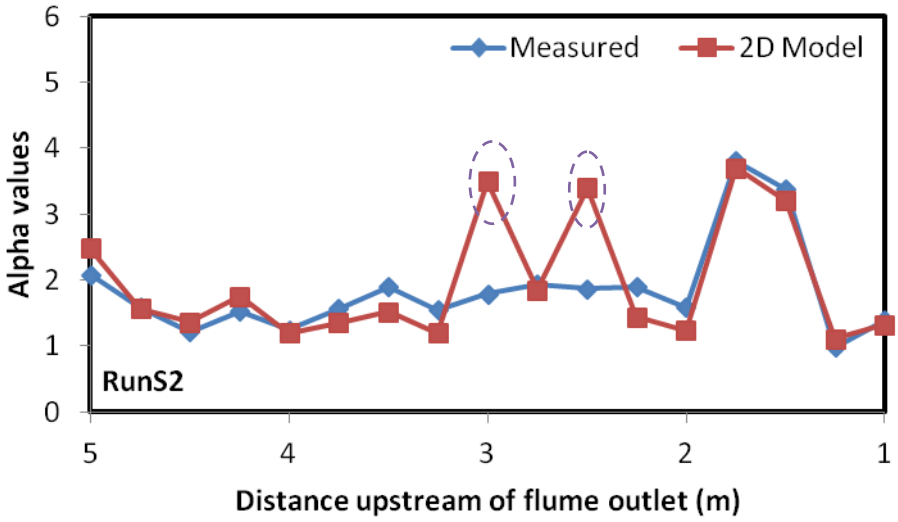
Measured
2D Model
Alpha values
RunS2
Distance upstream of flume outlet (m)

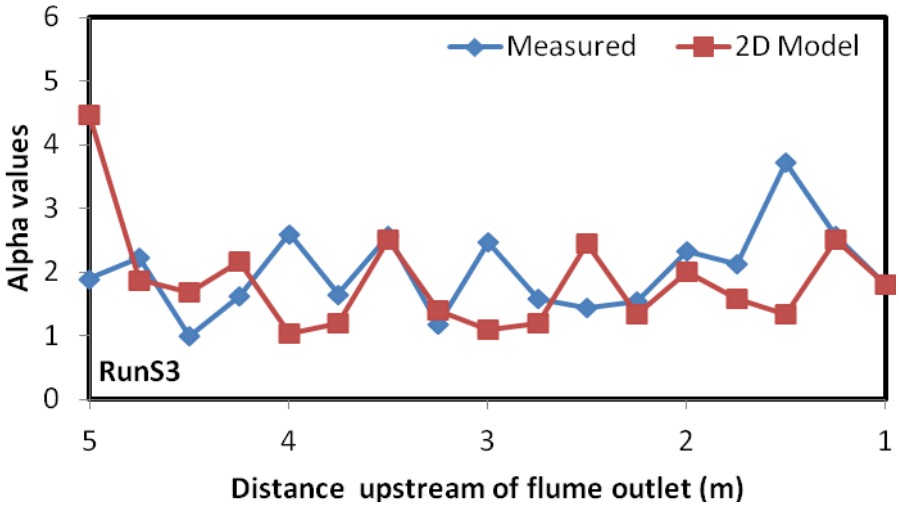
Measured
2D Model
Alpha values
RunS3
Distance upstream of flume outlet (m)

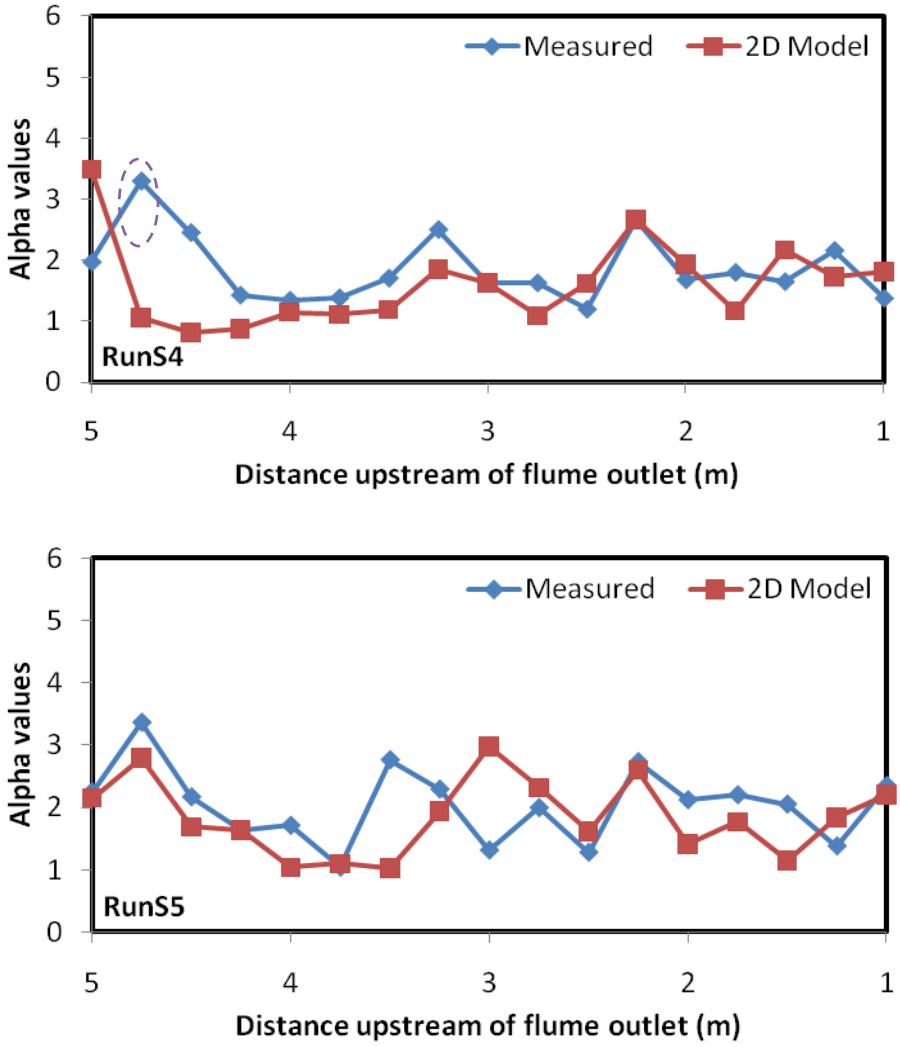


**Figure 7-16 Comparison of gamma shape parameter determined using measured and simulated data**

As expected, shape parameter values close to the flume inlet are much higher than anywhere else in the flume, although this does not appear to be true for RunS2 and to some extent for RunS5. The reason is probably, as stated in chapters 5 and 6, that degradation was greatest in the upstream part of the flume, leading to flow confinement in one or two channels and a reduction in the variance of flow depth and boundary shear stress distributions.

Table 7-5 outlines the statistical relationships between alpha values calculated using measured and simulated flow parameters. The relationship between alpha values calculated using the two approaches is slightly weaker. The coefficient of determination for alpha is considerably lower, although these relationships remain significant at the 99 percent level.

Table 7-5 Statistical comparison of measured and modelled alpha values

| | RunS1 | | RunS2 | | RunS3 | | RunS4 | | RunS5 | |
|---|---|---|---|---|---|---|---|---|---|---|
| | Measured | 2D Model | Measured | 2D Model | Measured | 2D Model | Measured | 2D Model | Measured | 2D Model |
| No. of Obs. | 17 | 17 | 17 | 17 | 17 | 17 | 17 | 17 | 17 | 17 |
| Mean | 2.11 | 2.05 | 1.83 | 2.47 | 2.01 | 1.95 | 1.87 | 1.6 | 2.03 | 1.84 |
| Std. Deviation | 1.26 | 0.7 | 0.72 | 0.33 | 0.66 | 0.84 | 0.56 | 0.69 | 0.6 | 0.6 |
| $r^2$ | 0.38 | | 0.25 | | 0.05 | | 0.11 | | 0.3 | |
| P(T<=t) | 0.18 | | 0.07 | | 0.54 | | 0.23 | | 0.34 | |

Figure 7-16 shows that the overall similarity in longitudinal pattern of alpha values determined using the two approaches is reasonable. However, notable differences are observed at some sections close to the flume inlet and mid-flume for some runs; shape parameters determined using simulated shear stresses tend to be higher in most of these cases. In the following section, these differences will be investigated for selected channel cross-sections in more detail. For example, there appears to exist significant variation between alpha values at mid-flume for RunS2 (at locations X=3m and X=2.5m from the flume outlet, as circled with a dashed line in Figure 7-16). Differences in alpha values derived using the two approaches can be attributed to a wide range of sources of error and uncertainty. One of the reason for differences in alpha values is the significant difference in flume and model cross section bed elevations (see Figure 7-17A and B). The bed topography at model cross sections appears to be drowned out, and as a result flow is confined in one big channel for both cross sections (Figure 7-17C and D) unlike the flume cross sections, where in this case flow occupies at least two channels (Figure 7-17E and F). This difference in topography has affected the distribution of flow depth patterns, especially for X=2.5m where the location of the maximum flow depth is entirely shifted (Figure 7-17G and H). Flume flow depths show greater variability with standard deviations of 1.15mm and 1.1mm (which means lower alpha) compared to 0.8mm and 0.7mm for the model flow depth at X=2.5m and 3m respectively (the variance of model flow depths is 17% and 21% lower than for the flume flow depths). There appears to be a significant difference in the mean shear stress estimated using the flume measurements and modelled flow variables, although results from the previous section (section 7.5) indicate that the mean shear stress derived from the simple depth-slope product is a reasonably reliable estimator of the true reach averaged shear stress as determined from the two-dimensional hydraulic model. In addition, the variance of the shear stress distribution was 53% and 22% lower (for X=2.5m and X=3m, respectively)

when determined using the two-dimensional hydraulic model compared to that calculated for the mean channel slope.

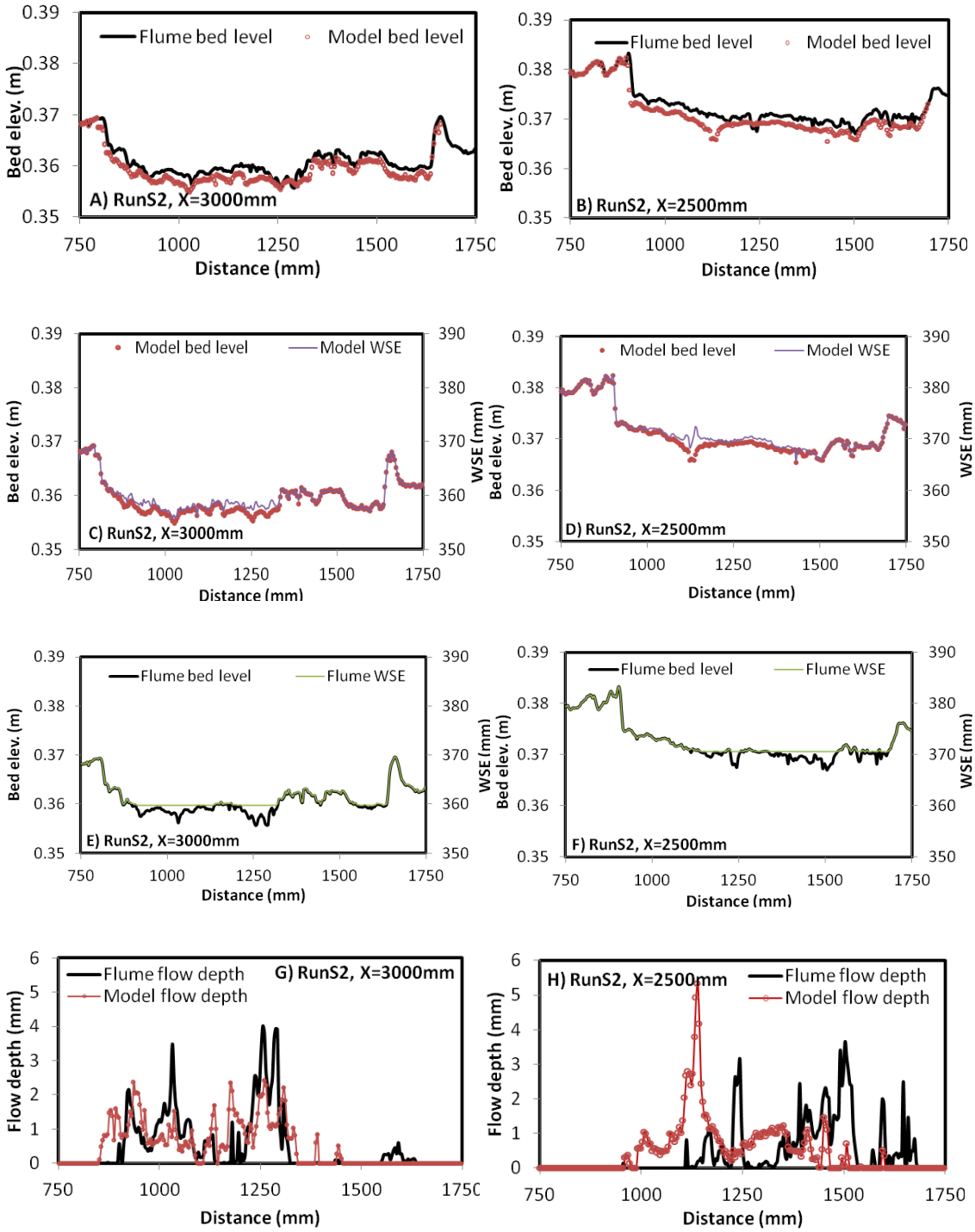

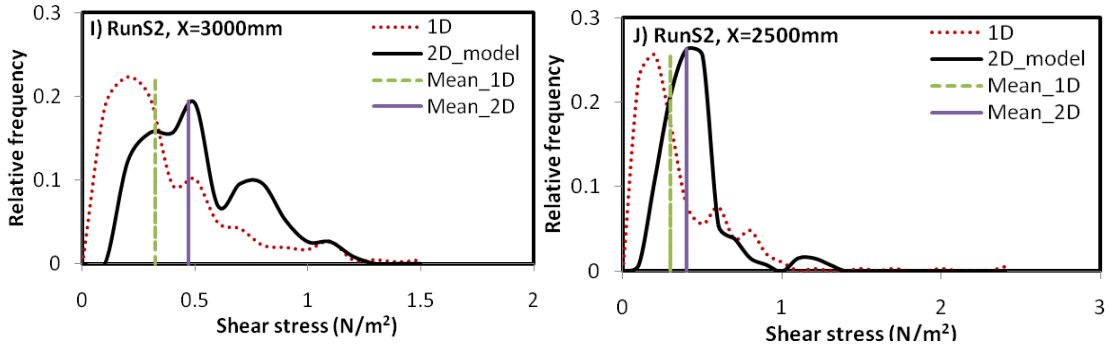


**Figure 7-17 Comparison of measured and modelled flow variables at two sections around the middle of the flume (RunS2, X=2500 & X=3000mm)**

Another significant difference between alpha values is evident at X=4500mm for RunS1 and X=4750mm for RunS4. Flume and model cross-sections do not show significant differences at X=4500mm for RunS1 (Figure 7-18A). However, model predicted flow depths are much higher than the measured flow depth (Figure 7-18C). This is probably due to the difficulty of measuring the flow depth in steep upstream channels, where channel banks are near vertical, rather than error in model predictions. Shear stress distributions determined using local flow depths and mean channel slope yield much higher mean shear stresses than those determined for the same data using local predictions of both depth and energy slope (Figure 7-18E). The result of this is underestimation of modelled α although the variance of the modelled shear stress distribution was much less than that determined using the depth-slope product (with standard deviations of 0.05 and 0.2 $N/m^2$ for modelled and measured shears, respectively). This suggests that the value of the shape parameter α depends on both the variability of flow depth or shear stress and also on the mean value of flow depth or shear stress at the section. In contrast, at X=4750mm for RunS4, there is significant deviation in bed elevations between the model and flume cross-sections bed elevations (Figure 7-18B). This in turn shifts the width of the flow depth distribution. Statistically, the shear stress dataset appears to be similar (within the same standard deviation of 0.23 and 0.27 $N/m^2$ for model and flume data, respectively). However, the mean shear stress determined using the local flow depth and mean channel slope is almost 50% higher than the modelled shear stress (Figure 7-18F). As a result, the value of α estimated using the product of local flow depth and mean channel slope is larger than the one estimated using the modelled shear stress.

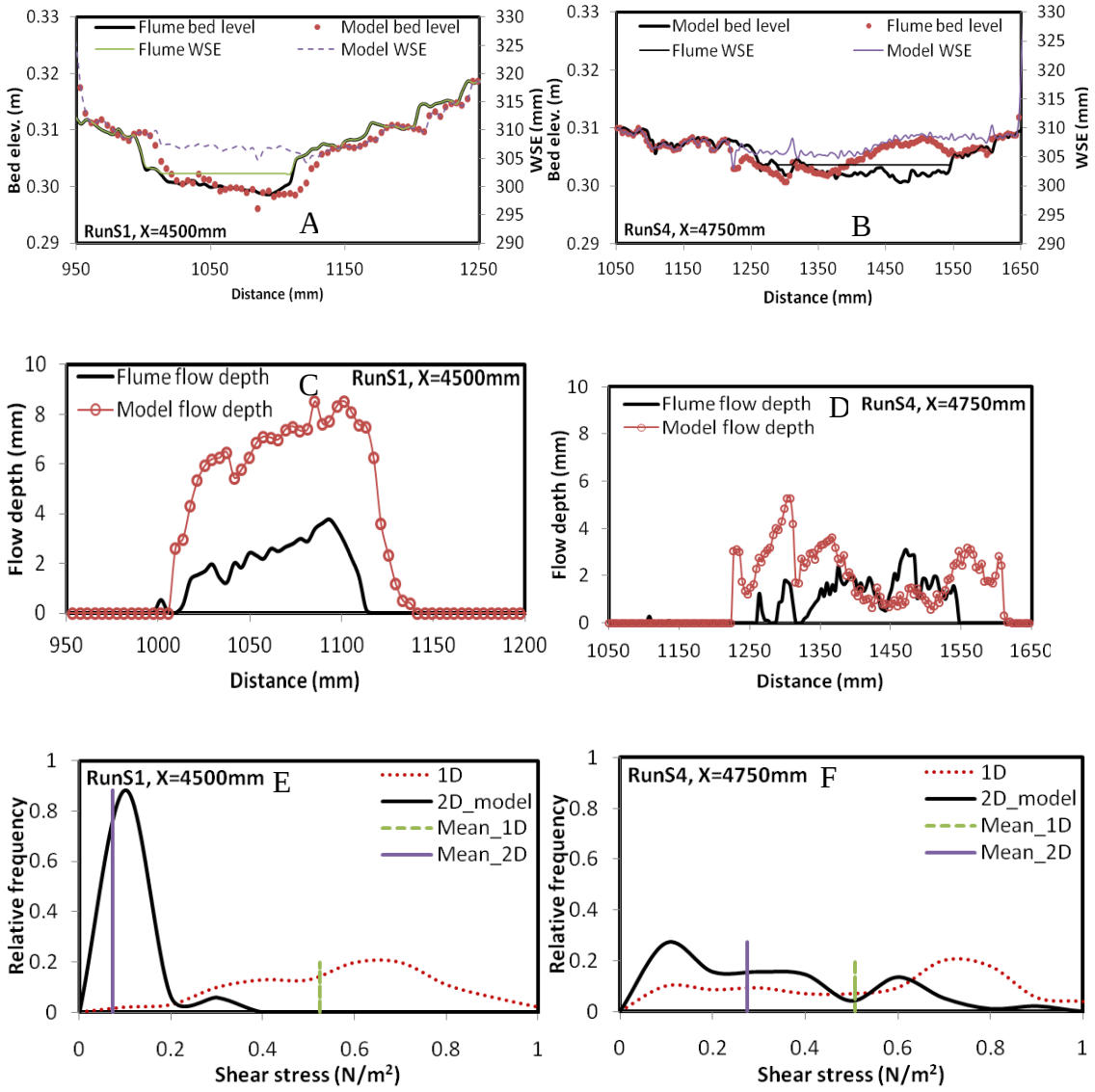


**Figure 7-18 Comparison of measured and modelled flow variables at two sections at flume inlet (RunS1, X=4500 & RunS4, X=4750mm)**

Figure 7-19 shows a plot of the values of α for different values of model derived mean shear stress. Values of α were computed by dividing the whole length of the experimental flume into four sections (each 1m long) and combining the shear stress data from each section and normalizing it by the reach-averaged shear stress and fitting it to the gamma PDF. The shear stress plotted represents the mean for each 1m long reach. The shape parameter α appears to follow a general trend when plottted against the mean shear stress in this way. The overall value of α tends to increase with an increase in mean shear stress. This is the case because a relatively high shear stress means a relatively high intensity of sediment transport, which suggests that the channel is

degrading. As a channel degrades bed topography will be drowned out and hence spatial variation in flow depth (that increases the value of α) will be reduced. This is also consistent with predictions of Nicholas (2002) and Bertoldi *et al* (2009). The dashed line shows the critical shear stress determined based on an experimentally determined value of Shields parameter of 0.11 and the $d_{50}$ of 0.47 mm. It appears that as the mean shear stress approaches the critical value, the pattern of points tends to bend highly than anywhere else in the curve. It is clear that values of alpha are sensitive to the mean shear stress and the critical value of shear stress for sediment transport, although there are not enough points to support this.

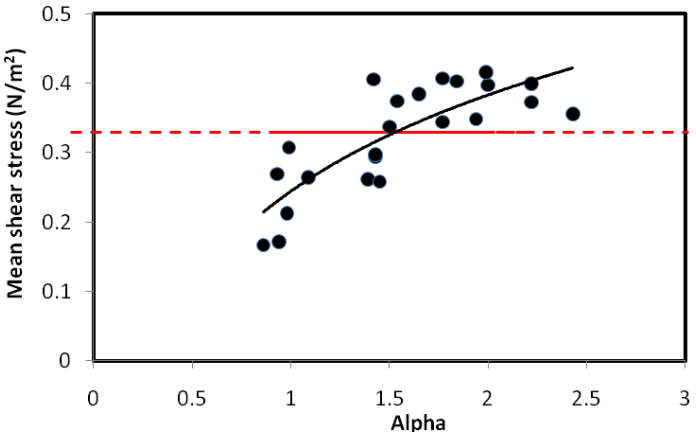


**Figure 7-19 Model derived reach mean shear values for the experimental run are plotted against best-fit α**

In chapter 6 it was shown that there appears to exist a systematic variation between the shape parameter α and changes in bed topography. Based on this an investigation was carried out to look for a relationship between the shape parameter and a morphological parameter (in this case, the areal change in aggradation or degradation). As in the previous case, values of α were computed by dividing the whole length of the experimental plot into four sections (each 1m long), and combining the shear stress data from each section, normalizing it by the reach-averaged shear stress and fitting it to the gamma PDF. The net change in area (NA) quantifies the net change in cross-sectional area of a transect and is computed as:

$$\Delta NA = \sum_{i=1}^{n} (Z_{ib} - Z_{ia})\, w \qquad 7\text{-}10$$

Where $Z_{ib}$ and $Z_{ia}$ refer to channel bed elevations before and after a given time interval (in this case, the time between two DEMs) and w is the width of the channel. However, a channel may appear to be stable where amounts of erosion and deposition in different

parts of the channel balance each other. Consequently, a computed net change in area of zero may incorrectly characterize the channel. To avoid this potential problem, the absolute change in area (AA) is also used:

$$|\Delta AA| = \sum_{i=1}^{n} |Z_{ib} - Z_{ia}|\, w \qquad 7\text{-}11$$

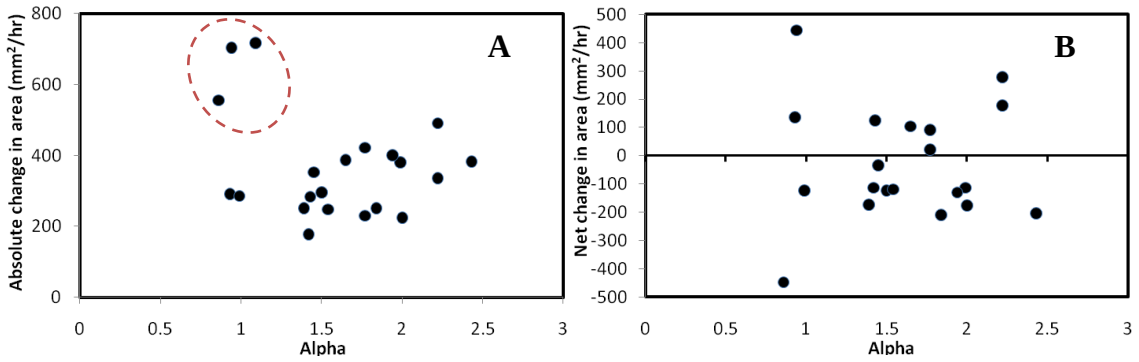


**Figure 7-20 Relationship between (A) absolute change in area and alpha (B) Net change in area and alpha**

Figure 7-20 shows that there is no clear relationship between the absolute (or net) change in area and the shape parameter α. Most of the data (other than those circled by the dashed line) suggest that as the absolute change in area of the channel increases, the shape parameter also increases slightly although the coefficient of determination is very low (0.21). This could be explained if most of the contribution to the absolute change in area is from degradation, because degradation might lead to flow confinement and less variance in flow depth (shear stress) and hence higher alpha values. It appears from Figure 7-20B that as the channel degrades (lower part of the chart), alpha values increase slightly as the volume of erosion increases. However, there is no clear relationship when the channel is aggrading (upper part of the chart). Overall, there is little evidence that a relationship exists between the shape parameter and the absolute (net) change in area.

## 7.7. SUMMARY

Despite the existence of some differences in bed elevation between cross-sections used to derive 'measured' flow properties and cross-sections extracted from the model DEM, the two-dimensional hydraulic model is capable of replicating measured patterns of flow depth in most of the cross sections considered. There is also good agreement between the measured and simulated water surface elevation. The fit between measured and modelled flow depths is optimised for low values of effective roughness ($R_d$),

which is around $0.21d_{50}$-$0.64d_{50}$. Clifford *et al.* (1992) showed that higher multipliers of effective roughness (e.g., $R_d=3.5d_{84}$) represent a measure of total flow resistance that incorporates contributions from both individual grains and larger bedforms. By separating these two components they showed that grain-scale roughness alone could be quantified by $R_d=0.4d_{50}$. In this series of experiments, although the bedform roughness may be substantial, it is represented by the topography in the model DEM. However, the value of $R_d$ in the model is only meant to represent the roughness at scales finer than the model grid (i.e. a few mm) and that is expected to correspond to grain roughness. This suggests that the value of effective roughness used in the model may be reasonable and may be thought to represent the grain roughness component. Moreover, grain resistance is largely a function of relative submergence ($Y/d_{50}$). This means that the effect of grain resistance therefore declines with increasing flow depth (Knighton, 1998;Wohl, 2000). As flow depth is very small in most sections of the experimental channel, it is likely that the grain resistance may be significant in this case.

A comparison of the shear stress distributions derived using the two-dimensional hydraulic model and with those estimated using the 1D reach-averaged equation (i.e. the depth-slope product) shows a close correspondence between the two. Mean shear stresses determined using local depth and mean channel slope are roughly comparable to those determined for the same data using local predictions of both depth and energy slope. This may be due to compensation of extreme flow depths by extremes in the local energy slope. However, the variance of the modelled shear stress distribution shows some differences to that calculated using the mean channel slope. One possible reason for this is due to variability in local water surface slope as the sections considered for comparison do not possess significant differences in bed elevation.

Frequency distributions of modelled shear stress were shown to fit a gamma distribution as has also been observed in several other studies (Paola, 1996;Nicholas, 2000). Longitudinal patterns of the gamma distribution shape parameter ($\alpha$) determined using the modelled shear stresses show some differences when compared with those computed using the 'depth-slope product'. The difference, in most cases, appears to be a result of differences in elevation between measured and DEM extracted cross sections. Moreover, the value of $\alpha$ is found to be dependent on both the variability in shear stress

and also on the mean shear stress. The value of α is shown to increase with the mean shear stress. Values of α obtained in this study range from 1 to 8, and are generally lower than those obtained by Bertoldi *et al.*(2009) for a laboratory braided river, but mostly in agreement with Nicholas (2000), who estimated typical values of α between 1 and 4, but as high as 8 in some sections and at high discharge for the Waimakariri River. However, Bertoldi *et al.*(2009) evaluated values of α directly from the transport rates rather than the transverse distribution of depth or shear stress and Nicholas (2000) used local flow depth. While Nicholas (2002) showed that using local flow depth instead of local shear stress does not introduce major errors in the flux calculation, computation of α values depends on whether depth or shear stress is used.

The design, implementation and output from the micro-scale physical model have been explained (Chapters 4 to 6); the resultant experimental data and DEM have been used in a two dimensional hydraulic numerical model (Chapter 7) to assist in the understanding of the controls on shear stress distribution and its effect on sediment transport and channel evolution. The next chapter will summarise the findings of the project, reflecting back to the original aims and objectives specified in Chapter 2 and reflecting the direction of future work in more detail using preliminary data collected from a river located at the highlands of North Ethiopia.

# 8. CONCLUSION

## 8.1. INTRODUCTION

This chapter begins by providing a short synopsis of the thesis, giving an overview of each of the chapters. The thesis objectives and aims are then revisited, incorporating a discussion of how the findings from this project have addressed these. Finally, the chapter comments on the wider implications of this research and the direction future research could take.

## 8.2. PROJECT SUMMARY

Overall, the aim of this research was to develop a micro-scale physical model of a braided river and use this to obtain an improved understanding of the lateral variability of sediment transport as a control on braided river evolution. In Chapters 1 and 2, the importance of understanding sediment transport dynamics in braided rivers was noted; this is of key importance in engineering and geomorphology, in the study, design and operation of hydraulic and flood control structures. Braided rivers can be agents of significant erosion and sediment transport, and can change their geometry rapidly, thereby modifying their boundaries and floodplains. This makes them problematic for engineers when designing channel or braidplain edge structures, such as bridges and roads or other hydraulic structures. Chapter 2 set the background of the thesis by providing a review of the state-of-the-art in braided river research to date and explaining why braided rivers are of importance. This review helped to identify the current lack of understanding that exists relating to the effects of lateral variation in hydraulics and sediment transport dynamics in braided rivers. Although there exist a number of ways to predict sediment transport in braided rivers, the effect of lateral variation of sediment transport was not systematically addressed in previous research. Moreover, the relationship between sediment transport and channel morphological indices (e.g., stream braiding and channel width to depth ratio), the role played by channel pattern indices and their contribution to sediment transport dynamics are less well known. The three main approaches that have been utilised in braided river research (field work, physical models and numerical models) were outlined in Chapter 3. The advantages and

disadvantages of employing each method were presented along with examples from the literature of their use in braided river research. Due to the difficulty, time taken and cost of acquiring high quality data in the field the chapter concluded that experimental physical modelling was the best solution for this research, as it allowed the processes occurring during river channel evolution to be observed in detail in a controlled environment. However, the importance of evaluation of the physical model output was stressed and a three-fold methodology was decided upon in which a numerical model would also be used to predict flow depths and shear stresses in the experimental channels, and similar data would also be collected from a field setting. The aim of this strategy was to allow comparison of the trends in key parameter(s) identified in the field, numerical model and the micro-scale physical model.

The substantive research of this thesis was presented in Chapters 4 to 8, with Chapters 4 to 6 focused on the physical model design, analysis and results. Chapter 4 described the experimental design including the rationale for the experimental conditions, the scaling relationships used and the input conditions of the five experimental scenarios. In Chapter 5 the changes in sediment storage and channel morphology in aggrading and degrading experimental braided rivers were presented. The results were discussed in the context of current understanding of braided river evolution. The sediment transport characteristics of experimental braided channels were presented in Chapter 6. The chapter outlined the effects of lateral variation in hydraulic parameters on sediment transport computation. It also discussed the relationship between channel pattern indices (width to depth ratio and braiding index) and sediment transport. In Chapter 7 the experimental data and digital elevation models were used in a two dimensional hydraulic model to predict flow depth and shear stress. The high resolution digital elevation models were then used to gain a better understanding of the controls on the shear stress distribution in the experimental channels and its influence on sediment transport and channel evolution.

## 8.3. RESEARCH AIMS REVISITED

In light of the research presented in the previous chapters, the aims of this investigation identified in Section 2.7 are revisited in the following sections.

1. **To develop a micro-scale physical model and exploit its potential for braided river evolution studies**

In this project a micro-scale physical model of a braided river was designed, and run. Five different experimental runs were carried out. Three of the experimental runs were degradation runs with no sediment supply from upstream and two of them were aggradation runs. All the runs were carried out one after the other without flattening the channel bed. However, in all runs the water discharge rate was held constant. The sediment supply rate fed to the aggrading systems was also constant.

The micro-scale physical model of braided river evolution designed and run for this research has been found to successfully replicate processes that have been observed on natural braided rivers. The experimental braided channels produced in this research differed slightly from those presented in previous studies by the fact that there is no any width limitation from the flume walls while the channel braids. Therefore, situations are considered where channel width is unrestricted by the experimental setup.

A continuous record of river morphology was achieved using high resolution laser profiling to quantify channel changes (fill, incision and lateral erosion) and section geometry. Several digital elevation models were also collected throughout the development of the channel. During all the runs, part of the evolution of the channel was recorded using a Canon HG10 digital video camera, and still imagery was collected at 2 minute intervals using Canon EOS10d digital cameras mounted overhead. At the downstream end of the basin a plastic gutter conveyed both the liquid and sediment flux to a constant head overflow tank. The tank rested on a high precision laboratory scale (accuracy 0.1g) which was used to measure the cumulative weight of exported sediment at 5 minute intervals. These data were used with observations of channel width at the downstream flume to derive sediment transport per unit river width.

Collecting the imagery during the experiments was straightforward and once the cameras were in position the image collection was automated; meaning that it was not very labour intensive and allowed attention to be focused on running the experiment and manual measurements rather than recording the channel evolution. However, the

imagery did not allow any quantitative analysis due to the fact that flow depth was extremely shallow, the sand is fully saturated so that identification of dry and wet parts of the channel becomes very difficult. The photographs were then used only for qualitative analysis and to provide information on channel evolution without the need to interrupt the experiment.

The experimental findings from this investigation demonstrate that the physical micro-scale model designed for this project simulated many of the processes observed on natural braided rivers. It enabled quantitative recording and analysis of the changes that occurred in the channel morphology and the changes in sediment transport capacity as the channel aggraded and degraded that, due to the timescales involved, would have been impossible to monitor in the field. The limitations of the technique (i.e. the time-consuming design and analysis processes) and errors within the data are far outweighed by the quantity and type of data produced.

Overall the experimental braided channels exhibited many of the feature characteristics of natural braided rivers during their evolution; these included an increase in braiding intensity, number of braid bars, pattern complexity and morphologically active braid plain width during channel agradation and vertical incision close to the flume inlet that sometimes extended to middle of the flume during degradation. Absence of sediment feed from upstream caused the flow to be concentrated into a single channel flanked by erosional terraces that ultimately left a greater proportion of the active channel exposed. The processes and channel configurations observed tend to agree with those from previous experimental braided river studies (Ashmore, 1991;Hoey and Sutherland, 1991;Germanoski and Harvey, 1993;Germanoski and Schumm, 1993;Madej *et al.*, 2009). This is the most prominent feature of the evolution of sand bed laboratory channels. However, in both aggradation and degradation cases the downstream portion of the channel aggraded due to the resultant influx of sediment arriving from the upstream reach. This is also in agreement with the laboratory experiments of Germanoski and Harvey (1993) and Germanoski and Schumm (1993). Another typical characteristic of degrading channels was a transformation in channel pattern from braided to single thread, especially in the upstream reach where the effects were acute. The channels in the upstream part of the flume became progressively narrower in time

and the length of the channel transformed to single thread also increased with time. This is an indicator of the fact that although the transformation towards a single thread channel was not completed in the series of runs, the ultimate consequence of continued degradation was evident from the trend.

There was substantial fluctuation in sediment output throughout the experiment. Several irregular phases of transport intensity were observed in the time series, which statistical analysis confirmed to posses a strong periodicity and dependence on previous transport rates. There is no significant difference in the magnitude of the sediment transport rate peaks for aggrading and degrading channels, but these peaks were higher in relative terms during degradation runs.

The experimental work presented here has shown that despite the lack of dynamic similarity conditions and simplification of overall similarity criteria, fairly consistent results could be obtained which can be interpreted in a generic sense. The similarity between the laboratory channels from this experiment and those previously investigated by different researchers with or without a field prototype utilizing the Froude modelling principle suggest that the laboratory channels are at least qualitatively transferable to the field.

**2. To obtain an improved understanding of lateral variability of sediment transport as a control in braided river evolution**

Analysis of the micro-scale physical model output has provided a wealth of data on how the channel morphology and sediment transport capacity of an experimental braided channel alter as it evolves. The high resolution digital elevation models attained and a number of channel cross section measurements obtained provide an extremely useful dataset. These data have helped to show how channel morphology and sediment transport changes, both as the experimental channel evolves and also with a change in the sediment supply rate.

The effect of cross section averaging of hydraulic parameters on sediment transport was investigated by comparing measured total sediment transport rates (time averaged) with

the predictions of the Meyer-Peter-Muller equation (MPM) using surveyed topographic cross sections and cross section averaged hydraulic parameters. Sediment transport rates predicted by the Meyer-Peter-Muller transport equation and cross section averaged hydraulic parameters under-predict actual transport rates. This demonstrates the significant influence of transverse variability of hydraulic parameters in controlling and predicting sediment transport rates in braided channels. Computation of the transport rates using the measured topographic cross sections and including lateral variability shows good agreement with the measured values.

A relationship exists between braiding intensity and sediment transport for the experimental braided channels. Earlier investigators that addressed this issue have reported that an increase in braiding intensity may promote higher rates of sediment transport (Nicholas, 2000;Warburton and Davies, 1994) as a result of increased spatial variability in flow depth and shear stress. However, Ashmore (1988) and Hoey and Sutherland (1991) argue that sediment transport rate decreases as braiding increases. Results from the experimental braided channels reported here reveal that sediment transport increased with braiding intensity. However, there seems to exist a threshold, beyond which, an increase in braiding intensity does not increase sediment transport and it may even reduce transport rates. This may be because of division of flow by the channels formed as a result of increase in braiding intensity, and hence increased flow width and lower mean shear stress. This will reduce the amount of flow to be conveyed by the "active" part of the channel.

There are some important issues in this respect. There is a tendency for channel multiplication to occur in aggrading reaches. Since bedload transport rate has a non linear relationship with excess shear stress ($\tau$-$\tau_c$), the total bedload flux in a channel depends not only on the mean values of $\tau$ and $\tau_c$, but also on their spatial variances within the reach under consideration (Ferguson, 2003). This promotes higher sediment transport rates as a result of increased spatial variability in flow depth and shear stress. Although increased flow variability (associated with braiding) increases sediment transport rates, braiding also increases channel width/depth ratio and reduces mean shear stress and these effects tend to reduce sediment transport rates. Moreover,

although the existence of those effects is undeniable, their magnitude is uncertain. Which of these effects tends to dominate is a key question and depends on the strength of the feedback between the sediment transport rate and change in channel morphology. This feedback strength can be measured by the temporal change in the measure of the shear stress variance $\alpha$, which is $(d\alpha/dt)$.

It is thought that a channel formed in erodible material has some maximum limit in the shear stress variance that can be sustained without the bank failing. That means the banks can withstand only a certain shear stress, after which bank retreat will occur. There is some channel configuration at which the shear stress variance is maximized and as a result the sediment transport is increased. Up to this point it is thought that the process does not modify mean flow depth and channel width appreciably. Beyond this point channel boundaries will fail and, although shear stress variance is increasing, its effect will be dominated by the increase in channel width resulting from bank failure. This process will increase channel width to depth ratio substantially and hence the mean shear stress will be reduced. This will ultimately reduce sediment transport. The overall process is elaborated in Figure 8-1.

The experimental data generated in this study provide a unique opportunity to observe in detail the spatial and temporal changes in sediment transport and channel morphology that occurred in the channels as they evolved. These data and digital elevation models were used in a two dimensional hydraulic model to attempt to gain a better understanding of the controls on the shear stress distribution in the experimental channels and its influence on sediment transport and channel evolution.

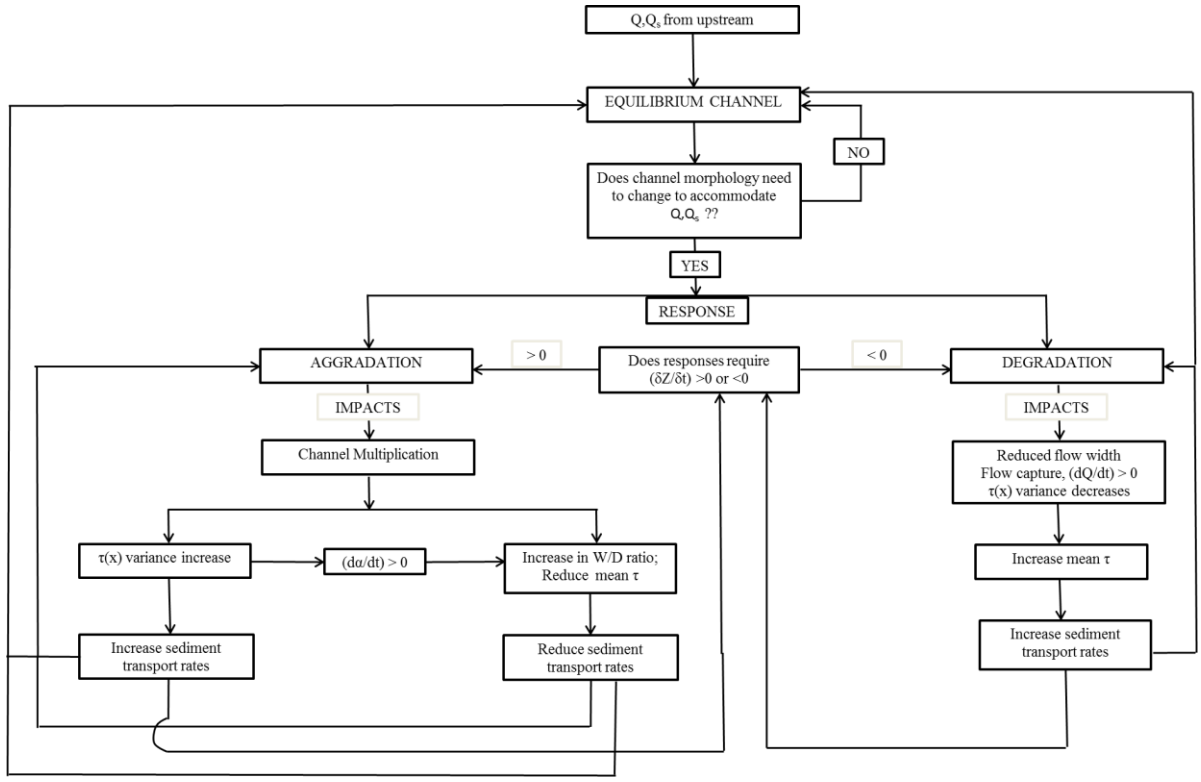


**Figure 8-1 Schematic representation of the controls on aggradation and degradation defined in terms of the effects of lateral flow variability in sediment transport and channel morphology. Q = water discharge, $Q_s$ = sediment discharge input from upstream; Z = mean bed elevation, t = time, τ = mean shear stress, W/D = channel width to depth ratio; α = measure of shear stress variance Based on the conceptual model of Hoey and Sutherland (1991), modified based on the results of this study.**

A comparison of the shear stress distributions derived using the two-dimensional hydraulic model and with those estimated using the one-dimensional reach-averaged equation (i.e. the depth-slope product) shows a close correspondence between the two. Mean shear stresses determined using local depth and mean channel slope are roughly comparable to those determined for the same data using local predictions of both depth and energy slope. This is probably due to compensation of extreme flow depths by local energy slope. This is encouraging as cross section averaged parameters to be used in equations like "the depth-slope product" can be obtained easily. Moreover, the equation is very simple and can be used by any field practitioner and river engineer at field level where management decisions are required.

The wealth of data on channel morphology and sediment transport dynamics produced by the micro-scale physical model has been discussed. Of particular importance to

current debate regarding braided rivers is the data that quantify the spatial and temporal variation of channel pattern indices, sediment transport and the parameter that describes the width of the shear stress distribution. The data extracted on the width of shear stress distribution shape parameter demonstrate that shape parameter (α) values decrease in the downstream direction slong the flume, indicating greater spatial variability in bed topography, although for the middle part of the flume (from 1.5m to 3.5m) variations in 'α' are small. In contrast, braiding intensity increases in the downstream direction. As with the shape parameter (α), the braiding intensity shows little variation around the middle of the flume. Maxima in braiding intensity and minima in shape parameter values occur around the flume outlet. In contrast, minima in braiding intensity and maxima in shape parameter values occur at the flume entrance.

Obtaining high resolution data that quantify aggradation and degradation scenarios on natural braided rivers over the course of their evolution is very difficult, mainly due to the time taken for the channel to evolve. In this respect, the experimental data obtained during this project provide the ideal solution. The detailed spatial and temporal patterns of channel pattern indices (e.g., width to depth ratio and braiding intensity) derived from the micro-scale physical model in this investigation enabled the establishment of a relationship between channel pattern indices (width to depth ratio) and the width of shear stress distribution shape parameter (α). The relationship between channel pattern index (width to depth ratio) and the width of shear stress distribution shape parameter (α) is based on data from each cross section of the experimental channels. This relationship clearly shows a slightly increasing trend of α with channel width to depth ratio.

## 8.4. FUTURE WORK

Most flume experiments to-date have considered idealised cases with constant inflow conditions (water discharge and sediment supply rate). The effect of varying sediment supply was introduced here but only in a simplistic way. There are a number of modifications that could be made to the experiments conducted here. Future work should attempt to address the effect of varying water discharge (using inflow hydrographs) to assess whether observed effects of varying sediment supply would

persist under varying flows. Moreover, an attempt could be made to evaluate the effect of bank stabilization on sediment transport dynamics and channel morphology. This could be realized by introducing vegetation, similar to the techniques used in the experimental work of Tal *et al* (2004) on meandering rivers. A more complex scenario of varying flows (using hydrographs) in combination with vegetation would help to provide understanding of the relationship between water discharge, sediment supply rate and vegetation on transport dynamics and channel patterns.

Further work related to the numerical modelling should involve development and testing of a one-dimensional numerical sediment routing model that includes lateral flow variability. The relationships between the width of the shear stress distribution shape parameter and channel pattern indices (e.g., braiding intensity or channel width to depth ratio) developed in this thesis can be used as an initial input for such a one-dimensional numerical model.

More importantly future work should focus on validating the experimentally generated relationship (chapter 6, Equation 6-19) between the width of shear stress distribution shape parameter and channel pattern indices (e.g., channel width to depth ratio) using field data. It normally require lots of channel morphological data to evaluate the shear stress distribution shape parameter (α), which is costly and time consuming. Moreover, it is very difficult to collect dataset representing different flow and morphological condition. So, validation of relationships like equation 6-19 is very crucial from this point of view.

Preliminary field work has been done to show important directions of future work regarding validation of experimentally generated relationship between the shape parameter (α) and the channel width to depth ratio. The following section discusses about this. The section starts by introducing the aim of the preliminary field work and describing the field site. Field data collection strategy and application of the two dimensional hydraulic model described in chapter 7 to generate additional data is addressed. Finally a relationship is generated between the shear stress width parameter and channel width to depth ratio and this relationship is compared with the one generated in chapter 6 (Equation 6-19).

### 8.4.1. Field Site

The aim of this section is to evaluate the applicability of the relationships established using the physical model. It is important to be clear that direct comparison of results between the experimental channels and the natural river is not undertaken. Given the nature of the experiments, there are a number of reasons that this cannot be done. The use of a generic micro-scale physical model means that it is not scaled to a specific field prototype and therefore, unlike a Froude-scale model, direct comparison cannot be made between the laboratory and the field, and verification of the physical model with field data is impossible. A further constraint in comparing the experimental findings from this project with the field is that the tightly controlled and constant input conditions (water discharge and sediment supply) from the experiment are not found in nature. As indicated above, therefore, the focus is on comparison of the trends observed in the experimental channels with those in the field. Longitudinal variations in the width of the shear stress distribution α and its relationship with other morphological parameters will be investigated for the study reach. An attempt will be made to establish a relationship between the shape parameter α and mean morphological parameters (e.g., the channel width to depth ratio). A comparison will then be made between the output of this analysis and the equivalent analysis of the experimental channels (chapter 6) to determine if the regression equation developed for the gamma shape parameter obtained from the experimental channels is realistic in nature.

The Megech River, which is about 75 km long, has a drainage area of about 850 $km^2$ and an average annual discharge of 11.1 $m^3/s$. This river is one of the main water sources flowing into Lake Tana from the north. Lake Tana represents a major hydrological system in the upper Blue Nile Basin and it is the largest lake in Ethiopia with a surface area of 3012 $km^2$ and a volume of 28 $km^3$ at its long term mean elevation of 1786 m.a.s.l. The highest elevation of the Megech watershed is around 2991 m above mean sea level, in its north eastern part. Four major tributaries join the Megech River: two from the right bank and the other two from the left. The Megech catchment is characterized as mountainous, wedge-shaped with mean catchment slope of (3.2%). The catchment of the Megech River is highly vulnerable to sheet, rill and gully erosions. During a field visit made in 2006 by groups of professionals responsible for the design

of the Megech Dam, it was observed that new gullies which directly ran into the Megech River were being formed as a result of the increased agricultural activities performed in the catchment such as cultivation of steep slopes steep area farming and intensive grazing. The proposed new dam currently under construction in Megech River is located southeast of Azezo and Tewodros airport about 3 km to the right of Gondar-Bahir Dar main road and Megech River crossing.

The climate of Megech catchment is marked by rainy season from May to October, with monthly rainfall varying from 67 mm in October to 3.6 mm in July. Mean annual precipitation is about 1100 mm in the upper part and is about 1000mm in the lower part. Rainfall over the catchment is mono-modal with 79% of annual rainfall occurring in the period June to September. The dry season, from November to April, has a total rainfall of about 8% of the mean annual rainfall. Dependable rainfall (85%) varies from less than 1.2mm during the dry season to 88-225mm/month during the period of June to July/August, equivalent to 55 to 75% of the average values. Temperature variations throughout the year are minor. Maximum temperatures vary from $23^0$c in July to $30^0$c in March, whereas minimum temperatures range from $11.5^0$c in January to $15.6^0$c in April and May. Humidity varies between 39% in March and 79% in August.

Table 8-1 shows estimated monthly rainfall over Megech reservoir which is located some 3 km upstream of the study reach. Table 8-2 shows stream flow data of Megech River at the hydrometric station near Azezo, which is very close to the study reach.

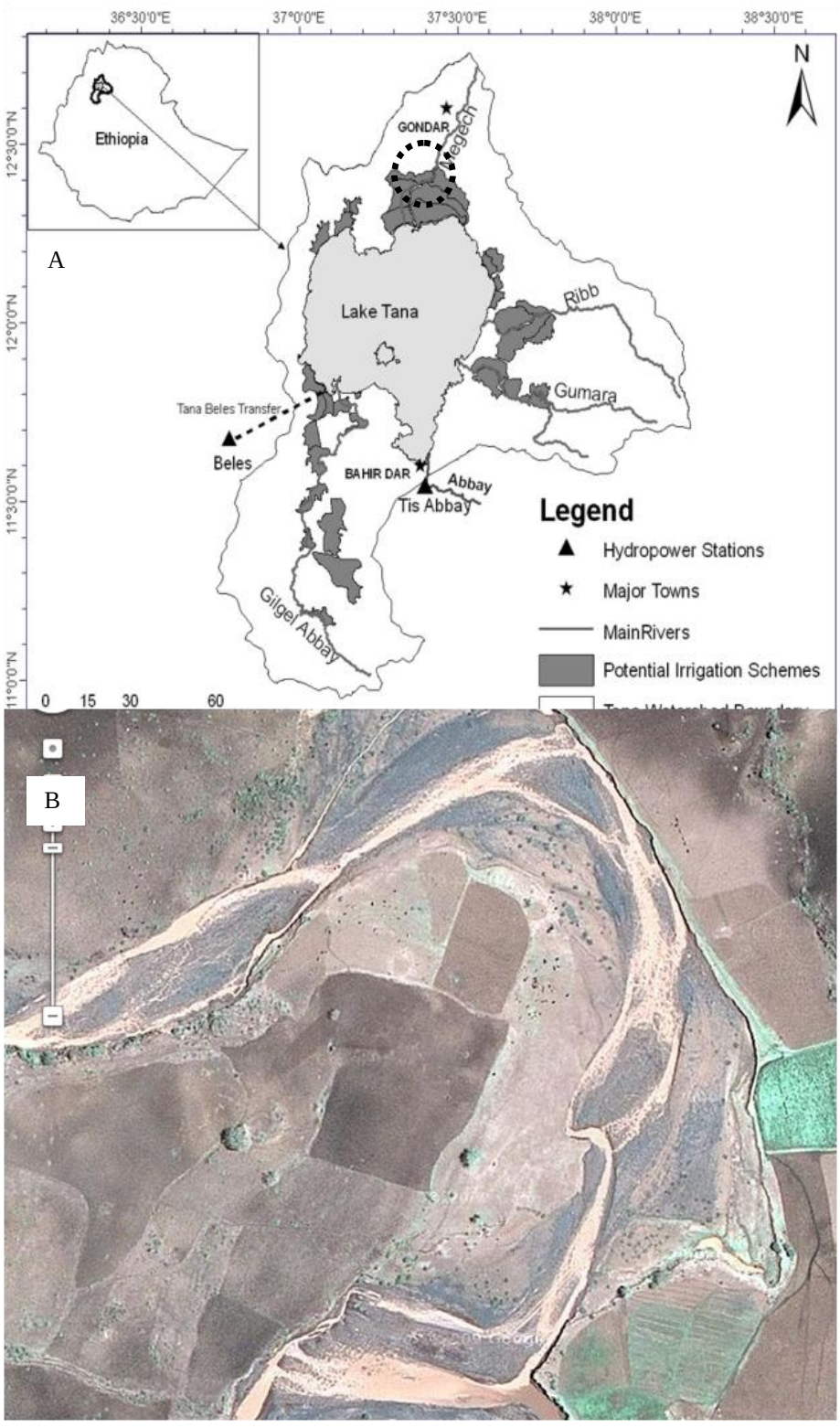


**Figure 8-2 Location map of the Lake Tana catchment showing (A) Major inflowing Rivers including Megech River; (B) Image extracted from Google Earth showing the planform of the river near the field site; Fieldwork site is circled by dashed line. (''A'' Taken from Megech Dam Feasibility Report, Volume 1)**

Table 8-1 Estimated monthly rainfall (mm) over Megech Reservoir (Taken from Megech Dam Feasibility Report, Volume 1)

| | Jan | Feb | Mar | Apr | May | Jun | Jul | Aug | Sep | Oct | Nov | Dec | Annual |
|---|---|---|---|---|---|---|---|---|---|---|---|---|---|
| Mean | 3.9 | 3.4 | 16.7 | 34.8 | 85.5 | 157.4 | 305.6 | 277.7 | 108.9 | 66.8 | 22.4 | 7.8 | 1090.9 |
| Max | 26.9 | 32.6 | 89.3 | 130.2 | 219.7 | 308.9 | 548.9 | 560.4 | 230.8 | 209.7 | 84 | 38.6 | 1514.6 |
| Min | 0.0 | 0.0 | 0.0 | 0.0 | 1.4 | 35.9 | 179.7 | 148.8 | 16.4 | 0.0 | 0.0 | 0.0 | 711.8 |

Table 8-2 Streamflow data of Megech River at the hydrometric station near Azezo, M $m^3$ (Taken from Megech Dam Feasibility Report, Volume 1)

| | Jan | Feb | Mar | Apr | May | Jun | Jul | Aug | Sep | Oct | Nov | Dec | Annual |
|---|---|---|---|---|---|---|---|---|---|---|---|---|---|
| Mean | 1.3 | 1 | 1.1 | 1.3 | 2 | 8.5 | 33.6 | 96.1 | 34.8 | 7.1 | 3.2 | 2.1 | 192.0 |
| Max | 10.2 | 7.9 | 11.9 | 11.8 | 14.8 | 97.9 | 116.1 | 334.7 | 125.5 | 28.9 | 16 | 12.4 | 429.3 |
| Min | 0.1 | 0.0 | 0.0 | 0.1 | 0.3 | 0.9 | 3.2 | 31.3 | 3.0 | 1.2 | 0.4 | 0.1 | 61.6 |

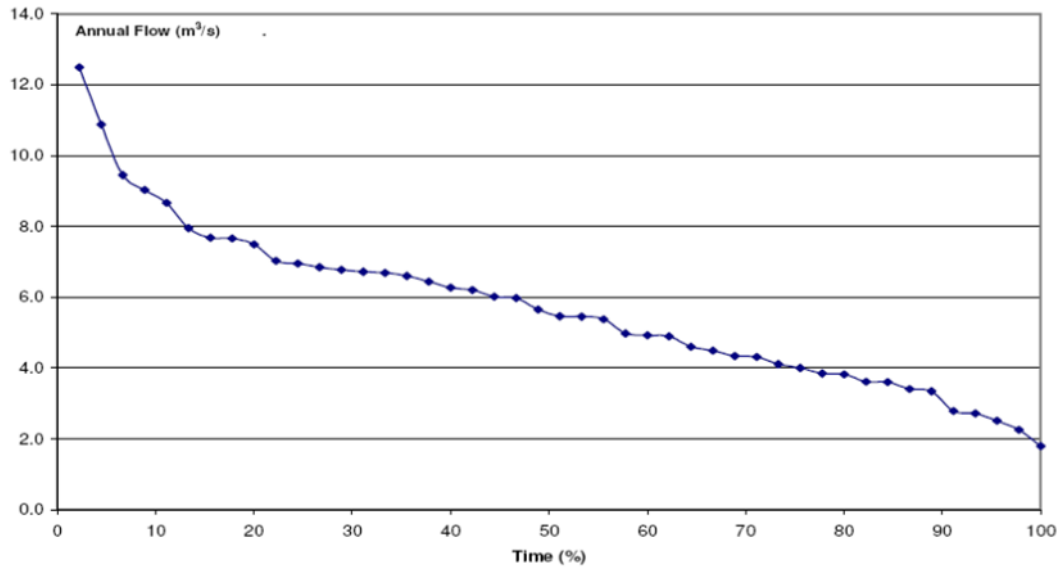


Figure 8-3 Annual historic flow duration curve for the period of 1960-2004 for Megech Dam site (Taken from Megech Dam Feasibility Report, Volume 1)

A significant part of the basin is designated for crop production using rain-fed agriculture. Because of the growing population pressure, cultivation is also practiced on marginal lands with a resulting increase in upstream soil erosion and sedimentation in downstream areas (SMEC, 2008c). The low-lying parts of the basin bordering Lake

Tana include extensive floodplains where recessional cultivation is practised. It was evident during the fieldwork visit that the Megech River in general and the study reach in particular are also characterized by serious bank erosion and mass movement (Figure 8-4). The eroded and transported sediment from the upstream highlands, bed and banks of the river ultimately reaches Lake Tana. Although an estimate is not available and research related to sediment transport and rates of bank erosion have not yet been carried out for River Megech, there is visual evidence that the contribution to Lake Tana sedimentation may be significant. On the other hand, farm landowners complain of bank erosion and channel shifting, which cause the loss of some parts of their valuable land. The bank erosion problem seems to be triggered by unmanaged in-stream gravel mining in some parts of the river. The mining activity on the right bank of the river appears to lower the bottom of the channel, making the bank almost vertical and unstable (Figure 8-4C). Siltation in the downstream reaches of the major rivers including Megech is one of the causes of overbank flow and flooding (SMEC, 2008a). Figure 8-4 E, F, G, and H shows that the river actually does not possess a typical morphology and it is included to ease interpretation of results later in the chapter.


**Figure 8-4 River bank erosion in the study reach, eroding agricultural land and River training works and pictures showing the nature of the river**

### 8.4.2. Field Data Collection

In order to be able to employ the hydraulic model used in chapter 7 to simulate flow within the surveyed section of the Megech River, Ethiopia, a brief but intensive field measurement campaign was undertaken. The surveyed reach is approximately 102.5m long and 34m wide and is bounded on the true left by a steep sloped bank. There is no clearly defined river bank on the true right of the river (Figure 8-5). Reach topography was surveyed in detail using Leica TPS1200+ total station and more than 2000 elevation points were recorded in a regular grid of 0.5m lateral and 2.5m longitudinal resolution. A digital elevation model was constructed from these data for use by the hydraulic model (Figure 8-5).

### 8.4.3. Velocity & Depth Measurement

Velocity and depth data provide a basis for evaluating how well the hydraulic model predicts flow conditions for various flow patterns. Therefore, field observation of depth and velocity were made at 0.5m interval across ten cross sections for depth and four cross sections for velocity. In all cases, flow depth was measured using stadia rod

to a resolution of +/-1cm and point velocity was measured using SEBA Mini current meter M1attached with SEBA Signal counter Z6-SEBA HAD with a time measurement accuracy of 0.01s and impulse frequency of 40 impulse/s. Despite the small diameter of the propeller (50mm), its physical dimensions limited the resolution of the profile and constrained the number of points obtainable in some areas of low water depth. A minimum of 3 and maximum of 9 measurements per velocity profile were obtained by varying elevation above the bed at regular intervals of 0.1Y to 0.9Y, where Y is the flow depth. A 9 mm diameter depth setting wading rod was used to position the propeller and a base plate was attached with the rod for resting on the river bed. The 10 flow depth measurement cross sections were placed in such away that they passed through different types of flow features within the channel (e.g. pools and riffles). Two cross sections from the upstream part of the reach and eight cross sections from the downstream section were chosen.

The section at the inlet of the reach is divided into a number of smaller segments. Local depth $Y_i$ measured directly and local mean velocity $U_i$ taken to be the velocity measured at 0.4Y above the bed were used to compute the discharge. Discharge through each segment is estimated by:

$$\boldsymbol{q_i = Y_i * U_i} \qquad 8\text{-}1$$

and the total discharge is estimated by:

$$\boldsymbol{Q = \sum q_i * b_i} \qquad 8\text{-}2$$

Where b is measured width of the channel. The discharge at the time of measurement was $0.35 m^3 s^{-1}$.

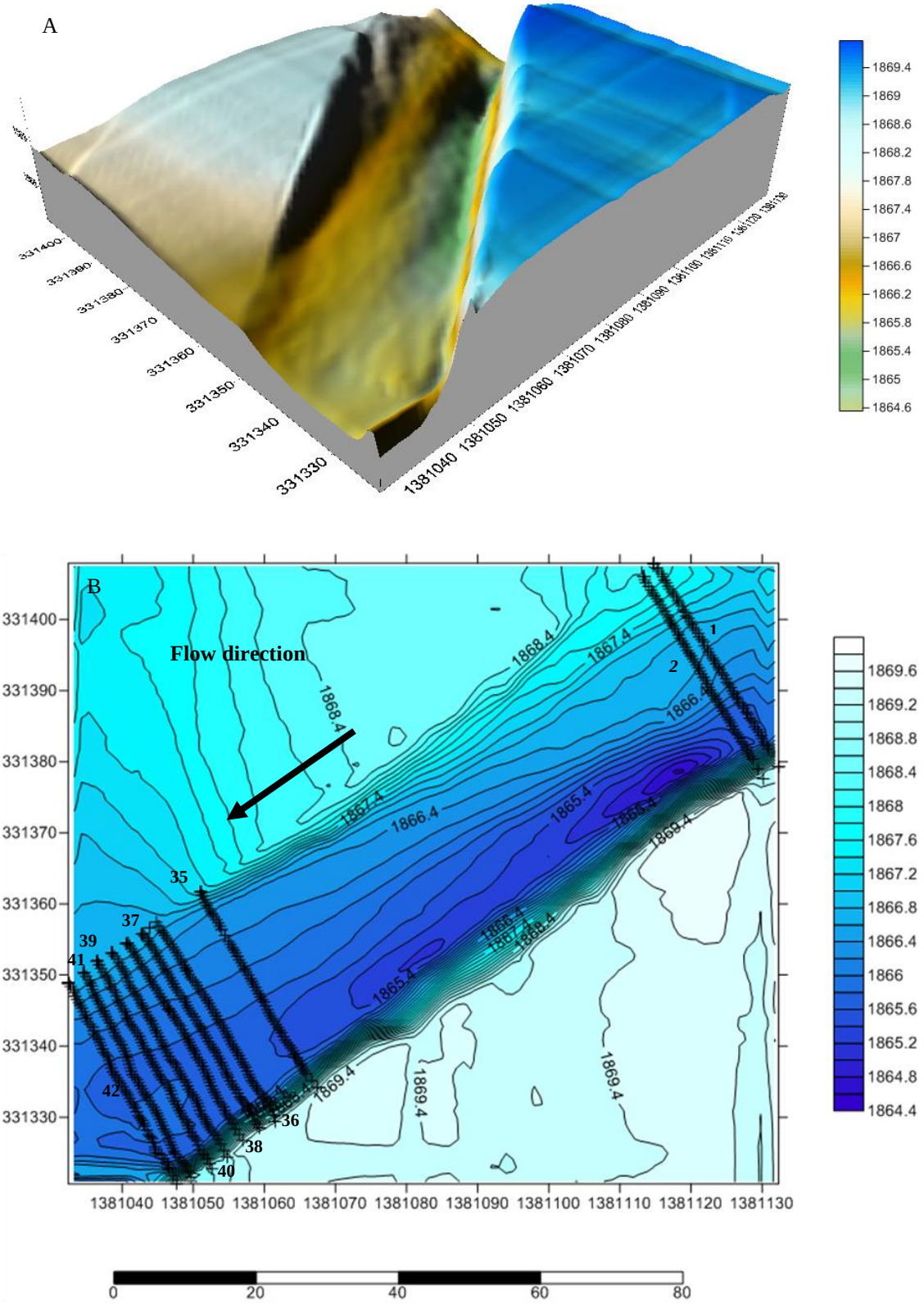


**Figure 8-5 A) 3D surface map and (B) Topographic map of the study area with measurement locations.**

### 8.4.4. Model Application

In the next sections, the two-dimensional hydraulic model described in section 7.2 is applied using the data collected from Megech River. The model is used to generate flow depth and flow velocity using the digital elevation model described in section 8.3, Figure 8.5. Model predictions of flow depth and flow velocity are compared with measured values.

### 8.4.5. Model Depth Predictions

Model depth predictions were compared against cross sectional data for quantitative analysis and spatial patterns. Model results replicate flow depths measured in the field at different sections of the river including where flow is divided by channel bars although the highest depths are under predicted. The possible reason for this under prediction is that the low points are missed from the DEM used for simulation. This is clearly indicated in Figure 8-6.

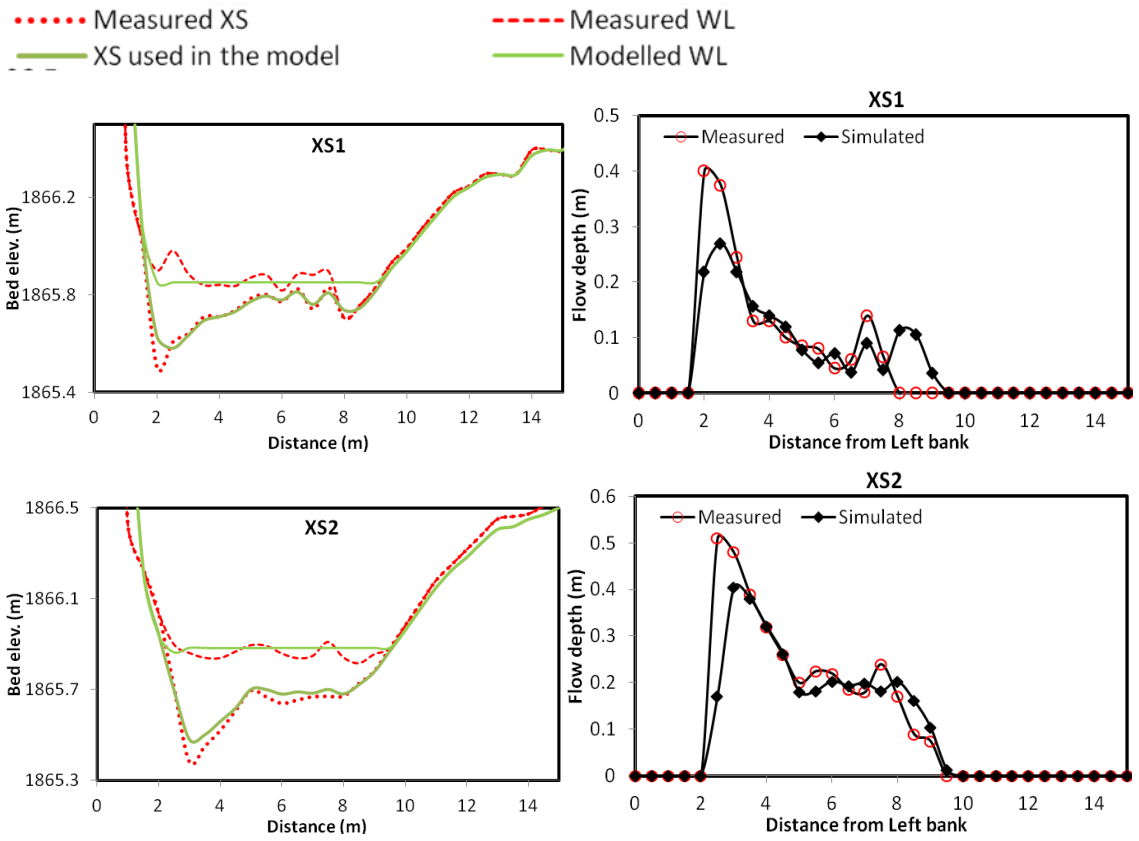

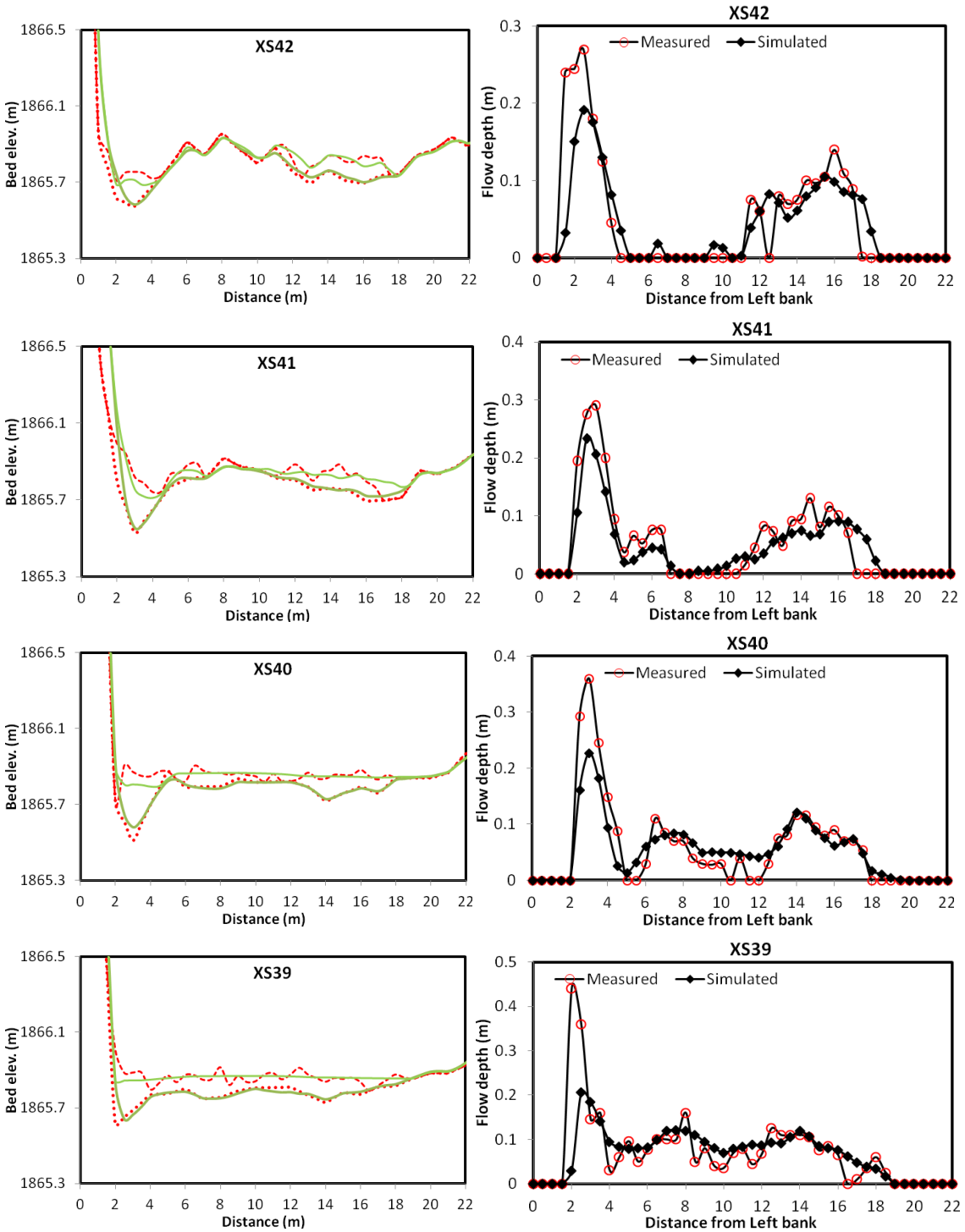
XS42
Bed elev. (m)
Distance (m)
XS42
Measured
Simulated
Flow depth (m)
Distance from Left bank
XS41
Bed elev. (m)
Distance (m)
XS41
Measured
Simulated
Flow depth (m)
Distance from Left bank
XS40
Bed elev. (m)
Distance (m)
XS40
Measured
Simulated
Flow depth (m)
Distance from Left bank
XS39
Bed elev. (m)
Distance (m)
XS39
Measured
Simulated
Flow depth (m)
Distance from Left bank

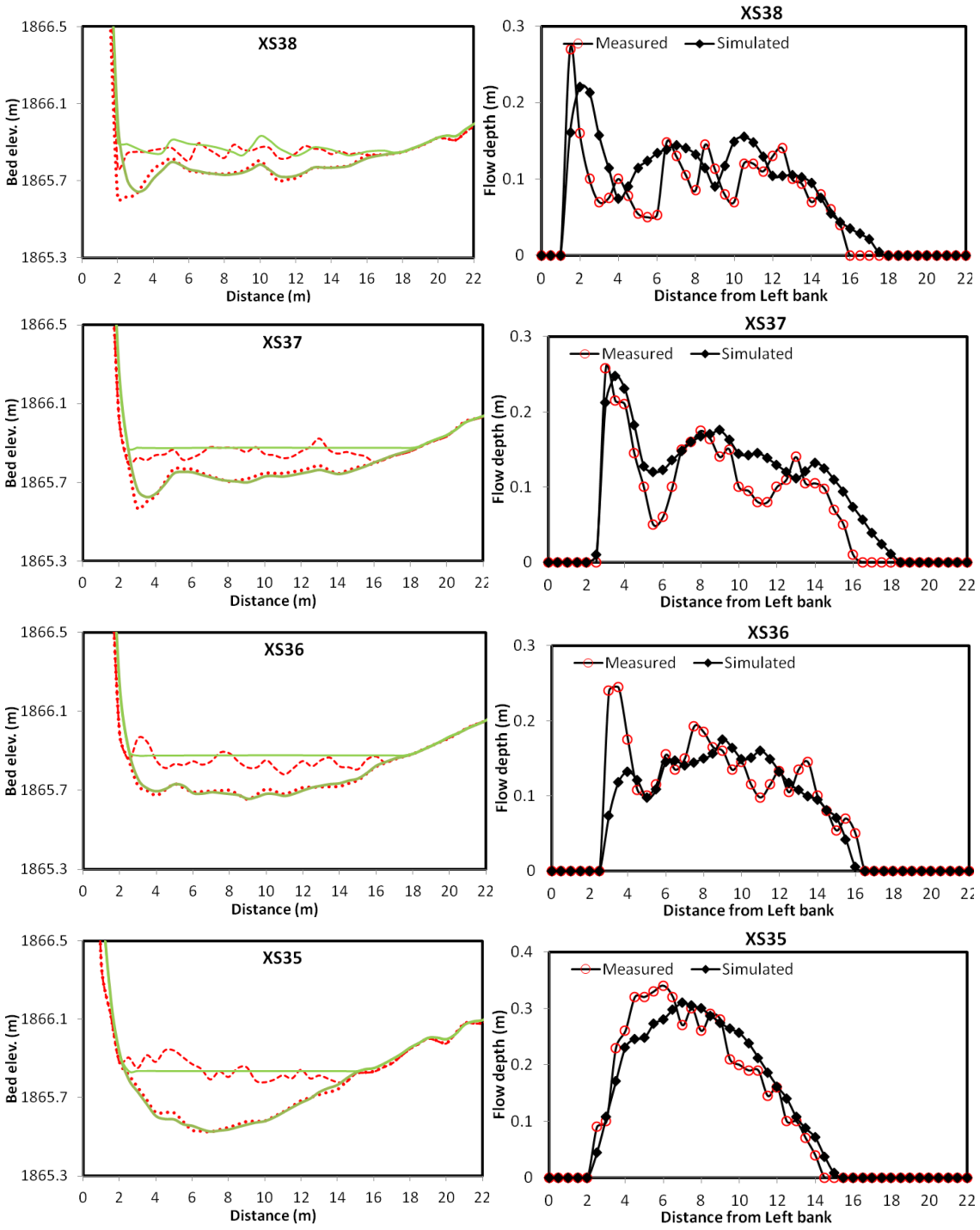


**Figure 8-6 Predicted and measured flow depth along the channel of the study reach.**

Table 8-3 summarizes the results of the sensitivity analysis for point values of simulated and measured flow depth conducted using different values of the roughness depth $R_d$ and the roughness constant $R_c$ using the structural analysis presented in chapter 6 and 7 (Webster, 1997). The coefficient of determination for the relationship between

measured and simulated flow depth is relatively insensitive to various combinations of $R_c$ and $R_d$ values. However, the best fit lines between measurements and model predictions suggest an optimum roughness depth between 0.01 and 0.04 at lower resistance (low values of the constant $R_c$).

The results presented above for low flow conditions illustrate that there is a high level of correspondence between the measured and simulated depths in most areas of the study reach and generally the model replicates the patterns observed in the field data. Differences between model results and field data can be attributed to a wide source of errors and uncertainty. One uncertainty might be the presence of small scale topographic variability between the measured and DEM extracted cross sections that made the model unable to capture flow depths at the deepest sections. From the comparison figure it appears that depth prediction error was attributable to error in the DEM and was not primarily an error of the 2D model itself since in some sections where there is no significant difference in bed elevations of measured and DEM extracted cross sections, the model replicates the measured flow depth.

**Table 8-3 Results of sensitivity analysis for simulated and measured flow depth using different values of effective roughness $R_d$**

| | **Roughness values $R_d$** | | |
|---|---|---|---|
| **$R_c$** | 0.01 | 0.04 | 0.07 |
| 24 | $r^2$ =0.76 | 0.71 | 0.74 |
| | B = 0.84 | 0.9 | 0.94 |
| 15 | $r^2$ = 0.79 | 0.75 | 0.74 |
| | B = 0.83 | 0.94 | 0.96 |
| 5 | $r^2$ = 0.79 | 0.74 | 0.74 |
| | B =0.99 | 1.03 | 1.05 |

Pasternack *et al*. (2004) addressed the issue of DEM accuracy in terms of topographic survey (resolution and accuracy) and DEM generation methodology. In this study, the bed was surveyed with a resolution of 1 point every 1.21 $m^2$, which appeared to be in the higher side as compared to those specified to capture typical gravel bed morphology(Brasington and Richards, 2000;Brasington *et al.*, 2000). It might be possible to reduce error of 2D model predictions at individual nodes by having higher point densities. Second, it was very difficult to accurately predict the discharge due to extreme shallowness of the flow in one of the channels. Although the current meter used for measuring flow velocity was particularly suitable for shallow flows, the coarse bed material made use of the current meter difficult or impossible in some places.

### 8.4.6. Model Velocity Predictions

The general trends in observed lateral variations in velocity were captured by the 2D model (Figure 8-7).

Table 8-4 summarizes the results of the sensitivity analysis for point measurements of modelled and measured velocity conducted using different values of the roughness depth $R_d$ and the roughness constant $R_c$ using the structural analysis presented in chapter 7 (Webster, 1997). The coefficient of determination for the relationship between measured and simulated velocity is considerably lower than that of the relationship between measured and simulated flow depth and insensitive to various combinations of $R_c$ and $R_d$ values. However, the best fit lines between measurements and model predictions suggest an optimum roughness depth between 0.01 and 0.04 at lower resistance (low values of the constant $R_c$), consistent with that of model predictions for flow depth. These relationships are best evaluated and explained by considering the distributed patterns of measured and modelled flow velocities at individual cross sections shown in Figure 8-7 and Figure 8-8. Velocity data comparison is shown only for four sections as detail velocity measurements were carried out only for those cross-sections. Gaps in the velocity data at some cross sections in Figure 8-7 reflect the fact that no measurement were obtained in very shallow flows. XS2 and XS42 showed a general over-prediction, with more than double over-prediction near the true left bank. Coefficients of determination for those two sections are 0.34 and 0.71,

respectively. In both locations flow depth was under-predicted. However, there are also locations where there was no error in depth prediction, although velocity was over-predicted. The other cross-sections showed a close match between observed and predicted velocities; although there is still some degree of over-prediction and coefficients of determination are considerably lower (0.32 and 0.18 for cross sections 1 and 41).

**Table 8-4 Results of sensitivity analysis for modelled and measured velocity using different values of effective roughness $R_d$**

| | **Roughness values $R_d$** | | |
|---|---|---|---|
| **$R_c$** | 0.01 | 0.04 | 0.07 |
| 24 | $r^2$ =0.08 | 0.17 | 0.13 |
| | B = 3.33 | 2.03 | 1.56 |
| 15 | $r^2$ = 0.25 | 0.23 | 0.22 |
| | B = 2.13 | 1.61 | 1.33 |
| 5 | $r^2$ = 0.29 | 0.25 | 0.23 |
| | B =1.21 | 0.98 | 0.81 |

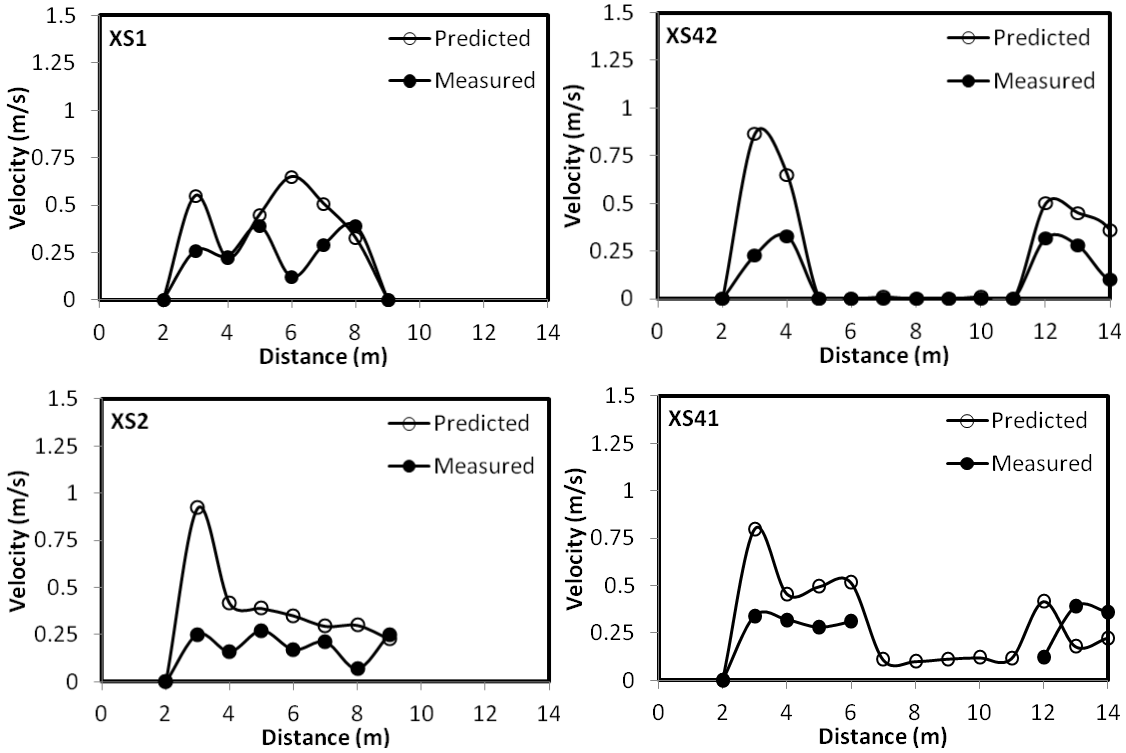


**Figure 8-7 Comparison of observed versus predicted velocities at four cross sections. Distances are from true left bank.**

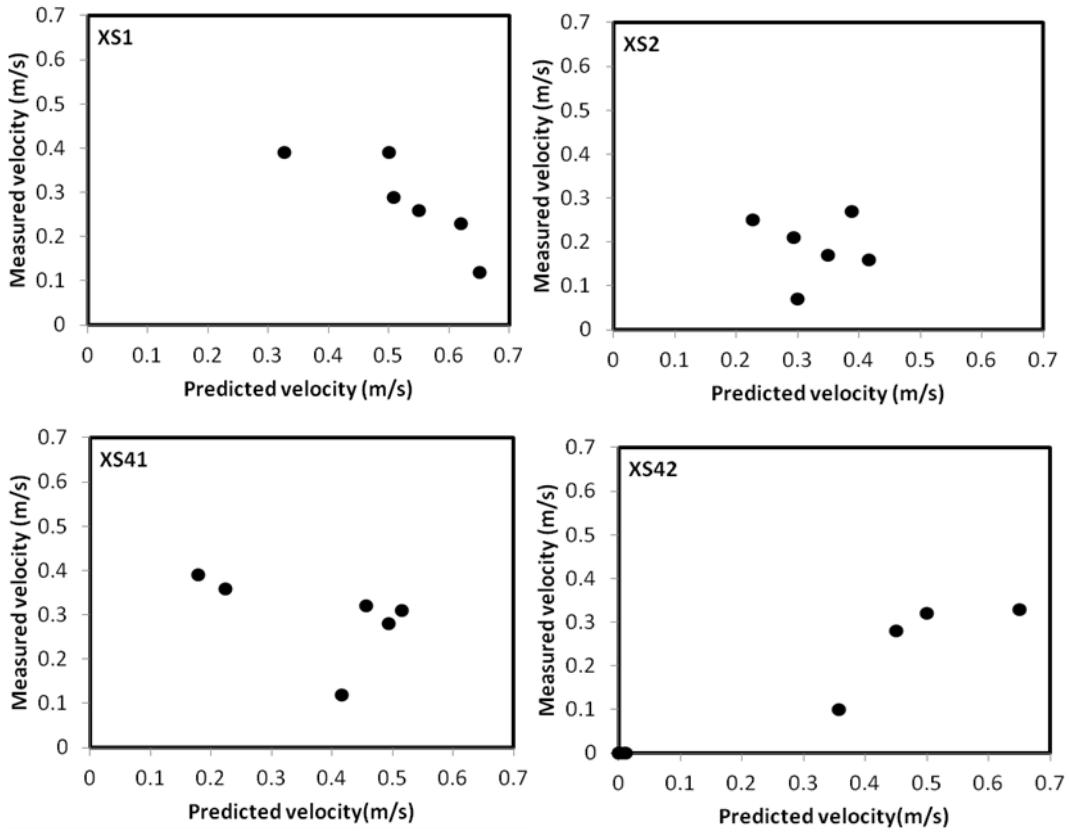

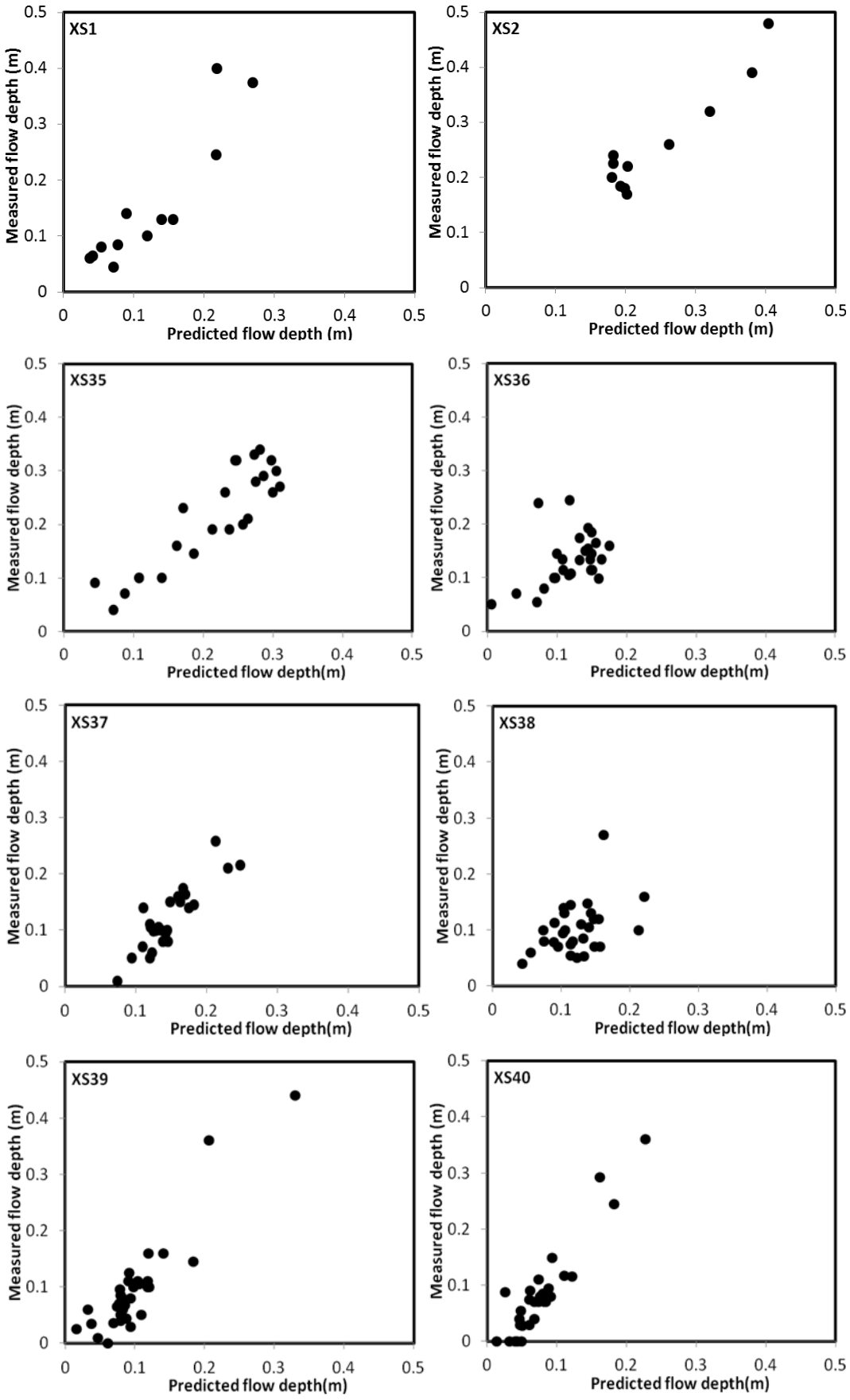
XS1
XS2
XS35
XS36
XS37
XS38
XS39
XS40
Measured flow depth (m)
Predicted flow depth (m)
Predicted flow depth(m)
0
0.1
0.2
0.3
0.4
0.5

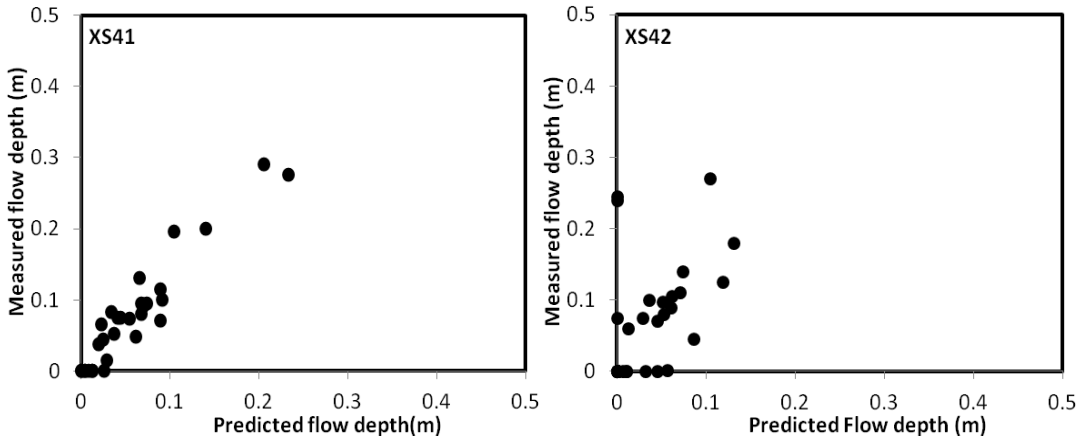


**Figure 8-8 Scatter plot of measured and predicted velocity and flow depth at four sections.**

In most cases locations with worst predictability occurred close to the pool entrance near the river true left bank; however, differences between measured and predicted velocities do not appear to vary systematically with either flow depth or distance from channel banks. A scatter plot of velocity and depth is presented for four cross sections (Figure 8-8). Moreover, the hydraulic model solves the momentum equation written in conservative form, so unit discharge and depth are the primary variables that the model solves for, rather than depth and velocity. Predictions of unit discharge may be much better than those of velocity. Also (as you do mention) poor velocity predictions are inevitable where depth is poorly predicted, and are also very likely in extremely shallow flows, as here.

Figure 8-9 shows spatial patterns of velocity vectors (A) and unit discharge vectors (B) derived from the longitudinal and lateral components of velocity and unit discharge. Vectors are scaled by the magnitude of velocity and unit discharge and contours overlain on these plots indicate flow depth magnitude for a discharge at the time of measurement which is equal to $0.35 m^3 s^{-1}$. Discharge at the time of measurement was calculated based on the approach mentioned in section 8.4.3. Both vectors are associated with two zones of high velocity and unit discharge that are found at the entrance and exit of the reach, although unit discharge values are also higher at the middle of the reach. Flow is also concentrated in the narrower portion of the section near the true left bank where the channel bed is scoured.

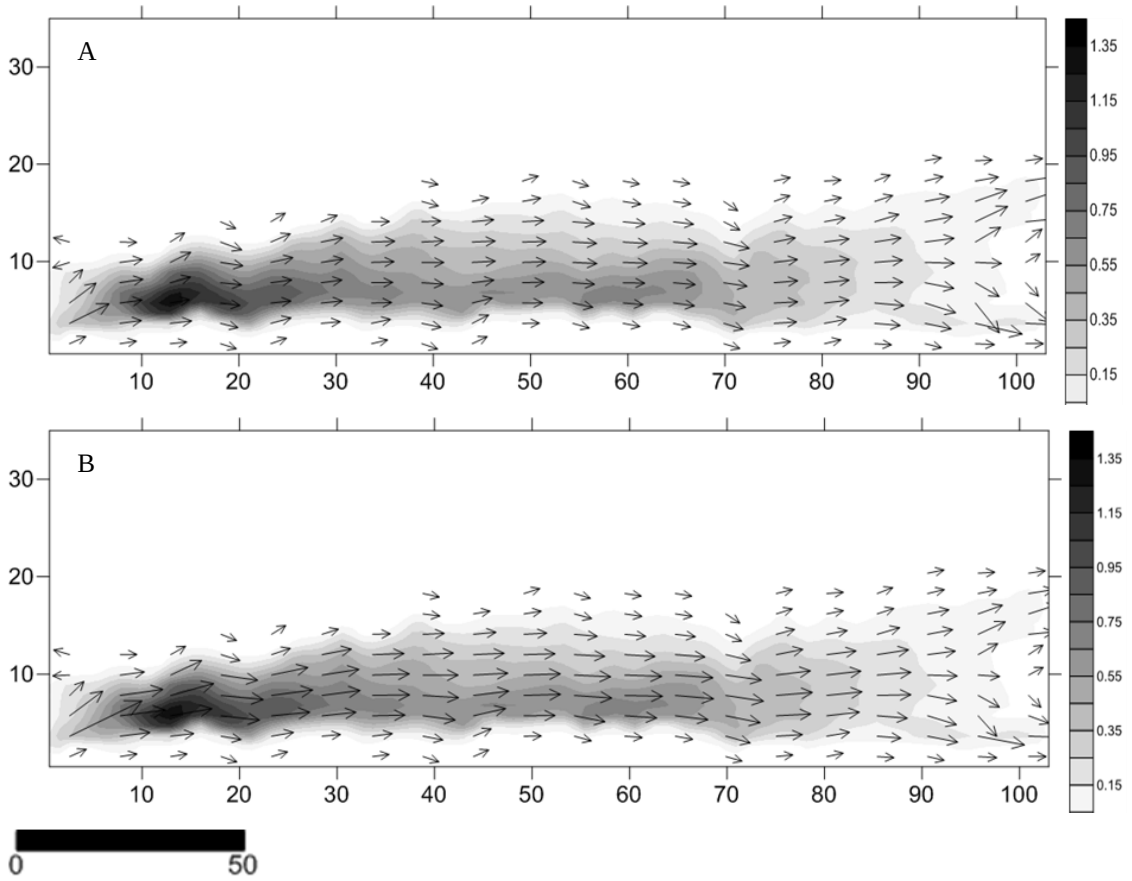


**Figure 8-9 Model simulation for the study reach at a discharge of 0.35 $m^3/s$. Shading corresponds to depth solutions and arrows correspond to (A) velocity vectors; (B) unit discharge vectors (both scaled to magnitude).**

### 8.4.7. Simulated Hydraulics at Higher Discharges

Flow patterns within the study reach were simulated for higher discharge values of 2, 3, 6, 8 and 10 (equivalent to the average annual discharge) $m^3s^{-1}$. Flow values were obtained from a flow duration curve prepared for a dam site located at about 1km above the study reach (Figure 8-3). Based on this flow duration curve, the discharge available 50% of the time is nearly 6 $m^3/s$. The purpose of these additional model runs was not to test the model in the same way as for low flows, since no field measurements could be obtained at higher discharges. But, the objective was twofold. Firstly, to evaluate the potential for using the model to quantify depth, velocity and shear stress frequency distributions for a range of discharges. Secondly, simulated flow depth and shear stress values will be fitted to the two-parameter gamma probability density function and values of the shape parameters will be obtained (see chapter 7, section 7.6 for explanation of this approach). The shape parameters obtained by fitting model extracted shear stress will then be compared with the shape parameters from the regression

equations developed from flume studies as a function of total water surface width and mean flow depth in chapter 6 (section 6.9).

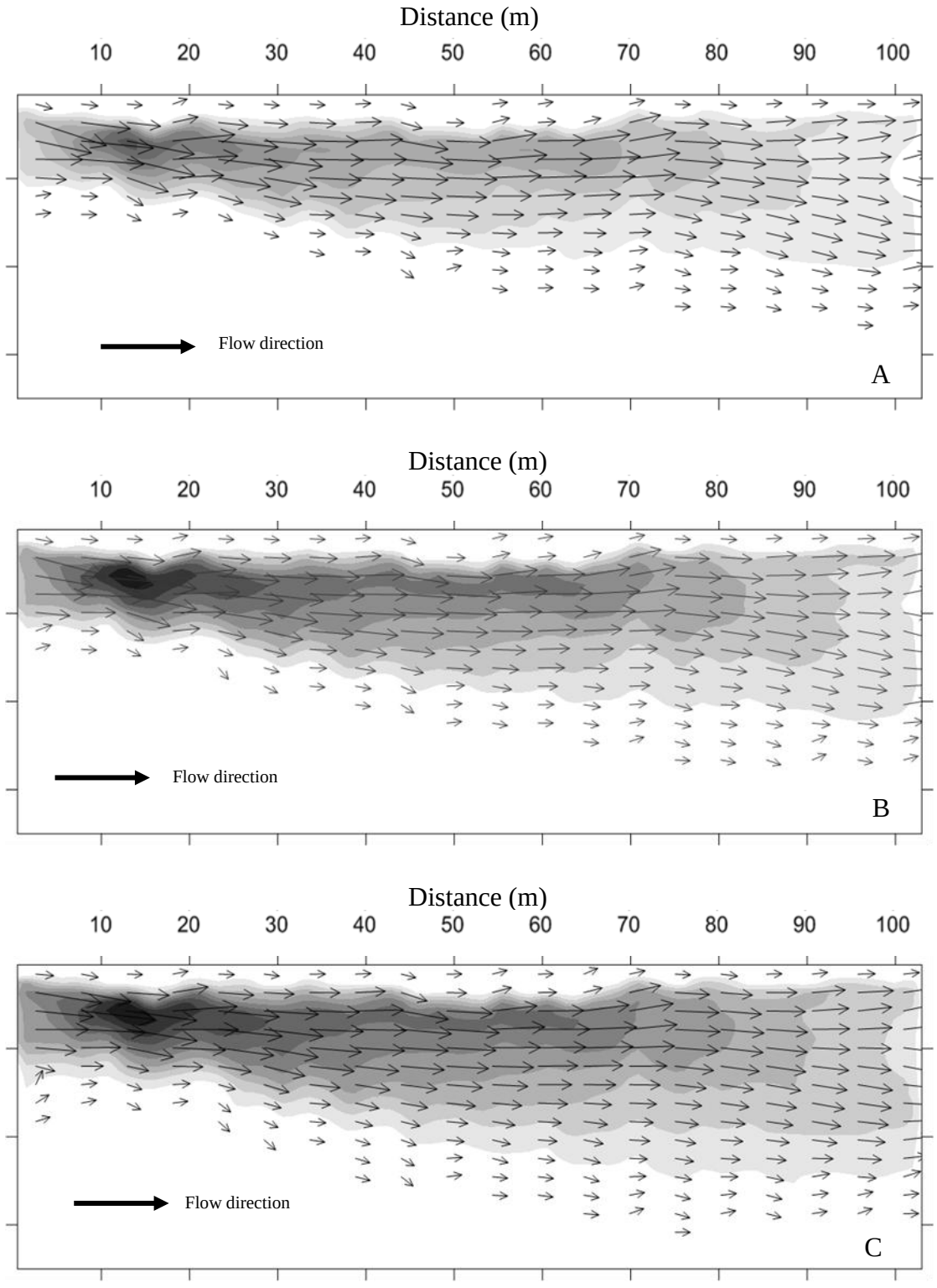

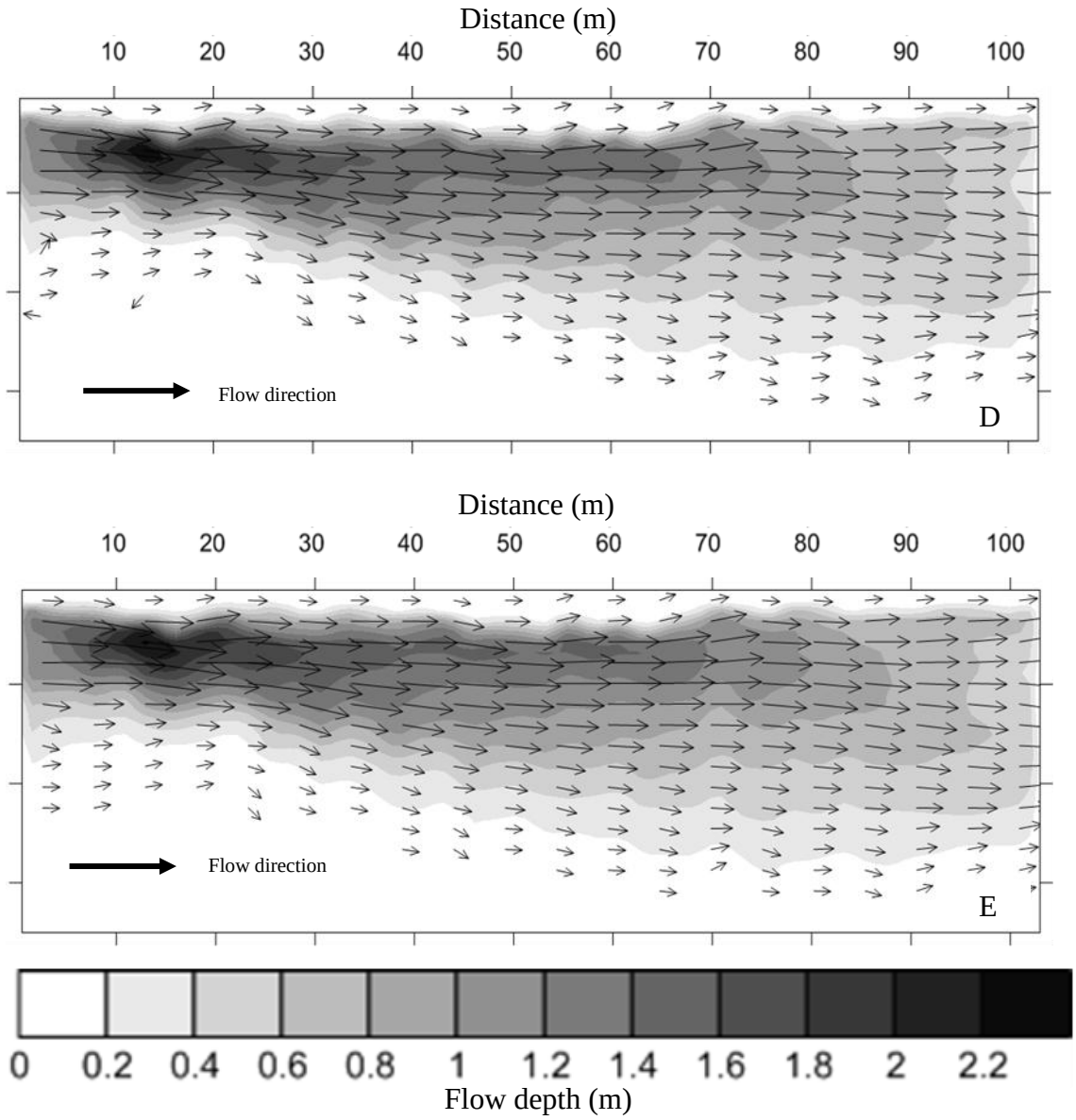


**Figure 8-10 Simulated patterns of flow depth within the study reach for discharges of (a) 2 $m^3$/s, (b) 3 $m^3$/s, (c) 6 $m^3$/s, (d) 8 $m^3$/s, and (e) 10 $m^3$/s. In the scale flow depth is represented in meters.**

The maximum discharge value simulated was limited to 10 $m^3$ $s^{-1}$ because at higher discharges the surveyed channel extent was overtopped and there were no topographic data available beyond the 35m wide channel surveyed. Figure 8-10 shows the simulated flow depths within the study reach at discharges of 2, 3, 6, 8 and 10$m^3$/s. At low flow water is confined to the deepest channel at the true left bank of the river. This area is a pool which mostly contains ponded water and extends up to beyond the middle of the study reach. There was a gradual rise in thalweg bed elevation along the flow direction that limits the extent of the pool. As discharge rises there is an increase in the area of

flow on higher surfaces towards the true right bank of the river and a tendency for increased flow depth towards the true left bank of the river. As the left bank is characterized by highly erodible and nearly vertical steep slope, there was no significant increase in flow surface area on the left as discharge rises. The result is that the change in width as discharge increases is small compared to the change in depth, and hence a slightly declining width to depth ratio (Figure 8-11A). Photographs in Figure 8-4 E, F, G and H can help in interpreting flow patterns shown in Figure 8-10 to what is actually in the field.

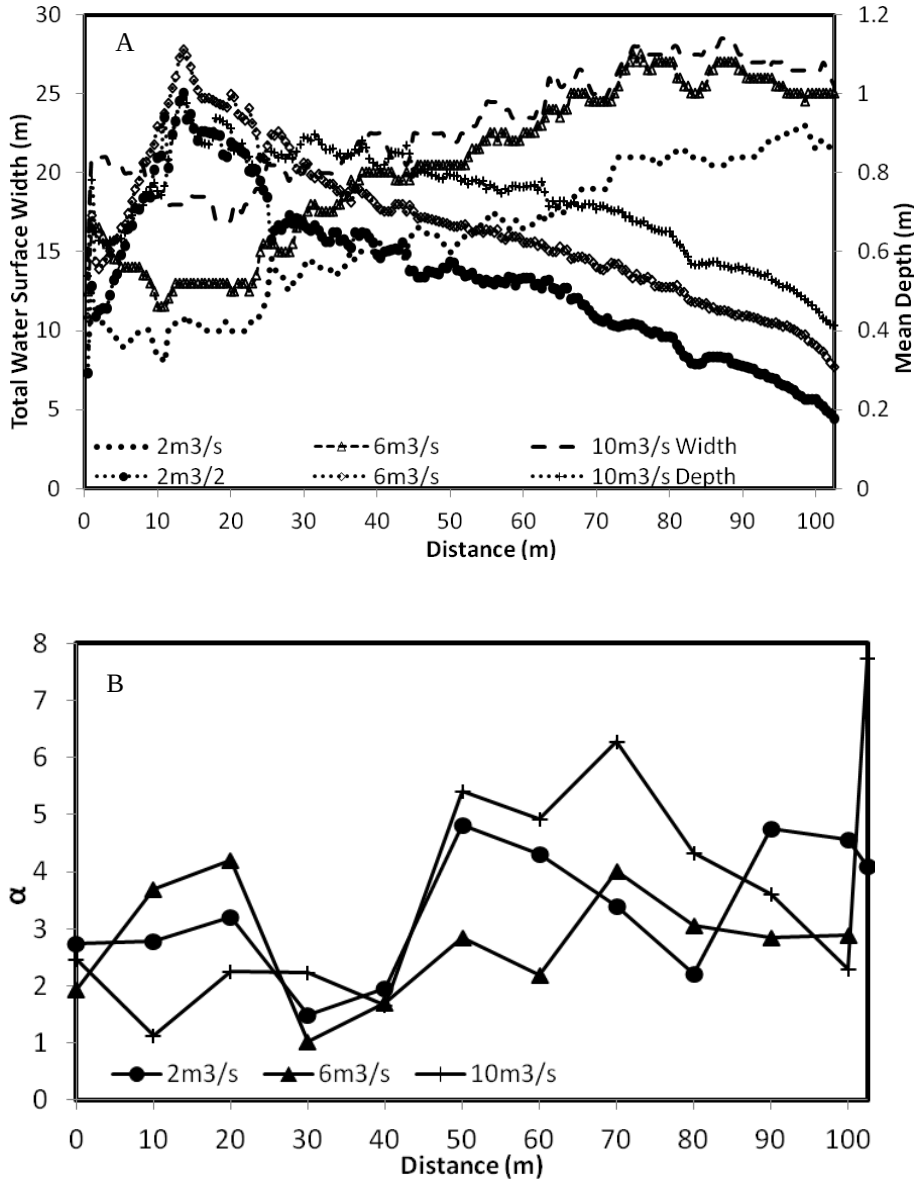


**Figure 8-11 Longitudinal variation in channel characteristics along the River Megech; A) Water surface width and flow depth for three discharges; and C) the gamma distribution shape parameter (α) determined from surveyed cross section topography for three discharges.**

Figure 8-11 shows changes in channel characteristics along the Megech River. Total water surface width increases in the downstream direction although it does not show noticeable changes at the middle reach where the pool is located. Longitudinal variation of mean flow depth also follows two patterns. Flow depth appear to increase continuously in the downstream direction up to the pool (around 15m from the inlet) and then it decreases after it exits the pool (Figure 8-11A). Longitudinal variations in the gamma probability density function shape parameter (α) are shown in Figure 8-11B for three discharges. α are determined by fitting model derived shear stress to a two-parameter gamma PDF (refer to chapter 7, section 7.5 for explanation of this). It can be seen from the figure that α decreases in an upstream direction. This indicates greater spatial variability in bed topography in the upstream part of the reach. For most of the middle reach, α value remains high indicating small spatial variability associated with the pool. However, the relationship between discharge and shape parameter α is not clear, although there is an indication of increase in α value with discharge at the entry and exit of the study reach. Previous investigators (Paola, 1996;Nicholas, 2000) have observed a clear trend of increase in α value as discharge rises. However, Nicholas (2000) also noticed that longitudinal trends in shape parameter α are more marked at peak discharges than mean annual flow for the case of Waimakariri River. Moreover, Paola (1996) also observed a weak tendency for α to increase with discharge for Ohau River. In this case simulations were carried out for much smaller discharges than the peak due to the limited availability of topographic information. This might be the reason for absence for a clear relationship between discharge and the shape parameter.

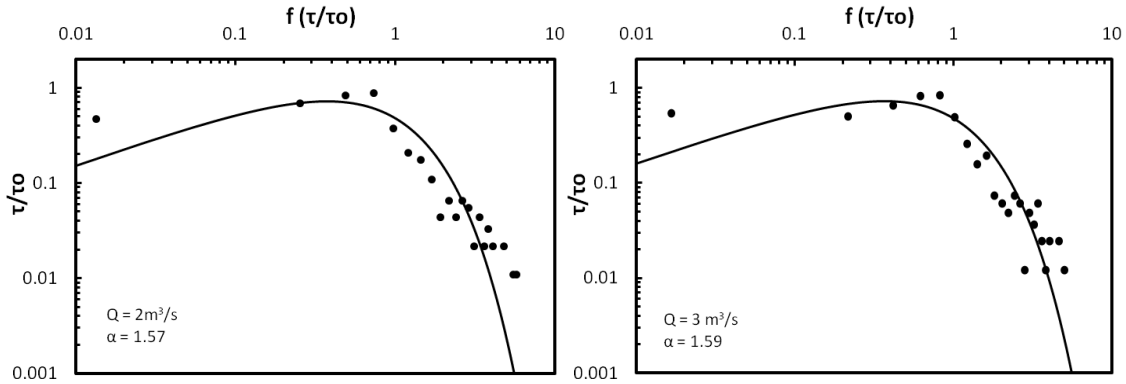

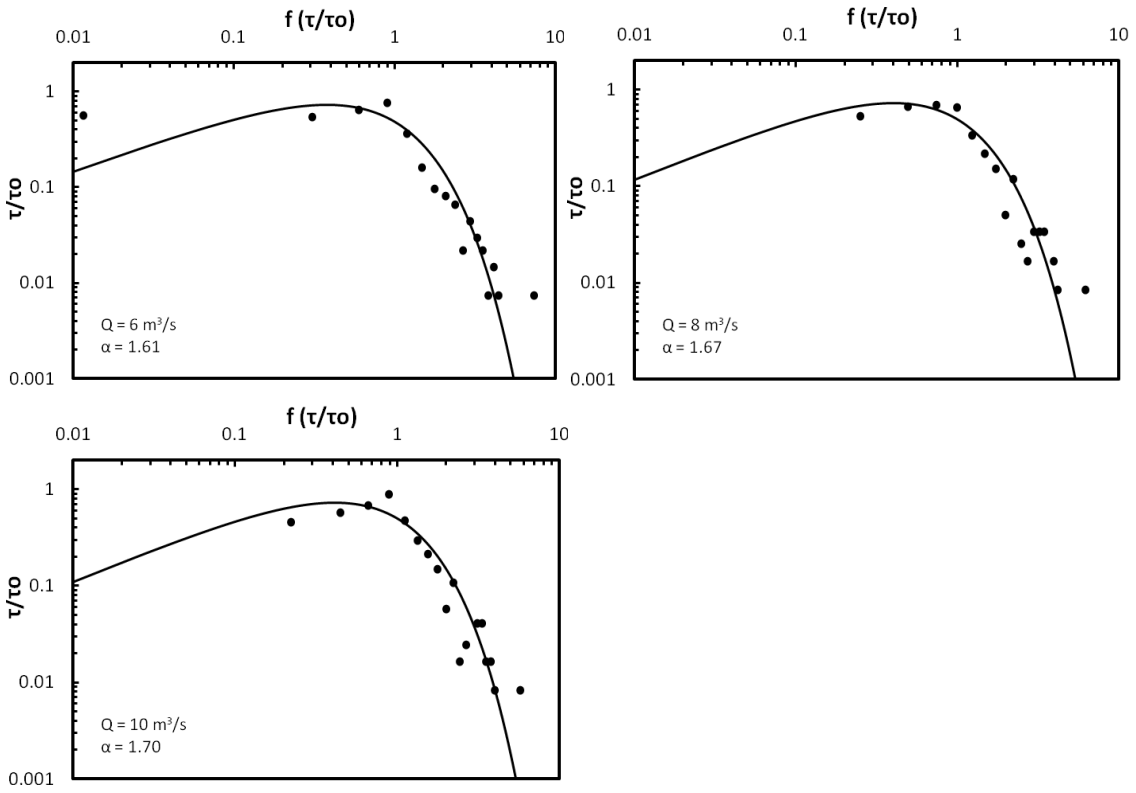


**Figure 8-12 Gamma distribution fitted to simulated boundary shear stress distribution for five discharges.**

Paola (1996) used the data obtained by Mosley (1982) to calculate shear stress distributions for Ohau River at three different discharges. A similar procedure was carried out here using the modelled shear stress calculated by applying the procedure in chapter 7, section 7.5. Boundary shear stresses determined at each point of the ten cross sections where there are measured data were merged together and fitted to a two parameter gamma distribution (equation 7.9 in section 7.6). Distributions of this form fitted to the modelled shear stresses within the study reach for five discharges are shown in Figure 8-12. Although at a low rate, these relationships illustrate a trend towards an increase in α at higher flows. This is consistent with the trend observed by Paola for Ohau River and Nicholas (2003) of Avoca River, New Zealand and is indicative of a reduction in the variance of the boundary shear stress distribution at high discharges.

One of the drawbacks of stochastic approaches to bed load prediction is the fact that the method requires a large amount of channel morphology data in order to derive the input parameters of the distribution at a range of discharges (Bertoldi *et al.*, 2009). The difficulty and lack of a relationship for estimating the gamma distribution shape parameters from mean morphological parameters was also one of the reasons that

hindered the development of this method. Based on this, in chapter 6 (section 6.9) it was attempted to develop a regression equation to calculate the gamma distribution shape parameter (α). The equation was developed as a function of total water surface width and mean flow depth and reads as:

$$\alpha = 0.00935(W/h) + 1.0035 \qquad 8\text{-}3$$

Where α is the gamma distribution shape parameter, W is total water surface width and h is mean flow depth. Application and testing of equation 8.3 for the field study reach directly by using measured data is difficult as it requires data like total water surface width and mean flow depth for different discharges. One way identified to investigate the validity of this relationship for the field study reach, therefore, was to run the two dimensional hydraulic model for the field study reach and extract the required information (water surface width and mean flow depth) to calculate the shape parameter α using equation 8.3 for a range of discharges. This was done for the cross sections with measured data. Further to this, based on outputs of the hydraulic model, shear stress was calculated using the approach mentioned in chapter 7 (section 7.5) for cross sections with measured data. This shear stress was then normalized and fitted to a two parameter gamma probability density function (equation 7.9 in chapter 7) to determine a series of α values for a range of discharges and various cross sections. Figure 8-13 shows relationship between α values determined from the regression equation (equation 8.3) and by fitting modelled and normalized shear stress values to the two parameter gamma PDF for the 10 the cross sections of the field reach with measured data.

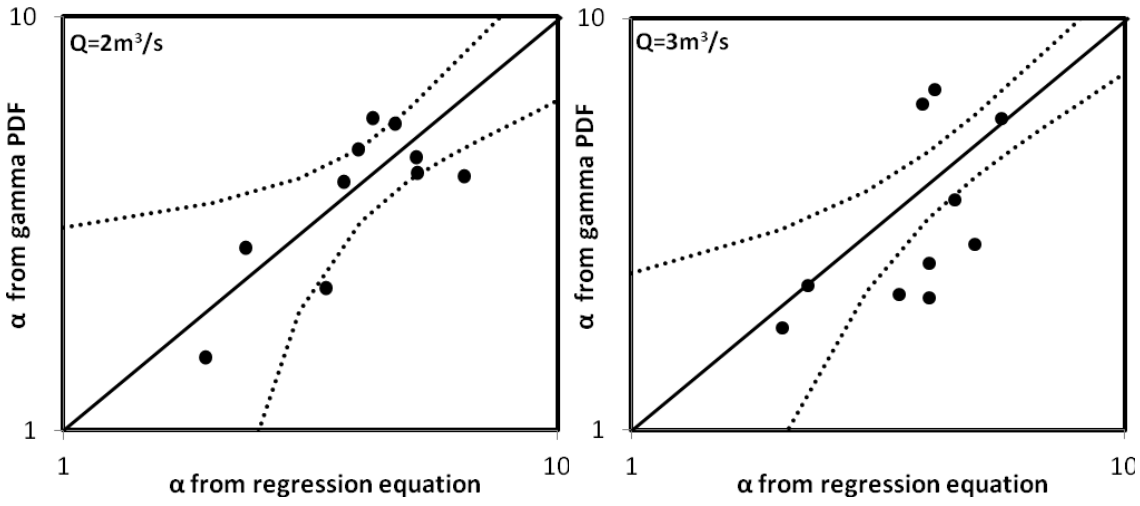

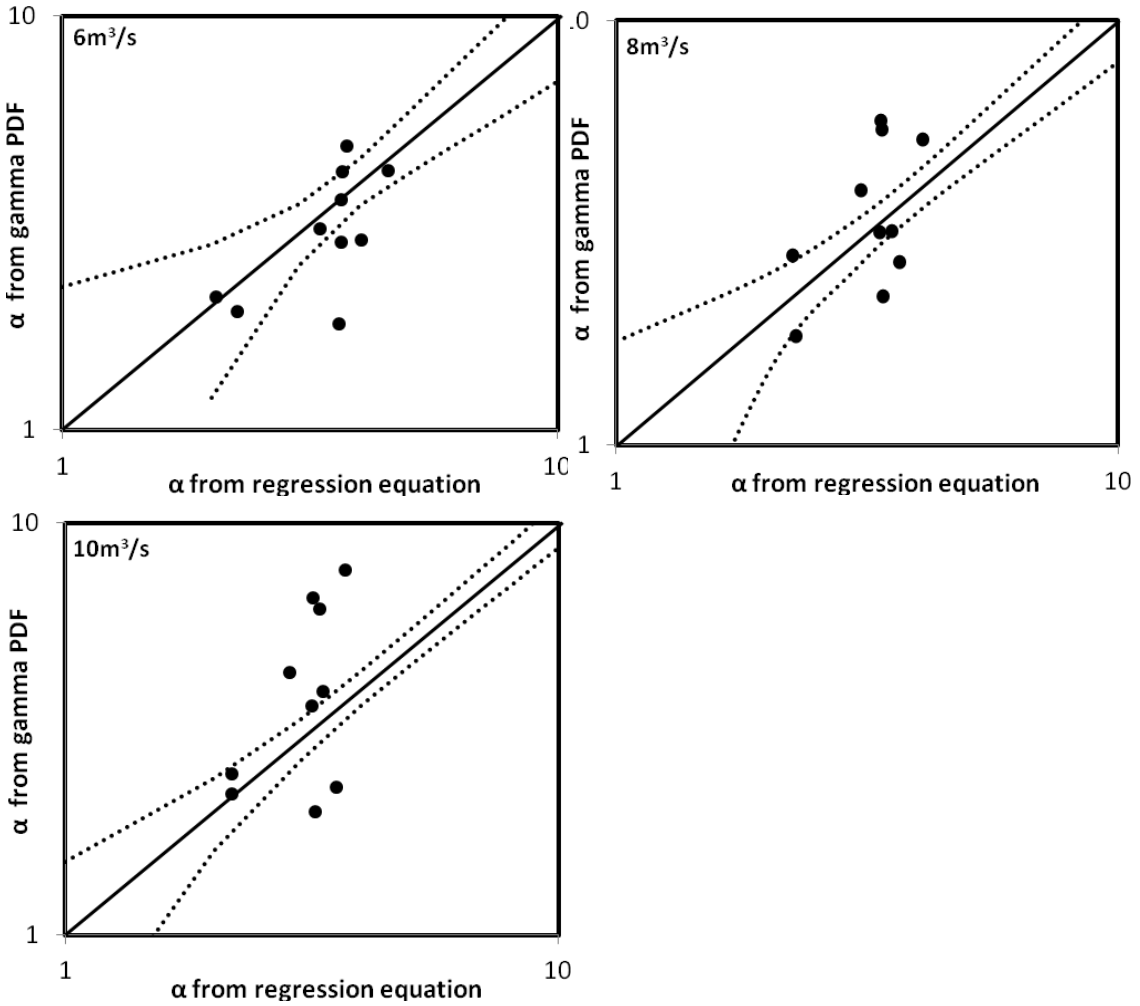


**Figure 8-13 Relationship of alpha values obtained by fitting modelled and normalized shear stress data to gamma PDF and from the regression equation (equation 8.7). Solid line is 1:1 while dashed lines are 95% confidence limits.**

For a discharge of 2m$^3$/s, more than 70% of the predicted α values fell within the 95% confidence limits of α-values obtained by fitting the 2D shear stress to a gamma PDF. However, as discharge rises it appeared that there is much more scatter in the data, although this is not consistent for all discharge values. As discharge rises, the depth increases much faster than the water surface width in the middle part of the reach (where there is measured data) due to the nature of the topography. This made the ratio (w/h), and hence the overall value of α, reduce as discharge rises. This will potentially underestimate the value of α. However, it has been shown that the magnitude of the effect of α varies with average stream power and is greatest at low stream power (low shear stress) (Bertoldi *et al.*, 2009, Fig. 5). On the basis that higher discharge will contribute to high flow depth and hence high shear stress, it is thought that the effect of underestimation of α value at increasing discharge may not add significantly to the error

in sediment transport estimation. The magnitude of α values predicted using the two methods is typically between 1 and 4, but as high as 8, depending on topography, flow stage and channel slope, which is consistent with previous studies (Nicholas, 2000). Despite the unaccountable sources of error inherent in the derivation of the regression equation from flume data and the hydraulic model, the equation gives a good first-hand estimate of α value that can be used when other topographic information is unavailable.

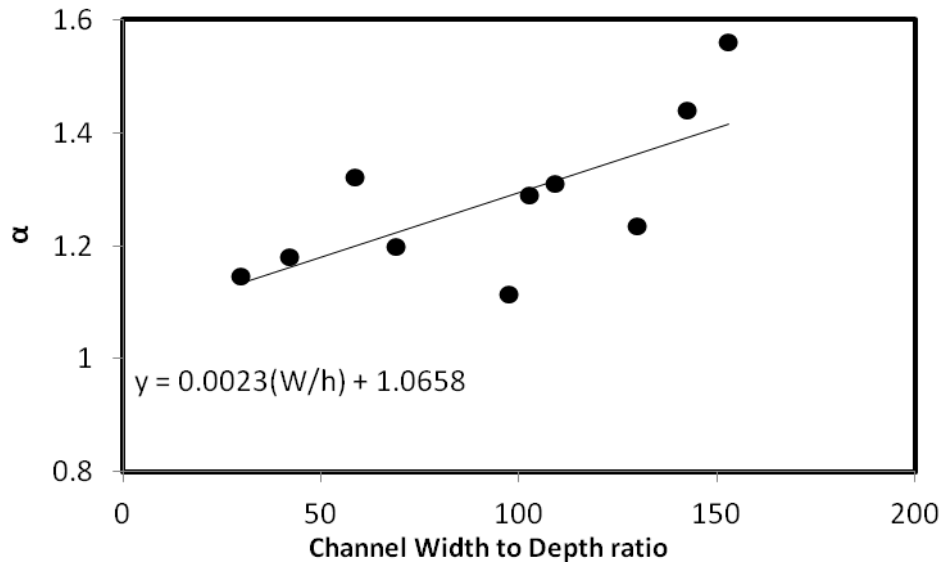


**Figure 8-14 Relationship between channel width to depth ratio and gamma shape parameter for Megech River**

Figure 8-14 shows the relationship between measured channel width to depth ratio and the gamma shape parameter α. α values were obtained by fitting shear stress calculated by using the measured flow depth and the 'depth-slope product' shear stress equation to a gamma PDF. A simple linear regression was performed on the data to determine if there was significant relationship between α and channel width to depth ratio. The results are reasonably encouraging, although the points are scattered with a lower correlation (0.5) for the relationship obtained between field measured parameters. There are some points to make about the comparison of the equation from the flume (chapter 6, section 6.9) and field measurements. There is high level of variance in the equations generated from different sections of the flume. This relates in part to the problem inherent in the assumptions used to obtain the required data (water surface width and mean flow depth), which will limit its application. Field measurement technique was better with respect to reliability than the case applied in the flume, although there was some uncertainty with very shallow flows. However, field measurements were done

only for few cross sections. It is interesting that both field and laboratory data follow the same trend, although it is counter to the idea that alpha will increase at higher flows (greater depths). However, it appears that alpha has very little dependency on flow depth especially for shallow flows. In both the experiments and the field study, flow depth was relatively small. In both of the equations generated from the flume and field measurement, the slope of the regression line is low indicating the fact that there is weak dependency of α value on channel width to depth ratio. That means at high values of width to depth ratio (which are characteristics of braided rivers), alpha values do not increase significantly. A t-statistic was used to test the significance of the slope. The t-statistic for the slope was significant at the 0.05 critical alpha level, with a t value of 2.8, p = 0.023. The constant term from both equations is almost equivalent.

As summary a lot of important information have been generated by the application of the two dimensional hydraulic model. Consequently, the two dimensional hydraulic models are proved effective and powerful tools capable of generating hydraulic information that would be difficult to obtain in the field at an equivalent spatial resolution (Nicholas, 2003). Comparison of simulated and measured hydraulic variables at measured flow conditions illustrates that the model replicates the systematic trends especially in measured flow depths. Considering the difficulty of obtaining high quality field data at times of peak flow, simulations conducted for a range of discharges demonstrate the potential for using two dimensional hydraulic models to quantify the reach-scale hydraulic characteristics of gravel bed rivers. Results presented in this case demonstrate that modelled shear stress distributions exhibit trends that are consistent with previous investigations. This is important as the distributed hydraulic information extracted from the model can be used in the development of statistical models of braided river flow characteristics that can be used to derive bedload transport rates of braided rivers (Nicholas, 2000;Paola, 1996).

As noted in chapter 6, a relationship between the width of the shear stress distribution (α) and channel morphological parameter is very important as it avoids the huge amount of data required to calculate α. The approach followed in this section is important and provides a means of investigating relationships between shear stress frequency distribution characteristics, bedload transport and indices of channel morphological

parameter (e.g., width to depth ratio or braiding index). Based on the collected data, a relationship has been developed between channel width to depth ratio and the gamma shape parameter α. The relationship is established based on data from only a small reach of the river and for a particular flow condition. This may limit its application. Visual comparison of this equation with the one developed from flume data in chapter 6 shows that the slope of the linear regression line is several times less than the slope of the equation developed from flume data. However, in both cases the dependency of α on width to depth ratio is weak.

The Megech River is undergoing frequent changes in channel morphology due to activities occurring upstream, especially gravel mining. There is also an ongoing dam project for irrigation and water supply purposes. It would be interesting to re-survey the river channel to identify the changes in channel pattern and sediment transport dynamics that result from these effects (especially dam construction). The area of interest could also be expanded in length and width. Model simulations for the river couldn't be made for higher discharges due to the fact that topographic data were not available. More fieldwork would also enable collection of better resolution data which could help to improve the accuracy of the DEMs produced, more flow depth and velocity measurements from a greater number of cross sections, allowing more general comparisons to be drawn on the trends of some parameters between the output from the experimental runs and the conditions on the Megech gravel bed river. Although the results would not be Froude-scaled to the field prototype, some scaling could be made to ensure similar conditions and so the results would still be of interest in determining how the channel may, potentially, respond in the future.

## 8.5. FINAL CONCLUSION

The micro-scale physical model developed in this project has proved its value as a tool for investigating braided channel evolution. Moreover, the effects of aggradation and degradation processes observed were comparable to those that have been noted in field studies. Despite limitations of scale, and therefore the inability to verify the results with a natural river prototype, the micro-scale model nevertheless has substantial value as a means of investigating aggradation and degradation scenarios and the effects of lateral

variability of sediment transport in braided channels. Based on the results of this study it is suggested that experimental micro-scale physical modelling of braided rivers provides a valuable tool with which to investigate channel processes that occur in longer timescales and obtaining insights into other aspects of fluvial morphodynamics.

The results obtained here provide an understanding of how braided rivers may respond to changes in sediment supply that might be used to predict, in a general sense, likely river responses to upstream land use change or dam construction. This investigation has also shown that, although channel pattern indices (such as braiding intensity) will vary with discharge, pattern changes associated with aggradation and degradation will be visible at any single discharge. The detailed spatial and temporal patterns of channel pattern indices (width to depth ratio and braiding intensity) and the width of shear stress distribution shape parameter ($\alpha$) over the course of the experimental channel evolution provided insight into how lateral flow variability should be incorporated into one dimensional numerical sediment routing models. The data also demonstrate that channel aggradation increases sediment transport by promoting lateral flow variability. This in turn feeds back to further aggradation depending on the response of the channel. This process will continue up to a point where there is no substantial variation in channel width to depth ratio. Beyond this point, there will be a reduction in sediment transport rates as a result of reduction in mean shear stress. This may in turn feed back to promote further aggradation.

# REFERENCES

ACKERS, P. & CHARLTON, F. 1970. Meander geometry arising from varying flows. *Journal of hydrology,* 11**,** 230-252.

AHNERT, F. 1970. A comparison of theoretical slope models with slopes in the field. *Zeitschrift für Geomorphologie, Berlin, Supplementband***,** 88-101.

ASCE 2000. Hydraulic modeling: Concepts
and practice. *Manual and Report No. 97, ASCE, Reston, Va.*

ASHMORE, P. 1991. Channel morphology and bed load pulses in braided, gravel-bed streams. *Geografiska Annaler. Series A. Physical Geography***,** 37-52.

ASHMORE, P. 1991. Channel morphology and bed load pulses in braided, gravel-bed streams. *Geografiska Annaler: Series A, Physical Geography,* 73**,** 37 - 52.

ASHMORE, P. 1993. Anabranch confluence kinetics and sedimentation processes in gravel-braided streams. *Geological Society: London: Special Publications,* 15**,** 129 - 146.

ASHMORE, P. 2001. Braiding phenomena: statics and kinetics. *Gravel Bed Rivers V***,** 95-121.

ASHMORE, P. & CHURCH, M. 1998. Sediment transport and river morphology: a paradigm for study. Water Resources Publications: LLC Highlands Ranch, CO.

ASHMORE, P. & CHURCH, M. 1998. Sediment transport and river morphology: a paradigm for study. *Water Resources Publications LLC, Highlands Ranch, Colorado***,** 115-148.

ASHMORE, P. E. 1982. Laboratory modelling of gravel braided stream morphology. *Earth Surface Processes and Landforms,* 7**,** 201-225.

ASHMORE, P. E. 1988. Bed load transport in braided gravel bed stream models. *Earth Surface Processes and Landforms,* 13**,** 677-695.

ASHMORE, P. E. 1988. Bed load transport in braided gravelbed stream models. *Earth Surface Processes and Landforms,* 13**,** 677-695.

ASHMORE, P. E. 1991a. Channel morphology and bed load pulses in braided, gravel-bed streams. *Geografiska Annaler. Series A. Physical Geography***,** 37-52.

ASHMORE, P. E. 1991a. Channel morphology and bed load pulses in braided, gravel-bed streams. *Geografiska Annaler. Series A, Physical Geography,* 73**,** 37-52.

ASHMORE, P. E. 1991b. How do gravel-bed rivers braid. *Canadian Journal of Earth Sciences,* 28**,** 326-341.

ASHMORE, P. E. 1991b. How do gravel-bed rivers braid? *Canadian Journal of Earth Sciences,* 28**,** 326-341.

ASHMORE, P. E. 1993. Anabranch confluence kinetics and sedimentation processes in gravel-braided streams. *Geological Society, London, Special Publications,* 75**,** 129.

ASHMORE, P. E. & CHURCH, M. 1998. Sediment transport and river morphology: a paradigm for study. *Water Resources Publications LLC, Highlands Ranch, Colorado***,** 115-148.

ASHMORE, P. E., SERVICES, A. E. P. & DIVISION, A. A. E. R. M. 1985. *Process and form in gravel braided streams: laboratory modelling and field observations,* Alberta Environment, Environmental Protection Services, Research Management Division.

ASHWORTH, P., BEST, J., LEDDY, J. & GEEHAN, G. 1994. The physical modelling of braided rivers and deposition of fine-grained sediment. *Process models and theoretical geomorphology***,** 115–139.

ASHWORTH, P. & FERGUSON, R. 1986. Interrelationships of channel processes, changes and sediments in a proglacial braided river. *Geografiska Annaler. Series A. Physical Geography***,** 361-371.

ASHWORTH, P., FERGUSON, R. & POWELL, M. 1992. Bedload transport and sorting in braided channels. *Dynamics of gravel-bed rivers***,** 497-513.

ASHWORTH, P. J., BEST, J. L. & JONES, M. 2004. Relationship between sediment supply and avulsion frequency in braided rivers. *Geology,* 32**,** 21.

ASHWORTH, P. J., BEST, J. L. & JONES, M. 2004. Relationship between sediment supply and avulsion frequency in braided rivers. *Geology,* 32**,** 21 - 24.

ASHWORTH, P. J., BEST, J. L. & JONES, M. 2006. The relationship between channel avulsion, flow occupancy and aggradation in braided rivers: insights from an experimental model. *Sedimentology***,** 1 - 17.

ASHWORTH, P. J., BEST, J. L., LEDDY, J. O. & GEEHAN, G. W. 1994. The physical modelling of braided rivers and deposition of fine-grained sediment. *In:* KIRKBY, M. J. (ed.) *Process Models and Theoretical Geomorphology*. Chichester, UK: John Wiley and Sons Ltd.

BABAEYAN-KOOPAEI, K., ERVINE, D., CARLING, P. & CAO, Z. 2002. Velocity and turbulence measurements for two overbank flow events in River Severn. *Journal of Hydraulic Engineering,* 128**,** 891.

BAGNOLD, R. 1973. The nature of saltation and of'bed-load'transport in water. *Proceedings of the Royal Society of London. A. Mathematical and Physical Sciences,* 332**,** 473-504.

BATHURST, J. 1997. Environmental river flow hydraulics. *Applied fluvial geomorphology for river engineering and management***,** 69-93.

BATHURST, J., GRAF, W. & CAO, H. 1987. Bed Load discharge equations fo steep mountain rivers.

BERTOLDI, W., ASHMORE, P. & TUBINO, M. 2009. A method for estimating the mean bed load flux in braided rivers. *Geomorphology,* 103**,** 330-340.

BHALLAMUDI, S. M. 1991. Numerical modeling of aggradation and degradation in alluvial channels. *Journal of hydraulic engineering,* 117**,** 1145.

BIRON, P. M., ROBSON, C., LAPOINTE, M. F. & GASKIN, S. J. 2004. Comparing different methods of bed shear stress estimates in simple and complex flow fields. *Earth Surface Processes and Landforms*, 29**,** 1403-1415.

BLUCK, B. 1979. Structure of coarse grained braided stream alluvium. *Transactions of the Royal Society of Edinburgh,* 70**,** 181-221.

BONDESAN, M. 2001. with a contribution by Castaldini, D., 2001. Hydrography. In: Castiglioni, G.B., Pellegrini, G.B. (Eds.), Illustrative Notes of the Geomorphological Map of Po Plain (Italy), Suppl. Geogr. Fis. Dinam. Quat. IV. 33–44.

BRADBROOK, K., LANE, S. & RICHARDS, K. 2000. Numerical simulation of three-dimensional, time-averaged flow structure at river channel confluences. *Water resources research,* 36**,** 2731-2746.

BRAS, R. L., TUCKER, G. E. & TELES, V. 2003. Six myths about mathematical modeling in geomorphology. DTIC Document.

BRASINGTON, J. & RICHARDS, K. 2000. Turbidity and suspended sediment dynamics in small catchments in the Nepal Middle Hills. *Hydrological processes,* 14**,** 2559-2574.

BRASINGTON, J., RUMSBY, B. & MCVEY, R. 2000. Monitoring and modelling morphological change in a braided gravel-bed river using high resolution GPS-based survey. *Earth Surface Processes and Landforms,* 25**,** 973-990.

BRICE, J. 1960. Index for description of channel braiding. *Geological Society of America Bulletin,* 85**,** 581-586.

BRICE, J. C. 1964. *Channel patterns and terraces of the Loup Rivers in Nebraska,* US Government Printing Office.

BRIDGE, J. S. 1993. The interaction between channel geometry, water flow, sediment transport and deposition in braided rivers. *Geological Society, London, Special Publications,* 75**,** 13.

BRISTOW, C. & BEST, J. 1993. Braided rivers: perspectives and problems. *Geological Society, London, Special Publications,* 75**,** 1-11.

BRYANT, M., FALK, P. & PAOLA, C. 1995. Experimental study of avulsion frequency and rate of deposition. *Geology,* 23**,** 365.

CAO, Z. & CARLING, P. Mathematical modelling of alluvial rivers: reality and myth. Part 2. Special issues. 2002. Telford, 297-307.

CAO, Z. & CARLING, P. Mathematical modelling of alluvial rivers: reality and myth. Part 2: Special issues. 2002. London: Published for the Institution of Civil Engineers by Thomas Telford Ltd., c2000-c2003., 297-308.

CARSON, M. 1984. Observations on the Meandering-Braided River Transition, the Canterbury Plains, New Zealand: Part One. *New Zealand Geographer,* 40**,** 12-19.

CARSON, M. A. & GRIFFITHS, G. A. 1987. Bedload transport in gravel channels. *Journal of Hydrology, New Zealand,* 26.

CARSON, M. A. & GRIFFITHS, G. A. 1989. Gravel transport in the braided Waimakariri River: mechanisms, measurements and predictions. *Journal of hydrology,* 109**,** 201-220.

CARSON, M. A. & GRIFFITHS, G. A. 1989. Gravel transport in the braided Waimakariri River: mechanisms, measurements and predictions. *J. Hydrol.,* 109, 201–220.

CHANSON, H. 1999. The Hydraulics of Open Channel Flow: An Introduction. Physical Modelling of Hydraulics.

CHEW, L. & ASHMORE, P. E. 2001. Channel adjustment and a test of rational regime theory in a proglacial braided stream. *Geomorphology,* 37**,** 43-63.

CHOW, V. T. 1959. Open-channel hydraulics.

CHOW, V. T. 1964. Handbook of applied hydrology: a compendium of water-resources technology. *McGraw-Hill Book Co. New York,(SW/2778), 1964, 1500*.

CHURCH, M. 1978. Palaeohydrological reconstructions from a Holocene valley fill. *Fluvial sedimentology,* 5**,** 743-772.

CHURCH, M. 1983. Pattern of instability in a wandering gravel bed channel.

CHURCH, M. 1995. Geomorphic response to river flow regulation: Case studies and time-scales. *Regulated Rivers: Research & Management,* 11**,** 3-22.

CHURCH, M. & GILBERT, R. 1975. Proglacial fluvial and lacustrine environments. *Publ. by: Society of economic paleontologists and mineralogists, Tulsa, Oklahoma(USA), 1975, 22-100, Soc. Econ. Paleontol. Mineral., Spec. Publ. 23*.

CHURCH, M., MCLEAN, D. & WOLCOTT, J. 1987. River bed gravels: sampling and analysis: in Thorne, CR, Bathurst, JC, and Hey, RD, eds., Sediment Transport in Gravel-bed Rivers. Chichester, Wiley.

CHURCH, M. A., D. G. MCLEAN, AND J. F. WOLCOTT 1987. *River bed gravels: Sampling and analysis, in Sediment transport in gravel-bed rivers*, John Wiley & Son Ltd.

CLARKE, L., QUINE, T. A. & NICHOLAS, A. 2010. An experimental investigation of autogenic behaviour during alluvial fan evolution. *Geomorphology,* 115**,** 278-285.

CLIFFORD, N., ROBERT, A. & RICHARDS, K. 1992. Estimation of flow resistance in gravel-bedded rivers: A physical explanation of the multiplier of roughness length. *Earth Surface Processes and Landforms,* 17**,** 111-126.

CONSULTANTS, N. H. 1983. Causes of river bed degradation. *Water Resources Research,* 19**,** 1057-1090.

COULTHARD, T., HICKS, D. & VAN DE WIEL, M. J. 2007. Cellular modelling of river catchments and reaches: Advantages, limitations and prospects. *Geomorphology,* 90**,** 192-207.

CUI, Y., PAOLA, C. & PARKER, G. 1996. Numerical simulation of aggradation and downstream fining. *Journal of Hydraulic Research,* 34**,** 185-204.

CUI, Y. & PARKER, G. 2005. Numerical model of sediment pulses and sediment-supply disturbances in mountain rivers. *Journal of hydraulic engineering,* 131**,** 646.

CULLEN, L. E., DUNCAN, R. P., WELLS, A. & STEWART, G. H. 2003. Floodplain and regional scale variation in earthquake effects on forests, Westland, New Zealand. *Journal of the Royal Society of New Zealand,* 33**,** 693-701.

DALRYMPLE, R. A. 1985. Introduction to Physical Models in Coastal Engineering. *Physical Modeling in Coastal Engineering. Rotterdam, Netherlands***,** pp 3-9.

DAVIES, T. 1987. Problems of bed load transport in braided gravel-bed rivers. *Sediment Transfer in Gravel-Bed Rivers. John Wiley & Sons New York. 1987. p 793-811, 3 fig, 36 ref.*

DAVIES, T. & MCSAVENEY, M. 2001. Anthropogenic fanhead aggradation, Waiho River, Westland, New Zealand. *Gravel-Bed Rivers V***,** 531-553.

DAVIES, T. R. & LEE, A. 1988. Physical hydraulic modelling of width reduction and bed level change in braided rivers. *Journal of Hydrology(New Zealand) JLHYAD*, 27.

DAVIES, T. R. H., MCSAVENEY, M. J. & CLARKSON, P. J. 2003. Anthropic aggradation of the Waiho River, Westland, New Zealand: microscale modelling. *Earth Surface Processes and Landforms*, 28**,** 209-218.

DAVINROY, R. D. Micro Scale Sediment Modeling (Micro Modeling) of Inland Waterways. 1996a.

DAVINROY, R. D. 1996b. Sedimentation Study of the Mississippi River, Santa Fe Chute, Doolan Chute, Hydraulic Micro Model Investigation. ARMY ENGINEER DISTRICT ST LOUIS MO APPLIED RIVER ENGINEERING CENTER.

DAVINROY, R. D. 1997. Method and apparatus for micro modeling the sediment transport characteristics of a river. Google Patents.

DAVOREN, A. & MOSLEY, M. 1986. Observations of bedload movement, bar development and sediment supply in the braided Ohau River. *Earth Surface Processes and Landforms*, 11**,** 643-652.

DEAN, R. G. 1985. Physical Modeling of Littoral Processes. *Physical Modeling in Coastal Engineering, Rotterdam, The Netherlands***,** pp 119-139.

DELLA MORTE, R. 2004. *River flow 2004*, Taylor & Francis.

DEVRIES, M., KLAASSEN, G. & STRUIKSMA, N. 1989. On the Use of Movable Bed Models for River Problems: State of Art, Symp. *River Sedimentation, Beijing, China*.

DIKAU, R. 1999. The need for field evidence in modelling landform evolution. *Process modelling and landform evolution***,** 1-12.

DINGMAN, S. L. 1984. Fluvial hydrology.

DOEGLAS, D. 1962. The structure of sedimentary deposits of braided rivers. *Sedimentology,* 1**,** 167-190.

DOESCHL-WILSON, A. B. & ASHMORE, P. E. 2005. Assessing a numerical cellular braided-stream model with a physical model. *Earth Surface Processes and Landforms,* 30**,** 519-540.

DUC, B. M., WENKA, T. & RODI, W. 2004. Numerical modeling of bed deformation in laboratory channels. *Journal of hydraulic engineering,* 130**,** 894.

EATON, B. & LAPOINTE, M. 2001. Effects of large floods on sediment transport and reach morphology in the cobble-bed Sainte Marguerite River. *Geomorphology,* 40**,** 291-309.

EGOZI, R. & ASHMORE, P. 2008. Defining and measuring braiding intensity. *Earth Surface Processes and Landforms,* 33**,** 2121-2138.

EINSTEIN, H. A. 1950. *The bed-load function for sediment transportation in open channel flows,* US Dept. of Agriculture.

EL-BELASY A.M 1996. M.Sc Thesis, HH275. *IHE Delft, the Netherlands*.

ENGELUND, F. & SKOVGAARD, O. 1973. On the origin of meandering and braiding in alluvial streams. *Journal of Fluid Mechanics,* 57**,** 289-302.

ETTEMA, R. & MAYNORD, S. Framework for Evaluating Very Small Hydraulic Models of Channel-Control Works. 2004. ASCE.

FAHNESTOCK, R. K. 1963. *Morphology and hydrology of a glacial stream--White River, Mount Rainier, Washington,* US Govt. Print. Off.

FERGUSON, R. 1993. Understanding braiding processes in gravel-bed rivers: progress and unsolved problems. *Geological Society, London, Special Publications,* 75**,** 73.

FERGUSON, R. 2003. The missing dimension: effects of lateral variation on 1-D calculations of fluvial bedload transport. *Geomorphology,* 56**,** 1-14.

FERGUSON, R. 2007. 2 Gravel-bed rivers at the reach scale. *Developments in Earth Surface Processes,* 11**,** 33-53.

FERGUSON, R., ASHMORE, P., ASHWORTH, P., PAOLA, C. & PRESTEGAARD, K. 1992. Measurements in a braided river chute and lobe 1. Flow pattern, sediment transport, and channel change. *Water resources research,* 28**,** 1877-1886.

FERGUSON, R. & ASHWORTH, P. 1991. Slope-induced changes in channel character along a gravel-bed stream: The Allt Dubhaig, Scotland. *Earth Surface Processes and Landforms,* 16**,** 65-82.

FERGUSON, R. & ASHWORTH, P. 1992. Spatial patterns of bedload transport and channel change in braided and near-braided rivers. *Dynamics of gravel bed rivers. Ed. P. Billy, RD Hey, CR Thorne and P. Tacconi. John Wiley & Sons*.

FERGUSON, R. & WERRITTY, A. 1983. Bar development and channel changes in the gravelly River Feshie, Scotland.

FREDSQE, J. 1978. Meandering and braiding of rivers.

FRINGS, R. M., KLEINHANS, M. G. & VOLLMER, S. 2008. Discriminating between pore filling load and bed structure load: a new porosity based method, exemplified for the river Rhine. *Sedimentology,* 55**,** 1571-1593.

FUJITA, Y. 1989. Bar and channel formation in braided streams. *River Meandering. Water Resources Monograph 12. American Geophysical Union, Washington. 1989. p 417-462, 30 fig, 3 tab, 75 ref.*

FUKUOKA, S. 1989. Finite amplitude development of alternate bars. *River meandering***,** 237-265.

GAINES, R. A. & MAYNORD, S. T. 2001. FORUM-Microscale Loose-Bed Hydraulic Models. *Journal of Hydraulic Engineering-Reston,* 127**,** 335-338.

GASSER, M. M. 1996. Impact of high Aswan Dam on Egypt. *Issues and directions in hydraulics***,** 377-417.

GERMANOSKI, D. 1993. Asynchronous terrace development in degrading braided channels. COLORADO STATE UNIV FORT COLLINS DEPT OF EARTH RESOURCES.

GERMANOSKI, D. & HARVEY, M. D. 1993. Asynchronous terrace development in degrading braided channels. DTIC Document.

GERMANOSKI, D. & SCHUMM, S. 1993. Changes in braided river morphology resulting from aggradation and degradation. *The Journal of geology,* 101**,** 451-466.

GERMANOSKI, D. & SCHUMM, S. 1993. Changes in braided river morphology resulting from aggradation and degradation. *The Journal of Geology***,** 451-466.

GILBERT, G. K. 1917. *Hydraulic-mining debris in the Sierra Nevada,* US Gov't Print. Off.

GILBERT, G. K. & MURPHY, E. C. 1914. *The transportation of debris by running water,* Govt. print. off.

GILVEAR, D. J. 1993. River management and conservation issues on formerly braided river systems; the case of the River Tay, Scotland. *Geological Society, London, Special Publications,* 75**,** 231-240.

GLAZIK, G. 1984. Influence of river model distortion on hydraulic similarity of structures arranged at the channel. *Symposium on scale effects in modelling hydraulic structures, International Association of Hydraulic Research, Esslingen, Germany.*

GOFF, J. & MCFADGEN, B. 2002. Seismic driving of nationwide changes in geomorphology and prehistoric settlement--a 15th Century New Zealand example. *Quaternary Science Reviews,* 21**,** 2229-2236.

GOFF, J. R. & ASHMORE, P. 1994. Gravel transport and morphological change in braided Sunwapta River, Alberta, Canada. *Earth Surface Processes and Landforms,* 19**,** 195-212.

GOMEZ, B. 1991. Bedload transport. *Earth-Science Reviews,* 31**,** 89-132.

GOMEZ, B. & CHURCH, M. 1989. An assessment of bed load sediment transport formulae for gravel bed rivers. *Water Resources Research,* 25**,** 1161-1186.

GOMEZ, B., NAFF, R. L. & HUBBELL, D. W. 1989. Temporal variations in bedload transport rates associated with the migration of bedforms. *Earth Surface Processes and Landforms,* 14**,** 135-156.

GRAF, W. H. 1984. *Hydraulics of sediment transport,* Water Resources Pubns.

GRIFFITHS, G. 1979. Recent sedimentation history of the Waimakariri River, New Zealand. *Journal of Hydrology(New Zealand),* 18.

GRIFFITHS, G. A. 1989. Conversion of braided gravel-bed rivers to single-thread channels of equivalent transport capacity. *J. Hydrology (NZ),* 28**,** 63–75.

GUJAR, V. G. 1981. Determination of scales for mobile bed models with special reference to river models. *Irrig. Power,* 38(2), New Delhi, India.

HALL, R. J. 2012. Waiho River: Optimal Future Management.

HAM, D. G. & CHURCH, M. 2000. Bed-material transport estimated from channel morphodynamics: Chilliwack River, British Columbia. *Earth Surface Processes and Landforms,* 25**,** 1123-1142.

HANCOCK, G. R., NUAKE, J. & FITYUS, S. G. 2006. Modelling of sediment dynamics in a laboratory-scale experimental catchment. *Hydrological Processes,* 20**,** 67 - 84.

HANCOCK, G. R. & WILLGOOSE, G. R. 2001. The interaction between hydrology and geomorphology in a landscape simulator experiment. *Hydrological Processes,* 15**,** 115 - 133.

HANCOCK, G. R. & WILLGOOSE, G. R. 2003. A qualitative and quantitative evaluation of experimental model catchment evolution. *Hydrological Processes,* 17**,** 2347 - 2363.

HARDY, R. 2008. Geomorphology Fluid Flow Modelling: Can Fluvial Flow Only Be Modelled Using a Three-Dimensional Approach? *Geography Compass,* 2**,** 215-234.

HARTEN, A., LAX, P. D. & VAN LEER, B. 1983. On upstream differencing and Godunov-type schemes for hyperbolic conservation laws. *SIAM review***,** 35-61.

HASBARGEN, L. E. & PAOLA, C. 2000. Landscape instability in an experimental drainage basin. *Geology*, 28**,** 1067-1070.

HASBERGEN, L. E. & PAOLA, C. 2000. Landscape instability in an experimental drainage basin. *Geology*, 28**,** 1067 - 1070.

HAYASHI, T. & OZAKI, S. 1980. Alluvial bedforms analysis. I. Formation of alternating bars and braids. *Application of Stohastic Processes in Sediment Transport***,** 1-40.

HAYTER, E. J., BERGS, M. A., GU, R., MCCUTCHEON, S. C., SMITH, S. J. & WHITELEY, H. J. 1999. HSCTM-2D, a finite element model for depth-averaged hydrodynamics, sediment and contaminant transport. *Report, National Exposure Research Laboratory, Office of Research and Development, US EPA, Athens, Georgia*.

HEC 1993. HEC-6: Scour and Deposition in Rivers and Reservoirs, User's Manual. August.

HENDERSON, F. 1966. Open Channel Flow, 522 pp. Macmillan, New York.

HIBMA, A., SCHUTTELAARS, H. & DE VRIEND, H. 2004. Initial formation and long-term evolution of channel-shoal patterns. *Continental shelf research*, 24**,** 1637-1650.

HICKIN, E. J. 1995. Hydraulic geometry and channel scour, Fraser River, British Columbia, Canada. *Wiley: Chichester***,** 155-167.

HICKS, D. M., DUNCAN, M. J., LANE, S. N., TAL, M. & WESTAWAY, R. 2007. 21 Contemporary morphological change in braided gravel-bed rivers: new developments from field and laboratory studies, with particular reference to the influence of riparian vegetation. *Developments in Earth Surface Processes*, 11**,** 557-584.

HICKSON, T. A., SHEETS, B. A., PAOLA, C. & KELBERER, M. 2005. Experimental test of tectonic controls on three-dimensional alluvial facies architecture. *Journal of Sedimentary Research,* 75**,** 710 - 722.

HOEY, T. 1992. Temporal variations in bedload transport rates and sediment storage in gravel-bed rivers. *Progress in physical geography,* 16**,** 319.

HOEY, T., CUDDEN, J. & SHVIDCHENKO, A. 2001. The consequences of unsteady sediment transport in braided rivers. *Gravel Bed Rivers V***,** 121-140.

HOEY, T. B. & SUTHERLAND, A. J. 1991. Channel morphology and bed load pulses in braided rivers: a laboratory study. *Earth Surface Processes and Landforms,* 16**,** 447 - 462.

HOEY, T. B. & SUTHERLAND, A. J. 1991. Channel morphology and bedload pulses in braided rivers: a laboratory study. *Earth Surface Processes and Landforms,* 16**,** 447-462.

HONG, L. & DAVIES, T. 1979. A study of stream braiding: Summary. *Geological Society of America Bulletin,* 90**,** 1094-1095.

HOOKE, R. L. & ROHRER, W. L. 1979. Geometry of alluvial fans: effect on discharge and sediment size. *Earth Surface Processes and Landforms,* 4**,** 147 - 166.

HOOKE, R. L. B. 1968. Steady-state relationships on arid-region alluvial fans in closed basins. *American Journal of Science,* 266**,** 609.

HOWARD, A. D., KEETCH, M. E. & VINCENT, C. L. 1970. Topological and geometrical properties of braided streams. *Water Resources Research,* 6**,** 1674-1688.

HUBBELL, D. 1987. Bed load sampling and analysis. *Sediment Transport in Gravel-Bed Rivers. John Wiley and Sons New York. 1987. p 89-118, 8 fig, 1 tab, 12 ref.*

HUDSON, R. Y., HERRMANN, F. A., SAGER, R. A., WHALIN, R. W., KEULEGAN, G. H., CHATHAM & C. E., H., L. Z. 1979. Coastal Hydraulic Models. *Special Report No. 5. US Army Corps of Engineers, Waterways Experiment Station, Vicksburg, MS.* .

HYDRAULICS, D. 1999. Delft 3D Users' Manual. *The Netherlands: Delft Hydraulics*.

J. TUNNICLIFFE, D. M. H., J. WALSH, M. DUNCAN 2010. parameterizing spatial variability in shear stress and bed surface grain size in braided channels. *Gravel Bed Rivers VII: Tadoussac, QC, Canada*.

JANSEN, P. P., VAN BENDEGOM, L., VAN DEN BERG, J., DE VRIES, M. & ZANEN, A. 1979. *Principles of river engineering: the non-tidal alluvial river*, Pitman.

JARAMILLO, W. F. 1984. Aggradation and Degradation of Alluvial-Channel Beds. *Journal of hydraulic engineering,* 110**,** 1072.

KAMPHUIS, J. W. 1991. Alongshore sediment transport rate. *Journal of Waterway, Port, Coastal and Ocean Engineering,* 117**,** 624-640.

KIRKBY, M. 1971. Hillslope process-response models based on the continuity equation. *Inst. Br. Geogr. Spec. Publ,* 3**,** 15-30.

KIRKBY, M. J. 1996. A role for theoretical models in geomorphology? *Geomorphology,* 10.

KNIGHTON, A. 1989. River adjustment to changes in sediment load: the effects of tin mining on the Ringarooma River, Tasmania, 1875–1984. *Earth Surface Processes and Landforms,* 14**,** 333-359.

KNIGHTON, D. 1998. *Fluvial forms and processes: a new perspective*, Arnold, Hodder Headline, PLC.

KNIGHTON, D. 1998. Fluvial forms and processes: London. *Edward Arnold*.

KORUP, O. 2005. Geomorphic imprint of landslides on alpine river systems, southwest New Zealand. *Earth Surface Processes and Landforms,* 30**,** 783-800.

KOSS, J. E., ETHRIDGE, F. G. & SCHUMM, S. 1994. An experimental study of the effects of base-level change on fluvial, coastal plain and shelf systems. *Journal of Sedimentary Research,* 64**,** 90.

KOSS, J. E., ETHRIDGE, F. G. & SCHUMM, S. A. 1994. An experimental study of the effects of base level change of fluvial, coastal plain and shelf systems. *Journal of Sedimentary Research,* B64**,** 90 - 98.

KURABAYASHI, H., SHIMIZU, Y. & JANG, C. L. 2001. Numerical calculation of bed deformation inbraided stream, Proceedings of the 2nd International Symposium on River, Coastaland Estuarine Morphodynamics,Obihiro, Japan, 2001.

LAGUE, D., CRAVE, A. & DAVY, P. 2003. Laboratory experiments simulating the geomorphic response to tectonic uplift. *Journal of Geophysical Research,* 108.

LAGUE, D., CRAVE, A. & DAVY, P. 2003. Laboratory experiments simulating the geomorphic response to tectonic uplift. *Journal of Geophysical Research,* 18**,** 3.1 - 3.20.

LANE, E. W. 1957. *A study of the shape of channels formed by natural streams flowing in erodible material,* US Army Engineer Division, Missouri River.

LANE, S. 2000. The measurement of river channel morphology using digital photogrammetry. *The Photogrammetric Record,* 16**,** 937-961.

LANE, S., BRADBROOK, K., RICHARDS, K., BIRON, P. & ROY, A. 1999. The application of computational fluid dynamics to natural river channels: three-dimensional versus two-dimensional approaches. *Geomorphology,* 29**,** 1-20.

LANE, S., RICHARDS, K. & CHANDLER, J. 1995. Morphological estimation of the time-integrated bed load transport rate. *Water resources research,* 31**,** 761-772.

LANE, S. N. & RICHARDS, K. S. 1997. Linking river channel form and process: time, space and causality revisited. *Earth Surface Processes and Landforms,* 22**,** 249-260.

LANE, S. N. & RICHARDS, K. S. 1998. High resolution, two-dimensional spatial modelling of flow processes in a multi-thread channel. *Hydrological Processes,* 12**,** 1279-1298.

LANE, S. N. & RICHARDS, K. S. 2000. High resolution, two dimensional spatial modelling of flow processes in a multi-thread channel. *High resolution Flow Modelling in Hydrology and Geomorphology. Wiley, Chichester***,** 105-124.

LANE, S. N., WESTAWAY, R. M. & MURRAY HICKS, D. 2003. Estimation of erosion and deposition volumes in a large, gravel-bed, braided river using synoptic remote sensing. *Earth Surface Processes and Landforms,* 28**,** 249-271.

LATTEUX, B. 1986. The LNH experience in modelling sediment transport under combined wave and current action. *Symp. on Scale Effects in Modelling Sediment Transport phenomenon, supplement, International Association for Hydraulic Research*.

LAWLESS, M. & ROBERT, A. 2001. Scales of boundary resistance in coarse-grained channels: turbulent velocity profiles and implications. *Geomorphology,* 39**,** 221-238.

LE, B. 1978. *A Study of Stream Braiding: A Thesis Submitted in Partial Fulfilment of the Requirements for the Degree of Master of Agricultural Science in Agricultural Engineering in the University of Canterbury, Lincoln College.* University of Canterbury.

LE, B. & DAVIES, T. 1979. A study of stream braiding. *Geological Society of America Bulletin,* 82**,** 1251-1266.

LEE, L. J. & HENSON, B. L. 1977. The interrelationships of the longitudinal profiles and channel pattern for the Red River. *Journal of hydrology,* 35**,** 191-201.

LEOPOLD, L. B. & WOLMAN, M. G. 1957. *River channel patterns: braided, meandering, and straight*, US Govt. Print. Off.

LIEBS, W. 1942. *Die Nachbildung von Flüssen mit beweglicher Sohle im Modell: Grundlagen, Durchführg d. Modellversuche, Übertragbarkeit d. Ergebnisse.* Preuß. Versuchsanst. f. Wasser-, Erd-u. Schiffbau.

MADEJ, M. A., SUTHERLAND, D. G., LISLE, T. E. & PRYOR, B. 2009. Channel responses to varying sediment input: A flume experiment modeled after Redwood Creek, California. *Geomorphology,* 103**,** 507-519.

MALVERTI, L., LAJEUNESSE, E. & MÉTIVIER, F. 2008. Small is beautiful: upscaling from microscale laminar to natural turbulent rivers. *Journal of Geophysical Research,* 113**,** F04004.

MALVERTI, L., LAJEUNESSE, É. & MÉTIVIER, F. 2007. Experimental investigation of the response of an alluvial river to a vertical offset of its bed. *Dohmen-Janssen & Hulscher (eds) River, Coastal and Estuarine Morphodynamics, Taylor & Francis Group: London*.

MARSTON, R. A., GIREL, J., PAUTOU, G., PIEGAY, H., BRAVARD, J. P. & ARNESON, C. 1995. Channel metamorphosis, floodplain disturbance, and vegetation development: Ain River, France. *Geomorphology,* 13**,** 121-131.

MARTIN, J. H. 1993. A review of braided fluvial hydrocarbon reservoirs: the petroleum engineer's perspective. *Geological Society, London, Special Publications,* 75**,** 333-367.

MARTIN, Y. & CHURCH, M. 1995. Bed-material transport estimated from channel surveys: Vedder River, British Columbia. *Earth Surface Processes and Landforms,* 20**,** 347-361.

MARTIN, Y. & CHURCH, M. 1995. Bed material transport estimated from channel surveys: Vedder River, British Columbia. *Earth Surface Processes and Landforms,* 20**,** 347-361.

MAYNORD, S. T. 2006. Evaluation of the micromodel: An extremely small-scale movable bed model. *Journal of hydraulic engineering,* 132**,** 343.

MCARDELL, B. W. & FAEH, R. 2001. A computational investigation of river braiding. *Gravel Bed Rivers V,* 11-46.

MCCARTNEY, M., SULLIVAN, C., ACREMAN, M. & MCALLISTER, D. 2000. Ecosystem impacts of large dams. *Thematic review II,* 1.

MCLEAN, D. Sensitivity analysis of bedload equations. 1985. 1-15.

MCLEAN, D. G. 1990. The relation between channel instability and sediment transport on Lower Fraser River.

MCLEAN, D. G. & CHURCH, M. 1999. Sediment transport along lower Fraser River: 2. Estimates based on the long-term gravel budget. *Water resources research,* 35**,** 2549-2559.

MCLEAN, D. G., CHURCH, M. & TASSONE, B. 1999. Sediment transport along lower Fraser River: 1. Measurements and hydraulic computations. *Water Resources Research,* 35**,** 2533-2548.

MCLELLAND, S., ASHWORTH, P., BEST, J., RODEN, J. & KLAASSEN, G. 1999. Flow Structure and Transport of Sand-Grade Suspended Sediment around an Evolving Braid Bar, Jamuna River, Bangladesh. *Fluvial sedimentology VI,* 43-57.

MCLELLAND, S. J., ASHWORTH, P. J. & BEST, J. L. 1996. The origin and downstream development of coherent flow structures at channel junctions. *Coherent flow structures in open channels***,** 459-490.

MEIROVICH, L., LARONNE, J. B. & REID, I. 1998. The variation of water-surface slope and its significance for bedload transport during floods in gravel-bed streams. *Journal of Hydraulic Research,* 36**,** 147-157.

MÉTIVIER, F. & MEUNIER, P. 2003. Input and output mass flux correlations in an experimental braided stream. Implications on the dynamics of bed load transport. *Journal of hydrology,* 271**,** 22-38.

MEUNIER, P. & MÉTIVIER, F. 2000. Permanence des flux de masse d'une rivière en tresses expérimentales: Permanent transport regime of an experimental braided river. *Comptes Rendus de l'Académie des Sciences-Series IIA-Earth and Planetary Science,* 331**,** 105-110.

MEUNIER, P. & MÉTIVIER, F. Effective stream power and dynamics of bedload transport in experimental braided streams. 2003. 10219.

MEUNIER, P. & MÉTIVIER, F. 2006. Sediment transport in a microscale braided stream: from grain size to reach scale.

MEYER-PETER, E. & MÜLLER, R. Formulas for bed-load transport. 1948. 39–64.

MIALL, A. D. 1977. A review of the braided-river depositional environment. *Earth-Science Reviews,* 13**,** 1-62.

MIGLIO, A., GAUDIO, R. & CALOMINO, F. 2009. Mobile-bed aggradation and degradation in a narrow flume: Laboratory experiments and numerical simulations. *Journal of Hydro-environment Research,* 3**,** 9-19.

MINGHAM, C. & CAUSON, D. 1998. High-resolution finite-volume method for shallow water flows. *Journal of Hydraulic Engineering,* 124**,** 605.

MORETON, D. J., ASHWORTH, P. J. & BEST, J. L. 2002. The physical scale modelling of braided alluvial architecture and estimations of subsurface permeability. *Basin Research,* 14**,** 265 - 285.

MOSLEY, M. 1983. Response of braided rivers to changing discharge. *Journal of hydrology,* 22.

MOSLEY, M. P. 1981. Semi-determinate hydraulic geometry of river channels, South Island, New Zealand. *Earth surface processes and landforms,* 6**,** 127-137.

MOSLEY, M. P. 1982. Analysis of the effect of changing discharge on channel morphology and instream uses in a braided river, Ohau River, New Zealand. *Water Resources Research,* 18**,** 800-812.

MOSLEY, M. P. & ZIMPFER, G. 1978. Hardware models in geomorphology. *Progress in Physical Geography,* 2**,** 438.

MURRAY, A. B. & PAOLA, C. 1994. A cellular model of braided rivers.

MURRAY, A. B. & PAOLA, C. 1997. Properties of a cellular braided-stream model. *Earth Surface Processes and Landforms,* 22**,** 1001-1025.

MURRAY, A. B. & PAOLA, C. 2003. Modelling the effect of vegetation on channel pattern in bedload rivers. *Earth Surface Processes and Landforms,* 28**,** 131-143.

MUTO, T. & SWENSON, J. B. 2005. Large-scale fluvial grade as a nonequilibrium state in linked depositional systems: Theory and experiment. *Journal of Geophysical Research,* 110**,** F03002.

NEILL, C. R. 1971. River bed transport related to meander migration rates. *Journal of the Waterways, Harbors and Coastal Engineering Division,* 97**,** 783-786.

NEILL, C. R. 1987. Sediment balance considerations linking long-term transport and channel processes. *Sediment Transport in Gravel-Bed Rivers. John Wiley and Sons New York. 1987. p 225-249, 9 fig, 25 ref.*

NICHOLAS, A. 2000. Modelling bedload yield in braided gravel bed rivers. *Geomorphology,* 36**,** 89-106.

NICHOLAS, A. 2003. Investigation of spatially distributed braided river flows using a two-dimensional hydraulic model. *Earth Surface Processes and Landforms,* 28**,** 655-674.

NICHOLAS, A. 2003. Investigation of spatially distributed braided river flows using a two dimensional hydraulic model. *Earth Surface Processes and Landforms,* 28**,** 655-674.

NICHOLAS, A. & SAMBROOK SMITH, G. 1999. Numerical simulation of three-dimensional flow hydraulics in a braided channel. *Hydrological Processes,* 13**,** 913-929.

NICHOLAS, A., THOMAS, R. & QUINE, T. 2006. Cellular modelling of braided river form and process. *Braided Rivers***,** 137-151.

NICHOLAS, A. P. 2000. Modelling bedload yield in braided gravel bed rivers. *Geomorphology,* 36**,** 89-106.

NICHOLAS, A. R. & MCLELLAND, S. J. 2004. Computational fluid dynamics modelling of three-dimensional processes on natural river floodplains. *Journal of Hydraulic Research,* 42**,** 131-143.

OLESEN, K. W. & TJERRY, S. 2002. Morphological modelling of the Chaktomuk Junction. *In Bousmar, D. and Zech, Y., editors, River flow 2002. Proceedings of the international conference on fluvial hydraulics. Louvain-LaNeuve, Belgium, 4– 6 September 2002. Lisse: A.A. Balkema Publishers, 2, 879– 87.*

OSTERKAMP, W. 1978. Gradient, discharge, and particle-size relations of alluvial channels in Kansas, with observations on braiding. *American Journal of Science,* 278.

PAIGE, A. D. & HICKIN, E. J. 2000. Annual bed-elevation regime in the alluvial channel of Squamish River, Southwestern British Columbia, Canada. *Earth Surface Processes and Landforms,* 25**,** 991-1009.

PAOLA, C. 1996. Incoherent structure: turbulence as a metaphor for stream braiding. *Coherent Flow Structures in Open Channels***,** 705–723.

PAOLA, C. 2000. Quantitative models of sedimentary basin filling. *Sedimentology,* 47**,** 121-178.

PAOLA, C., PARKER, G., MOHRIG, D. C. & WHIPPLE, K. X. 1999. The influence of transport fluctuations on spatially averaged topography on a sandy, braided fluvial fan. *SPECIAL PUBLICATION-SEPM,* 62**,** 211-218.

PARKER, G. 1976. On the cause and characteristic scales of meandering and braiding in rivers. *Journal of Fluid Mechanics,* 76**,** 457-480.

PARKER, G. 1978. Self-formed straight rivers with equilibrium banks and mobile bed. Part 2. The gravel river. *Journal of Fluid Mechanics,* 89**,** 127-146.

PARSONS, A. J. & ABRAHAMS, A. D. 2009. Geomorphology of desert environments. *Geomorphology of Desert Environments***,** 3-7.

PASTERNACK, G. B., WANG, C. L. & MERZ, J. E. 2004. Application of a 2D hydrodynamic model to design of reach-scale spawning gravel replenishment on the Mokelumne River, California. *River Research and Applications,* 20**,** 205-225.

PEAKALL, J., ASHWORTH, P. & BEST, J. Physical Modelling in Fluvial Geomorphology: Principles, Applications and Unresolved Issues. 1996. John Wiley & Sons, 221.

PEAKALL, J., ASHWORTH, P. J. & BEST, J. L. 1996. Physical modelling in fluvial geomorphology: principles, applications and unresolved issues. *In:* RHOADS, B. L. & THORN, C. E. (eds.) *The Scientific Nature of Geomorphology.* Proceedings of the 27th Binghampton Symposium in Geomorphology: 27 - 29 September 1996: John Wiley and Sons Ltd.

PEAKALL, J. & WARBURTON, J. 1996. Surface-tension in small hydraulic river models–the significance of the Weber number. *Journal of Hydrology (NZ),* 35**,** 199-212.

PETTS, G. E., MÖLLER, H. & ROUX, A. L. 1989. Historical change of large alluvial rivers: Western Europe.

PICKUP, G. & HIGGINS, R. 1979. Estimating sediment transport in a braided gravel channel--The Kawerong River, Bougainville, Papua New Guinea. *Journal of Hydrology,* 40**,** 283-297.

PIÉGAY, H., GRANT, G., NAKAMURA, F. & TRUSTRUM, N. 2006. Braided river management: from assessment of river behaviour to improved sustainable development.

POPOV, I. 1962a. A sediment balance of river reaches and its use for the characteristics of the channel process. *Trudy GGI,* 1962**,** 3-21.

POPOV, I. 1962b. Application of morphological analysis to the evaluation of the general channel deformations of the River Ob'. *Trudy GGI,* 1962**,** 22-86.

R DOANE, M., R DOANE, N. & DUMITRIU, D. 2003. Geomorphological evolution of longitudinal river profiles in the Carpathians. *Geomorphology*, 50**,** 293-306.

REID, I. & LARONNE, J. B. 1995. Bed load sediment transport in an ephemeral stream and a comparison with seasonal and perennial counterparts. *Water Resources Research,* 31**,** 773-781.

REINFELDS, I. & NANSON, G. 1993. Formation of braided river floodplains, Waimakariri River, New Zealand. *Sedimentology*, 40**,** 1113-1127.

RICHARDSON, W. R. & THORNE, C. R. 1998. Secondary currents around braid bar in Brahmaputra River, Bangladesh. *Journal of hydraulic engineering*, 124**,** 325.

RUNDLE, A. 1985a. The mechanism of braiding. *Z. Geomorphol. NF, Suppl. Bd,* 55**,** 1-13.

RUNDLE, A. 1985b. Braid morphology and the formation of multiple channels; the Rakaïa, New Zealand. *Zeitschrift fqr Geomorphologie. Supplementband (55)***,** 15-37.

RUST, B. R. 1978. A classification of alluvial channel systems. *Fluvial sedimentology,* 5**,** 123-126.

SABERSKY, R. H., ACOSTA, A. J. & HAUPTMANN, E. G. 1971. *Fluid flow: a first course in fluid mechanics,* Macmillan New York.

SAPOZHNIKOV, V. B. & FOUFOULA-GEORGIOU, E. 1997. Experimental evidence of dynamic scaling and indications of self-organized criticality in braided rivers. *Water Resources Research,* 33**,** 1983 - 1991.

SCHLICHTING, H. & GERSTEN, K. 2000. *Boundary-layer theory*, Springer Verlag.

SCHOKLITSCH 1934. Bedload and bedload movement. *Wasserwirtschaft, Heft (1934), p. 4.*

SCHUMM, S. & KHAN, H. 1971. Experimental study of channel patterns.

SCHUMM, S. & KHAN, H. 1972. Experimental study of channel patterns. *Geological Society of America Bulletin,* 83**,** 1755.

SCHUMM, S. & KHAN, H. 1972. Experimental study of channel patterns. *Geological Society of America Bulletin,* 83**,** 1755-1770.

SCHUMM, S. & WINKLEY, B. 1994. The character of large alluvial rivers. *The variability of large alluvial rivers***,** 1-9.

SCHUMM, S. A. 1960. *The shape of alluvial channels in relation to sediment type: erosion and sedimentation in a semiarid environment,* US Government Printing Office.

SCHUMM, S. A. 1961. Effect of sediment characteristics on erosion and deposition in ephemeral-stream channels. *Geological Survey professional paper,* 352.

SCHUMM, S. A., MOSLEY, M. P. & WEAVER, W. 1987. Experimental fluvial geomorphology.

SHEETS, B. A., HICKSON, T. A. & PAOLA, C. 2002. Assembling the stratigraphic record: depositional patterns and time-scales in an experimental alluvial basin. *Basin Research,* 14**,** 287 - 301.

SHIELDS, A. 1936. Anwendung der Ähnlichkeitsmechanik und der Turbulenzforschung auf die Geschiebebewegung. Mitt. der Preuss. Versuchsanstalt für Wasserbau und Schiffbau. H.

SHIELDS, A., OTT, W. & VAN UCHELEN, J. 1936. Application of similarity principles and turbulence research to bed-load movement.

SHVIDCHENKO, A. & KOPALIANI, Z. 1998. Hydraulic modeling of bed load transport in gravel-bed Laba River. *Journal of Hydraulic Engineering,* 124**,** 778-785.

SIEGRIST, K. 2001. Virtual laboratories in probability and statistics.

SLINGERLAND, R. & SMITH, N. D. 1986. Occurrence and formation of water-laid placers. *Annual Review of Earth and Planetary Sciences,* 14**,** 113.

SMEC 2008a. Hydrological study of the Tana-Beles Sub-basins: Surface water investigation. Addis Ababa, Ethiopia: Ministry of Water Resources.

SMEC 2008c. Hydrological study of the Tana-Beles Sub-basins: Main Report. Addis Ababa, Ethiopia: Ministry of Water Resources.

SMITH, N. D. 1974. Sedimentology and bar formation in the upper Kicking Horse River, a braided outwash stream. *The Journal of Geology***,** 205-223.

SMITH, N. D. & MINTER, W. 1980. Sedimentological controls of gold and uranium in two Witwatersrand paleoplacers. *Economic Geology,* 75**,** 1-14.

SMITH, N. D. & SMITH, D. G. 1984. William River: An outstanding example of channel widening and braiding caused by bed-load addition. *Geology,* 12**,** 78-82.

SNOW, R. S. & SLINGERLAND, R. L. 1987. Mathematical modeling of graded river profiles. *The Journal of Geology***,** 15-33.

SOUTHARD, J. B., SMITH, N. D. & KUHNLE, R. A. 1984. Chutes and lobes: newly identified elements of braiding in shallow gravelly streams. *Sedimentology of gravels and conglomerates***,** 51–59.

STEFFLER, P. & BLACKBURN, J. 2002. River2D–Introduction to Depth Averaged Modelling and User's Manual. *University of Alberta***,** 23.

STOJIC, M., CHANDLER, J. H., ASMORE, P. & LUCE, J. 1998. Assessment of sediment transport rates by automated digital photogrammetry. *Photogrammetric Engineering,* 64**,** 387 - 395.

STRICKLER, A. 1923. Some contributions to the problem of velocity formula and roughness coefficient for rivers, canals, and closed conduits. *Mitteilungen des edgenossishen Amtes fur Wasserwirtscaft, Bern, Switzerland*.

STRUIKSMA, N. Scale effects in the reproduction of the overall bed topography in river models. 1986.

STRUIKSMA, N., KLAASSEN, G.J. 1986. On scale effects in movable-bed river models. *Symposiumon scale effects in modelling sediment transport phenomena, Toronto, Canada*.

SUGA, K. 1973. Some notes on hydraulic model tests of river channels. *IAHR Int. symp. on River Mechanics, Bangkok, Thailand*.

SURIAN, N. 2006. Effects of human impact on braided river morphology: examples from Northern Italy.

SURIAN, N. & RINALDI, M. 2003. Morphological response to river engineering and management in alluvial channels in Italy. *Geomorphology,* 50**,** 307-326.

TAL, M., GRAN, K., MURRAY, A. B., PAOLA, C. & HICKS, D. M. 2004. Riparian vegetation as a primary control on channel characteristics in multi-thread rivers. *In:* BENNETT, S. J. & SIMON, A. (eds.) *Riparian Vegetation and Fluvial Geomorphology: Hydraulic, Hydrologica and Geotechnical Interaction.* American Geophysical Union Monograph.

TAL, M. & PAOLA, C. 2007. Dynamic single-thread channels maintained by the interaction of flow and vegetation. *Geology,* 35**,** 347.

THMOAS, R. 2003. Development and Evaluation of A Cellular Model to simulate Braided River Dynamics. *Unpublished PhD Thesis,* University of Exeter**,** 362.

THOMAS, R. 2003. *Development and evaluation of a cellular model to simulate braided river dynamics.*

THOMAS, R. & NICHOLAS, A. 2002. Simulation of braided river flow using a new cellular routing scheme. *Geomorphology,* 43**,** 179-195.

THOMAS, R., NICHOLAS, A. & QUINE, T. 2002. Development and application of a cellular model to simulate braided river process-form interactions and morphological change. *River Flow 2002***,** 783-791.

THOMPSON, S. 1985. Transport of gravel by flows up to 500 m3/s, Ohau River, Otago, New Zealand. *Journal of Hydraulic Research,* 23**,** 285-303.

TOCKNER, K. & STANFORD, J. A. 2002. Riverine flood plains: present state and future trends. *Environmental conservation,* 29**,** 308-330.

TOCKNER, K., WARD, J. V., ARSCOTT, D. B., EDWARDS, P. J., KOLLMANN, J., GURNELL, A. M., PETTS, G. E. & MAIOLINI, B. 2003. The Tagliamento River: a model ecosystem of European importance. *Aquatic Sciences-Research Across Boundaries,* 65**,** 239-253.

VAN HEIJST, M. W. I. M. & POSTMA, G. 2001. Fluvial response to sea-level changes: a quantitative analogue experimental approach. *Basin Research,* 13**,** 269 - 292.

VAN LEER, B. 1977. Towards the ultimate conservative difference scheme. IV. A new approach to numerical convection. *Journal of computational physics,* 23**,** 276-299.

WARBURTON, J. 1996. Active braidplain width, bed load transport and channel morphology in a model braided river. *Journal of Hydrology (New Zealand),* 35**,** 259 - 285.

WARBURTON, J. 1996. Active braidplain width, bed load transport and channel morphology in a model braided river. *Journal of Hydrology (NZ),* 35**,** 259-285.

WARBURTON, J. 1996. A brief review of the hydraulic modelling of braided gravel-rivers in New Zealand. *Journal of Hydrology (New Zealand),* 35**,** 157 - 173.

WARBURTON, J. & DAVIES, T. 1994. Variability of bedload transport and channel morphology in a braided river hydraulic model. *Earth Surface Processes and Landforms,* 19**,** 403-421.

WARBURTON, J., DAVIES, T., GRIFFITHS, G., HOEY, T. & YOUNG, W. 1996. Future prospects for the use of hydraulic models in the management of New Zealand braided gravel-bed rivers. *Journal of hydrology. New Zealand,* 35**,** 287-302.

WARBURTON, J., DAVIES, T. & MANDL, M. 1993. A meso-scale field investigation of channel change and floodplain characteristics in an upland braided gravel-bed river, New Zealand. *Geological Society, London, Special Publications,* 75**,** 241.

WARBURTON, J. & DAVIES, T. R. H. 1994. Variability of bed load transport and channel morphology in a braided river hydraulic model. *Earth Surface Processes and Landforms,* 19**,** 403 - 421.

WATER, D. 2002. Environment (2003). *MIKE21 and MIKE3 particle analysis and oil spill analysis user guide*.

WEBSTER, R. 1997. Regression and functional relations. *European Journal of Soil Science,* 48**,** 557-566.

WHIPPLE, K. X., PARKER, G., PAOLA, C. & MOHRIG, D. 1998. Channel dynamics, sediment transport, and the slope of alluvial fans: Experimental study. *The Journal of geology,* 106**,** 677-694.

WHIPPLE, K. X., PARKER, G., PAOLA, C. & MOHRIG, D. 1998. Channel dynamics, sediment transport, and the slope of alluvial fans: Experimental study. *The Journal of geology***,** 677-693.

WHITING, P. & DIETRICH, W. 1989. Boundary shear stress and sediment transport in river meanders of sand and gravel.

WHITING, P. J. & DIETRICH, W. E. 1991. Convective accelerations and boundary shear stress over a channel bar. *Water Resources Research,* 27**,** 783-796.

WIBERG, P. L. & SMITH, J. D. 1991. Velocity distribution and bed roughness in high-gradient streams. *Water Resources Research,* 27**,** 825-838.

WILCOCK, P. R. 1996. Estimating local bed shear stress from velocity observations. *Water Resources Research,* 32**,** 3361-3366.

WILCOCK, P. R. 2001. Toward a practical method for estimating sediment-transport rates in gravel-bed rivers. *Earth Surface Processes and Landforms,* 26**,** 1395-1408.

WILKINSON, R. 1984. A method for evaluating statistical errors associated with logarithmic velocity profiles. *Geo-marine letters,* 3**,** 49-52.

WILLIAMS, G. P. 1983. Paleohydrological methods and some examples from Swedish fluvial environments. I. Cobble and boulder deposits. *Geografiska Annaler. Series A. Physical Geography***,** 227-243.

WILLIAMS, G. P. & WOLMAN, M. G. 1984. *Downstream effects of dams on alluvial rivers,* US Government Printing Office Washington, DC.

WILLIAMS, J. J. 1995. Drag and sediment dispersion over sand waves. *Estuarine, Coastal and Shelf Science,* 41**,** 659-687.

WINTERBOTTOM, S. J. 1995. An analysis of channel change on the Rivers Tay and Tummel, Scotland, using GIS and remote sensing techniques.

WINTERBOTTOM, S. J. 2000. Medium and short-term channel planform changes on the Rivers Tay and Tummel, Scotland. *Geomorphology,* 34**,** 195-208.

WINTERBOTTOM, S. J. & GILVEAR, D. J. 1997. Quantification of channel bed morphology in gravel-bed rivers using airborne multispectral imagery and aerial photography. *Regulated Rivers: Research & Management,* 13**,** 489-499.

WOHL, E. E. 2000. *Mountain rivers,* Amer Geophysical Union.

WONG, M. & PARKER, G. 2006. Reanalysis and correction of bed-load relation of Meyer-Peter and Müller using their own database. *Journal of hydraulic engineering,* 132**,** 1159.

WU, W. 2001. CCHE2D sediment transport model. Version 2.1, Technical Report No. NCCHE-TR-2001-3, The University of Mississippi, Mississippi, USA.

WU, W. 2007. *Computational river dynamics,* CRC.

YALIN, M. 1963. An expression for bed-load transportation. *J. Hydraul. Div. ASCE,* 89**,** 221-250.

YALIN, M. S. 1971. *Theory of hydraulic models,* Macmillan.

YOUNG, W. & DAVIES, T. 1991. Bedload transport processes in a braided gravel-bed river model. *Earth Surface Processes and Landforms,* 16**,** 499-511.

YOUNG, W. & DAVIES, T. 1991. Bedload transport processes in a braided gravel bed river model. *Earth Surface Processes and Landforms,* 16**,** 499-511.

YOUNG, W. & WARBURTON, J. 1996. Principles and practice of hydraulic modelling of braided gravel-bed rivers. *Journal of Hydrology (NZ),* 35**,** 175-198.

YOUNG, W. J. & WARBURTON, J. 1996. Principles and practice of hydraulic modelling of braided gravel-bed rivers. *Journal of Hydrology (NZ),* 35**,** 175-198.

ZOLEZZI, G., BERTOLDI, W. & TUBINO, M. 2006. Morphological analysis and prediction of channel bifurcations. *Braided Rivers: Process, Deposits, Ecology and Management. Edited by GH Sambrook-Smith, JL Best, CS Bristow, and GE Petts. Special Publication,* 36**,** 227-250.

ZOLEZZI, G., BERTOLDI, W. & TUBINO, M. 2006. Morphological analysis and prediction of river bifurcations.